Evaluating mangrove proxies for quantitative relative sea-level reconstructions

SEFTON, JULIET,PERRY

EVALUATING MANGROVE PROXIES FOR QUANTITATIVE RELATIVE SEA-LEVEL RECONSTRUCTIONS

JULIET PERRY SEFTON

A THESIS

submitted for the

Degree of Doctor of Philosophy

in Physical Geography

at

the Department of Geography

DURHAM UNIVERSITY

2020

Abstract

Deciphering the timing, magnitude, and geographic variability of relative sea-level changes from geological records is critical for projecting future sea-level changes. Mangrove sediments provide an archive of past sea-level changes because they occupy intertidal zones along coastlines in low latitude locations. Such locations are important because they are far from present and former polar ice sheets that influence relative sea levels via glacio-isostatic adjustment. However using mangrove sediments for quantitative relative sea-level reconstructions is challenging due to variable fossil preservation and issues with radiocarbon dating. To evaluate the utility of mangrove sediments for high-resolution relative sea-level reconstructions, I studied two mangroves on Mahé, Seychelles.

To determine what materials are best suited for radiocarbon analysis, I compared radiocarbon ages from bulk sediments, organic concentrates, and macrofossils. I find that radiocarbon ages from bulk sediment and organic concentrate are indistinguishable and therefore both methods likely sample younger carbon. These results demonstrate that macrofossils sourced from above-ground (e.g. leaves) are the most reliable materials for constructing radiocarbon chronologies in mangrove sediments.

I examined the utility of mangrove pollen as a sea-level indicator through vegetation mapping and pollen trapping in two Seychelles mangroves. Mangrove species are broadly zoned according to elevation, but the results from annual pollen traps demonstrate pollen rain is poorly associated with vegetation. Additionally, low pollen concentrations in surface sediments suggest that it is unlikely pollen-based proxies will improve existing uncertainties on relative sea-level reconstructions in Seychelles.

To test the utility of geochemical properties for relative sea-level reconstructions in Seychelles mangroves I characterised the TOC, TIC and lipid biomarker compositions in surface sediments at two mangroves sites. Sedimentation is controlled by hydrogeomorphological factors, and therefore TOC and TIC do not provide sufficient information alone to reconstruct past elevation changes. However, biomarker distributions may be indicative of different vegetation and elevation zones.

Contents

List of figures

List of tables

Statement of copyright

Acknowledgements

I would like to thank my supervisors Sarah Woodroffe and Erin McClymont for helping develop and support this project over the last three years. They have facilitated incredible opportunities for me in the Department of Geography and beyond and I am very grateful. I would also like to thank my external supervisor Philippa Ascough at the University of Glasgow and the Scottish Universities Environmental Research Centre for your support, expertise, and for hosting me in the laboratory in the grand metropolis of East Kilbride.

This project would not have been possible without funding from a number of sources. Firstly, thanks to the Van Mildert College Trust who generously funded my stipend and some annual research costs – it has been a pleasure to join your community. Secondly, thank you to the Department of Geography who funded my student fees, and conference attendance. I would also like to thank a number of organisations for providing essential funds for my two fieldwork seasons (in no particular order): the Royal Geographical Society, the Quaternary Research Association, the International Association for Sedimentologists, the British Sedimentological Research Group, and the Estuarine and Coastal Science Association. Radiocarbon analyses undertaken as part of this project were funded by NERC (Radiocarbon Analysis Allocation Number 2119.0418).

I had amazing support in the field from Louise Best, Wilfred Woolf, my partner Richard Selwyn Jones, and my supervisor Sarah. Thanks for trudging around the mangroves and battling the tides, spiders, wasps, and mosquitoes every day with a smile. Richard – I am sorry about the dengue fever…

I would like to thank the Seychelles National Park Authority, and in particular Isabelle Ravinia for their support in the field and for facilitating our science permits.

The laboratory technical team in the Department of Geography have been very helpful during my time in the labs. Thank you to (in no particular order) Frank Davies, Eleanor Ross, Amanda Hayton, Martin West, Chris Longley, Merv Brown, Neil Tunstall, Kathryn Melvin, and Michael Heslop for all their expertise, support, and chats. Michael – I haven't watched Crocodile Dundee yet but I'll get round to it soon. I would also like to thank Charlotte Spencer-Jones who spent many dedicated hours in the lab teaching me the alchemy of biomarker analysis. Thank you for your expertise, support, and mentorship.

Thanks also to Kathy Wood, Lianne Percival, and all the wonderful support staff in the Department of Geography. Also big thanks to John Thompson – no matter how busy you are your door is always open and you are always so welcoming despite all the teaching fiascos! Such a large department cannot function without folks like you.

Thanks to all the folks who let me tag along on other projects and taught me lots – Ian Shennan, Louise Best, Martin Brader, Emmanuel Bustamante-Fernandez, Matt Brain, Simon Engelhart, Andy Kemp. I learnt so much during extra fieldtrips to Greenland, Scotland, Micronesia – thanks for letting me tag along Sarah, and teaching me the craft of coring. Maybe I will even like Troels-Smith descriptions someday..

Thanks to all the wonderful PhD peers I have shared offices with over the last three years. I have learnt so much from you all and you have massively enriched my experience here at Durham. Mateja, Zoe, Liz… thanks for the coffee breaks, chats, drinks and dinners. Your friendship means so much to me.

Last but certainly not least, thank you to my partner Richard Selwyn Jones for your unwavering support and enthusiasm in my development as a scientist. Although somehow I doubt you'll be entering a mangrove again anytime soon..

Chapter 1: Introduction

1.1 Rationale

Sea-level rise is one of the major threats to society as a result of anthropogenic climate change (Mengel et al., 2018; Steffen et al., 2018). Projections of global mean sea-level rise by 2100 CE (Common Era) range from decimetres to over one metre (IPCC, 2019) — an uncertainty that partially reflects our imperfect understanding of the processes governing ice sheet instability, climate, and sea-level changes on timescales greater than instrumental and satellite observations. To determine the rate, magnitude, mechanisms, and geographical variability of relative sea-level changes on longer timescales, we must use geological archives (Milne et al., 2009). This approach allows us to understand sea-level variability in response to climate changes over centennial to millennial timescales, which allows for more precise projections of future sea-level rise (Dutton et al., 2015a; Horton et al., 2018).

There are a number of outstanding questions, and therefore motivations, for using geological data to understand past sea-level changes (Khan et al., 2019a). How much grounded ice was present during the Last Glacial Maximum (LGM) ~20,000 years before present? What are the mechanisms behind possible periods of rapid sea-level changes in the past? Were the major ice sheets melting during the Late Holocene and immediate pre-industrial era (from ~4,000 years ago until the 19th century)? These questions remain challenging to address because sea-level changes are not uniform over time or space.

Relative sea level (RSL) is the height of the ocean surface relative to a local, land-based reference. RSL in any one location can be attributed to multiple processes: a) changes to global land-based ice volume (termed 'eustasy'), b) changes to ocean temperature, salinity, circulation, and tidal range c) local or regional tectonic uplift or subsidence, and d) the oceanic and solid Earth response to loading and unloading of ice masses, termed glacial isostatic adjustment (GIA). Regions far from past and present centres of grounded ice (known as 'far-field') are ideal for understanding past eustatic sea-level changes because RSL in these regions is less influenced by GIA processes (Clark et al., 1978).

1.1.1 Mid- and Late Holocene RSL changes

Far-field RSL data, and in particular data derived from corals, are used as primary constraints for ice sheet volumes in geophysical models (Bradley et al., 2016; Lambeck et al., 2014; Peltier, 2002; Peltier et al., 2015). These models report variable quantities and timings of ice sheet melt during the Mid- to Late Holocene (~6,000 years to present). There are key differences in the timing of cessation of major (>1 metre) eustatic sea-level rise; for example, whether metre-scale contribution of continental ice sheet melt to global mean sea-level rise ceased around or before 4,000 years ago (Milne et al., 2005; Peltier, 2002; Peltier et al., 2015) or continued into the Late Holocene (Bradley et al., 2016; Lambeck et al., 2014; Nakada and Lambeck, 1989). A major component of this variability relates to uncertainty in the contribution of the Antarctic Ice Sheet to Mid- to Late Holocene eustatic sea level, which is largely due to a paucity of observations close to the Antarctic Ice Sheet (Cuzzone et al., 2016; Lecavalier et al., 2014; Simms et al., 2018; Ullman et al., 2016; Whitehouse et al., 2012; Zurbuchen and Simms, 2019).

To test hypotheses about the timing and sources of ice sheet melt and the suitability of geophysical models, researchers typically select sites where RSL records require minimal amounts of correction for non-eustatic components. This is challenging, as there are no locations across the globe where eustasy is the only component of relative sea-level change, as non-eustatic contributions are not uniform over time and space. Despite this, there are some locations where modelled RSL patterns are largely insensitive to different model assumptions or parameters, and where non-eustatic signals are small (e.g. ± 1 metre or less). Such locations may help determine the timing, source, and existence of significant (>1 metre) eustatic sea-level changes over the last 4,000 years.

1.1.2 Mangrove sea-level data

Mangroves are salt-tolerant forests that are important sedimentary depositional environments in far-field regions. As mangroves generally only inhabit the upper half of the intertidal zone (Tomlinson, 2016), their sediments are potentially precise sea-level indicators. Many researchers consider mangroves to be the tropical equivalent of salt marshes, which can record decimetre-scale RSL fluctuations largely owing to the well-preserved microfossils that are employed to create transfer functions of past marsh surface elevations (Barlow et al., 2013; Gehrels, 2000; Kemp et al., 2009; Zong and Horton, 1999). However, mangroves present a number of unique challenges to sea-level researchers.

Microfossils such as foraminifera and diatoms that are traditionally used as sea-level indicators are often poorly preserved in mangrove sedimentary sequences (Berkeley et al., 2007; Khan et al., 2019b; Woodroffe et al., 2005), and radiocarbon-derived chronologies can be problematic as modern roots penetrate older sediments (Gischler, 2006; Woodroffe et al., 2015b). Further development of established and new sea-level proxies are required if mangrove sediments are to be used to precisely determine RSL changes in far-field regions.

1.2 Thesis aims

The overarching aim of this thesis is to *evaluate the utility of mangrove sediments for high resolution, quantitative relative sea-level reconstructions*. To address this aim, I have selected the case study site of the Seychelles, because it has coastal mangrove environments, and because the previous work undertaken here to quantify Mid- to Late Holocene RSL resulted in low-precision reconstructions. Seychelles is a critical location where we can test new proxy-based and chronological approaches with the aim to increase the precision of existing Mid- to Late Holocene RSL data.

My research questions and associated objectives are as follows:

1) **What materials in mangrove sediments are best suited for constructing radiocarbon age models?**

Radiocarbon dating is the most widely applied chronological method for reconstructing RSL changes from mangrove sediments, largely due to their abundance of organic carbon for radiocarbon measurements. However there are a number of challenges to obtaining reliable chronologies, the primary problem being the penetration of large and fine roots into underlying sedimentary sequences. Roots introduce younger carbon into the sediment record, which has the potential to affect our ability to measure the 'true' age of deposition at a given stratigraphic depth. Similarly, bulk sediment radiocarbon measurements may inadvertently sample fine roots and an unknown mix of carbon that may or may not reflect deposition age. Plant macrofossils or specific sediment fractions such as organic or pollen concentrates may better reflect depositional age (Woodroffe et al., 2015b), but studies which compare multiple materials collected from the same depth are required. The objectives of this work are to:

a) Characterise what plant materials (e.g. bulk, macrofossils) are available for radiocarbon measurements in Seychelles mangrove sediments;
b) Develop a method for isolating mangrove pollen for radiocarbon measurements from Seychelles mangrove sediments;
c) Systematically compare radiocarbon measurements on different materials (bulk, macrofossil, pollen concentrates) collected from the same depths in Seychelles mangrove sediments, and evaluate new radiocarbon ages in the context of previous ages produced by Woodroffe et al. (2015a).

2) Does mangrove pollen provide a reliable alternative to other microfossils for quantitative RSL reconstructions in Seychelles mangroves?

While foraminifera and diatoms are typically not well preserved in mangrove sediments, mangrove pollen has been widely used to understand past sea-level changes in mangrove environments (Ellison, 1989; Engelhart et al., 2007). Pollen is not necessarily deposited autochthonously (as foraminifera or diatoms are assumed to be), however mangrove species are often zoned according to inundation patterns and therefore their pollen, if locally dispersed, shows potential as a sea-level indicator. To assess this proxy as a sea-level indicator, a better understanding of mangrove pollen transport processes is required. How does modern mangrove pollen enter the sedimentary sequence, and does pollen faithfully reflect modern vegetation patterns? The objectives of this work are to:

a) Characterise mangrove species zonation in modern mangrove environments in Seychelles;
b) Construct pollen traps that will measure modern pollen rain above tidal inundation levels for one year;
c) Characterise the pollen composition of pollen traps and mangrove surface sediments;
d) Evaluate the suitability of mangrove pollen as a quantitative RSL indicator in Seychelles mangroves.

3) Are geochemical properties potential proxies for quantitative RSL reconstructions in Seychelles mangroves?

In the last decade, several geochemical techniques have been tested as alternative to microfossil-based RSL reconstructions (Engelhart et al., 2013; Kemp et al., 2010; Milker et al., 2015). Stable carbon isotopes, carbon/nitrogen ratios, and total organic carbon compositions have been investigated in both salt marsh and mangrove environments, but researchers have often found it difficult to distinguish different vegetation zones using bulk sediment measurements (Kemp et al., 2017; Khan et al., 2019b). Analysis of more specific organic fractions (such as lipid biomarkers) may be able to better distinguish different elevation zones in modern mangrove environments, but this approach has not yet been tested in the context of reconstructing RSL. The objectives of this work are to:

a) Characterise the total organic carbon (TOC) and total inorganic carbon (TIC) composition of modern mangrove sediments from Seychelles;
b) Characterise the lipid biomarker distributions in modern mangrove sediments from Seychelles;
c) Evaluate the utility of TOC, TIC, and lipid biomarker distributions for RSL reconstructions by testing the relationship between the observed values and measured environmental variables (elevation, grainsize, vegetation zone, and distance from shore).

Overall, these findings from modern mangroves in Seychelles will allow me to provide recommendations for future studies wishing to use mangrove sediments for high resolution (decimetre-scale) quantitative RSL reconstructions.

1.3 Study site: Seychelles

1.3.1 RSL change in Seychelles

The Seychelles is in a unique location where only minor GIA corrections to Mid- and Late Holocene RSL are required to infer a eustatic sea-level curve. The contribution of non-eustatic GIA components (ocean loading, ice loading, and ocean siphoning) to modelled RSL in Seychelles is small, and RSL in this region is modelled to be within 1 metre of eustatic sea level during the last 6,000 years (Milne and Mitrovica, 2008). These modelled results are also largely insensitive to different Earth viscosity profiles (Milne and Mitrovica, 2008; Woodroffe

et al., 2015a). The model-corrected RSL signal therefore closely approximates a eustatic sea-level signal. However, due to the range of eustatic functions used in existing GIA models, these models produce a range of Mid to Late-Holocene RSL predictions for the Seychelles (Woodroffe et al., 2015a). Comparing GIA-corrected RSL data from Seychelles to different GIA model predictions can provide an important test of the eustatic function in each model (Bradley et al., 2016, 2011; Lambeck et al., 2014; Peltier, 2004; Peltier et al., 2015). In turn, important new information can be provided on the magnitude and the temporal and spatial pattern of Mid- to Late Holocene ice sheet melt.

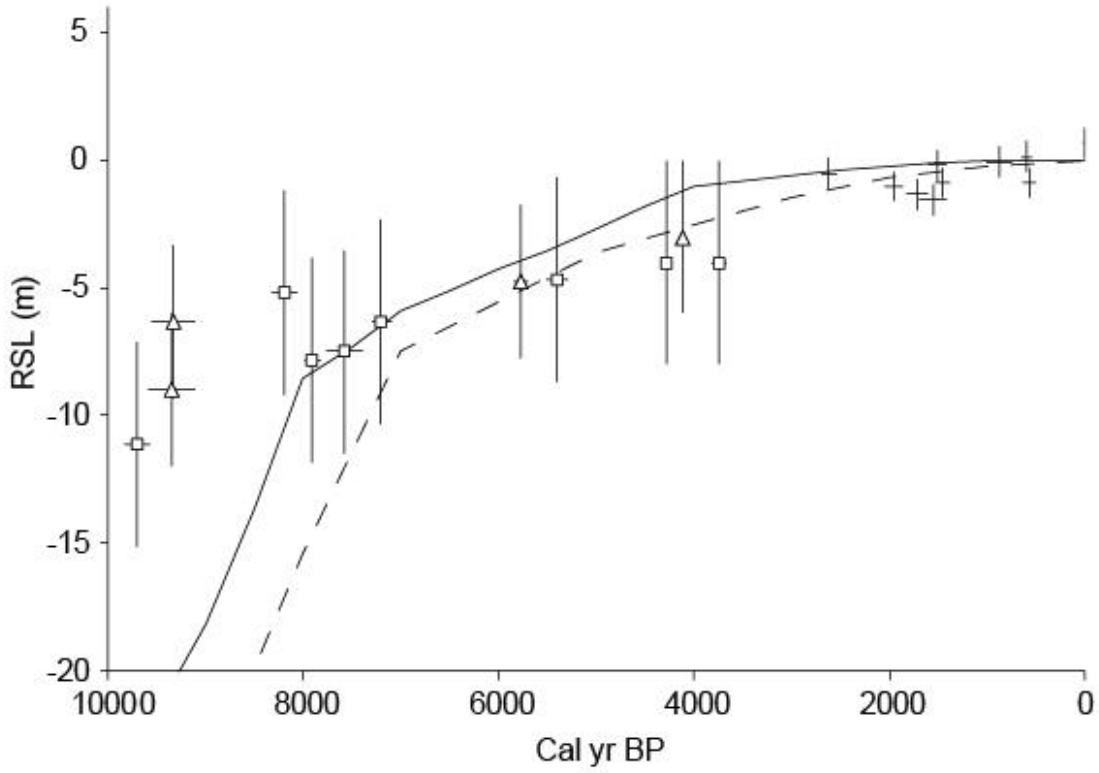

Figure 1.1: Holocene RSL data and modelled RSL from ice models ICE-5G (solid line) and EUST3 (dotted line) in Seychelles from Woodroffe et al., (2015a). Coral RSL data are the open squares and triangles (coral debris and framework coral, respectively), with vertical and age uncertainties displayed. Mangrove RSL data are the plain crosses which range the vertical and age uncertainties.

Previous studies that have investigated RSL changes in Seychelles use sea-level data derived from both coral and mangrove sediment (Braithwaite et al., 2000; Camoin et al., 2004; Woodroffe et al., 2015a). Coral and mangrove derived sea-level data collated from the island of Mahé (Figure 1.1) have metre-scale vertical uncertainties, which currently limit our ability to differentiate between different GIA models during the late Holocene (Woodroffe et al., 2015a). However, Woodroffe et al. (2015a) tentatively suggest that the RSL data from Mahé appear to be more consistent with a model where RSL continues to rise into the Late Holocene, and is therefore it is inferred that ice sheet melt continues into the Late Holocene.

Because foraminifera or diatoms were not preserved in the studied fossil mangrove sediments, the vertical uncertainty of mangrove sea-level data was ±0.6 metres (more than half the tidal range), which is an error that almost encompasses the likely sea-level changes themselves. Constructing radiocarbon age models from Seychelles mangrove sediments was also challenging, with different materials yielding significantly different and out-of-depth-sequence ages (Woodroffe et al., 2015a). To improve RSL reconstructions in the Seychelles, and in other environments with similar mangrove sedimentary sequences, new sea-level proxies and chronological approaches need to be investigated.

1.3.2 Study location

The Seychelles is a dominantly granitic archipelago located in the south-west Indian Ocean (~4-11°S) (Figure 1.2). These islands are situated on the Seychelles Bank, a shallow shelf platform generally less than 70 metres deep. Climate in Seychelles is characterised by annual wet and dry seasons, controlled by the shift in the position of the Intertropical Convergence Zone and prevailing trade-wind directions (Pfeiffer and Dullo, 2006). The region where the granitic islands are located (including Mahé, the island where my study areas are located) is very rarely impacted by cyclones (Bloemendaal et al., 2020). The Seychelles is considered tectonically stable on Quaternary timescales (Mart, 1988; Israelson and Wohlfarth, 1999; Dutton et al., 2015a), and therefore any RSL change during the Holocene is largely driven by eustatic sea-level changes and glacio- and hydro-isostatic adjustment (Dutton et al., 2015b; Woodroffe et al., 2015a; Vyverberg et al., 2018).

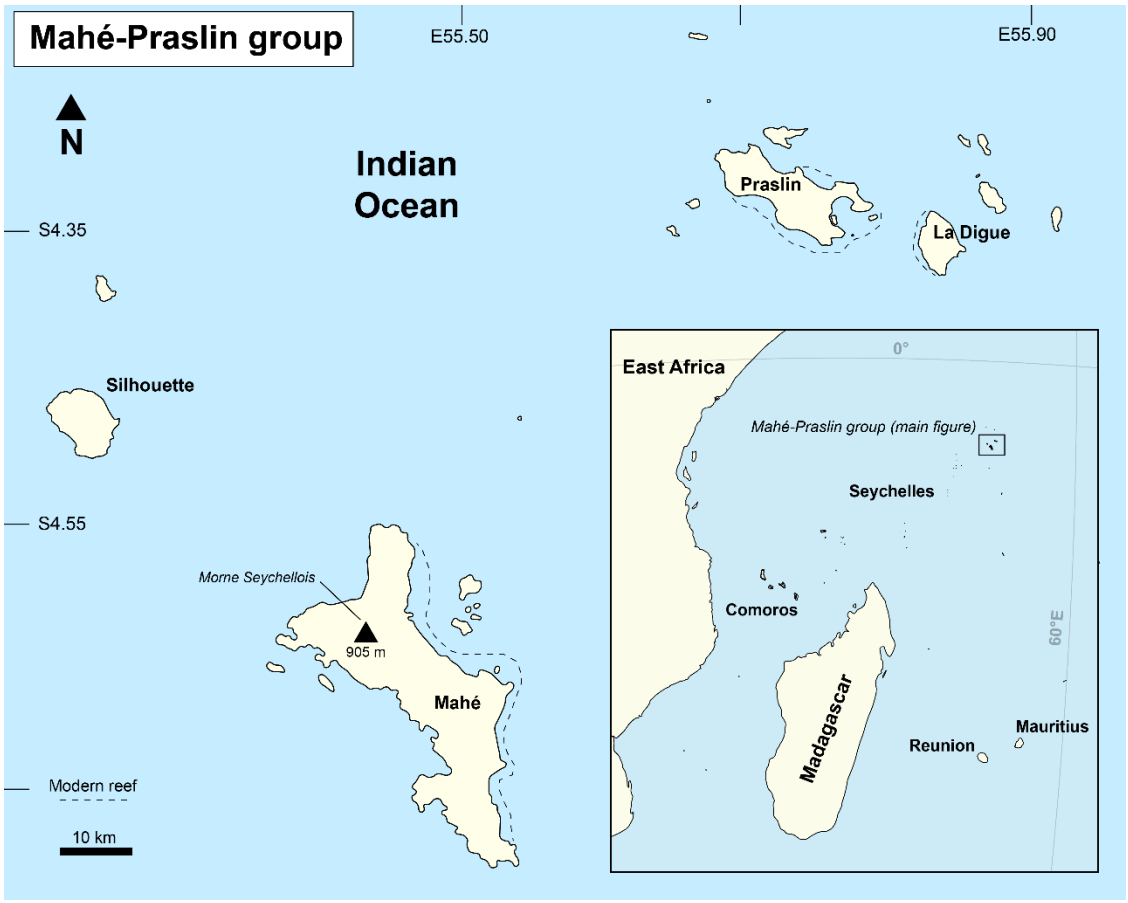

Figure 1.2: The Mahé-Praslin group (i.e. the granitic islands) is the northernmost island group in the Seychelles archipelago. The focus of this study is the largest and highest island, Mahé.

The Seychelles Bank was flooded after 9 ka BP (thousand years before 1950 CE) (Badyukov et al., 1989), and a ~26 m-thick Holocene fringing coral reef sequence developed up until ~3.7 ka BP (Braithwaite et al., 2000; Camoin et al., 2004). The reef sequence is characterised by coral debris, which are interpreted to be deposited during storms and are therefore not precise sea-level indicators. However, sea-level records across the SW Indian Ocean using coral records are broadly consistent, indicating sea levels reached present at around 3-2.5 ka BP (Camoin et al., 2004). There is limited evidence for a Holocene RSL highstand on the granitic islands of Seychelles, which has been previously attributed to hydro-isostatic subsidence of the Seychelles Bank in the mid-late Holocene (Camoin et al., 2004).

Mahé, the largest of the granitic islands, has relatively high topographic relief (up to 905 metres above sea level) and a narrow fringing reef; approximately one kilometre wide on the northeast coast and 200–300 metres wide in sheltered bays on the southwest coast (Figure 1.3). The tide gauge record at Point La Rue (Mahé, 1993 – present) has mixed semi-diurnal tides with a maximum tidal range of 2.1 metres (*Admiralty Tide Tables*, 2017). Mahé's coastline is characterised by rocky shores and sandy bays, and is backed by a narrow coastal

plain (<500 metres wide) composed of coral debris and carbonate sands of Late Holocene age (Woodroffe et al., 2015a). This coastal plain is interpreted as a beach plateau that formed when Holocene RSL rose to close to present, and the average plateau elevation is 10-15 cm above the modern storm ridge (Woodroffe et al., 2015a). After RSL stabilised in the Late Holocene, mangrove forests began to occupy areas of lower elevation behind the beach plateau and tombolos, which provided a coastal barrier and calmer hydrological conditions for mangrove establishment by 2 ka BP. Erosion of the beach plateau by rivers created further accommodation space for mangrove establishment. The vast majority of the mangrove forests behind the beach plateau have now been reclaimed as residential or agricultural land (Woodroffe et al., 2015a), and present day mangrove forests are generally restricted to the later-established riverine environments.

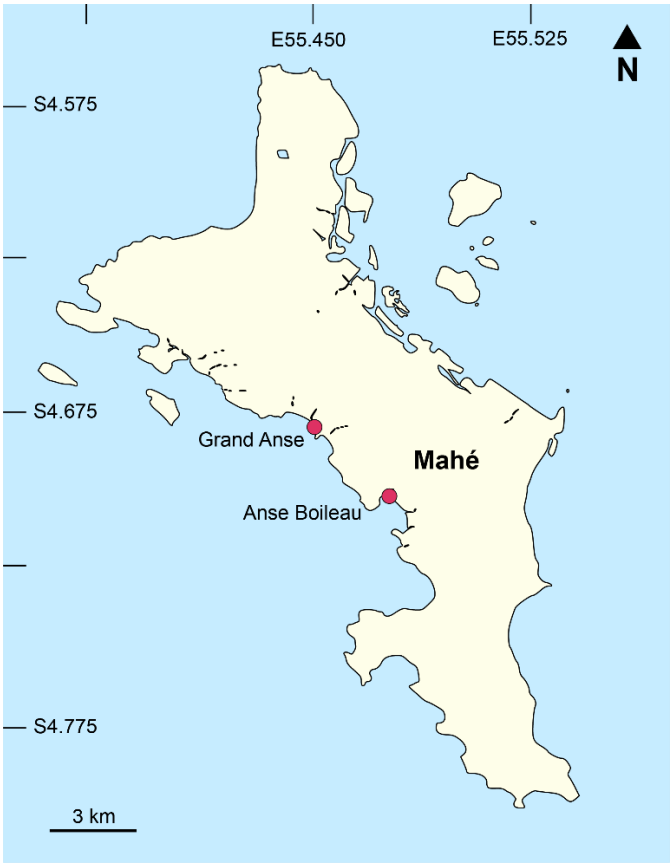

Figure 1.3: Mahé island and the location of the two mangrove areas studied here, Grand Anse and Anse Boileau.

Up to nine different mangrove species are reported from mangrove forests in the Seychelles (Spalding et al., 2010). Generally, mangrove forests on Mahé are characterised by five species: *Rhizophora mucronata*, *Sonneratia alba*, *Bruguiera gymnorrhiza*, *Avicennia marina* and *Lumnitzera racemosa*. Minor populations of *Xylocarpus granatum* and *Ceriops tagal* are present, as well as mangrove associates *Acrostichum aureum*, *Nypa fruticans* and *Pandanas*

sp. occurring near to the terrestrial forest transition. The adjacent terrestrial coastal plain is dominated by *Cocos nucifera* (coconut palm), *Terminalia catappa* (sea almond) and *Casuarina equisetifolia* (she-oak). The Mahé mangroves can be described as a mix of riverine and fringe mangroves, using the ecological classification of Lugo and Snedaker (1974), and are inundated daily by tides.

1.4 Thesis structure

This thesis has been constructed as a series of both review and research papers that are intended for publication in peer-reviewed journals. **Chapter two** provides a literature review of approaches to reconstructing past RSL using mangrove sediments, and provides a more detailed background and rationale for the following research chapters. I intend for the research chapters (three to five) to be read as stand-alone studies, but they also contain cross-references to other relevant chapters for connectivity. Because the methods that I used are generally specific to each chapter, they are included within the relevant chapter rather than as a separate methods section. Some repetition is included to keep chapters internally consistent. Each chapter contains a study location brief relevant to the chapter content, and Section 1.3 contains the overall study site introduction.

Chapter three, titled "*Comparing radiocarbon measurements of mangrove sediments from Mahé, Seychelles, for building reliable chronologies of relative sea-level change*" addresses research question. **Chapter four**, titled "*Assessing the use of mangrove pollen as a quantitative sea-level indicator on Mahé, Seychelles*", addresses research question 2. **Chapter five**, titled "*Testing the use of total organic carbon, inorganic carbon and lipid biomarker analyses as quantitative sea-level indicators from Seychelles mangrove sediments*", addresses research question 3. **Chapter six** presents a brief summary and discussion of key results presented in chapters three, four and five, and provides recommendations for future quantitative RSL reconstructions from mangrove sediments.

Chapter 2: Using mangroves to reconstruct relative sea level: problems and possibilities

2.1 Introduction

Global mean sea level is predicted to rise by the end of the 21st century, with projections varying from decimetres to more than a metre (Church et al., 2013; Horton et al., 2018). This large uncertainty owes partly to our incomplete understanding of the mechanisms and dynamics of sea-level change before the era of satellite and instrumental observations (IPCC, 2019). How do ice sheets respond to climate changes on centennial and millennial timescales, and how do resulting sea-level changes vary spatially and temporally? These questions can be addressed by reconstructing past sea-level changes from geological archives that extend geodetic records — they can provide a background signal that provides a baseline for future local and regional anthropogenic projections (Barlow et al., 2013; Gehrels and Woodworth, 2013).

In the far-field (which encompasses much of the low latitudes) ice-equivalent sea-level changes since the Last Glacial Maximum dominate other spatially-varying processes associated with Glacial-Isostatic Adjustment (GIA) (Clark et al., 1978; Fleming et al. 1998; Mitrovica et al. 2001; Peltier 2002; Milne and Mitrovica 2008; Whitehouse 2018). Mangrove forests, which consist of salt tolerant trees that inhabit a narrow ecological niche in the intertidal zone, are the dominant depositional environment capable of recording relative sea-level (RSL) changes in these regions (Tomlinson 2016, Spalding et al., 2010; Giri et al. 2011). Over millennial timescales mangrove sediments record changes in ice-equivalent sea level, GIA, tectonic movements and other processes that affect local RSL (Scholl and Stuiver 1967; Woodroffe et al. 1985; Hanebuth et al. 2000; Bird et al. 2010). They are ideal environments in which to reconstruct millennial, metre-scale RSL changes, but there are many challenges in producing higher precision (centennial, decimetre-scale) RSL records from mangroves. For example, mangrove sediment stratigraphy and chronology can be problematic due to penetration of large modern roots (Gischler 2006; Woodroffe et al. 2015b), and microfossils that are often used as sea-level indicators in intertidal sediments are variably preserved (Woodroffe et al. 2005; Berkeley et al. 2009a; Khan et al. 2019). The uncertainties that these difficulties create are undesirable particularly because they are — for many Late Holocene records (up to ~4,000 years before present) — the same or greater

magnitude than the likely RSL changes themselves (Woodroffe and Horton 2005; Barlow et al. 2013).

In this chapter, I review approaches to reconstructing Holocene RSL from mangrove sediments — outlining key challenges. I do not review the ecological processes and sedimentological response of modern mangrove environments to recent RSL rise (Blasco et al., 1996; Dahdouh-Guebas and Koedam 2008; McKee et al., 2012; Woodroffe et al. 2016; Friess et al. 2019), but rather provide a focussed perspective on mangroves as sea-level indicators using palaeoenvironmental and stratigraphic approaches. Here I define a 'mangrove sediment' (and/or peat) as any *in situ* plant or minerogenic material that has accumulated in the mangrove environment through time.

2.2 Background

2.2.1 Why do we need mangrove RSL reconstructions?

One major motivation for understanding RSL changes from geological data is to reconstruct the total amount of grounded ice present during the Last Glacial Maximum (Lambeck et al., 2014; Simms et al., 2019). In addition, of particular importance is to understand the melt histories of the large ice sheets during times of rapid climate warming in the past, and to quantify the amount of grounded ice melt occurring in the Late Holocene and the immediate pre-industrial era (~4,000 years ago to present). Key locations that allow us to achieve these goals are in the low latitudes.

Based on geophysical models, there are locations in the far-field where the GIA influences on RSL are small in comparison to the overall signal and are of opposite sign, therefore can almost cancel each other out (Figure 2.1) (Milne and Mitrovica, 2008). These coastlines are predominantly in the low latitudes where mangrove forests are the main coastal sedimentary environment. (Figure 2.2).

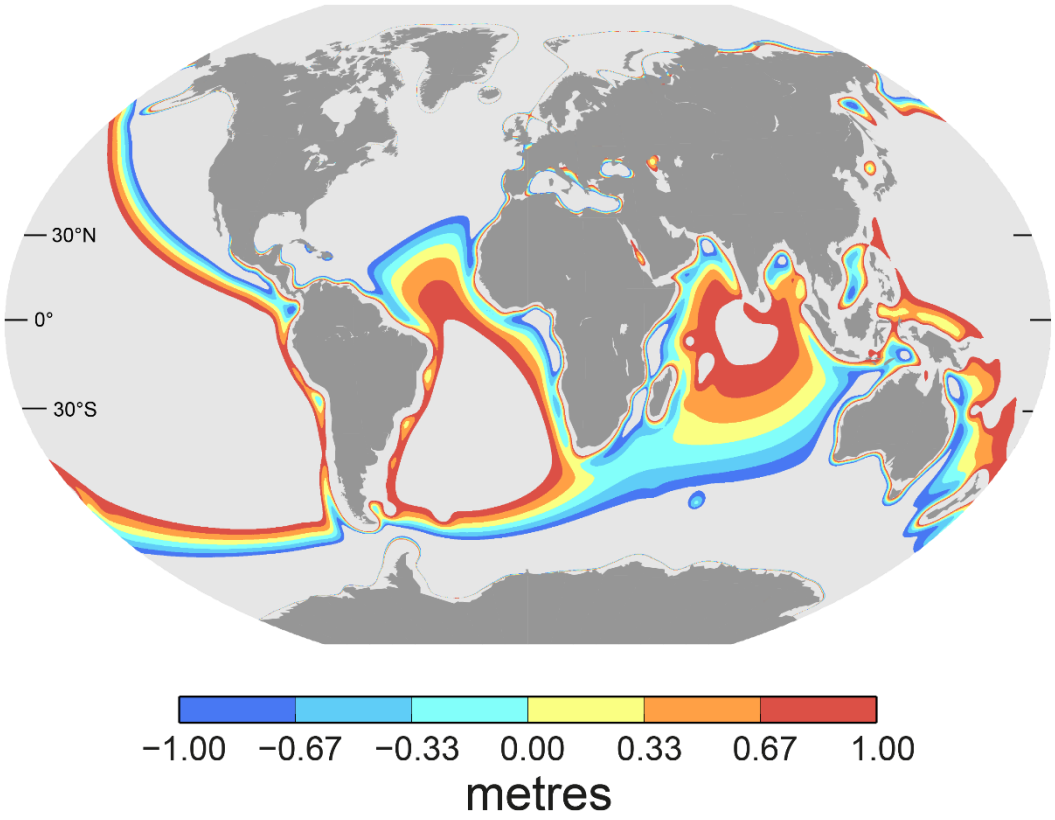

Figure 2.1: Modelled RSL changes where non-eustatic influences contribute ±1 metre from 6,000 years ago, from Milne and Mitrovica (2008). This can be seen as a 'treasure map' in terms of identifying study sites to precisely reconstruct ice-equivalent sea level changes during the mid-late Holocene.

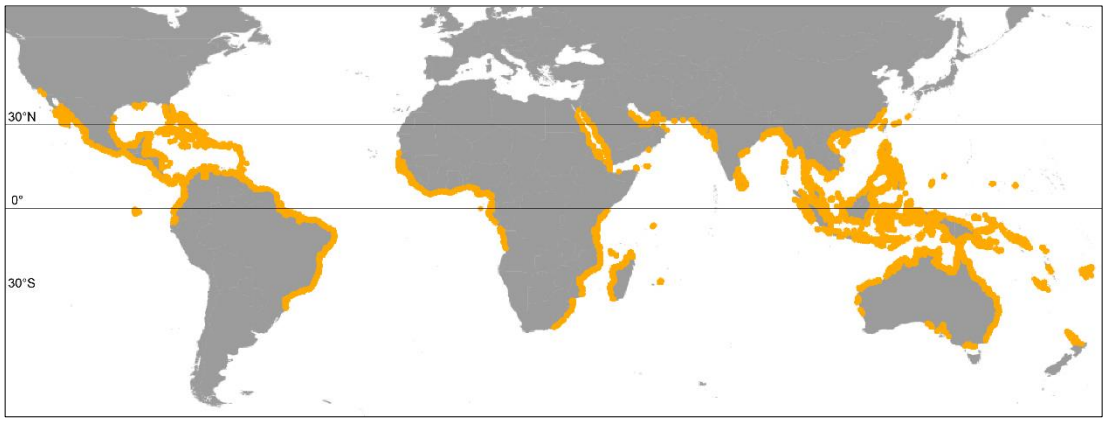

Figure 2.2: Modern global mangrove distribution (horizontally exaggerated) dataset from Giri et al. (2011).

At present, far-field RSL reconstructions are commonly derived from coral reef sequences (Bard et al., 1996; Chappell and Polach, 1991; Fairbanks, 1989; Peltier and Fairbanks, 2006), coastal geomorphic features (Chappell et al. 1982; Murray-Wallace et al. 2002; Angulo et al. 2006; Tamura et al. 2012; Stattegger et al. 2013), and sedimentary sequences such as shallow-marine sediments (Hanebuth et al., 2000) or intertidal sediments (e.g. mangrove sediments) (Larcombe et al. 1995; Punwong et al. 2013a; Woodroffe et al. 2015a).

The majority of these studies investigate RSL changes since the Last Glacial Maximum (LGM) and a few over multiple glacial cycles. There are fewer decimetre-resolution Mid- to Late-Holocene RSL studies from the far-field, which is a key time period for understanding globally where and how much grounded ice existed immediately prior to the industrial era (Woodroffe 2009; Woodroffe et al. 2012; Punwong 2013a). Coral reef records have large vertical uncertainty because coral can live in a range of water depths; 5-10 metres below Lowest Astronomical Tide is the smallest range for branching coral, and coral microatolls — which are potentially very precise — are not widely found (Lighty et al. 1982; Chappell 1983; Blanchon and Shaw 1995; Montaggioni et al. 1997; Hibbert et al. 2016). Mangroves are extremely common along these coastlines and have the potential to produce high-precision Late Holocene RSL data to address these outstanding questions, providing we can better understand these environments and their potential as sea-level indicators and limitations.

2.2.2 The outstanding problems

Despite the wealth of existing metre-scale RSL reconstructions from mangroves we are really no closer to being able to create centimetre- to decimetre-scale RSL reconstructions in these environments than we were a few decades ago (Geyh et al., 1979; Scholl, 1964a; Woodroffe et al., 1985). These sedimentary environments are difficult to interpret because of multiple factors. Complex sedimentation patterns and geomorphological interactions on a variety of scales are highly localised and are difficult to monitor on useful timescales (Furukawa et al., 1997; Cahoon and Lynch 1997; Adame et al. 2010; Krauss et al. 2014). Mangrove sediment accumulates in tropical temperatures, and in combination with oxygenation of the sediment column, this promotes rapid nutrient cycling and dissolution of microfossils (Debenay 2004; Berkeley et al. 2007). Bioturbation by mangrove roots and crabs mixes the sediment column on a decimetre to metre scale (Kristensen, 2008), which is compounded further in regions with a lack of Late Holocene sediment accommodation space and/or low sedimentation rates. In addition, there remains uncertainties around mangrove sediment compaction through time, and practical issues with safely accessing and surveying these environments.

To improve our ability to precisely reconstruct RSL (in particular Late Holocene RSL from these environments) we need better understanding of a) how surface depositional processes relate to sediment preserved in mangrove sediment archives b) which indicators produce the most reliable and precise RSL reconstructions, and c) how best to date these sediments to create credible age-depth models that we can use to precisely reconstruct RSL.

2.3 Approaches to reconstructing elevation change

2.3.1 Mangrove sediments as RSL indicators

Mangroves have inhabited tropical intertidal zones since the Paleocene approximately 55 million years ago (Plaziat et al., 2001). Mangroves sediments are ideal targets for RSL reconstruction in the far-field because they are extremely common coastal environments, and mangroves live in a narrow elevation range above mean sea level, which is generally the upper half of the local tidal range (McKee et al. 2012). They are often viewed as the low-latitude equivalent of salt marsh environments which can provide high-resolution Late Holocene RSL reconstructions (e.g. Gehrels et al. 2005; Kemp et al. 2011; Barlow et al. 2013; Long et al. 2014; Kemp et al. 2018).

Mangroves have evolved to tolerate periodic inundation with saline marine waters through salt rejection and secretion mechanisms (Tomlinson, 2016). Terrestrial plant species outcompete mangroves above the reach of the tides, but mangroves are also not adapted to sub-tidal conditions, as their roots systems require regular oxygenation. This characteristic alone makes mangrove sediments a definitive indicator of an intertidal depositional environment, making them a true sea-level indicator unlike shallow marine or terrestrial sediments that provide limiting information on the position of RSL only. Anaerobic conditions occur cyclically in mangrove sediments (dependent on tidal and groundwater variability), which can allow for preservation of sediments, macro- and microfossils that can be used for RSL reconstructions (Alongi, 2014; Ellison, 2008). The use of mangrove sediments for RSL reconstructions has generally focussed on records extending from the Mid-Holocene to recent because of the accessibility of fossil sediments in the present day intertidal and nearshore marine environment, although studies investigating sediments back to Pleistocene times and older do exist (e.g. Caratini and Fontugne 1992; Roberts et al. 2017).

The indicative meaning of mangrove sediments is often defined as ‘the upper half of the local tidal range’. Such definition has been used in recent mangrove-based RSL data compilations and databases (e.g. Khan et al. 2017; Zong, 2004), and in locations with very small tidal ranges this is a sensible approach (e.g. Pacific Ocean islands, such as Micronesia, Tonga or Fiji, Ellison, 1989; Fujimoto and Miyagi, 1993; Ellison and Strickland, 2015). A more accurate solution (although often less precise) and particularly useful at locations with larger tidal ranges is to measure the vertical elevation range of the modern mangrove zone at (or

near) the site of a RSL study to derive a local mangrove indicative meaning (e.g. examples in Table 2.1). Use of this indicative meaning assumes that tidal range has not changed through time, and that palaeo mangrove environments also occurred in the same elevation range (and relative to the same reference water levels) as present. A general issue with using this approach is that although it is often relatively easy to define the vertical range of modern mangroves in a particular location (e.g. Khan et al., 2019b), there is often no definitive way of differentiating mangrove from terrestrial organic sediments which formed in freshwater bogs immediately landward of mangrove environments within fossil cores on the basis of the physical characteristics of the sediment alone. This means it can be difficult to justify applying this indicative meaning to core sediments, without further information derived from macro- and microfossils.

Within the mangrove environment different mangrove species distribute themselves relative to the duration and frequency of tidal inundation, a variable which is strongly linked to elevation and salinity (Crase et al., 2013; Leong et al., 2018). Characterising this pattern can help to improve the precision of RSL reconstructions beyond just the presence of mangrove sediment, but understanding this zonation is not straightforward. Vertical zonation with respect to sea level emerging in any local mangrove environment is a result of complex interactions between mangrove ecology, succession and environmental gradients of tidal-inundation, geomorphology, groundwater, substrate, sedimentation rates and local climate (Woodroffe 1992; Woodroffe et al. 2016). In Queensland Australia, *Avicennia* sp. and *Sonneratia* sp. dominate the most seaward section of mangrove forests, followed by a *Rhizophora* sp. zone landwards (Chappell and Grindrod, 1984). In Fiji, *Rhizophora* sp. dominates the seaward fringe of the mangrove, followed by a landward *Bruguiera* sp. zone (Ellison and Strickland, 2015). In the Caribbean region, mangroves across the upper intertidal zone can be entirely *Rhizophora* sp. (McKee et al. 2007). This means that a local or regional understanding of mangrove zonation is required to inform understanding of fossil environments (Plaziat, 1995).

Mangrove fruit, propagules, flowers, leaves, roots and wood can help to determine whether an organic-rich sediment is from a mangrove environment or not (Plaziat, 1995). Invertebrates such as molluscs are also used to infer that a deposit is mangrove sediment (Perry et al. 2008). However, a challenge to using macrofossils to determine if sediments are from a mangrove environment is their poor preservation potential. Crabs — which dominate mangrove environments across the globe — also consume a large amount of mangrove leaf litter before it can be deposited and preserved in a sedimentary sequence

(Middleton and McKee 2001; Skov and Hartnoll 2002; Gillis et al. 2019). Additionally, in locations with low sedimentation rates, macrofossils decompose at the surface more quickly than they can be incorporated into sediments. Macrofossils are most often found in locations where sedimentation rates are high, for example in the Caribbean region where Holocene RSL rise has been continuous and has created accommodation space (McKee et al. 2007; Wooller et al. 2007; Monacci et al. 2009). The difficulty using macrofossils as opposed to general stratigraphy to indicate a particular zone within a mangrove is assigning a macrofossil with an indicative meaning beyond just being indicative of a mangrove deposit. Because of the potential for post-depositional processes and movement of macrofossils by tides, this is problematic and therefore macrofossils are most commonly used simply to confirm that a fossil sediment was formed under a mangrove.

While there is considerable scope to continue developing sedimentological approaches to reconstruct RSL in mangrove environments (in particular to quantify relationships between physical properties and elevation in the intertidal zone), macro- and micro-fossils are widely seen as potentially the best sea-level indicators in mangroves because they perform well in mid- and high-latitude salt marsh settings and therefore 'should' be applicable to low-latitude low-energy coastal environments as well.

Table 2.1: Table summarising studies using mangrove sediments for quantitative RSL reconstructions. A 'lithology' sea-level indicator refers to studies that use the presence of mangrove sediment (and the indicative range of mangroves at that locality). Others (pollen, diatoms, foraminifera, geochemistry) refine the 'lithology' sea-level indicator further either by using indicative assemblages or using transfer function approaches. MSL (mean sea level), MTL (mean tide level), MHWS (mean high water springs), MHWN (mean high water neaps), MHW (mean high water), MHHW (mean higher high water), HAT (highest astronomical tide), MHLW (mean lower low water), MLWS (mean low water springs).

Study	Locality	Sea-level indicators	Depositional environment	Indicative meaning
Belperio, 1979	Australia	Lithology	Mangrove	-0.076 – 1.424 m local height datum
Bird et al. 2007, Bird et al. 2010	Singapore	Lithology, bulk sediment and foraminifera stable $\delta^{13}C$	Mangrove	MSL, uncertainty half the elevation range between MSL - MHWS (0.63 m)
Boski et al. 2015	Brazil	Lithology, foraminifera	Mangrove	Upper half of tidal range (1.4 metre range)
Cohen et al. 2005	Brazil	Lithology	Mangrove	1 – 2.4 m MSL
Culver et al. 2015, Culver et al. 2013	Malaysia	Foraminifera	Mangrove, middle or high swamp determined by foraminifera assemblages	±0.18 m of transfer function reconstructed palaeo elevation
Ellison, 1989	Tonga	Pollen	Mangrove	0.4 – 0.8 m MSL, ± 0.3 m
			Rhizophora sp. dominated mangrove	0.4 – 0.7 m MSL, ± 0.3 m

Study	Locality	Sea-level indicators	Depositional environment	Indicative meaning
Ellison, 1993	Bermuda	Lithology	Mangrove	MSL – MHW
Ellison, 2005	Indonesia	Pollen	*Rhizophora* sp. dominated mangrove	0.15 – 1.1 m MSL
			Bruguiera sp. dominated mangrove	1.1 – 1.6 m MSL, ± 0.1 m
Ellison and Strickland, 2015	Fiji	Pollen	*Rhizophora* sp. dominated mangrove	-0.34 – 0.66 m MSL, ± 0.1 m
			Bruguiera sp. dominated mangrove	0.23 – 0.83 m MSL. ± 0.1 m
Engelhart et al. 2007	Indonesia	Pollen	Seaward mangrove	0.88 – 2.18 m local height datum
			Middle mangrove	1.86 – 2.13 m local height datum
			Rear mangrove	1.92 – 2.01 m local height datum
Fontes et al. 2017	Brazil	Lithology, pollen	Mangrove	Upper half of tidal range (1 metre range)
Fujimoto and Miyagi, 1993	Micronesia	Lithology	Mangrove	Local tidal range

Study	Locality	Sea-level indicators	Depositional environment	Indicative meaning
Fujimoto and Ohnuki, 1995	Okinawa, Japan	Lithology	Mangrove	MTL – MHWS
Geyh, 1979	South East Asia	Lithology	Mangrove	MHWN – MHWS
Grindrod 1985	Australia	Lithology	Mangrove	approximately MHWS
Grindrod and Rhodes, 1984	Australia	Lithology, pollen	Mangrove	MSL – MHW
			Rhizophora sp. dominated mangrove	1.5 – 3.0 m local height datum
			Non-*Rhizophora* sp. dominated mangrove	3.0 – 3.5 m local height datum
Hanebuth et al. 2000	South China Sea	Lithology	Mangrove	MSL – MHHW
Horton et al. 2005	Malay-Thai peninsula	Lithology	Mangrove, proximal to marine environment	HAT – MHHW

Study	Locality	Sea-level indicators	Depositional environment	Indicative meaning
			Mangrove, proximal to freshwater environment	MHHW – MHLW
Islam and Tooley, 1999	Bangladesh	Lithology	Mangrove	Upper half of tidal range (1.5 metre range)
Khan et al. 2019	Puerto Rico	Stable $\delta^{13}C$, C:N, TOC, Foraminifera to Theocambian ratio	Mangrove	MLW – HAT
			Brackish transition	> MHW
			Freshwater swamp	> HAT
			Avicennia basin	MHW – HAT
			Mixed-species riverine mangrove	MLW – MHW
Parkinson, 1989	USA	Lithology	Mangrove	Local tidal range
Punwong et al. 2018, Punwong et al. 2013a, 2013b	Tanzania	Lithology, pollen	Mangrove (Rufiji Delta)	2.57 m MTL, ± 0.9 m
			Mangrove (Makoba Bay, Zanzibar)	-0.08 m MTL, ± 1.55 m

Study	Locality	Sea-level indicators	Depositional environment	Indicative meaning
			Mangrove (Unguja Ukuu, Zanzibar)	0.92 m MTL, ± 0.95 m
			Lower intertidal mangrove	-0.08 m MTL, ± 0.23 m
			Middle intertidal mangrove	-0.08 m MTL, ± 0.86 m
			Higher intertidal mangrove	-0.08 m MTL, ± 0.47 m
Scholl and Stuiver 1967, Scholl 1964a, 1964b	USA	Lithology	Mangrove	Local tidal range
Stattegger et al. 2013, Tamura et al. 2009	Cambodia	Lithology	Intertidal (includes mangrove)	Local tidal range
Tam et al. 2018	Peninsula Malaysia	Diatoms, pollen	Upper mangrove	HAT – MHHW, ± 0.1 m
			Middle mangrove	MHHW – MHW
			Lower mangrove	MTL – MHW, ± 0.1 m
Wang and Chappell, 2001	Australia	Lithology	Mangrove	HAT – MLWS

Study	Locality	Sea-level indicators	Depositional environment	Indicative meaning
Woodroffe et al. 2015	Seychelles	Lithology	Mangrove	0.2 m MTL, ± 0.6 m
Woodroffe, 1981	Cayman Islands	Lithology	Mangrove	0.15 – 0.3 m MSL

2.3.2 Microfossils

Mangrove pollen is widely used to differentiate mangrove from other terrestrial organic-rich sediments, although it is relatively rare to use information gained on vertical zonation to improve the precision of RSL reconstructions (Ellison 2005; Engelhart et al. 2007; Punwong et al. 2018). Some studies have used other microfossils such as foraminifera and diatoms to create transfer functions to create quantitative RSL reconstructions (Ellison 1989; Zong and Hassan 2004; Barbosa et al. 2005; Woodroffe et al. 2005; Horton et al. 2007; Engelhart et al. 2007; Culver et al. 2013; Culver et al. 2015; Tam et al. 2018), however other microfossils such as testate amoebae and ostracodae have been little studied in mangrove settings (Escobar et al., 2008; Hussain et al., 2007).

2.3.2.1 Foraminifera

Foraminifera are single-celled zooplankton which live in a wide spectrum of marine and brackish environments. In the intertidal zone, different individuals and assemblages of species inhabit different elevation ranges, based primarily on their salinity tolerance (Gehrels, 2000; Horton, 1999). Foraminifera assemblages therefore make excellent sea-level indicators in mid- to high-latitude intertidal environments (Edwards and Wright, 2015; Gehrels et al., 2001; Hayward et al., 1999; Palmer and Abbott, 1986).

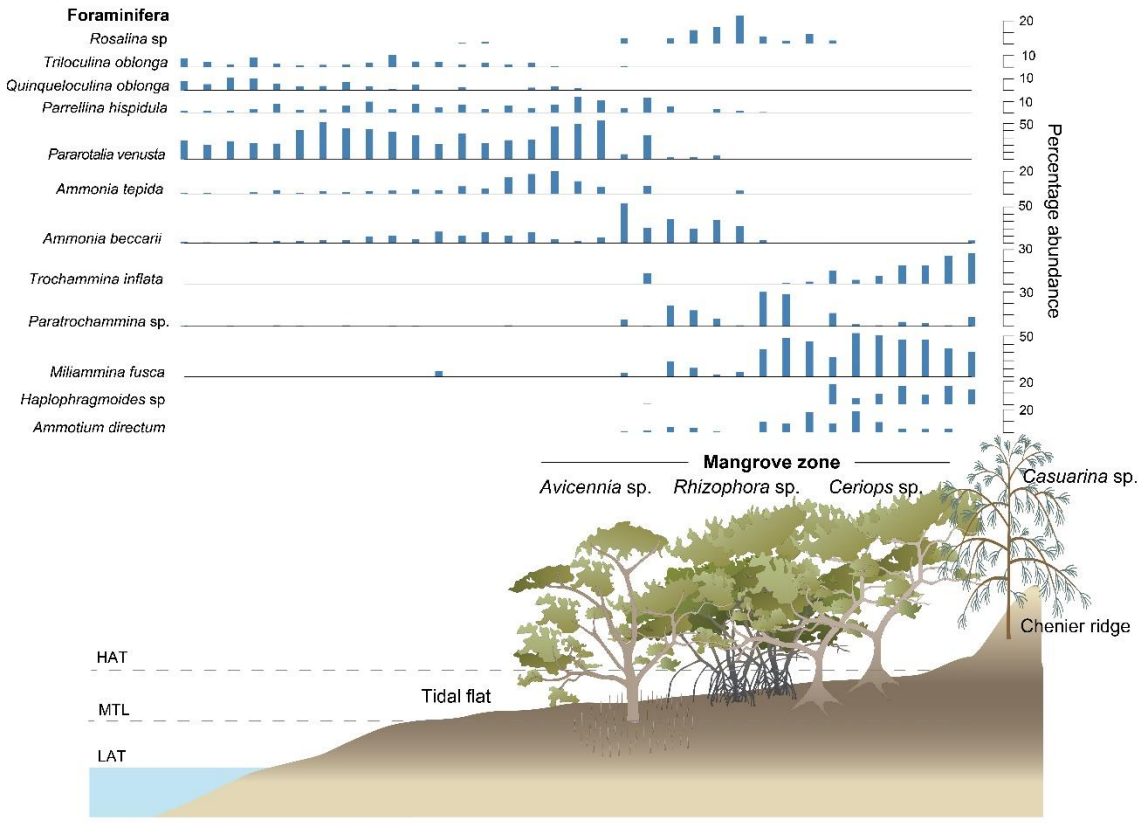

Figure 2.3: A schematic diagram of selected foraminifera and mangrove species zonation in an Australian mangrove environment, based on data from (Woodroffe et al., 2005). This cross-section is approximately ~600 m in length, and the local tidal range (HAT-LAT) is approximately 2.5 metres. Mangrove symbols are courtesy of the Integration and Application Network (ian.umces.edu/symbols/), University of Maryland Centre for Environmental Science.

Foraminifera are observed in surface mangrove sediments worldwide and their distribution is controlled primarily by elevation in the intertidal zone, which controls the duration and frequency of subaerial exposure (Culver 1990; Wang and Chappell 2001; Debenay et al. 2002; Horton et al. 2005; Woodroffe et al. 2005, 2007, 2009; Perry et al. 2008; Berkeley et al., 2007, Berkeley et al. 2009a; Dey et al. 2012). Foraminifera are used in a qualitative way but are also used to create quantitative RSL reconstructions in mangroves (Berdin et al., 2003; Boski et al., 2015; Culver et al., 2015; González et al., 2010; Hayward et al., 2004; Horton et al., 2007a; Khan et al., 2019b; Sen and Bhadury, 2017). Generally, calcareous foraminifera such as *Ammonia* sp. dominate the mostly-unvegetated tidal mud flats at the seaward fringe of mangrove zones (Debenay, Guiral, and Parra 2002; Woodroffe et al. 2005; Berkeley et al. 2009a). At higher elevations under the mangrove canopy, agglutinated foraminifera such as *Trochammina inflata* and *Miliammina fusca* dominate (Figure 2.3). Transfer function models that use modern training sets from upper intertidal environments yield vertical reconstruction uncertainties of between ± 0.07 m and ~±0.4 m (Horton et al., 2003, Woodroffe et al., 2005) and where subtidal foraminifera are included ~±4 m (Horton

et al., 2007a). Although modern foraminifera inhabit fairly tight elevation zones in the upper intertidal zone, they are variably preserved in the fossil record so this high level of transfer function model precision is often irrelevant when trying to reconstruct RSL (Woodroffe 2009). While elevation is considered the dominant control on mangrove foraminifera distribution, a range of other environmental factors can be important, such as the presence or absence of canopy vegetation in the mangrove which creates large temperature fluctuations over short distances that cause stress to foraminifera and complicate their vertical zonation (Debenay et al. 2000; Woodroffe et al. 2005).

As stated above, the long-term preservation potential of foraminifera in mangrove sediments is highly variable. Foraminifera (and in particular calcareous species) do not preserve well in acidic mangrove sediments, which are also well-oxygenated in the upper part of the sediment column, and have high ambient temperatures (Berkeley et al. 2007). Calcareous foraminifera tests are commonly dissolved and agglutinated foraminifera tests are often disaggregated in the sediment column within active mangrove rooting zones, which can be metres deep within the sediment column (Debenay et al., 2004; Hayward et al. 2004; Woodroffe et al. 2005; Berkeley et al. 2007; Perry et al., 2008; Berkeley et al. 2009a).

Other issues that appear to be unique to low-latitude intertidal environments include; a) relatively high numbers of infaunal (sediment-dwelling) foraminiferal species that can live up to 80 cm depth in oxygenated mangrove sediments (Culver et al., 2013), b) agglutinated foraminifera production rates under mangrove canopies are relatively low compared to in other environments (Debenay et al. 2004; Berkeley et al. 2007), c) foraminifera in more open mangrove canopies (or back-mangrove environments higher in the intertidal zone) are more prone to stress from higher temperatures and salinities (Debenay et al., 2002; Woodroffe et al. 2005), and d) low pH conditions caused by bacterial decomposition of leaf litter that can cause dissolution of calcareous species (Woodroffe et al. 2005). Any sites with notably different surface assemblages to fossil assemblages (i.e. sites with poor modern-analogues) need to assess the influence of post-depositional processes, sediment mixing and infaunal species production (Berkeley et al., 2009b).

2.3.2.2 Diatoms

Diatoms, which are a form of siliceous phytoplankton, are also observed in modern mangrove settings, but their ecology is less-studied than that of foraminifera (Zong and Horton 1999; Zong and Hassan 2004; Horton et al., 2007b). Only a few studies use diatom data to qualitatively or quantitatively reconstruct past RSL changes in mangrove settings

(Tamura et al. 2009; Rashid et al. 2013; Tam et al. 2018). For example, a tidal level transfer function using diatoms in Indonesian mangroves developed by Horton et al. (2007b) has a vertical error estimate of ±0.15 metres, but this was not tested on any fossil sequences. Diatoms can undergo dissolution in higher temperature conditions (Barker et al., 1994), which may lead to poor preservation in sedimentary sequences. Woodroffe et al. (2015a) note in their Seychelles study that while diatoms were present at the mangrove sediment surface, they were absent down-core (Figure 2.4). Where preserved, however, diatoms have the potential to produce high-resolution RSL reconstructions similar to those from mid- to high-latitude salt marshes (Long et al. 2012; Barlow et al. 2014).

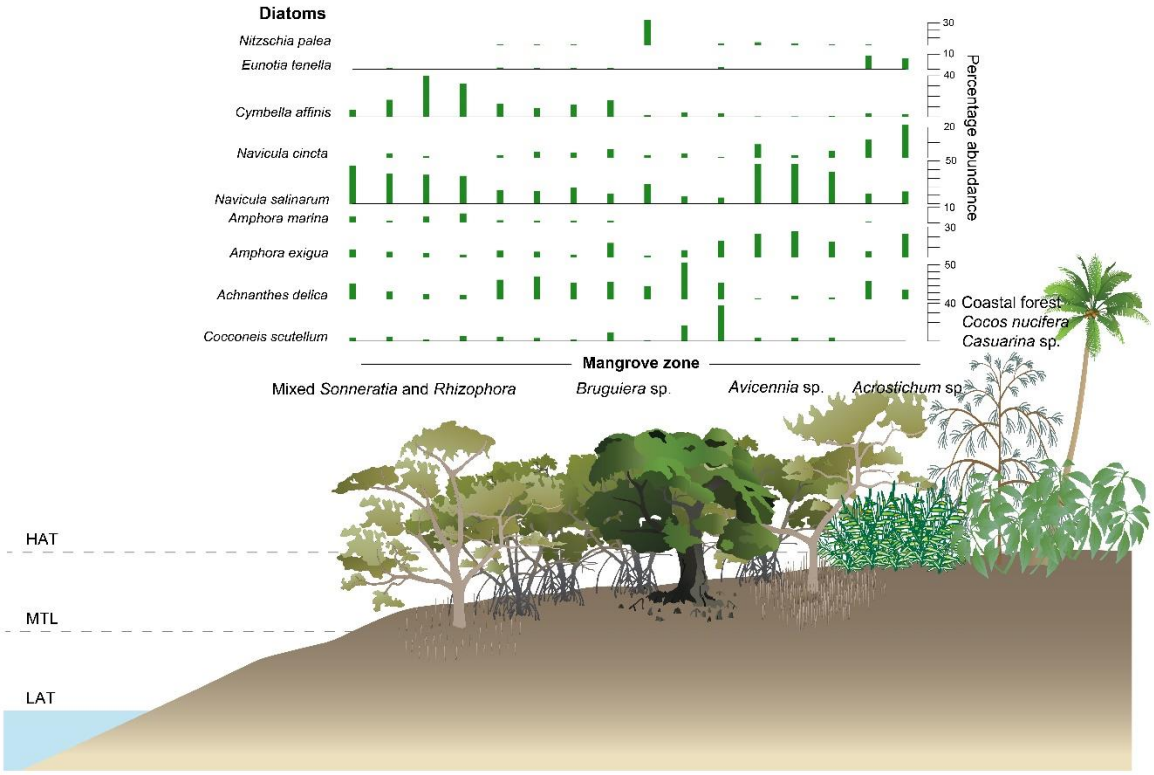

Figure 2.4: A schematic diagram of selected diatom and mangrove species zonation in a Seychelles mangrove environment (Woodroffe, unpublished). Mangrove symbols are courtesy of the Integration and Application Network (ian.umces.edu/symbols/), University of Maryland Centre for Environmental Science.

2.3.2.3 Pollen

Pollen shed from terrestrial plants during the reproduction process is widely distributed in terrestrial and marine environments and has been used extensively across the globe to reconstruct local and regional palaeoenvironments (Bernhardt and Willard, 2015). Pollen deposited in sedimentary archives can be indicative of local vegetation patterns, but also of regional vegetation, where wind and water mediums transport pollen. The use of pollen in

RSL studies is most commonly applied in combination with other proxy data, but pollen has also been used for quantitative reconstructions using transfer functions and other pollen ratio methods (Engelhart et al. 2007; Gehrels 2013; Punwong et al. 2018).

Mangrove pollen is most commonly used to reconstruct past mangrove vegetation dynamics, but also often to reconstruct RSL (Woodroffe et al. 1985; Ellison 1989; McKee and Faulkner 2000; Ellison 2005; Monacci et al. 2009; Punwong et al. 2013a; Urrego et al. 2013). Pollen is particularly well-preserved in mangrove sediments, as pollen grains are relatively resistant to decay in acidic and high temperature conditions, unlike foraminifera and diatoms (Grindrod, 1988). Zonation of pollen in surface sediments across modern mangrove environments broadly reflects the zonation of living mangrove plants, because mangrove pollen dispersal is highly localised (Ellison 1989; Grindrod et al. 1999; Behling et al. 2001; Ellison 2005; Mao et al. 2006; Engelhart et al. 2007; Cohen et al. 2008). Many mangrove species disperse pollen via insect and bird vectors (e.g. *Avicennia* sp.) and therefore have relatively low production rates, with the exception of *Rhizophora* species which generally use wind as a vector (Grindrod, 1985). Low production rates can mean that a regional terrestrial pollen signal dominates mangrove sediment concentrations, but concurrently the presence of mangrove pollen can indicate very close proximity, or definitively, mangrove depositional environments.

Broadly, the increase or decrease in the quantity of mangrove pollen preserved in shallow marine sediments can be used to reconstruct the proximity of the mangrove fringe to the core site, and therefore allow reconstruction of large-scale RSL changes over the Holocene (Bartlett and Barghoorn, 1973; Hendy et al., 2016; Van Campo and Bengo, 2004; Versteegh et al., 2004). Bartlett and Barghoorn (1973) also used pollen to infer RSL transgression over the Holocene in Panamá from relative increases and decreases in mangrove pollen in marine sediments. Woodroffe et al. (1985) used mangrove pollen distributions in modern mangrove environments of northern Australia as analogues to interpret environmental change in fossil cores collected in the intertidal zone, and found evidence of a regional expansion in mangrove area, dubbed the 'big swamp phase', which they interpret as occurring when RSL slowed and stabilised during the mid-Holocene. Ellison (1989) used pollen to confirm the presence of mangrove sediments to reconstruct RSL in Tonga. Engelhart et al. (2007) took a quantitative approach by creating a pollen-based transfer function from Indonesian mangroves resulting in a transfer function with a vertical uncertainty of ±0.22 metres, where the local tidal range is 1.5 metres.

Despite detailed modern observations, there is little information on the role of mangrove pollen redistribution via river and tidal currents, and the influence of the difference in pollen production and dispersal between mangrove species on creating pollen-based modern training sets (Chappell and Grindrod, 1984; Grindrod, 1988; Tomlinson, 2016; Urrego et al., 2010). One solution would be to monitor modern pollen rain in mangroves to evaluate any differences between local mangrove pollen production and the pollen in mangrove surface sediments. However this is a challenging objective because of periodic tidal inundation and high annual rainfall (Grindrod 1985; Behling et al. 2001; Jantz et al. 2013). We need a better understanding of why pollen preserved in surface mangrove sediments does or does not reflect modern vegetation patterns to increase the applicability and precision of pollen as quantitative sea-level indicators. An important point to note is that quantitative RSL reconstructions using fossil pollen require zonation of at least two mangrove species. Monospecific mangrove locations will not yield more precise sea-level data using pollen than by using the presence of mangrove sediments alone to reconstruct RSL, beyond using pollen to confirm that an organic sediment accumulated under a mangrove.

2.3.3 Geochemical approaches

As mangroves inhabit the intertidal zone, accumulating sediments can derive from both terrestrial and marine sources, which have different geochemical compositions. Analysing sediment geochemical composition has the potential to yield information about past increasing or decreasing marine vs. terrestrial influence, and thus qualitative and potentially quantitative reconstruction of RSL changes. Loss on ignition (LOI) measurements to determine organic and inorganic carbon content are widely applied to mangrove sedimentary sequences. LOI is often used to characterise the sediments as organic-rich, but is not usually able to distinguish mangrove from other terrestrial organic-rich sediments. LOI measurements are better used to identify terrestrial organic inputs in otherwise marine sediment sequences (e.g. Plater et al. 2015). Total sulphur and organic sulphur concentrations have also been used as a proxy for marine inundation, as sulphate ion concentrations are an order of magnitude higher in seawater than in freshwater and rainwater (Phillips et al. 1994). More recently, major and minor elemental analysis has shown some association with different terrestrial influences (e.g. Ca/Ti ratios) and elevation within a mangrove zone (Bourgeois et al., 2019; Yao and Liu, 2017). Rock-Eval pyrolysis has also shown promise for distinguishing terrestrial versus marine sediments, and for assessing the level of organic matter degradation post-deposition (Kemp et al. 2019).

2.3.3.1 Stable isotopes and total organic carbon

Total organic carbon (TOC), stable isotopes of sulphur ($\delta^{34}S$ ‰), carbon ($\delta^{13}C$ ‰), oxygen ($\delta^{18}O$ ‰), nitrogen ($\delta^{15}N$ ‰), and carbon and nitrogen isotope ratios (C:N) of bulk sediments have been used to qualitatively reconstruct vegetation changes and RSL in intertidal environments (Chmura et al. 1987; Chmura and Aharon 1995; Wilson et al. 2005; Lamb et al. 2006; Mackie et al. 2007; Bird et al. 2010; Kemp et al. 2010; Engelhart et al. 2013; Milker et al. 2015; Khan et al. 2015; Leng and Lewis 2017; Kemp et al. 2019). Organisms inhabiting different environments fractionate stable isotopes into their living tissues differently, which is a result of both biological and environmental processes. For example, terrestrial and aquatic plants fractionate carbon isotopes differently because of their varying photosynthetic pathways (Emery et al. 1967; Haines 1976; Chmura and Aharon 1995; Lamb et al. 2006; Khan et al. 2015). Similarly, environmental changes such as salinity and temperature can change the composition of the waters plants uptake, changing their stable isotopic composition.

Stable isotopic compositions of different plants and animals in a wide range of environments in tropical and temperate locations have been characterised for reconstructing palaeoenvironments (Haines 1976; Lamb, Wilson, and Leng 2006), and more specifically, environmental change in mangrove environments (Smallwood et al. 2003; Wooller et al. 2003a; Wooller et al. 2003b; Bouillon et al. 2008; Vane et al. 2013; Kemp et al. 2019). The motivation for using geochemical approaches to reconstruct RSL has largely risen from situations where microfossil preservation is poor and therefore researchers are looking for other proxy indicators that have a quantifiable vertical zonation in the intertidal zone (Engelhart et al., 2013; Khan et al., 2015; Khan et al., 2019). Despite this need, most applications of stable isotopes for RSL reconstructions are qualitative in nature, or are coarse palaeoenvironmental reconstructions to aid other sedimentological or microfossil proxies (Törnqvist et al. 2004; Bird et al. 2007, 2010; Hawkes et al. 2011; Engelhart et al. 2013; Khan et al. 2015). Some studies also report difficulties in differentiating between mangrove and freshwater environments which is the same issue as using the physical properties of the sediment alone (Kemp et al., 2019; Khan et al., 2019b).

Applications of $\delta^{13}C$ ‰, $\delta^{15}N$ ‰ and C:N environmental proxies in mangrove settings is still in its infancy. Multiple studies in Belize mangroves have explored the use of $\delta^{13}C$ ‰ and $\delta^{15}N$ ‰ as proxies for past nutrient limitation in mangrove ecosystems (Smallwood et al. 2003; McKee et al. 2002; Wooller et al. 2003a). Wooller et al. (2003a) investigated the use of $\delta^{13}C$

‰ and $\delta^{15}N$ ‰ from mangrove leaves as a proxy for past mangrove eco-physiology, as modern dwarf and tall *Rhizophora mangle* have distinctive isotopic compositions. Whether a mangrove environment is dominated by dwarfed or tall species can indicate environmental and/or ecological stress conditions, such as those caused by RSL rise or fall (McKee and Faulkner 2000; McKee et al. 2002; Wooller et al. 2003a). Wooller et al. (2007) and Monacci et al. (2009) used this approach to assess, qualitatively, past RSL changes in Belize. Nutrient availability in these mangroves is at least partly controlled by seawater inundation, and is thus considered to be a significant control on mangrove isotopic composition (Monacci et al., 2009; Wooller et al., 2007).

Following promising applications to temperate salt marsh sediments (Kemp et al. 2010; Engelhart et al. 2013), Khan et al. (2019) tested TOC, $\delta^{13}C$ ‰ and C:N bulk sediment compositions in a mangrove environment in Puerto Rico, alongside foraminifera and theocambian-derived RSL reconstructions. While the foraminifera data did not display a relationship with elevation (making it unsuitable for a RSL reconstruction), a combination of both the geochemical compositions and a foraminifera/theocambian ratio were able to reconstruct palaeo mangrove elevations, which inform palaeoenvironmental interpretations. Sen and Bhadury (2017) used a similar approach to reconstruct Holocene RSL in the Sundarbans mangroves in India and Bangladesh. They found a relationship in modern mangrove sediments between $\delta^{13}C$ ‰ composition and elevation above mean sea level, but not for TOC or C:N. The sampling strategies vary significantly between these two studies, but their comparison highlights the likely large influence of local factors on TOC, $\delta^{13}C$ ‰ and C:N, and the importance of applying multiple proxies (Khan et al., 2019b).

A number of experimental and modern studies have shown that $\delta^{18}O$ ‰ composition of mangrove plant material is the same as the $\delta^{18}O$ ‰ composition of the source water (e.g. Ish-Shalom-Gordon et al. 1992; Verheyden et al. 2004). Wooller et al. (2007) used $\delta^{18}O$‰ composition of mangrove plant macrofossils as a tracer for water sources from a Holocene mangrove peat sequence in Belize. Here in the tropics, rainfall (freshwater) generally tends to have more negative $\delta^{18}O$ ‰ values than ocean water. Therefore, variations in mangrove $\delta^{18}O$ ‰ through the sediment column may provide information on relative marine or terrestrial influences over time. However because of the variation in $\delta^{18}O$ ‰ composition of source waters between seasons, $\delta^{18}O$ ‰ composition of mangrove plant material can only be used as a qualitative sea-level proxy, and in combination with other environmental proxies (Wooller et al., 2007).

Sulphur and nitrogen stable isotopes have been little studied for past RSL and palaeoenvironmental reconstructions in Holocene sediment sequences. $\delta^{34}S$ ‰ and $\delta^{15}N$ ‰ compositions in mangroves have been characterised almost solely for application to nutrient and food-web studies, and both show large variability over very short distances (Fry and Ewel 2003; Bouillon et al. 2008). Estuarine plants generally have relatively lower $\delta^{34}S$ ‰ values, but the reasons for this trend are not well-known due to the poor understanding of fractionation processes at the root–interstitial water–sediment interface (Fry et al., 1982). Like nitrogen, sulphur fractionation also occurs in the sediment column post-deposition due to bacterial decomposition, which can also vary in response to aerobic or anaerobic conditions (Bouillon et al. 2008).

We need a better understanding of isotopic fractionation processes in mangrove environments, as well as further study on post-depositional influences (such as microbial decomposition) on sediment compositions to enable stable isotopes to be used as reliable sea-level indicators. Studies in saltmarshes note significant alteration of carbon isotopic compositions via lignin degradation (Khan et al., 2015). C:N ratios in sediments from a salt marsh in North Carolina (USA) were similar across the elevation gradient, despite the fact that the modern plants present at different elevations had large differences in C:N values (Kemp et al. 2010). Isotopic analyses still need to be supplemented with palynological analyses to confirm isotopic changes are environmental and not a result of species succession, or diagenetic changes (Wooller et al., 2007; Xia et al., 2015). Mangroves are exclusively C3 plants which means their compositional range in $\delta^{13}C$ ‰ and C:N space is limited and similar to other terrestrial freshwater plants (e.g. Khan et al. 2015). Even in saltmarshes where C3 and C4 plant species are identified living at different elevations, bulk $\delta^{13}C$ ‰ and C:N can show dominantly C3 inputs (Kemp et al., 2017). Mangrove species zonation is therefore unlikely to be registered in sediments using $\delta^{13}C$ ‰ and C:N without allochthonous inputs from proximal C4 plants, aquatic plants or bacteria. Additionally, allochthonous marine and terrestrial organic matter (transported by rivers or tidal currents) presents problems in interpreting bulk sediment compositions (Lamb et al. 2007; Kemp et al. 2012; Khan et al. 2015).

2.3.3.2 Lipid biomarkers

Biomarkers, which are the molecular remains of plants, animals and microorganisms preserved in geological archives, are also a potential proxy sea-level indicator in mangrove environments. These molecular remains are chemical compounds which can be directly

identified as originating from a particular genus or species that would otherwise not be preserved as fossils in the sedimentary record (Eglinton and Eglinton, 2008; Meyers, 2003).

Characterisation of biomarkers from mangrove species and other intertidal environments is an area of active research (He et al., 2014; Hernandez et al., 2001; Koch et al., 2011; Scourse et al., 2005; Smallwood et al., 2003; Tulipani et al., 2017). A key research objective is to identify mangrove biomarkers preserved in sedimentary archives that have a species-specific origin. For example, *Rhizophora* sp. leaf lipids contain higher taraxerol (a higher plant biomarker) concentrations than other mangrove species. Versteegh et al. (2004) use the peak of both taraxerol and *Rhizophora* sp. pollen in surface and sediment cores offshore south-west Africa as evidence towards a proxy for *Rhizophora* sp. input to sediment archives. Koch et al. (2011) examined mangrove cores in northern Brazil and also found that taraxerol (as well as biomarkers germanicol and β-amyrin) in combination with palynology is a good proxy for *Rhizophora mangle* input to sediments. While both studies indicate that taraxerol likely has good preservation potential in sediments, further studies are required to test possibly biomarker degradation through time and for biomarkers specific to other mangrove species (He et al., 2018).

In a number of mangrove species in Australia, Micronesia and Florida, local salinity changes have been recorded by changes to the fractionation of hydrogen isotopes (δD): as salinity increases, deuterium is increasingly discriminated from mangrove leaf lipid *n*-alkanes and taraxerols (He et al., 2017; Ladd and Sachs, 2017, 2015a, 2015b, 2012). $\delta^{13}C$ ‰ in leaf lipids increased in response to increasing salinity in *Avicennia marina* mangroves in Australia (Ladd and Sachs, 2013). These studies link these salinity changes to measured rainfall patterns, as mangroves uptake water when a fresher source is available. However, it is acknowledged that the relationship between compound-specific isotopic composition and salinity needs further testing to ensure a definitive mangrove or species-specific source for the target *n*-alkanes and taraxerol. A major aim of these studies is to define a salinity proxy derived from mangrove compound-specific stable isotope analysis, to better understand palaeoprecipitation patterns (e.g. Sachse et al. 2012; Ladd 2014; Nelson and Sachs 2016).

While the interaction between environmental water and mangrove isotopic compositions with changing precipitation, freshwater runoff and sea-level changes is highly complex and needs further investigation. The studies described here prove the potential for mangrove biomarker proxies of palaeoenvironmental changes. Biomarkers and their isotopic compositions have potential to be more precise than similar compositional measurements

on bulk sediments, if compounds can be confidently attributed to specific sources of organic matter (Kemp et al. 2010; Vane et al. 2013; Khan et al. 2015).

2.4 Approaches to dating mangrove sediments

Attributing an absolute age to a sea-level indicator is a necessary process as part of a RSL reconstruction. A RSL reconstruction with a high resolution age model (placed on a regular geological timescale) allows not only the examination of magnitude and spatial variability of RSL changes, but also the rates of changes. A number of dating methods can be applied to mangrove RSL sequences, but the most commonly applied techniques are the radiocarbon (^{14}C), ^{210}Pb and ^{137}Cs dating techniques.

2.4.1 Radiocarbon

The radiocarbon method is the mostly widely applied dating technique for mangrove sedimentary sequences. Mangrove sediments typically contain relatively large amounts of carbon-rich material produced *in-situ*, which can be extracted and analysed for ^{14}C. The radiocarbon method can be applied to sediments deposited over the past ~40,000 years, and has relatively small measurement uncertainties. However, despite the abundance of material for ^{14}C measurement, there are challenges to generating reliable radiocarbon-derived chronologies from mangrove sediments. The processes of carbon cycling in mangrove ecosystems (above and below ground) are not well understood, and there is often uncertainty in the relationship between a radiocarbon measurement and the RSL event a sea-level researcher is trying to date. Obtaining radiocarbon chronologies from mangrove sediments therefore requires careful evaluation, from initial sample selection to interpretation of ^{14}C measurements.

Mangrove root systems make up a large proportion of carbon material in mangrove sediments (Huxham et al., 2010; McKee and Faulkner, 2000). Living mangrove roots can penetrate up to two metres into the underlying sediment (Grindrod, 1988; Kristensen, 2008), which disturbs the sedimentary sequence and introduces young carbon material. This presents a problem for generating a RSL history — ^{14}C measurements from roots will not be the same as the age of the time of deposition at a given stratigraphic depth. Carbon deposited in mangrove sediments is also derived from above-ground mangrove plant material, but also from algae, bacteria, fungi, insects and other invertebrates, all of which

are invariably recycled or partly recycled before they are preserved within the sedimentary archive (Bouillon et al. 2008; Alongi 2014). Carbon is also imported and exported from mangrove sediment through surface current activity, bioturbators such as crabs, and below-ground pore-water transport, driven by ground-water fluctuations associated with tidal and fluvial processes (Adame and Lovelock, 2011; Dittmar et al., 2006). Storms and extreme events such as tsunamis can also redistribute carbon from adjacent marine and terrestrial environments. Carbon material in mangrove sediment is therefore an often unknown mix of autochthonous and allochthonous material (but relative contributions can be informed by $\delta^{13}C$ measurements).

^{14}C measurements on bulk sediment (i.e. a sample of mangrove sediment where organic remains are unidentifiable) is a common and straightforward approach to generating chronologies. Radiocarbon ages from bulk-sediment samples are a result of the combined mean age of the multiple carbon sources present in the samples. While a bulk-sediment radiocarbon age may have a high precision value (a small uncertainty on a ^{14}C measurement), it is often difficult to assign the age to a particular sedimentation event or organism death that is indicative of RSL changes. Previous studies report out-of-sequence radiocarbon ages when sampling bulk sediment (Geyh et al. 1979; Grindrod and Rhodes 1984; Larcombe et al. 1995; Tamura et al. 2009; Punwong et al. 2013a, 2013b; Woodroffe et al. 2015a).

Researchers have recommended avoiding samples with visible mangrove roots in sedimentary sequences for radiocarbon measurement, and that any bulk sediment radiocarbon age should be considered a minimum age due to potential contamination from decomposed roots (Woodroffe 1981; Fujimoto and Miyagi 1993; Larcombe et al. 1995; Gischler 2006). Others use above-ground plant macrofossils such as leaves (Wooller et al., 2007). Leaves are more likely to have entered the sedimentary sequence shortly after the death of the plant tissue (i.e. the senescence of the leaf), and they should therefore record the age of sediment deposition. High sedimentation rates and ample accommodation space favour the preservation of above-ground macrofossils — for instance Caribbean sites which have experienced continuous late Holocene RSL rise (McKee et al. 2007; Wooller et al. 2007; Monacci et al. 2009). Preservation is rare in places with low sedimentation rates as plant macrofossils are more likely to decompose or be consumed at the sediment surface before burial, as seen in places where accommodation space is limited because of Late Holocene RSL fall (Punwong et al., 2013a, 2013b; Woodroffe et al. 2015a).

Radiocarbon ages of specific organic concentrates extracted from mangrove sediments are an alternative dating approach. Using a core taken from a mangrove in Tanzania, Woodroffe et al., (2015b) found that using radiocarbon ages from the 10–63 µm sediment size fraction produced in-sequence Holocene ages, where bulk sediment radiocarbon ages did not (Punwong et al., 2013b). This sediment size fraction was chosen to avoid large root fragments, and to better concentrate pollen or other small above-ground plant materials. These results show targeting specific sediment fractions may improve mangrove chronologies. In order to better measure the relationship between the timing of sediment deposition and ^{14}C measurements, we need further testing of approaches that target specific carbon sources (e.g. pollen).

2.4.2 Other dating techniques

Other radionuclide methods can be used to provide mangrove sediment chronologies on shorter timescales than radiocarbon, usually <100 years. Natural radionuclides such as ^{210}Pb (a ^{238}U decay series product) and anthropogenic radionuclides from nuclear testing fallout ^{137}Cs and $^{239+240}Pu$ are often applied to quantify historical sediment accumulation rates in mangrove environments, and therefore to provide RSL reconstructions (Lynch et al. 1989; Rogers et al. 2005; Sanders et al. 2010; Swales et al. 2015; Sanders et al. 2016). These approaches work well in environments with continuous sedimentation and a source of fine-grained minerogenic sediment, as these isotopes adsorb readily onto clay and silt-sized particles (Corbett and Walsh, 2015). Notably, these isotopes do not readily adsorb onto organic sediments, which can be a limiting factor in mangrove settings. ^{210}Pb approaches are more useful in continental settings (as opposed to oceanic settings) as atmospheric and therefore depositional fluxes are distinctly higher (Baskaran, 2011).

Anthropogenic chronohorizons such as heavy metals from industrial activity and pollen and charcoal markers have been used to inform palaeoenvironmental changes in mangrove settings. Mangrove sediments can store heavy metals related to the onset of local and regional mining activity (de Souza et al., 2017; Veerasingam et al., 2015). Changes in pollen and charcoal types and abundances in mangrove sedimentary sequences can relate to the timing of the increase in nearby human crop cultivation, or deforestation (Bocanegra Ramírez et al., 2019; Figueroa-Rangel et al., 2016; González et al., 2010; Punwong et al., 2017).

Other methods of dating mangrove sediments are not well-established or applied, mainly because the carbon-rich nature of mangrove sediments lends itself to the radiocarbon method, however difficult that may be. Volcanic ash layers (tephra) provide definitive chronohorizons if they can be identified to a known eruption. Tephra are rarely investigated in mangrove sedimentary sequences, as they are either not well preserved or difficult to identify without finer-scale microscope and geochemical analysis. Adame et al. (2015) were able to identify a tephra horizon in a mangrove sediment profile in southwest Mexico, which provided a precise horizon to which they could calculate organic carbon sequestration rates over the twentieth century. Preservation of this ash layer was more likely due to the size of the eruption and the proximity of the mangrove environment to the volcanic centre. This study highlights that in localities with active volcanoes (or that were during the Holocene) and that produce explosive eruptions, volcanic ash layers could form an important part of a mangrove sediment chronology. Recent studies have included optically stimulated luminescence (OSL) ages on beach ridges, which are often geomorphic features associated with mangrove deposits on millennial timescales (Culver et al., 2015; Mallinson et al., 2014). Further development in OSL dating techniques to utilise broader sample types and higher precision (i.e. less than millennial timescales) could provide good chronological data for high-resolution mangrove RSL reconstructions. The application of chronological methods independent of the radiocarbon technique should be used where possible, to produce more robust age models and to test the reliability of ^{14}C ages.

2.5 Other challenges

Another issue is that in many parts of the far-field (i.e. not in the coloured area of Figure 2.1), RSL was falling during the late Holocene, and to use sea-level indicators from this time period in these locations they need to preserve well under conditions of falling RSL. Using multiple types of sea-level indicators and enhancing our understanding of how they form is key to increasing the precision of far-field RSL reconstructions.

2.5.1 Bioturbation

Previous studies investigating palaeoenvironmental changes in mangrove environments commonly suggest that bioturbation limits the resolution that past changes can be deciphered, as sedimentary layers are homogenised and boundaries are obscured (Grindrod and Rhodes 1984; Behling et al., 2001; Debenay et al., 2004; Berkeley et al. 2007; Perry et al., 2008; Berkeley et al. 2009a). Many invertebrates (e.g. crabs and molluscs) are known to

create burrows (at a centimetre scale) in mangrove sediments, in some places up to one metre depth from the surface (Stieglitz et al. 2000; Koch et al. 2005; Hogarth 2015). As previously discussed, microfauna like foraminifera also live and burrow in the sediment column, which have been observed living at up to 80 cm depth in mangroves in Malaysia (Culver et al., 2013).

The degree of bioturbation in mangrove sediments is rarely described or quantified, in the context of a palaeoenvironmental study. Berkeley et al. (2007) found that bioturbation is an important control on the composition of foraminifera assemblages in intertidal mangrove environments. Bioturbation transports not only the foraminifera themselves to other depths, but also oxygenates the sediment column and transmits surface material to underlying sediments (Debenay et al. 2004; Perry et al. 2008). Oxygenation modifies decomposition rates and thus influences the preservation potential of organic matter, and therefore sediment composition within a sedimentary sequence (Gillis et al., 2019; Kristensen, 2008). The sediment-water/air interface extends into deeper layers through bioturbation, and therefore any material (and not solely foraminifera) used to create a sea-level index point may be 'vertically-smeared' by the same amount as the depth of bioturbation, depending on rates of mixing and sedimentation rates (Berkeley et al., 2009b, 2007). Rates of bioturbation can vary greatly between sub-environments within mangroves – for example between a high-elevation mangrove zone and that proximal to a low-elevation mud-flat (Berkeley et al. 2008).

Careful observations in the modern environment can help quantify the impact bioturbation has on a mangrove RSL reconstruction, such as counting number and size of burrows in a given sediment surface area (Perry et al. 2008), and avoiding coring sites close to areas of high burrow density (Culver et al., 2013). Consideration of the 'burial trajectory' of sediments (Berkeley et al. 2014), and evaluating any compositional changes to stratigraphy rather than depth in the sediment column (Berkeley et al. 2009b) may also help to account for bioturbation when interpreting sedimentary sequences. However, despite bioturbation, many studies report identifiable palaeoenvironmental changes (and thus RSL changes) from mangrove sedimentary sequences that would not be preserved had bioturbation completely mixed and blurred the stratigraphy (Behling et al. 2001; Hayward et al. 2004; Punwong et al. 2013a; Culver et al. 2015).

2.5.2 Physical challenges in mangrove environments

Mangrove sediments are not only hard to interpret, but also challenging to work in physically. Tropical regions that mangroves thrive in typically have high daytime temperatures and humidity, and often severe precipitation events which make sampling difficult. In some sites, density of vegetation makes accessing mangrove sites difficult either on foot or by boat. Dense vegetation and potentially high vegetation canopies also means that surveying (both manually and with GPS methods) is challenging and time-consuming. Because of canopy effects, remote sensing or aerial photography does not provide the resolution necessary for mapping elevations and has to be ground-truthed (e.g. Leong et al. 2018). These effects mean that it is quite difficult to assess site geomorphology in the field, in comparison to other coastal settings like salt marshes.

2.6 Summary

Mangroves are a valuable sedimentary archive of RSL changes over the Holocene. They have provided — and will continue to do so — necessary RSL data to answer questions relating to past environmental, ice volume and climatic changes in the pre-industrial era. Mangrove sediments have unique benefits and challenges, which need to be carefully considered to improve RSL reconstructions. Mangrove sea-level index points may have greater vertical uncertainty values compared to other coastal environments like salt marshes due to the challenge of levelling in these types of environments, preservation of microfossils, and mixing through bioturbation. Bulk sediment radiocarbon ages should be considered minimum ages due to root penetration. While these factors may seem unsurmountable for quantitative RSL reconstructions, it is unlikely that these errors are greater than the uncertainty determined from the indicative range of mangrove sediments. State-of-the-art sea-level databases that require details of such errors calculate uncertainty for sea-level index points as the square root of the sum of squared errors (Hijma et al., 2015; Khan et al., 2019a; Shennan, 1986), and the error derived from the indicative range typically dominates this overall uncertainty.

Chapter 3: Comparing radiocarbon measurements of mangrove sediments from Mahé, Seychelles, for building reliable chronologies of relative sea-level change

3.1 Introduction

Mangroves are salt-tolerant trees that inhabit a narrow ecological niche along tropical coastlines worldwide (Lugo and Snedaker, 1974; Tomlinson, 2016). They occupy distinct parts of the intertidal zone and therefore naturally respond to changes in relative sea level (RSL) (Friess et al., 2019; McKee et al., 2012; Woodroffe, 1990). Mangrove sedimentary deposits are valuable archives of past environmental changes, and in particular provide important observations of 'far-field' sea-level changes (i.e. locations far from the influence of glacio-isostatic adjustment processes that occur near ice sheets) during the Mid- and Late Holocene (Scholl, 1964; Woodroffe et al., 1985; Ellison, 2005; Culver et al., 2015; Woodroffe et al., 2015; Tam et al., 2018). Reliable chronologies are critical to such studies, but the nature of mangrove sediments presents unique challenges particularly when applying the radiocarbon dating method. Modern mangrove roots penetrate up to two metres into underlying sediments, which introduces carbon material that is younger than the age of sediment deposition (Beaman et al., 1994; Gischler, 2006; Grindrod and Rhodes, 1984; Woodroffe, 1981). Burrowing fauna such as crabs that inhabit mangroves also mix younger and older carbon material at decimetre scales within the sediments (Kristensen, 2008; Stieglitz et al., 2000). These issues are undesirable because in many locations we require closely spaced, reliable ages from shallow mangrove sedimentary sequences (<2 metres) to provide constraints on past RSL and palaeoenvironmental changes.

In this chapter I investigate which components of mangrove sediments are most suitable for obtaining reliable radiocarbon chronologies from mangrove sediments. I used sediments collected from a mangrove site on Mahé island in the Seychelles archipelago (Figure 1.3). Seychelles is in one of the few regions of the world where RSL is modelled to be within 1 metre of eustasy during the last 6,000 years, and where corrections for glacio-isostatic adjustment (GIA) are relatively insensitive to models using different Earth viscosity profiles (Milne and Mitrovica, 2008; Woodroffe et al., 2015a). I compare and evaluate AMS radiocarbon ages derived from bulk sediments, organic concentrates, pollen concentrates,

and macrofossils, as well as with those collected in a previous RSL at the same study site (Woodroffe et al., 2015a). I then provide recommendations for future palaeo-sea level and other studies using mangrove sediments to improve the reliability of radiocarbon derived chronologies.

3.2 Radiocarbon dating of mangrove sediments

During photosynthesis, mangroves synthesize carbon from the atmosphere and so are purely constructed from a terrestrial carbon reservoir. As mangroves are rooted within the intertidal zone, mangrove-derived carbon entering the sedimentary sequence is largely produced *in situ*, both above ground in the form of leaves, branches and trunks, and below ground as roots (Figure 3.1) (Bouillon et al., 2008; Krauss et al., 2014). Marine and terrestrial environments that fringe mangroves can also be sources of carbon in mangrove sedimentary sequences, for example, seagrass and other marine algae such as *Sargassum* can be transported into mangrove forests during flood tides and storm events (Gonneea et al., 2004; Jaffé et al., 2001; Kemp et al., 2019).

3.2.1 Bulk sediment

Dating of bulk mangrove sediments has been the most common approach for constructing chronologies for mangrove sedimentary sequences. Bulk sediments are composed of many different carbonaceous and non-carbonaceous materials, and the carbon fraction can itself be a mix of allochthonous or autochthonous carbon of potentially different ages. Bulk sediment samples are mostly humified organics, but can also contain macrofossils like roots and leaf material, bacteria, algae, pollen, fungi, and dissolved organic carbon from sediment pore waters. Previous mangrove RSL studies have reported out-of-sequence ages when bulk sediments are used for radiocarbon measurements (Geyh et al., 1979; Grindrod and Rhodes, 1984; Larcombe et al., 1995; Punwong et al., 2013a). This is likely due to the large range of possible carbon sources that make up a bulk sediment sample, as any radiocarbon measurement will be a combined mean age of multiple carbon sources. Therefore, it is difficult to confidently link bulk sediment ages to a target phenomenon (i.e. RSL changes) (Törnqvist et al., 2015).

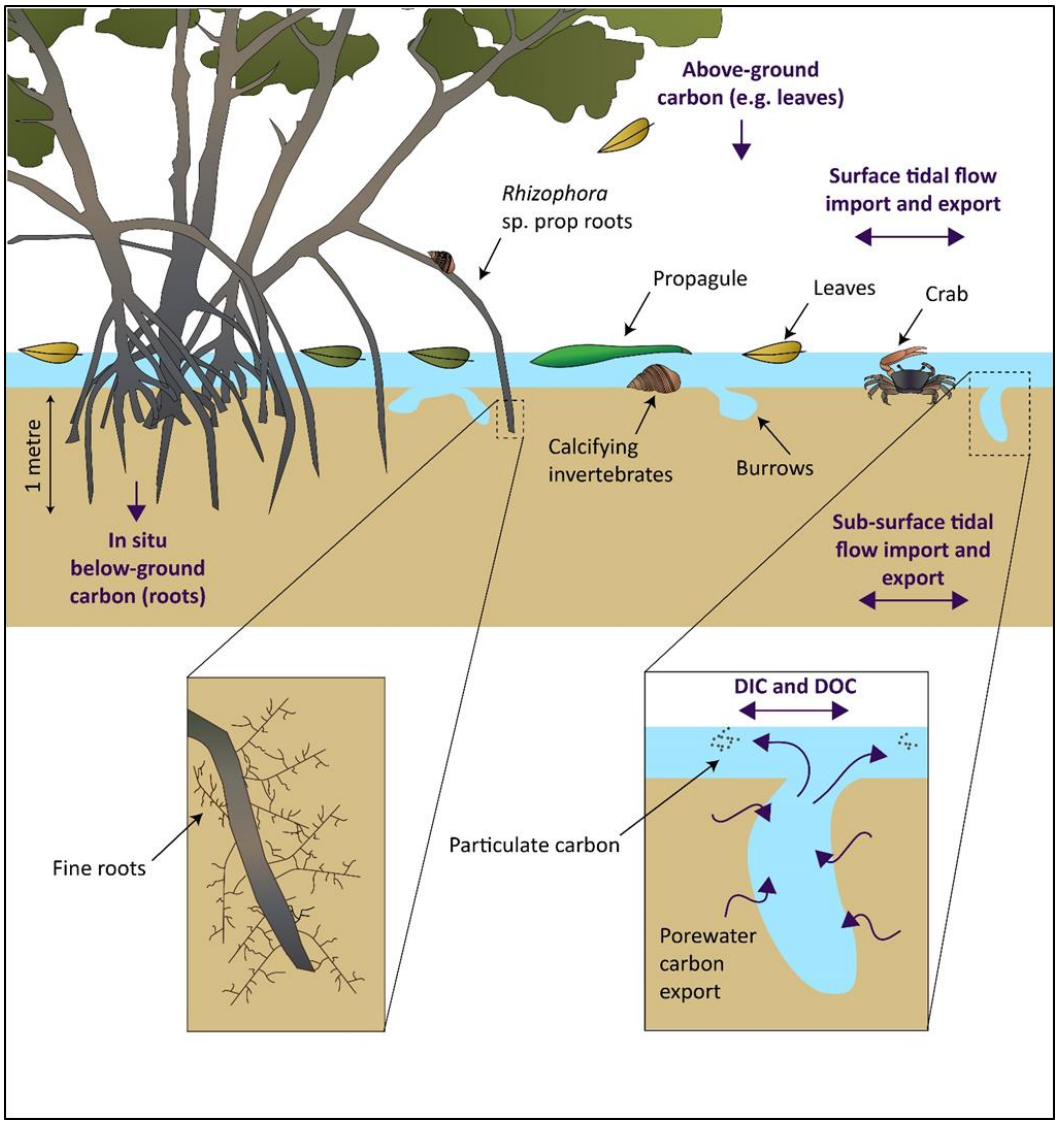

Figure 3.1: Processes and components of a modern mangrove environment that influence carbon preservation and degradation. Mangrove sediment archives develop through biogenic accretion (primarily through root production and leaf litter) and through minerogenic sedimentation from marine and terrestrial environments.

3.2.2 Roots and bioturbators

While mangrove root systems are relatively shallow in comparison to other terrestrial trees (owing to their need to be oxygenated in a saline environment), their roots can extend multiple (vertical) metres into underlying sediments (Figure 3.1) (Grindrod, 1988). This presents a problem for radiocarbon dating of mangrove sedimentary sequences, as the roots are younger than the sediment they penetrate. Roots can make up a large proportion of mangrove total biomass, particularly in locations with low minerogenic sediment delivery such as carbonate islands in the Caribbean (McKee et al., 2007; McKee and Faulkner, 2000). In other settings such as estuaries and deltas, mangrove biomass is more dominated by

above ground timber as canopies tend to be taller (Krauss et al., 2010), or roots shallower (Lovelock et al., 2007). Roots can therefore make up a sizeable percentage of mangrove carbon entering the sedimentary sequence (Huxham et al., 2010; McKee and Faulkner, 2000). Some researchers have suggested avoiding large roots when selecting radiocarbon samples to remedy this problem (Larcombe et al., 1995; Woodroffe, 1990, 1981). However mangroves also produce fine roots that decompose more quickly than larger woody roots (McKee et al., 2007), and these are more difficult to identify and isolate when sampling. Bulk sediment samples therefore are likely younger than their true deposition age due to the addition of decomposed, fine root-derived carbon (Gischler, 2006).

Crabs and other fauna (e.g. molluscs, shrimp, and foraminifera) can bioturbate mangrove sediments up to one metre depth (Koch et al., 2005; Stieglitz et al., 2000). This reworks young and old carbon, and also oxygenates the sedimentary column which affects preservation by enhancing aerobic decomposition (Debenay et al., 2004; Deng et al., 2006; Grindrod and Rhodes, 1984; Perry et al., 2008). The degree to which bioturbation affects palaeoenvironmental records in mangroves is difficult to quantify (see section 2.5.1). However many studies have still produced sensible and regionally-consistent palaeoecological changes using metre-scale core records despite the influence of bioturbation (e.g. Punwong et al., 2013a; Culver et al., 2015).

3.2.3 Macrofossils

Plant macrofossils derived from above ground carbon material (i.e. anything not a root, such as leaves and seeds) are considered the most reliable material for constructing radiocarbon chronologies in mangrove sediments. Above-ground plant material is more likely to enter the sedimentary sequence very shortly after its death, and is thus more likely to record the age of sediment deposition. In salt marshes — which inhabit the same ecological niche as mangroves but in temperate climates — leaves and seeds are commonly preserved and are used to construct high-resolution age models for decimetre-scale RSL reconstructions (Barnett et al., 2019; Kemp et al., 2018; Long et al., 2012). Where they are preserved and can be identified, mangrove plant macrofossils provided reliable sequences of radiocarbon ages (Grand Pre et al., 2012; Monacci et al., 2009; Wooller et al., 2007). High sedimentation/burial rates promote the preservation of macrofossils in sedimentary sequences, whereas at sites with low sedimentation rates, surface plant material decomposes or is consumed before it is buried within the sediment (at much faster rates than in salt marshes with more temperate climates). For example, at sites in the Caribbean

where Holocene RSL rise has been continuous to present day (i.e. continuous sediment accommodation space), mangrove leaves are often preserved within sedimentary sequences (Monacci et al., 2009; Wooller et al., 2007). At sites with limited sediment accommodation space such as the Indian Ocean region where Late Holocene RSL is falling or stable, mangrove plant macrofossils within sediment sequences are much more rare (Punwong et al., 2013a, 2013b; Woodroffe et al., 2015a). For instance, mangrove leaves are an order of magnitude larger than the leaves of plants from other similar environments such as salt marshes. This further reduces the chance of sampling a macrofossil in a core, and also reduces the potential resolution of a radiocarbon age as a deposited leaf can span multiple centimetres within a sedimentary sequence.

3.2.4 Organic and pollen concentrates

Where mangrove plant macrofossils are not available, researchers have turned to other carbon materials for constructing chronologies. Woodroffe et al. (2015b) tested the use of organic concentrate radiocarbon ages against bulk sediment ages in Tanzanian mangrove sediments for RSL reconstructions. The organic concentrate ages (a 10-63 µm sediment size fraction) are older than bulk sediment ages collected from a similar depth — in some instances over 1,000 calendar years older. These results suggest that by sieving out larger organic fragments, organic concentrates sample an older carbon fraction, which is presumably closer to the 'true' depositional age than bulk sediment ages which still contain younger root material (Woodroffe et al., 2015b; Kemp et al., 2019). Whilst organic concentrates isolate a particular size fraction for dating, they still contain a mix of carbon from an unknown number of sources. Radiocarbon dating of pollen concentrates is a method developed for use in lacustrine and freshwater bog sediments (Howarth et al., 2013; Neulieb et al., 2013; Newnham et al., 2007; Vandergoes and Prior, 2003), but has yet to be applied to mangrove sediments. By isolating mangrove pollen (an above-ground carbon source), this reduces the potential of sampling and dating organics that are not representative of the depositional age. Some researchers have found pollen reworking from surrounding terrestrial and marine environments, and therefore ages that are too old (Howarth et al., 2013; Kilian et al., 2002; Li et al., 2014; Neulieb et al., 2013). Further isolation of organics such as compound-specific radiocarbon dating have been successful in other environments (Ohkouchi and Eglinton, 2008; Pancost et al., 2000; Smittenberg et al., 2004), but have not been attempted in mangrove sediments.

There remains a need to test, comprehensively, mangrove radiocarbon dating approaches — in particular those that are alternatives to macrofossils. Here we analyse different sample types (bulk sediment, organic concentrates, pollen concentrates, and macrofossils) collected from the same depths in four different cores from a mangrove site from Mahé, Seychelles (Figure 3.2).

3.3 Study site and previous work

The mangrove area at Grand Anse, Mahé was selected for this radiocarbon comparison study (Figure 1.3). A previous study that investigated Late Holocene RSL changes in Seychelles used data derived from the Grand Anse mangrove sediments (Woodroffe et al., 2015a). However, the radiocarbon ages were difficult to interpret as a number were out-of-depth-sequence, and woody and root macrofossils yielded different ages to bulk sediment samples. Despite this, the RSL reconstruction demonstrates that mangroves had begun to occupy intertidal and river channel areas behind the carbonate-sand beach plateau by 2 ka BP (see Section 1.3.2), suggesting RSL stability. Critically, the uncertainty in radiocarbon dating from the mangrove sediments at Grand Anse did not allow Woodroffe et al. (2015a) to make confident conclusions regarding Late Holocene eustatic sea-level change.

Figure 3.2: Location of cores collected in the Grand Anse mangrove. Orange circles were collected as part of this study, purple circles collected as part of the Woodroffe et al. (2015a) study. White dotted line is the approximate extent of the mangrove zone, and the light blue line is the River Dauban.

3.4 Methods

A series of bulk sediments, macrofossils, organic concentrates and pollen concentrates were prepared for ^{14}C measurements, to compare results collected at the same depth in four cores collected across the study site (Figure 3.3).

I collected cores manually using a Russian-type corer. To ensure we had enough sediment or macrofossils at a certain depth for analysis, we collected duplicate cores at the same coring site. Cores were sampled into plastic tubes, sealed with plastic and stored at 4°C until sampling.

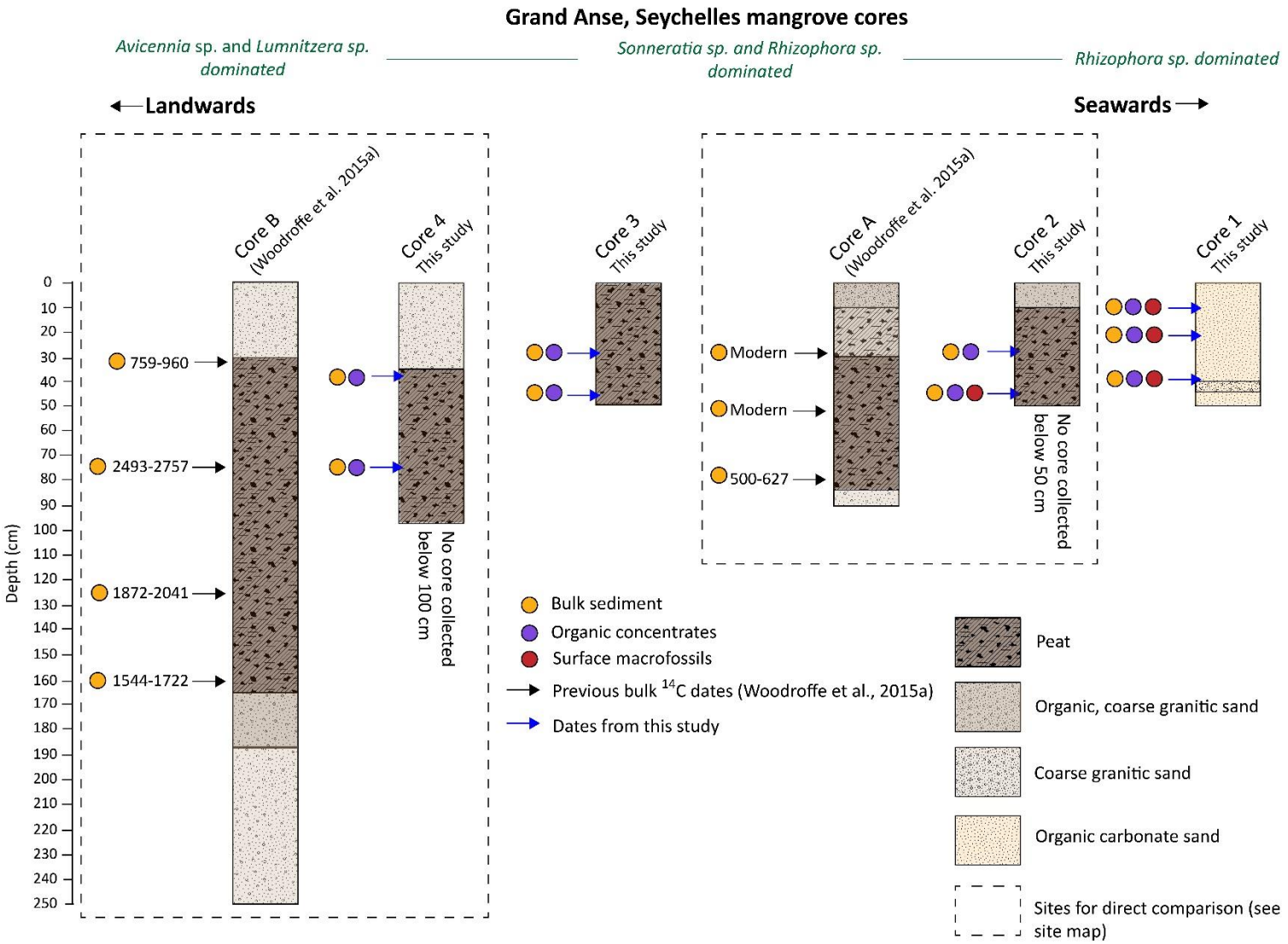

Figure 3.3: Stratigraphy and depths of radiocarbon samples collected at Grand Anse mangrove. Detailed core descriptions available in Table A11.

3.4.1 Sample pre-treatments

3.4.1.1 Bulk sediment and macrofossils

Bulk sediment was extracted from sediment cores using sterilised scalpels and utensils, and transferred to aluminium foil for storage and transport to the radiocarbon facility. Bulk sediment samples underwent further pre-treatment at the NERC Radiocarbon Laboratory (Environment) at the Scottish Universities Environmental Research Centre (SUERC), where they underwent standard acid-alkali-acid treatment which removes any carbonates and humic compounds (De Vries and Barendsen, 1954; Dunbar et al., 2016). Samples were digested in 2M hydrochloric acid (HCl) at 80°C for 8 hours. Samples were washed free of acid using deionised water, and then further digested in 1M potassium hydroxide (KOH) at 80°C for 2 hours. The KOH digestion was repeated (washing with deionised water in between) until no further humic material was extracted (i.e. the supernatant was clear). Samples were rinsed free of KOH and then digested again with 1M HCl at 80°C for 2 hours. Samples were then rinsed again with deionised water, dried, and homogenised ready for AMS ^{14}C measurements.

Macrofossils were extracted from sediment cores using sterilised scalpels and utensils, or isolated through wet sieving with de-ionised water at 90 µm and 63 µm in stainless steel mesh. Samples were examined by light microscopy to visually identify different plant material, photographed, and then dried and transferred to either aluminium foil or glass vials for storage and transport to the radiocarbon facility. Further pre-treatment of macrofossils was undertaken at the NERC Radiocarbon Laboratory and followed the same procedure as stated above (with the exception of the KOH digestion which used a concentration of 0.5M instead of 1M).

3.4.1.2 Organic concentrates

Organic concentrates were prepared using a modified method reported in Woodroffe et al. (2015b). Sediment was extracted from the core using sterilised scalpels and utensils and transferred to furnaced glassware. 1M HCl was added to the samples in excess, and this was heated and stirred in a water bath at 60°C for 30 minutes. Samples were rinsed free of acid using deionised water and then wet sieved at 63 µm and 10 µm stainless steel mesh sieves. Sieves were re-used between samples instead of using new nylon mesh sieves as nylon it has the tendency to shed fibres and introduce plastic particles into a sample. Stainless steel

sieves were sonicated in a water bath for >45 minutes in three changes of deionised water between samples to remove any contaminants. Small aliquots of the sieved 10-63 µm fraction were isolated with a furnaced glass pipette to create microscope slides to further identify plant material, and the >63 µm was examined under a microscope for any macrofossils (see above). The remaining 10-63 µm fraction was oven-dried at 40°C, and transferred to glass vials for storage and transport to the radiocarbon facility. Three process standards of known ages (Tiri barley mash, 96H humin, and anthracite) were also processed using the same method to measure any contamination during the sample preparation process. These covered an age range from modern to ^{14}C background levels.

3.4.1.3 Pollen concentrates

Pollen concentrates were prepared using methods modified from Newnham et al. (2007), Howarth et al. (2013) and Dahl (2019). Sediment was extracted from the core (one centimetre-thick samples) using sterilised scalpels and utensils and transferred to furnaced glassware. 1M HCl was added to the samples in excess, and this was heated and stirred in a water bath at 60°C for 30 minutes. Samples were rinsed free of acid using deionised water and then heated at 60°C in excess 1.5M KOH for five minutes. The KOH digestion was repeated (washing with deionised water in between) until no further humic material was extracted (i.e. the supernatant was clear). Samples were rinsed free of KOH and then digested again with 1M HCl at 60°C for 10 minutes. Samples were rinsed free of acid with deionised water and wet-sieved through 90 µm and 10 µm stainless steel sieves. The >90 µm was examined for any macrofossils suitable for dating (see above), and the <10 µm fraction was discarded as a majority of pollen grains are >10 µm in any diameter (Howarth et al., 2013). The 10-90 µm sediment fraction was transferred with deionised water to new and pre-cleaned plastic 50 mL centrifuge tubes, and centrifuged at 4000 revolutions per minute (rpm) for five minutes. The water was carefully pipetted off the separated sediment using furnaced glass pipettes to remove as much water from the sample as possible. 30 mL of 1.8 sg sodium polytungstate (SPT) was added in the centrifuge tube and vortexed to thoroughly mix. This mixture was allowed to settle for 10-30 minutes and then centrifuged for 10 minutes at 2000 rpm (avoid denser particles dragging down and trapping lighter ones) (Dahl, 2019). The separated lighter material (<1.8 sg) was pipetted away and rinsed and centrifuged with deionised water, carefully pipetting away the supernatant each time. The heavier (>1.8 sg) separated fraction was rinsed with deionised water. Small aliquots of both the lighter and heavier fractions were pipetted onto microscope slides to examine pollen

concentrations. The process of separation with SPT was repeated with a progressively less dense mixtures (1.6, 1.5, 1.4, 1.3, and 1.2 sg), with microscope slides of each fraction being prepared and examined at each stage to determine the sediment fraction with the greatest pollen concentration. Selected fractions were transferred to glass vials, dried and weighed for storage and transport to the radiocarbon facility. Three process standards of known ages (Tiri barley mash, 96H humin, and anthracite) were also processed using the same method to measure any contamination.

3.4.2 ^{14}C age determination

At the NERC Radiocarbon Laboratory, dried homogenised samples were converted to CO_2 gas using a CuO by combustion in pre-cleaned quartz tubes (Vandeputte et al., 1996). Evolved sample CO_2 was cryogenically purified before conversion to graphite by Fe/Zn reduction (Slota et al., 1987), after which sample $^{14}C/^{13}C$ ratios were measured by accelerator mass spectrometry (AMS) at the SUERC AMS Laboratory in East Kilbride, UK. Measured $^{14}C/^{13}C$ ratios were background corrected and normalised to $\delta^{13}C$-VPDB ‰ = -25 using the $\delta^{13}C$ values from sample aliquots measured on a dual inlet stable isotope mass spectrometer (Thermo Fisher Delta V). All ^{14}C ages are calibrated using either the SHCal13 curve (Hogg et al., 2013) or the Calibomb calibration curve for Southern Hemisphere Zone 3 (Hua et al., 2013) using OxCal v.4.3 (Bronk Ramsey, 2009).

After conversion to graphite, one macrofossil sample (UCIAMS-223878) was too small for measurement on the SUERC Laboratory AMS. This sample was measured by AMS at low current, at the Keck Carbon Cycle AMS Facility, University of California, Irvine, United States of America. The $^{13}C/^{12}C$ ratio was measured by AMS during ^{14}C determination and used to correct and normalise ^{14}C data to $\delta^{13}C$-VPDB ‰ = -25. The $^{13}C/^{12}C$ ratio is appropriate to correct for isotopic fractionation but it is not necessarily representative of the $\delta^{13}C$ of the original sample material, so a $\delta^{13}C$ value for this sample is not included in Table 3.1. The sample was corrected for modern carbon contamination as per Santos et al. (2007), and for modern carbon contamination (using data from process background and standard materials) and for samples <100 µg of carbon a correction based on small NIST Oxalic acid II to account for the effect of old carbon which becomes significant for those sample sizes.

3.5 Results

3.5.1 Organic and pollen concentrate fractions

Sieving sediment samples for radiocarbon dating invariably isolated the larger macrofossil and root material within a sample. The >63 µm fraction removed during the organic concentrate process contained large and fine roots (Figure 3.4) of varying stages of decomposition as well as sand and gravel-sized siliclastic grains (dominantly quartz). The organic concentrate fractions used for dating (10-63 µm) were examined under a high-powered microscope. The organic concentrates contain a mix of organic and non-organic material, which has been qualitatively described here using classifications of Tyson (1995) and McArthur et al. (2017). The organic concentrates are dominated by structureless organic matter particles, but they also contain siliclastic particles (silt and clay sized quartz), dark rectangular structureless organic matter, and degraded and well-preserved 'wood' particles (Figure 3.5). There are also minor amounts of membranous tissues (palynowafers), and trace amounts of algae, fungal hyphae and bodies, and pollen. Evidence of bacterial and fungal attack on organic fragments (structureless and woody) is common (Figure 3.5).

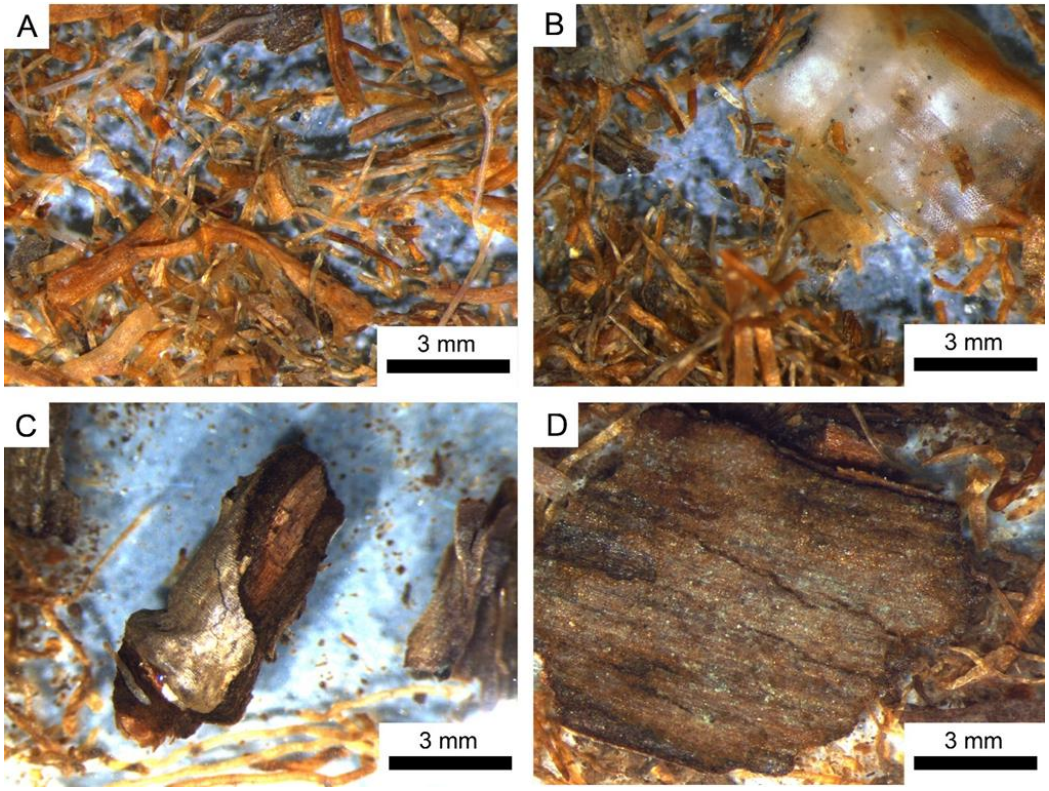

Figure 3.4: Microscope images of the >63 µm fraction sieving during organic concentrate pre-treatment. Figures A and B are from Core 2, Figures C and D are from Core 4.

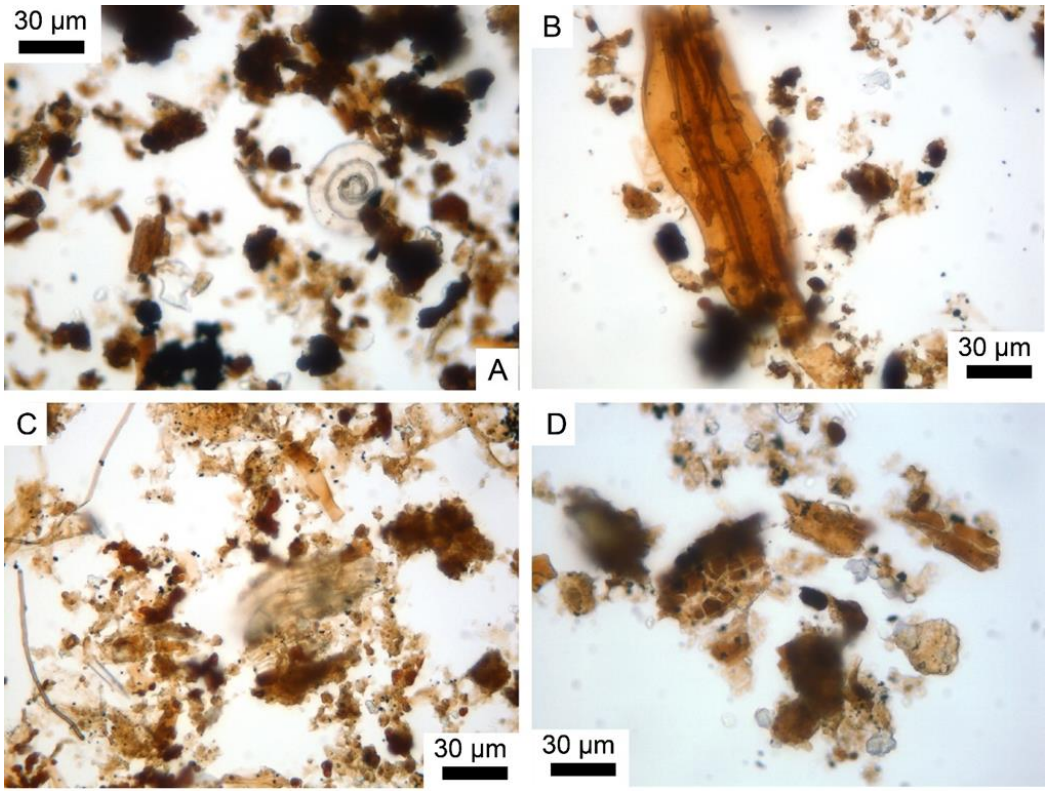

Figure 3.5: Microscope images of 10-63 µm organic concentrate samples. Figures A, B and C are from Core 4, Figure D is from Core 2.

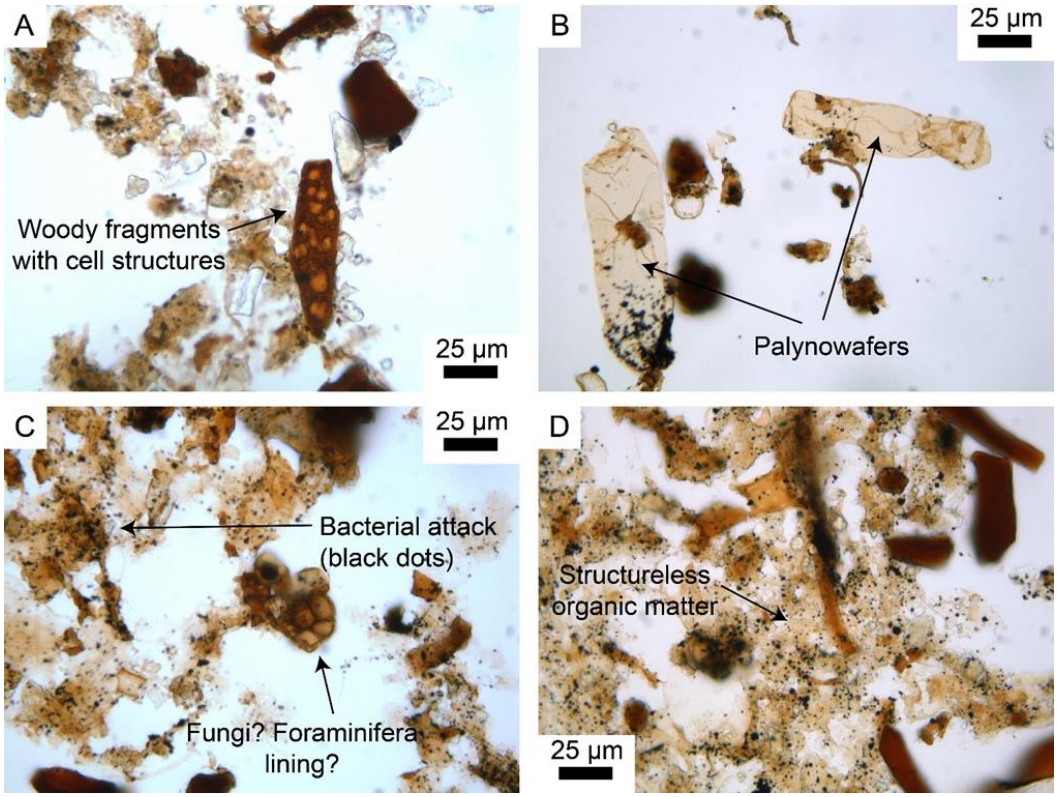

Figure 3.6: Microscope images of 10-90 µm fraction sieved during pollen concentrate sample processing. Figures A, B and C are from Core 4, Figure D is from Core 3. Annotations are organic structures found in all samples, with structureless organic matter becoming less common in later heavy liquid separations and rectangular woody fragments becoming more dominant.

The composition of the pre-treated pollen concentrates 10-90 µm fraction is largely similar to the organic concentrates (Figure 3.6), but with notably larger siliclastics (fine sand-sized) and slightly larger organic fragments. Each progressive step with SPT removed denser material: first siliclastics (>1.8 sg), then structureless organic matter (>1.6 sg), then the larger rectangular 'woody' particles (>1.4 sg). Any pollen was concentrated into the <1.3 sg fraction, but any fraction lighter than 1.4 sg was still dominated by smaller-sized 'woody' particles. While the percentage of pollen in each sample was not quantitatively determined, only one of the <1.3 sg fractions visibly contained a high enough concentration of pollen for ^{14}C measurements. This fraction was sent to the SUERC Radiocarbon Facility and converted to CO_2 gas, but with insufficient material in this one-centimetre-thick slice of sediment for a viable AMS ^{14}C measurement. Unfortunately, we do not have any pollen concentrates to compare in this study. However, we do have measurements on process standards for the PC method (Table 3.1), which prove that the method does not introduce contamination.

3.5.2 Core results

Radiocarbon measurements from this study and Woodroffe et al. (2015a) are listed in Table 3.1 and displayed in Figure 3.7.

*Table 3.1: List of radiocarbon measurements mentioned in this study. * 95% range calibrated Common Era (cal CE), using OxCal 4.3 (Bronk Ramsey, 2009). ** NERC Radiocarbon Laboratory process standard values are 0.21 ± 0.12% modern ^{14}C for anthracite, 3397 ± 35 ^{14}C years BP for 96H humin, and modern values for Tiri barley mash.*

CORE NAME	DEPTH IN CORE (CM)	SAMPLE TYPE	^{14}C AGE ±1σ	PERCENT MODERN CARBON (%)	MINIMUM CALIBRATED AGE, CAL CE*	MAXIMUM CALIBRATED AGE, CAL CE*	$\delta^{13}C_{VPDB}$‰ (± 0.1)	LAB ID	REFERENCE
Core B	32-33	Bulk	983 ± 37	88.48 ± 0.41	1025	1179	-28.9	SUERC-29500	(Woodroffe et al., 2015a)
Core 4	34-35	Bulk	1522 ± 37	82.74 ± 0.38	500	650	-29.2	SUERC-84524	This study
Core 4	34-35	Organic Concentrate	1577± 35	82.18 ± 0.36	423	601	-28.225	SUERC-86973	This study
Core B	75-76	Bulk	2559 ± 39	72.72 ± 0.36	-799	-491	-27.6	SUERC-30458	Woodroffe et al., 2015a)
Core 4	75-76	Bulk	1913 ± 37	78.81 ± 0.36	57	233	-27.7	SUERC-84525	This study
Core 4	75-76	Organic Concentrate	1847 ± 37	79.46 ± 0.36	119	340	-27.6	SUERC-86974	This study
CORE 4	128-129	Bulk	1998 ± 35	77.98 ± 0.34	-48	117	-26.6	SUERC-29501	Woodroffe et al., (2015a)
CORE 4	161-162	Bulk	1733 ± 37	80.59 ± 0.37	248	417	-28.3	SUERC-29502	(Woodroffe et al., 2015a)
Core 3	28-29	Bulk	n/a	101.36 ± 0.46	1918	1953	-28.6	SUERC-84528	This study
Core 3	28-29	Organic Concentrate	34 ± 37	99.58 ± 0.46	1700	1946	-27.16	SUERC-86982	This study
Core 3	46-47	Bulk	644 ± 37	92.29 ± 0.42	1298	1409	-28.9	SUERC-84529	This study
Core 3	46-47	Organic Concentrate	832 ± 37	90.16 ± 0.41	1185	1284	-27.699	SUERC-86983	This study
Core 2	28-29	Bulk	8 ± 35	99.90 ± 0.44	1707	1954	-28.1	SUERC-84526	This study
Core 2	28-29	Organic Concentrate	231 ± 37	97.17 ± 0.44	1637	…	-27.411	SUERC-86978	This study
Core A	28-29	Bulk	n/a	100.47 ± 0.44	1951	1959	-28.3	SUERC-29503	(Woodroffe et al., 2015a)

CORE NAME	DEPTH IN CORE (CM)	SAMPLE TYPE	^{14}C AGE ±1σ	PERCENT MODERN CARBON (%)	MINIMUM CALIBRATED AGE, CAL CE*	MAXIMUM CALIBRATED AGE, CAL CE*	$\delta^{13}C_{VPDB}$‰ (± 0.1)	LAB ID	REFERENCE
Core 2	45-46	Bulk	552 ± 37	93.36 ± 0.43	1329	1454	-29.1	SUERC-84527	This study
Core 2	45-46	Organic Concentrate	486 ± 35	94.13 ± 0.41	1410	1606	-27.742	SUERC-86979	This study
Core 2	45-46	Macrofossil: bark	915 ± 37	89.24 ± 0.41	1045	1262	-29.1	SUERC-88308	This study
Core A	53-54	Bulk	n/a	101.30 ± 0.47	1951	1959	-27.7	SUERC-29506	(Woodroffe et al., 2015a)
core a	80-81	Bulk	504 ± 37	93.92 ± 0.43	1402	1482	-28.2	SUERC-29507	(Woodroffe et al., 2015a)
Core 1	13.5-14.5	Bulk	n/a	106.74 ± 0.49	1957	2010	-29.6	SUERC-88309	This study
Core 1	13.5-14.5	Organic Concentrate	n/a	108.55 ± 0.50	1957	2004	-28.7	SUERC-88310	This study
Core 1	13.5-14.5	Macrofossil: *Terminalia* seed	n/a	105.03 ± 0.48	1957	…	-27.2	SUERC-88307	This study
Core 1	25-26	Bulk	n/a	110.64 ± 0.51	1958	2001	-29.2	SUERC-84534	This study
Core 1	25-26	Organic Concentrate	n/a	111.95 ± 0.49	1958	1998	-28.442	SUERC-86980	This study
Core 1	25-26	Macrofossil: *Terminalia* seed	n/a	106.43 ± 0.46	1957	2010	-27.4	SUERC-88306	This study
Core 1	25-26	Macrofossil: misc. flowers	20	102.96 ± 0.2	1956	1957	n/a	UCIAMS-223878	This study
Core 1	40-41	Bulk	n/a	110.45 ± 0.50	1958	2001	-29.3	SUERC-84533	This study
Core 1	40-41	Organic Concentrate	n/a	110.46 ± 0.51	1958	2001	-26.746	SUERC-86981	This study
Process standards**									
	Tiri barley mash	Organic Concentrate	n/a	116.71 ± 0.53				SUERC-86984	This study
	96H humin	Organic Concentrate	3390 ± 37	65.57 ± 0.53				SUERC-86989	This study

CORE NAME	DEPTH IN CORE (CM)	SAMPLE TYPE	^{14}C AGE ±1σ	PERCENT MODERN CARBON (%)	MINIMUM CALIBRATED AGE, CAL CE*	MAXIMUM CALIBRATED AGE, CAL CE*	$\delta^{13}C_{VPDB}$‰ (± 0.1)	LAB ID	REFERENCE
	Anthracite	Organic Concentrate	53697 ± 342	0.13 ± 0.01				SUERC-86990	This study
	Tiri barley mash	Pollen Concentrate	n/a	116.50 ± 0.53				SUERC-88315	This study
	96H humin	Pollen Concentrate	3394 ± 37	65.54 ± 0.30				SUERC-88316	This study
	Anthracite	Pollen Concentrate	53762 ± 325	0.12 ± 0.00				SUERC-88317	This study

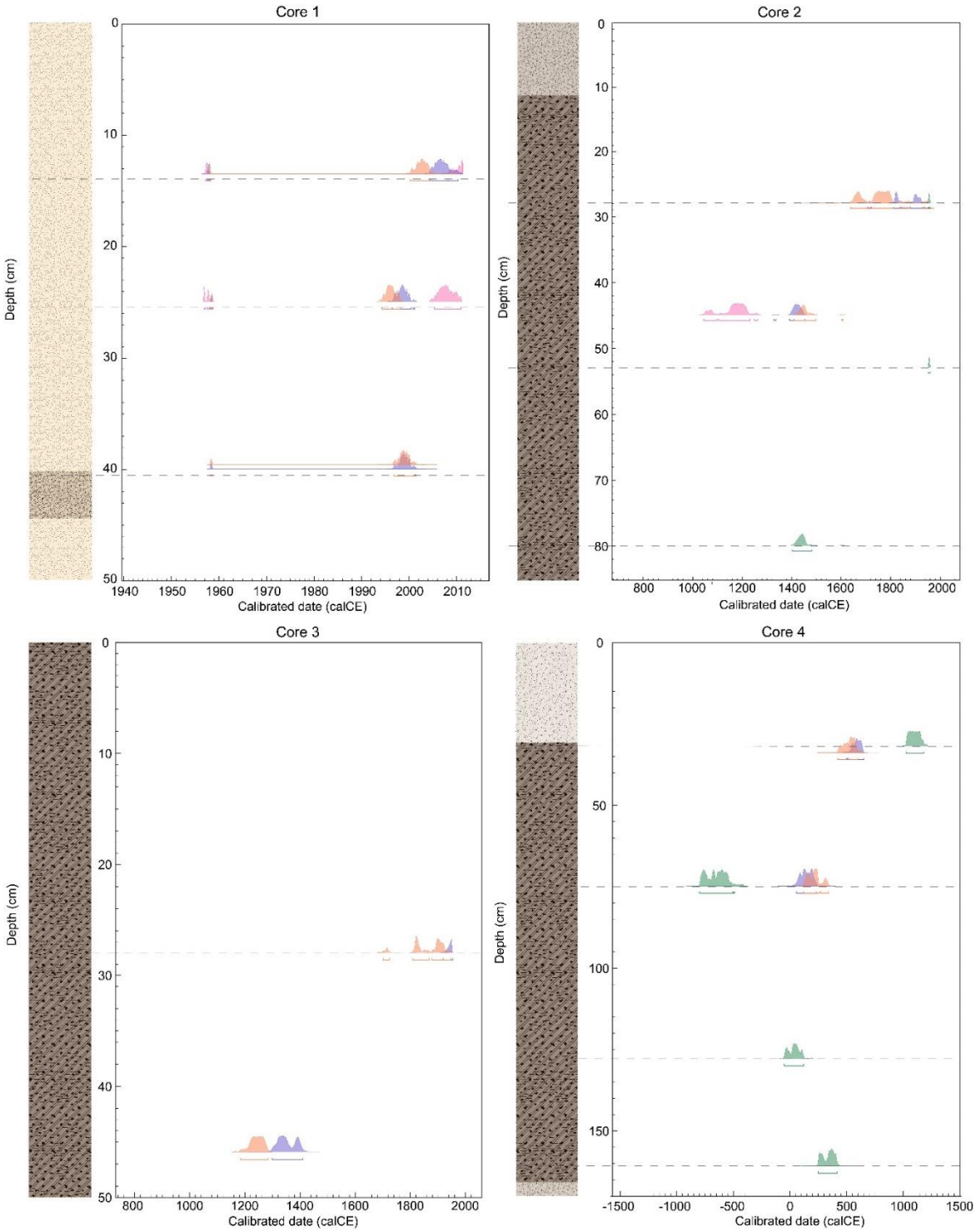

Figure 3.7: Probability distributions of calibrated ages (CE) with depth in Cores 1-4. Ages from Woodroffe et al. (2015a) are in green, bulk sediment ages from this study are in purple, OC ages are in orange, and macrofossil ages in pink. Core stratigraphy key is the same as in Figure 3.3. Plotted age ranges are the 95% range using OxCal 4.3 (Bronk Ramsey, 2009).

In Core 1, which is the site with highest quantities of carbonate sand and closest to the modern beach, I compare bulk, organic concentrate and macrofossil 2σ calibrated ages collected from three depths: 13.5 cm, 25 cm, and 45 cm depth. All ages at all depths in this core were calibrated using the Calibomb calibration curve (Hua et al., 2013), and all ages in the entire core overlap at 2σ ranges (Figure 3.7). However, the comparable bulk and organic concentrate ages appear closer in age than equivalent macrofossils, which are in this case large >3 cm diameter *Terminalia catappa* seeds, (a common tree on the coastal plain of Mahé), and some small (~500 µm to 1 mm), unidentified flowers. Further material (identified under a microscope) that had potential for ^{14}C measurements was found at all three depths and was mostly composed of chitin. The flower macrofossil sample at 25 cm depth has a narrow age range (1956-1957 cal CE) which overlaps with the older portion of age ranges from other samples at that depth. Unfortunately, these samples did not yield enough CO_2 gas for AMS measurements.

In Core 2, I can compare the new calibrated ages with those collected by Woodroffe et al. (2015a) who obtained modern ^{14}C ages at the comparable stratigraphic ranges (at 28 cm and 53 cm). Two new bulk and organic concentrate 2σ age ranges at 28 cm are older than the Woodroffe et al. (2015a) bulk sediment sample, but overlap each other (Figure 3.7). At 45 cm, bulk and organic concentrate ages also overlap and are several hundred years older than the Woodroffe bulk sediment sample at 53 cm. A bark macrofossil also collected at 45 cm depth is ~100 cal CE years older than the comparable bulk and organic concentrate ages. A further sample at 80 cm depth is out of sequence because is younger than the macrofossil sample higher in the sediment sequence.

In the Core 3, with a simpler sand and gravel-rich mangrove peat stratigraphy, I compare two sets of bulk and organic concentrate ages at 28 cm and 46 cm. Bulk and organic concentrate ages overlap at 28 cm and 46 cm depth, but both organic concentrate age ranges stretch slightly older than bulk sediment ages (Figure 3.7).

In Core 4, I can compare the new calibrated ages alongside those collected by Woodroffe et al. (2015b). There are three ages to compare at 32-34 cm (Figure 3.7). New bulk and organic concentrate 2σ age ranges overlap, and the Woodroffe et al. (2015a) bulk sediment sample at 32 cm is several hundreds of years younger than the new dates. At 75 cm there are also three ages to compare, and the bulk and organic concentrate 2σ age ranges also overlap. The Woodroffe et al. (2015a) bulk sediment sample is several hundred years older then the other two organic concentrate and bulk samples at the same depth. Further data (two bulk

sediment radiocarbon measurements, at 128 and 161 cm) previously collected by Woodroffe et al. (2015a) below 75 cm in this sedimentary sequence are out of sequence (one is younger despite being deeper in sequence).

In summary, the new organic concentrate ages are not consistently older than the comparable new bulk sediment ages. One macrofossil sample is older than the equivalent bulk and organic concentrate ages in a pre-bomb sequence (core 2), but this is not consistent with macrofossils collected from a post-bomb sedimentary sequence (core 1).

3.5.2.1 Process standard results

Both the organic and pollen concentrate process standard measurements were within 2σ of the consensus values (for the Tiri Barley Mash and Humin), and within error of the process background for anthracite (Table 3.1).

3.5.2.2 Stable carbon isotopes

Stable carbon isotopes ($\delta^{13}C$ ‰) on all samples are consistent with values from mangrove plant material and sediments in previous literature (e.g. Khan et al., 2019; Vane et al., 2013). This gives confidence that carbon sampled for radiocarbon measurements is mangrove-derived (Figure 3.8), and consistent with a terrestrial origin with no evidence of a contribution from marine carbon. The median value for bulk sediment samples from this study and from the Woodroffe et al. (2015a) study is -28.45 ‰. Median values for OC and macrofossils samples are -27.7 ‰ and -27.4 ‰, respectively.

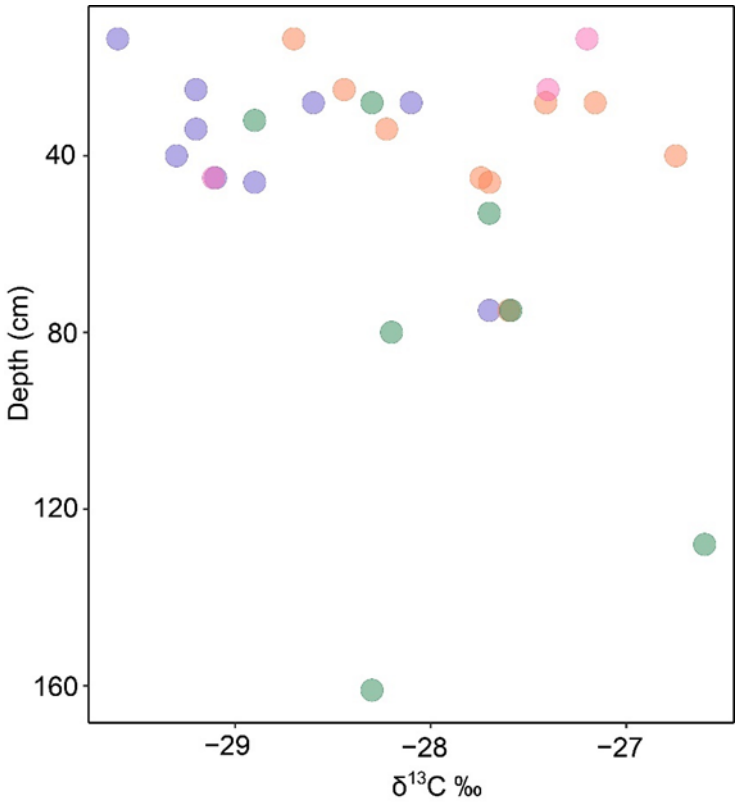

Figure 3.8: $\delta^{13}C$ ‰ values for all radiocarbon samples from this study and Woodroffe et al. (2015a), plotted against sample depth. Errors are ± 0.1 ‰ and are smaller than the points on the graph. Ages from Woodroffe et al. (2015a) are in green, bulk sediment ages from this study are in purple, OC ages are in orange, and macrofossil ages in pink

3.6 Discussion

3.6.1 Bulk sediment vs. organic concentrates

The results demonstrate that at Grand Anse, bulk sediment and organic concentrate samples from mangrove sediment cores are both from carbon sources that cannot be distinguished using radiocarbon measurements. Organic concentrate samples from mangrove cores in Tanzania are considerably older than their equivalent bulk sediment samples (Woodroffe et al., 2015a), leading to the suggestion that older carbon more representative of the 'depositional age' of the sediment is concentrated into finer sediment fractions. The Seychelles cores presented here are not consistent with this hypothesis, as bulk and organic concentrate age ranges overlap.

The $\delta^{13}C$ values collected as part of the radiocarbon measurements indicate that both bulk and organic concentrate samples are likely sampling a mangrove organic carbon pool (Figure 3.8), as values are consistent with those measured in other mangrove sediments (Kemp et al., 2019; Khan et al., 2019b; McKee et al., 2002; Sen and Bhadury, 2017). Fine root material (of the size 10-63 µm) and/or degraded root material may still be present in relatively large amounts in the organic concentrates at Grand Anse. Fine root material and degraded structureless organic matter are visible under light microscopy in the organic concentrate samples (Figure 3.5).

Another possibility as to why bulk and organic concentrate ages from the Grand Anse cores are similar could be because above-ground mangrove carbon contributes very little to peat formation. This scenario means that it is mostly root matter that is available for radiocarbon measurements in all sediment size fractions, and this is therefore not representative of the depositional age of the sediment at that elevation. Carbon derived from above-ground sources like leaf litter or timber is considered a contributor to mangrove sediment/peat formation in general, but quantitative constraints on this are rare or non-existent and there is large geographic variation (Krauss et al., 2014). Timber and roots are more resistant to degradation than leaf litter (Castañeda-Moya et al., 2011; Middleton and McKee, 2001; Saintilan et al., 2013). While mangroves generally produce large amounts of leaf litter (Saenger and Snedaker, 1993), there are specific conditions that lead to their preservation in the sediment column: limited tidal flushing of leaves, low numbers of leaf-consuming crabs, high sedimentation and/or accretion rates and low rates of decomposition (McKee, 2011; Middleton and McKee, 2001; Sukardjo et al., 2013). Unless these conditions are met (in both the present and past), it is more likely that roots and large pieces of timber contribute to peat formation rather than leaf litter. Therefore, it is plausible that humified above-ground carbon is not readily available for radiocarbon dating in an organic concentrate sample.

Even if above-ground carbon makes its way into the sediment column, it can be preferentially degraded or exported in comparison to root-derived carbon. Recent studies have highlighted the importance of porewater exchange in the oxidation and export of carbon deposited in mangrove sediments (Bouillon et al., 2007; Maher et al., 2017; Tait et al., 2016). Tidal pumping and river discharge drive the transport of both particulate and dissolved organic carbon from mangrove sediments, and crab burrows are considered major conduits (Gleeson et al., 2013; Stieglitz et al., 2013). Importantly, Maher et al. (2017) find that it is not just modern organic carbon being exported but also century-old mangrove carbon that is remineralised and exported through porewater exchange. These studies

demonstrate that even if above-ground carbon makes its way into the sediment column, it is still susceptible to being 'leached out' through post-depositional oxidation via tidal and groundwater pumping and crab burrowing.

The Woodroffe et al. (2015a) bulk sediment samples are younger than samples collected stratigraphically above in cores 2 and 4 (Figure 3.7), which suggests that these samples contain higher amounts of younger carbon than organic concentrate or macrofossil samples. In Core 4, the deepest sample (at 161 cm) is nearly 1,000 years younger than a sample nearly one metre above (at 75 cm). While we do not have any organic concentrate or macrofossil ages to compare below 75 cm, this variation suggests that carbon preservation and/or degradation is highly variable across a site (even at short distances), and that one core chronology may not be representative of sedimentation through the whole mangrove at a single core site.

3.6.2 Above-ground macrofossils

The lack of surface macrofossils in the Grand Anse cores indicates that mangrove leaves, seeds, flowers etc. are either being consumed, degraded, or transported away from the mangrove environment before they can be buried and preserved, or post-deposition. At Grand Anse, there are large numbers of both fiddler and red mangrove crabs that rapidly consume fallen mangrove leaves and propagules, meaning the surface sediment is largely clear of any plant debris. Despite this, occasional plant macrofossils were preserved in the cores: *Terminalia catappa* seeds (in Core 1), and undifferentiated bark (in Core 2).

The *Terminalia* seeds may be more likely to be preserved because when they are released from the tree, they tend to fall from a considerable height and hit the ground with a force that embeds them into the upper few centimetres of the surface sediment. Upon deposition they are already partially buried, and their hard outer shells means they are less available for consumption by crabs compared to leaves. However, it is more likely that the sedimentation rate at this part of the mangrove is the reason the *Terminalia* seeds were preserved, as the radiocarbon ages from the *Terminalia* macrofossils are post-1950 in age even at 40 cm depth. In Core 1, the macrofossil radiocarbon ages overlap with the bulk and organic concentrate ages, despite the bulk samples containing modern mangrove roots. The rapid sedimentation rate may have lead to rapid carbon burial and less modern root activity, resulting in similar radiocarbon measurements from different sample types.

The bark sample found in the Core 2 is a dense, woody macrofossil, and this may have contributed to its preservation. Bark grows above ground on the trunks of mangrove trees, but also on mangrove roots (Tomlinson, 2016), so it is not a solely above-ground macrofossil. The radiocarbon measurement on the bark in core 2 is ~100 calibrated years older than the equivalent bulk and organic concentrate samples (Figure 3.7). This indicates that the bark might be closer to the 'true' depositional age than the bulk or organic concentrate as these samples will include a younger root component, although I cannot rule out that the bark could be from an older root rather than above-ground mangrove timber.

3.6.3 Pollen concentrates

Generally, mangrove pollen is considered a robust microfossil as it is more resistant to decay than other fossils such as foraminifera (Grindrod, 1988). However, pollen production in mangroves is seasonal and generally low as the majority of mangrove species rely on insect and animal vectors for pollination (with the exception of *Rhizophora* sp.) (Tomlinson, 2016). Despite the presence of *Rhizophora mucronata* and other terrestrial pollen-producers in the Grand Anse mangrove environment and immediate surroundings, poor pollen preservation in sediments may be a contributing factor to why pollen concentrations were too low for radiocarbon measurements. See also Chapter 4: for further insight into pollen preservation in the Seychelles mangroves. As for the bulk, organic and macrofossil samples discussed above, the transport of pollen to the sedimentary sequence and its preservation potential may be affected by low rates of burial and potentially high rates of degradation in surface sediments at Grand Anse.

3.6.4 Implications

The results of this study indicate that obtaining reliable age/depth profiles that can be used for quantitative RSL reconstructions is challenging in the studied Seychelles mangrove sediment. In the absence of convincing above-ground macrofossils or pollen concentrates, the question remains as to whether a radiocarbon measurement from a bulk or organic concentrate sample can indeed be related to the true age of the deposition of the mangrove sediment at a given elevation.

Under rapidly rising RSL, accommodation space is created and this allows for mangrove sediment surface elevation gain via biogenic accretion and/or minerogenic sedimentation (Krauss et al., 2014; McKee et al., 2007; Murray-Wallace and Woodroffe, 2014). Continual elevation gain increases the likelihood that above-ground macrofossils like leaves are

preserved or contribute to peat formation, and therefore increases the likelihood of preserving older organic carbon more representative of the depositional age at any given elevation. Rapid sedimentation and accretion also reduces the amount of time that sediment at any given elevation is subject to decomposition via crab burrowing and porewater exchange. For example, leaf macrofossils are well preserved at mangrove sites in Belize, which has been undergoing subsidence and therefore continuous RSL rise over much of the Holocene due to the collapse of the forebulge of the Laurentide Ice Sheet (Monacci et al., 2009; Wooller et al., 2007).

During periods of RSL fall or stability, macrofossils and any above-ground carbon is more likely to decompose or be consumed before it is incorporated into the sediment column because it takes longer for the macrofossils to be buried. Similarly, limited accommodation space and therefore low rates of sedimentation or accretion means sediment at a given elevation will, for greater periods, be subject to both reworking via roots and bioturbation, and to degradation via oxidation, in the near-surface biological mixing zone (approximately 0-2 metres). RSL in the Seychelles has been stable and close to present for at least 3,000 years (Woodroffe et al., 2015a), which may be a reason why there is a limited amount of material that is representative of the true depositional age available for radiocarbon dating. Similarly, a global compilation investigating organic carbon storage in coastal wetlands (including mangroves) found that stable or falling RSL conditions over the Holocene generally lead to carbon loss as accommodation space is limited (Rogers et al., 2019).

Sites in Zanzibar, Tanzania experienced a Mid- Late Holocene highstand and RSL has been falling to present day, and organic concentrate ages from these cores are considerably older than their equivalent bulk sediment ages (Woodroffe et al., 2015b). It would appear that even under falling RSL, mangrove sediments in Tanzania have retained older carbon that may more closely represent the true age at the dated elevations. Climate in both coastal Tanzania and Seychelles is tropical and precipitation is dominantly controlled by the seasonal shift of the Intertropical Convergence Zone and Asian Monsoon (Pfeiffer and Dullo, 2006; Punwong et al., 2013a), making this an unlikely reason for any regional variability in organic carbon decomposition and preservation. The sedimentology of the stratigraphy sampled for radiocarbon dating varies slightly on a qualitative, descriptive basis: samples from Zanzibar are collected from an organic sand, whereas a majority of the samples from Seychelles cores are dominantly organic-rich (peat), but still have siliclastic sand and gravel components (Figure 3.3). Some studies have found that sediment texture and structure can influence mangrove root production (Gill and Tomlinson, 1977; McKee, 2001), and more generally,

sediments with higher bulk density decrease root growth (Kozlowski, 1999). However, sedimentology does not necessarily influence porewater exchange rates, and crab burrow density is thought to be a more important influence (Tait et al., 2016). Without further quantitative data on the Zanzibar sedimentology, we cannot rule out the influence of sedimentology on the apparent preservation of an older carbon fraction. Similarly, without observations of burrowing crab density and burrow depth, we cannot determine whether the Zanzibar site has less crab bioturbation, which might lead to better preservation of older carbon. Local hydrology and tidal flooding conditions may also contribute to root production, and to the preservation or degradation of older carbon (Castañeda-Moya et al., 2011; McKee et al., 2007; Poret et al., 2007).

A key difference in the Seychelles study compared with the Zanzibar study is a majority of the Seychelles samples are collected from the sediment depth (0-2 metres) within the near-surface biological mixing zone. While this is still the case for the Zanzibar study, the Zanzibar samples are deeper within the sediment column and may be less influenced by modern bioturbation. As a unit of sediment at a given depth transitions out of the near-surface biological mixing zone through sedimentation or accretion, a portion of this sediment unit no longer interacts with modern carbon sources and is preserved. While modern roots may still penetrate this sediment unit, it is to a much lesser extent and therefore likely contributes less younger carbon that higher up in the sediment column (Figure 3.1). Therefore, this is another potential reason why the Zanzibar organic concentrate samples are older than the bulk sediment samples. The Zanzibar organic concentrate samples may be a 'relict' of this organic carbon which was preserved *in situ* as that sediment depth transitioned out of the biological mixing zone, although the bulk sediment samples still contain the remnants of the last penetrating roots (and therefore produce younger ^{14}C ages).

3.7 Conclusions

While it is clear that we require further studies in different localities to test the reliability of using organic concentrate radiocarbon ages, it is likely that organic concentrate samples in both the Seychelles and in Zanzibar do not necessarily sample an older organic carbon source that is representative of the depositional age at a given elevation. The Seychelles samples show that when collecting samples in the modern mixing zone, bulk and organic concentrate ages are sampling the same organic carbon sources, but the Zanzibar samples show that once out of the mixing zone, organic concentrate samples do sample a relatively older carbon source than the bulk sediment sample. This shows that there is still value in

sieving a finer fraction for radiocarbon dating, as an organic concentrate sample is more likely to be closer to the true depositional age than one that still contains large root matter. However, organic concentrate samples may still be younger than the true depositional age due to their time spent in the mixing zone.

Researchers seeking to reconstruct Late Holocene sea level using mangrove sediments should therefore consider carefully the materials used for radiocarbon dating to create sea-level index points. Macrofossils that are distinctly from above-ground mangrove sources are the most ideal material to use for constructing age models. Organic concentrate samples are more reliable than bulk sediment ages, however these should be considered as minimum ages as it is likely the influence of roots and porewater exchange will result in a younger age. It is challenging to incorporate this unidirectional uncertainty from organic concentrate samples into horizontal and vertical error terms on a sea-level index point. Assigning uncertainty based on the maximum depth of mangrove root penetration and crab bioturbation and using an organic concentrate radiocarbon age to determine sedimentation rates is circular reasoning as organic concentrate ages are most likely to be younger than the age of deposition by an unknown amount. One potential method would be to use independent dating techniques to estimate sedimentation rates (e.g. ^{210}Pb or ^{137}Cs) to predict a likely radiocarbon age for a given depth and compare to a measured radiocarbon age that will presumably include additional younger carbon from its time in the mixing zone. In the absence of independent age control using these methods, uncertainty can only be considered qualitatively, where faster accumulating sequences have relatively smaller age uncertainties then slower accumulating sequences, which is likely affected by the nature of RSL changes during the period of investigation.

While our understanding of below-ground carbon dynamics in mangrove environments is increasing, further research should attempt to identify quantitatively what components of mangrove trees (e.g. timber, roots, leaf litter) contribute to peat and/or sediment formation (or are preferentially decomposed). Preferably, future work should focus on sites in a variety of settings, in particular those outside of the well-studied Caribbean region where studies often find well-preserved mangrove macrofossils for ^{14}C dating. In particular, identifying specific compounds formed uniquely by above-ground material such as mangrove leaves could be future targets for compound-specific radiocarbon dating (see Chapter 5:).

Chapter 4: Assessing the use of mangrove pollen as a quantitative sea-level indicator on Mahé, Seychelles

4.1 Introduction

Organic coastal sedimentary deposits are important archives of palaeoenvironmental change and are widely used to understand coastline evolution and reconstruct relative sea level (RSL) changes (Barlow et al., 2013; Ellison, 2008; Shennan, 1986). In temperate and high latitude regions, the organic sediments of salt marshes can provide high-resolution (decimetre-scale) RSL records using microfossil-based transfer functions (Gehrels, 2000; Kemp et al., 2009; Scott and Medioli, 1978; Woodroffe and Long, 2009; Zong and Horton, 1999). An enhanced global spread of detailed Holocene RSL reconstructions are necessary to improve our understanding of the climatic and geophysical processes influencing RSL prior to the satellite and historical eras (Horton et al., 2018). However, low latitude coastlines and their respective organic sediments are relatively under-studied compared to their temperate counterparts.

Mangroves occupy large areas of coast in low latitude regions and occupy a similar ecological niche to salt marshes, and have therefore been used to understand Holocene RSL changes (Bird et al., 2010; Horton et al., 2005a; Scholl, 1964a; Tam et al., 2018; Woodroffe, 2009b; Woodroffe et al., 2015a). Yet quantitative reconstructions remain challenging due to the poor preservation of fossil foraminifera and diatoms that are traditionally used for transfer functions (Barker et al., 1994; Debenay et al., 2004; Woodroffe et al., 2005). This preservation issue has meant a majority of palaeoenvironmental reconstructions from mangrove sediments are derived from pollen records (Behling et al., 2004; Grindrod, 1985; Urrego et al., 2013; Woodroffe et al., 1985). Mangrove sediments can provide conditions that are suitable for pollen preservation: anoxia and reducing conditions, low pH, and high salinity (Grindrod, 1988; Phuphumirat et al., 2015).

Mangrove species are thought to have highly localised pollen dispersal (Grindrod, 1985). This is an important observation, as unlike foraminifera or diatoms, pollen does not enter sedimentary sequences autochthonously. Mangrove pollen can be transported via birds, insects and mammals, winds, and tidal or fluvial currents before deposition, although a majority of mangrove species are pollinated via insect and bird vectors (Tomlinson, 2016). Mangrove species zonation is considered to be controlled by duration and frequency of tidal

inundation (Crase et al., 2013; Leong et al., 2018), which is strongly associated with elevation and salinity. Thus, mangroves with strong (elevation-controlled) zonation patterns and highly localised pollen dispersal are potential candidates for quantitative RSL reconstructions, if pollen assemblages in surface sediments accurately and precisely reflect modern vegetation zonation.

Pollen in mangrove surface sediments has been found to broadly reflect these zonation patterns in a number of modern mangrove environments (Behling et al., 2001; Cohen et al., 2008; Grindrod and Rhodes, 1984; Li et al., 2008; Mao et al., 2006; Urrego et al., 2009). This relationship has also led to the use of pollen assemblages for quantitative RSL reconstructions (Ellison, 1989; Engelhart et al., 2007; Punwong et al., 2018), which generally yield smaller uncertainties on sea-level index points than those constructed with a general mangrove sediment indicative range. However, despite detailed modern observations in mangroves, there is little information available on the exact process and timeline of the transport of mangrove pollen from tree to sedimentary deposit. Measuring modern pollen rain using pollen traps in mangroves is challenging because of the need to site traps above the level of tidal inundation and issues with high annual or seasonal rainfall that collects in and can overflow the traps taking with it the pollen rain (Behling et al., 2001; Grindrod, 1985; Jantz et al., 2013). Despite this difficulty, mangrove pollen transport processes need to be further investigated to increase the utility of pollen in quantitative RSL reconstructions.

To test the use of mangrove pollen as a quantitative sea level indicator in a small island microtidal mangrove environment, I investigated modern mangrove pollen from two mangroves from the Seychelles (Figure 1.3), using a combination of field mapping, pollen traps and surface sediment samples. I chose to work in the mangroves of the Seychelles because this is a critical location for understanding Late Holocene eustasy, and mangrove pollen distributions in small mangrove stands on tropical islands such as the Seychelles have not yet been fully investigated. Previous mangrove- and coral-derived RSL reconstructions from Seychelles provide a framework to test whether palynological approaches can improve vertical uncertainties and provide more detailed insight into Late Holocene eustasy (Braithwaite et al., 2000; Camoin et al., 2004; Woodroffe et al., 2015a).

I find that pollen collected in traps deployed over the whole elevation range of mangrove environments in the Seychelles for a year show that overall mangrove pollen production is relatively low compared to temperate intertidal settings (Long et al., 1999; Neulieb et al., 2013). I find that while modern vegetation zonation is related to elevation above mean tide

level (MTL), the association between plant and pollen trap data is not consistent between mangrove species. Additionally, very low pollen concentrations are detected in surface sediments which do not enable the assessment of pollen transport mechanisms. These results suggest that the Seychelles mangroves, with their small lateral extent and narrow connections to open marine environments, are not suitable for pollen-based quantitative RSL reconstructions. Sediment grainsize, variable sediment saturation levels, and low sedimentation rates may contribute to degradation of pollen post-deposition. Rather, the presence of mangrove pollen in a sediment sequence is indicative of a clear mangrove (and therefore intertidal) depositional environment and aids interpretation where depositional environment may be unclear from sedimentological descriptions (e.g. mangrove vs. freshwater peat).

4.2 Study site

Two mangrove areas were selected for the pollen trap study: Grand Anse and Anse Boileau (Figure 4.1) on the west coast of the island of Mahé (Figure 1.3). Up to nine different mangrove species are reported from mangrove forests in the Seychelles (Spalding et al., 2010). Generally, mangrove forests on Mahé are characterised by five species: *Rhizophora mucronata*, *Sonneratia alba*, *Bruguiera gymnorrhiza*, *Avicennia marina* and *Lumnitzera racemosa*. Minor populations of *Xylocarpus granatum*, *Ceriops tagal* and *Nypa fruitcans* are present, as well as minor and associate mangrove species *Acrostichum aureum*, *Casuarina equisetifolia* and *Pandanas* sp. occurring near to the terrestrial forest transition. The adjacent terrestrial coastal plain is mostly comprised of a beach plateau, which is a supratidal feature of the coastal zone around Mahé and formed during the Late Holocene as sediment supply from the fringing reef system moved onshore as RSL stabilised (Woodroffe et al., 2015a). Lowland forest on this coastal plain is dominated by *Cocos nucifera* (coconut palm), *Terminalia catappa* (sea almond), *Calophyllum inophyllum* (Takamaka) and *Mimusops* sp. (Vesey-Fitzgerald, 1940). The Mahé mangroves can be described as a mix of riverine and fringe mangroves, using the ecological classification of Lugo and Snedaker (1974), and are inundated daily by tides.

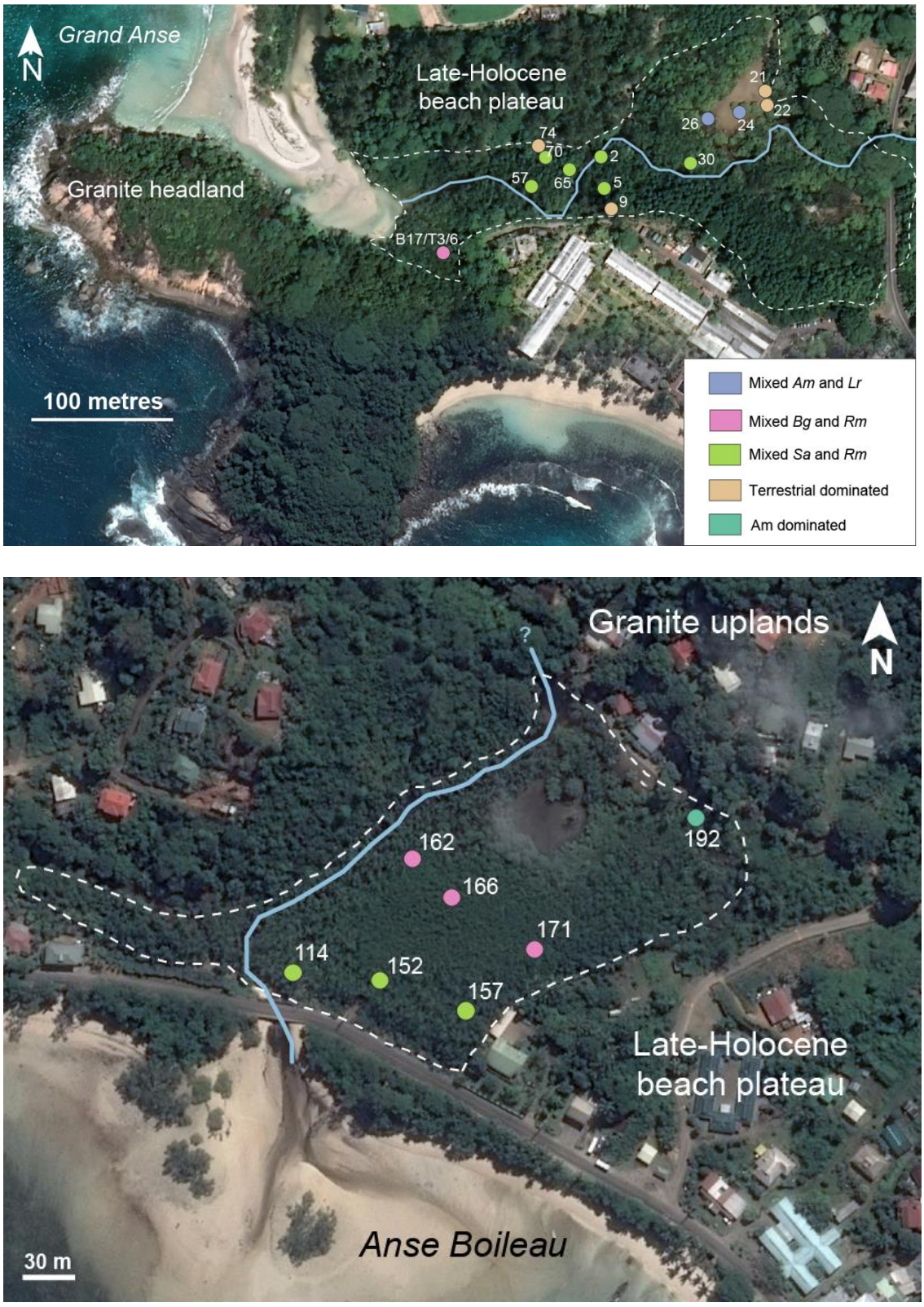

Figure 4.1: Top figure shows pollen trap and equivalent surface sample site locations at Grand Anse mangrove area. Sample sites are coloured by mapped vegetation zones, mangrove extent is marked by the dashed white line and light blue lines are site rivers (the River Dauban at Grand Anse, and the River Cayman at Anse Boileau). Mapped vegetation zone at each sample site is shown in the colour legend, where Bg or Bruguiera is Bruguiera gymnorrhiza, Am is Avicennia marina, Lr is Lumniztera racemosa, Sa is Sonneratia alba, and Rm is Rhizophora mucronata. Bottom figure as for top but for the Anse Boileau mangrove area.

4.3 Methods

4.3.1 Field methods

Vegetation was mapped and surveyed at a total of 188 sites (129 at Grand Anse, 59 at Anse Boileau) by recording key plant species within a <2 metre radius of the sample location within the mangrove zones (see Appendix Table A2 and A3). The non-mangrove vegetation identified was generally restricted to major species present on the beach plateau. Sample sites were selected to cover a range of geomorphological, sedimentological and plant species compositions within each of the mangrove sites. Site elevations were surveyed using a theodolite and staff, and a Van Essen Instrument water level logger was deployed to characterise the tidal timings and amplitudes at the Grand Anse mangrove for a duration of ~15 days. Data collected from the water level logger was compared to observations from the Point La Rue tide gauge (UHSLC 2019), and sample elevations were related to mean tide level (MTL) from timed water level measurements in calm-water locations in the mangrove. While there is a minor timing offset between the tide gauge measurements and the logger data (~25 minutes later at the west coast Grand Anse site compared to the east coast Point La Rue tide gauge), when this was corrected for the tidal amplitudes between Grand Anse and Point La Rue are comparable and within the 0.1 metre error resulting from the predicted tidal amplitudes (*Admiralty Tide Tables*, 2017). Given the proximity of the two sampled locations of Anse Boileau and Grand Anse (~3 km), the tidal logger data from Grand Anse is considered representative of both sites.

4.3.2 Pollen traps

Pollen traps were designed following previous modern pollen rain studies in mangroves (Behling et al., 2001) and tropical rainforests (Jantz et al., 2013). Traps were constructed from 50 mL plastic tubes (~11 cm in length, ~3 cm diameter opening), and filled with ~4 mL of liquid glycerol. The glycerol acts as a 'repository' medium for pollen entering the trap, as it is denser than the rainwater that would accumulate (and overflow) overtime in the trap. Trap openings were covered with mosquito netting to prevent insects entering the trap. Importantly, to avoid tidal inundation and hence preserve the modern pollen rain unaffected by tidal or fluvial flow, traps were attached to plastic-coated bamboo poles inserted into the sediment and above the predicted maximum tidal inundation level. The collecting period was one year between July 2017 and July 2018. A total of 33 traps were set in 2017, and 20

remained on collection in 2018 (Figure 4.1). After collection samples were refrigerated at 4°C until laboratory analysis could be undertaken. Trap samples were washed and centrifuged with deionised water to concentrate accumulated organic material. Pollen was isolated using standard laboratory methods (Moore et al., 1991), including addition of one *Lycopodium* spore tablet, alkali digestion, sieving at 180 µm, and acetolysis, and were stained before mounting on microscope slides.

4.3.3 Surface sediment samples

Surface sediment samples (top <1 cm of sediment) from immediately underneath each pollen trap location were collected at the same time as the traps (July 2018), and stored at 4°C until laboratory analysis could be undertaken. Surface sediment samples were also collected for grain size analyses (Chapter 5:) and total organic carbon (TOC) analyses (Chapter 5:). Pollen was isolated from mangrove sediment following standard procedures as above for the pollen trap samples, but with the inclusion of a hydrofluoric acid digestion step to remove minerogenic particles.

4.3.4 Pollen counting and identification

A minimum count of 200 pollen grains (not including *Lycopodium* spores) was attempted for each pollen trap and surface sediment sample. However as pollen concentrations were low, a number lower than 200 was used when more than two entire pollen slides per sample were required to achieve 200 counts. Pollen was identified using published references (Mao et al., 2012, 2006; Thanikaimoni, 1987) and the online Australasian Pollen and Spore Atlas (The Australasian Pollen and Spore Atlas, 2019). Mangrove pollen grains were identified to species level, with the exception of *Bruguiera* and *Ceriops* species, which are not distinguishable with light microscopy and are thus grouped together (Engelhart et al., 2007; Punwong et al., 2013a). The most commonly occurring non-mangrove pollen grains were identified to genus or species level, but were otherwise grouped together as 'non-mangrove'. The total sum excludes fungal spores, and for further analysis was amalgamated into two groups: mangrove and non-mangrove pollen. Total mangrove counts were also subdivided further into three groups: major, minor and associate elements as per (Mao et al., 2012; Tomlinson, 2016). Percentage counts of taxa, counts, and concentration calculations are available in Appendix Table A1. Pollen accumulation rates are likely to be under-estimates, because there was considerable variability in the condition of the mosquito nets on the traps upon collection (as the mosquito net reduces the area available for pollen

to accumulate). I calculate pollen accumulation assuming the net covering did not impede pollen accumulation and based on the saturated weights of the organic residue collected in pollen traps (and before laboratory treatment).

4.3.5 Statistical analyses

To evaluate the relationship between modern vegetation and pollen trap samples, I calculated a number of indices proposed by Davis (1984): 1) the association index (A) which measures whether the presence of a pollen type indicates the presence of the parent plant species in the local environment, 2) the under-representation index (U), which measures under-representation of pollen types when the parent plant species is present in the local environment, and 3) the over-representation index (O), which measures the over-representation of pollen types where a parent plant species is absent in the local environment. These indices are calculated by the formulae:

$$A = \frac{\mathrm{B}_0}{\mathrm{P}_0 + \mathrm{P}_1 + \mathrm{B}_0}$$

$$U = \frac{\mathrm{P}_1}{\mathrm{P}_1 + \mathrm{B}_0}$$

$$O = \frac{\mathrm{P}_0}{\mathrm{P}_0 + \mathrm{B}_0}$$

where B_0 is the number of sites where both the pollen type and the parent plant species are present in the local environment, P_0 is the number of sites where the pollen type is present but the parent plant species is absent in the local environment, and P_1 is the number of sites where the pollen type is absent but the a plant species is present in the local environment. These semi-quantitative indices are useful because the small areal extent of the Grand Anse and Anse Boileau mangroves does not permit traditional quantitative quadrat vegetation mapping, and therefore regression analysis between modern vegetation and pollen trap samples cannot be undertaken (e.g. Davis, 1984; Urrego et al., 2009).

To determine possible ordination of pollen trap data with respect to environmental variables, I performed canonical correspondence analysis (CCA), and to test ordination of data with respect to environmental variables (e.g. elevation, distance from open shore, and modern vegetation zone) (Engelhart et al., 2007; Urrego et al., 2010, 2009). The analyses were performed in *R* (version 3.6.1) using the 'vegan' and 'cluster' packages (Maechler et al., 2019; Oksanen, 2019), and plotting of results using 'ggplot2' and 'rioja' packages (Juggins, 2017; Wickham, 2016).

4.4 Results

4.4.1 Modern vegetation

At Grand Anse, sites proximal to the river channel are generally dominated by *Sonneratia alba* and *Rhizophora mucronata* mangroves, with *Bruguiera gymnorrhiza* and *Rhizophora mucronata* inhabiting more interior zones of the mangrove (Figure 4.3). Sites in the most landward section of the Grand Anse mangrove (and generally higher elevations) were dominated by a mix of *Avicennia marina* and *Lumnitzera racemosa*. *Acrostichum aureum* and *Casuarina equisetifolia* dominate the fringes of the mangrove zone near the terrestrial transition. At Anse Boileau (Figure 4.4), vegetation zonation is generally similar to Grand Anse, but more landward/higher elevation zones were dominated by *Avicennia marina* and *Lumnitzera racemosa* is notably absent. Residential development around the fringes of the Anse Boileau mangrove has limited the extent of the zone inhabited by *Acrostichum aureum* and *Casuarina equisetifolia* (which is present at Grand Anse).

Using this survey data from both mangrove sites, mangrove vegetation zones occupy a maximum elevation range between -0.58 to +0.82 m MTL, however different vegetation groups inhabit different elevation ranges (Figure 4.2). *Avicennia marina* and *Lumnitzera racemosa* tend to occupy narrower and higher elevation ranges within the mangrove zone (between +0.21 to +0.53 m MTL at Grand Anse, and between +0.06 and +0.45 m MTL at Anse Boileau), while mixed *Sonneratia alba* and *Rhizophora mucronata* stands occupy the whole of the mangrove zone. The terrestrial dominated vegetation zone is distinctly above all of the mangrove zones.

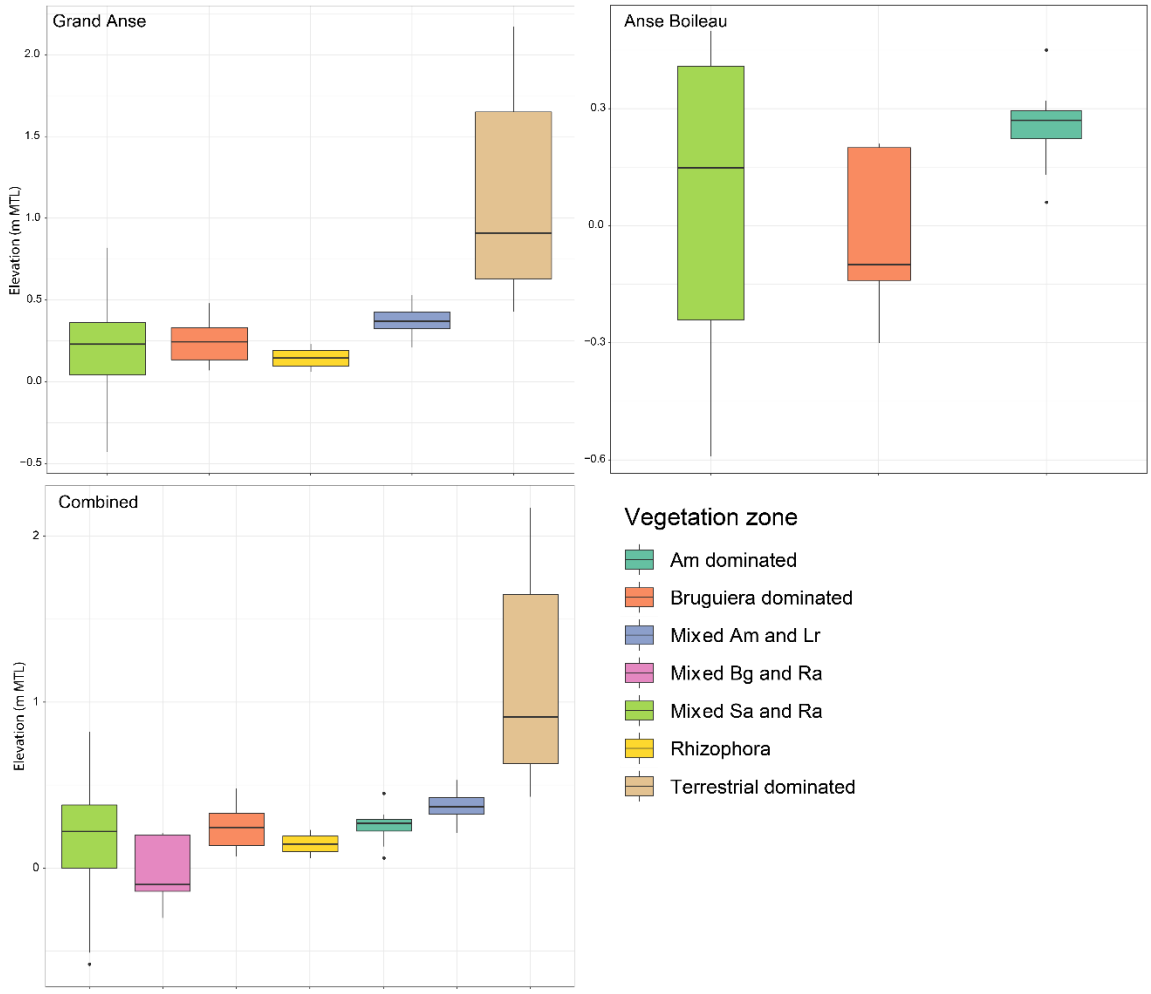

Figure 4.2: Box and whisker plot of mangrove vegetation zones surveyed from Grand Anse, Anse Boileau, and combined datasets (see Appendix Table A2 and A3 for vegetation zone data). Abbreviations in key are: Am (Avicennia marina), Lr (Lumniztera racemosa), Bg (Bruguiera gymnorrhiza), Rm (Rhizophora mucronata), Sa (Sonneratia alba). The Terrestrial dominated zone mapped here includes Casuarina equisetifolia, which although is classed as a minor mangrove species, occurs at the upper edges of the mangrove zone along with other non-mangrove species.

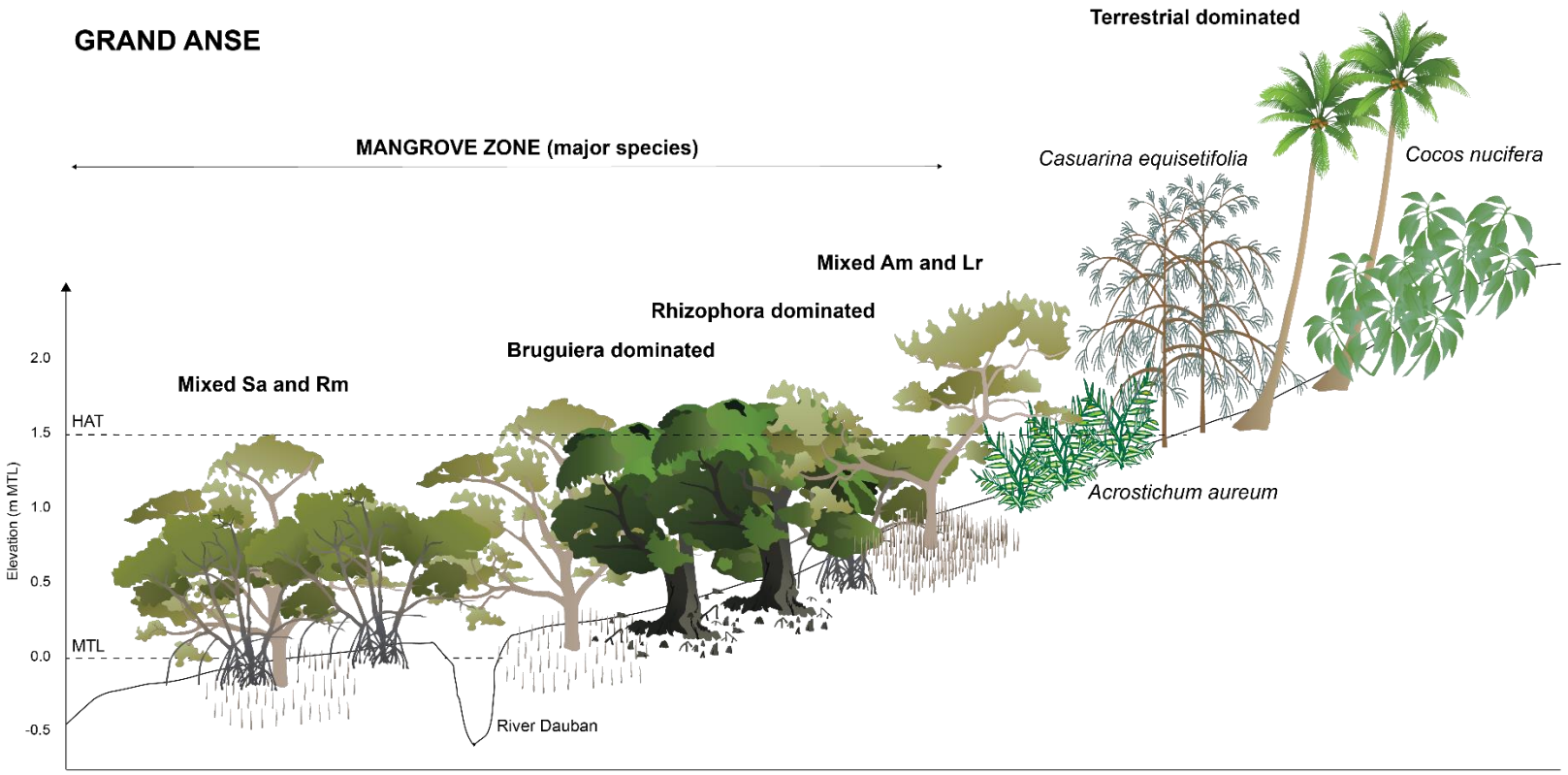

Figure 4.3: Schematic diagram of the surveyed vegetation zones at the Grand Anse mangrove. The overall mangrove zone includes the major species as per the Mao et al. (2012) classification. The zones relate qualitatively to the zones displayed in Figure 4.2. Vegetation key: Sa is Sonneratia alba, Rm is Rhizophora mucronata, Am is Avicennia marina and Lr is Lumnitzera racemosa. Mangrove symbols are courtesy of the Integration and Application Network (ian.umces.edu/symbols/), University of Maryland Centre for Environmental Science.

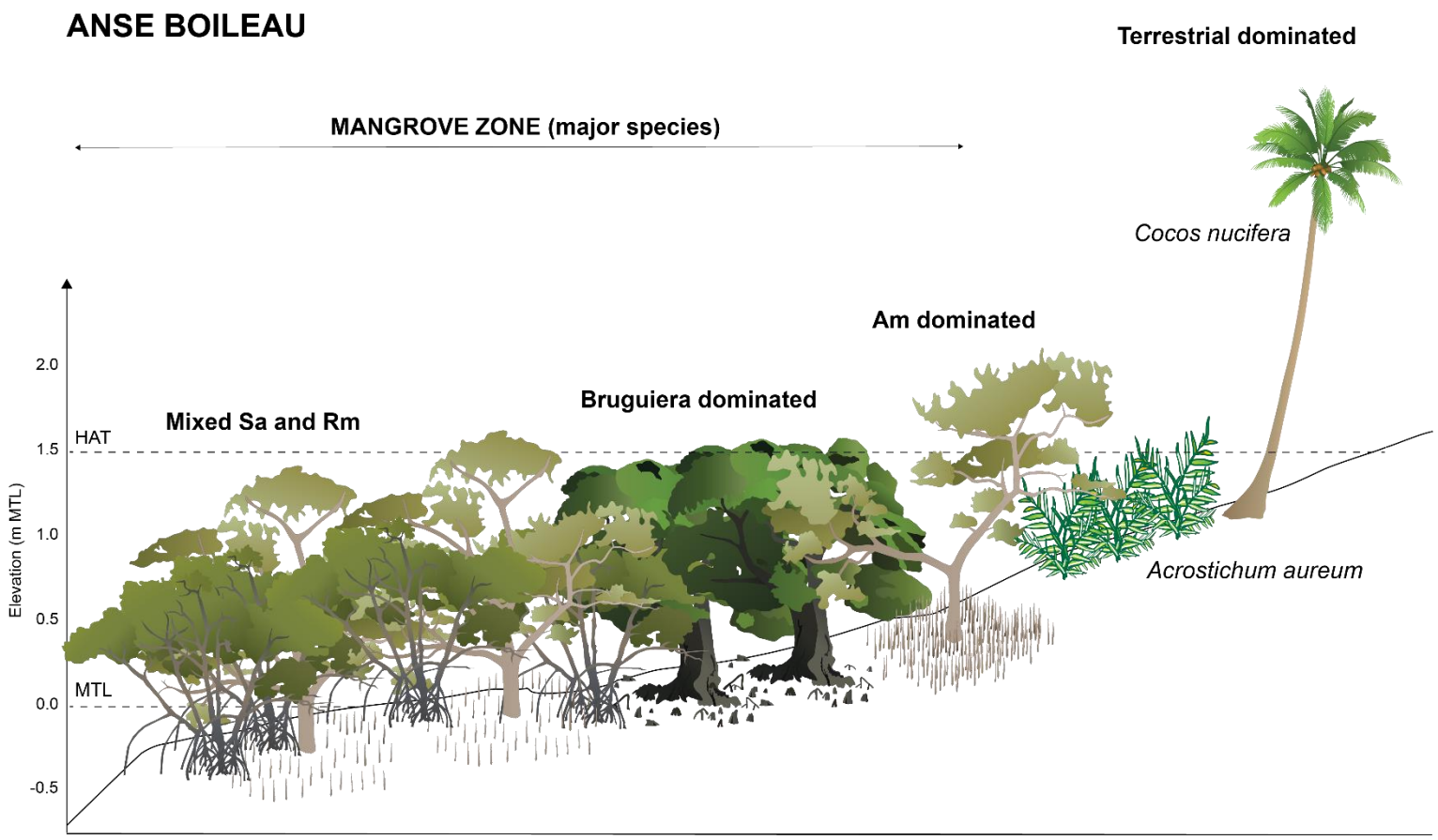

Figure 4.4: Schematic diagram of the surveyed vegetation zones at the Anse Boileau mangrove. The overall mangrove zone includes the major species as per the Mao et al. (2012) classification. The zones relate qualitatively to the zones displayed in Figure 4.2. Vegetation key: Sa is Sonneratia alba, Rm is Rhizophora mucronata, Am is Avicennia marina. Mangrove symbols are courtesy of the Integration and Application Network (ian.umces.edu/symbols/), University of Maryland Centre for Environmental Science.

4.4.2 Pollen trap data

Pollen trap sample abundances (of samples >5% abundance) and pollen group totals are presented along with pollen counts and concentrations in Figure 4.5 and Figure 4.6. Only 10 samples out of 20 pollen traps samples reached the minimum pollen sum of 200 grains, with five samples reaching only 50 grains from two pollen slides. Pollen traps contain five major mangrove pollen species, and considerable abundances of *Casuarina equisetifolia* and *Acrostichum aureum*. Total non-mangrove pollen varies from ~6–57 % abundance in the pollen trap samples, of which *Cocos nucifera* and *Terminalia catappa* are dominant species. At Grand Anse, major mangrove species abundance generally reduces with increasing elevation, while minor and associate mangrove species abundance generally increases with increasing elevation. This pattern is not evident in the Anse Boileau pollen trap data.

Pollen concentrations (grains/gram/year) vary greatly between mapped vegetation zones (Table 4.1). Terrestrial-dominated and mixed *Sonneratia alba* and *Rhizophora mucronata* vegetation zones have pollen concentrations an order of magnitude greater than all other vegetation zones. Averaged pollen trap concentration from Grand Anse is also higher than that of Anse Boileau.

Table 4.1: Average pollen concentrations by mapped vegetation zone.

Mapped vegetation zone	**Average pollen concentration (grains/gram/year)**
Terrestrial dominated (*n* = 4)	65487
Mixed Sa and Rm (*n* = 9)	67557
Mixed Bg and Rm (*n* = 4)	9879
Am dominated (*n* = 1)	1950
Mixed Am and Lr (*n* = 2)	5606
Grand Anse average (*n* = 13)	**58890**
Anse Boileau average (*n* = 7)	**22438**

The A (association), O (over-representation), and U (under-representation) indices are presented in Table 4.2. *Rhizophora mucronata* is the only major species with a high association index (i.e. A ≥ 0.5). *Pandanas tectorious* and *Lumnitzera racemosa* also have high association indices (A = 1.00), although these values are calculated from only one sample in both cases. *Avicennia marina* and *Bruguiera/Ceriops* species have intermediate values (A = ~0.3) which suggests there is still a reasonably close association between species presence and pollen occurrence. Species *Sonneratia alba*, *Casuarina equisetifolia* and *Acrostichum*

aureum have low values (A < 0.2), which indicates that presence of pollen has low association with presence of parent plant species. High over-representation indices can indicate either high or low pollen production rates. *Casuarina equisetifolia* and *Acrostichum aureum* have high O index values which likely indicates high pollen production rates, because their pollen abundances in pollen trap samples are relatively high (i.e. high $\bar{X}_p$ values). A majority of the other species have high O index values (e.g. *Sonneratia alba*) but these are more likely to be low pollen producers as pollen abundances in pollen trap samples are relatively low. *Avicennia marina* and *Sonneratia alba* have high under-representation indices (U = 0.5 and U = 0.67, respectively), and *Bruguiera/Ceriops* has intermediate values (U = 0.43). These three species/groups have concurrently high O index values, which suggests these species have low pollen production rates but have efficient pollen dispersal mechanisms. Species with low U index values and high O index values (e.g. *Nypa fruticans*) indicate poor pollen production and/or dispersal mechanisms.

Table 4.2: Association (A), over-representation (O), and under-representation (U) indices (Davis, 1984) for major, minor and associate mangrove species found in pollen trap sites at Grand Anse and Anse Boileau. B_0 equals the number of samples where both plant species and pollen type is present at a sample site, P_0 equals the number of samples where plant species is absent but pollen type is present at a sample site, and P_1 equals the number of samples where plant species are present but pollen type is absent. See main text for formulae. n is the number of sample sites used to determine indices. Additionally as per Davis (1984), $\bar{X}_p(n)$ is the average pollen percentages in a sample where parent plants are present (n = the number of samples in average calculation), and $\bar{X}_a(n)$ is the average pollen percentages in a sample when parent plants are absent (n = number of samples in average calculation).

Species	**B_0**	**P_0**	**P_1**	**A**	**O**	**U**	***n***	**$\bar{X}_p(n)$**	**$\bar{X}_a(n)$**
Rhizophora mucronata	12	8	0	0.6	0.40	0.00	20	51.8 (11)	11.1 (9)
Bruguiera/Ceriops	4	5	3	0.33	0.56	0.43	12	1.7 (6)	0.8 (14)
Sonneratia alba	1	8	2	0.09	0.89	0.67	11	8.1 (3)	4.2 (17)
Avicennia marina	3	4	3	0.30	0.57	0.50	10	1.3 (5)	0.2 (15)
Lumnitzera racemosa	1	0	0	1.00	0.00	0.00	1	8.3 (1)	0.0 (19)
Xylocarpus granatum	0	2	0	0.00	1.00	0.00	2	0 (0)	0.1 (20)
Heritiera littoralis	0	2	0	0.00	1.00	0.00	2	0 (0)	0.1 (20)
Acrostichum aureum	2	12	0	0.14	0.86	0.00	14	76.3 (2)	3.4 (18)
Nypa fruticans	1	7	0	0.13	0.88	0.00	8	0.4 (1)	0.6 (19)
Casuarina equisetifolia	1	17	0	0.06	0.94	0.00	18	71.4 (1)	19.5 (19)
Pluchea indica	0	2	0	0.00	1.00	0.00	2	0 (0)	0.1 (20)
Aegiceras corniculatum	0	1	0	0.00	1.00	0.00	1	0 (0)	0.1 (20)
Pandanas tectorious	1	0	0	1.00	0.00	0.00	1	0.8 (1)	0.2 (19)

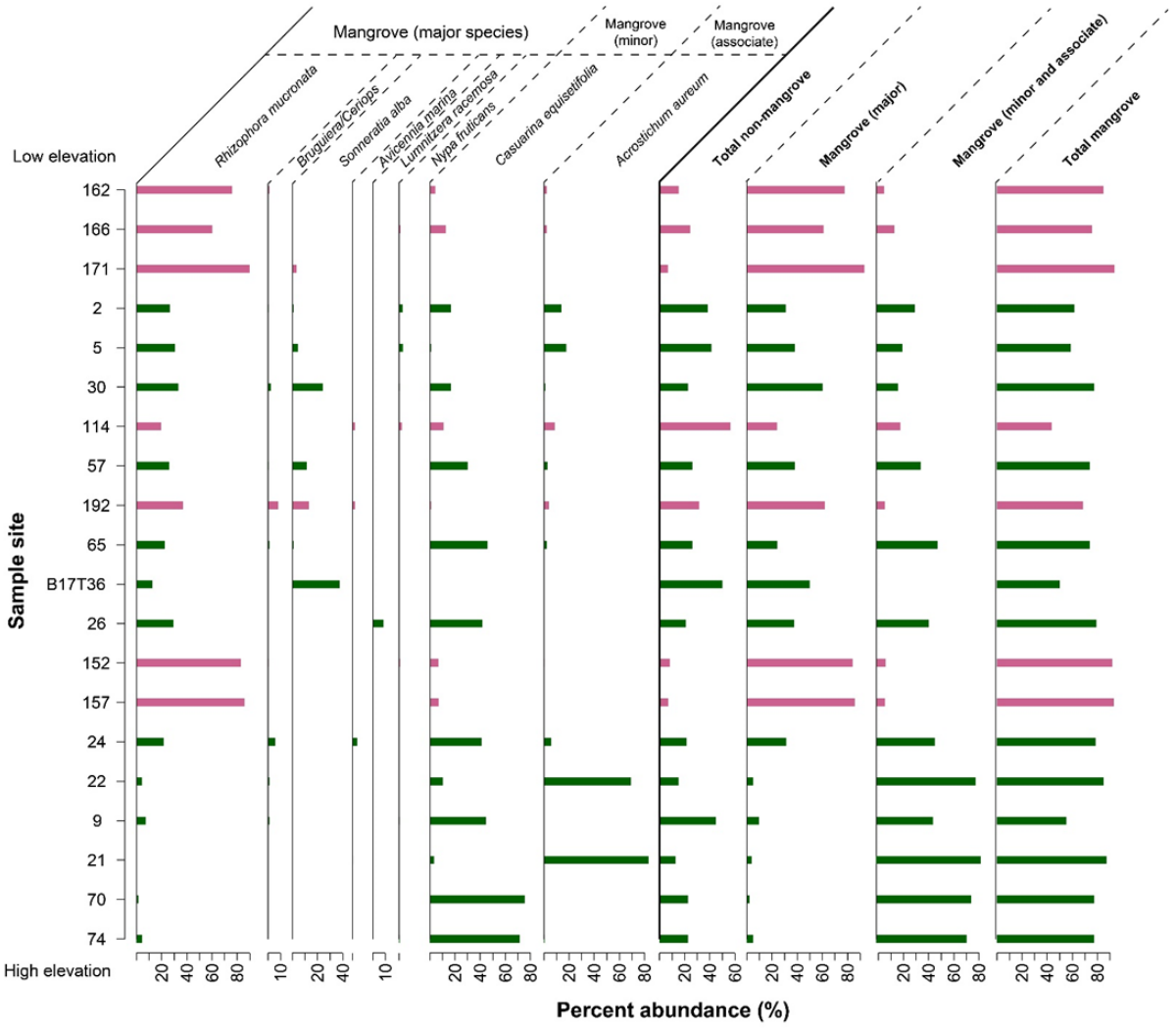

Figure 4.5: Pollen percent abundances for Grand Anse (green) and Anse Boileau (pink) mangrove area pollen traps. Sample sites are ordered by elevation (m MTL). Grouping of mangrove species is consistent with categories in Mao et al. (2012).

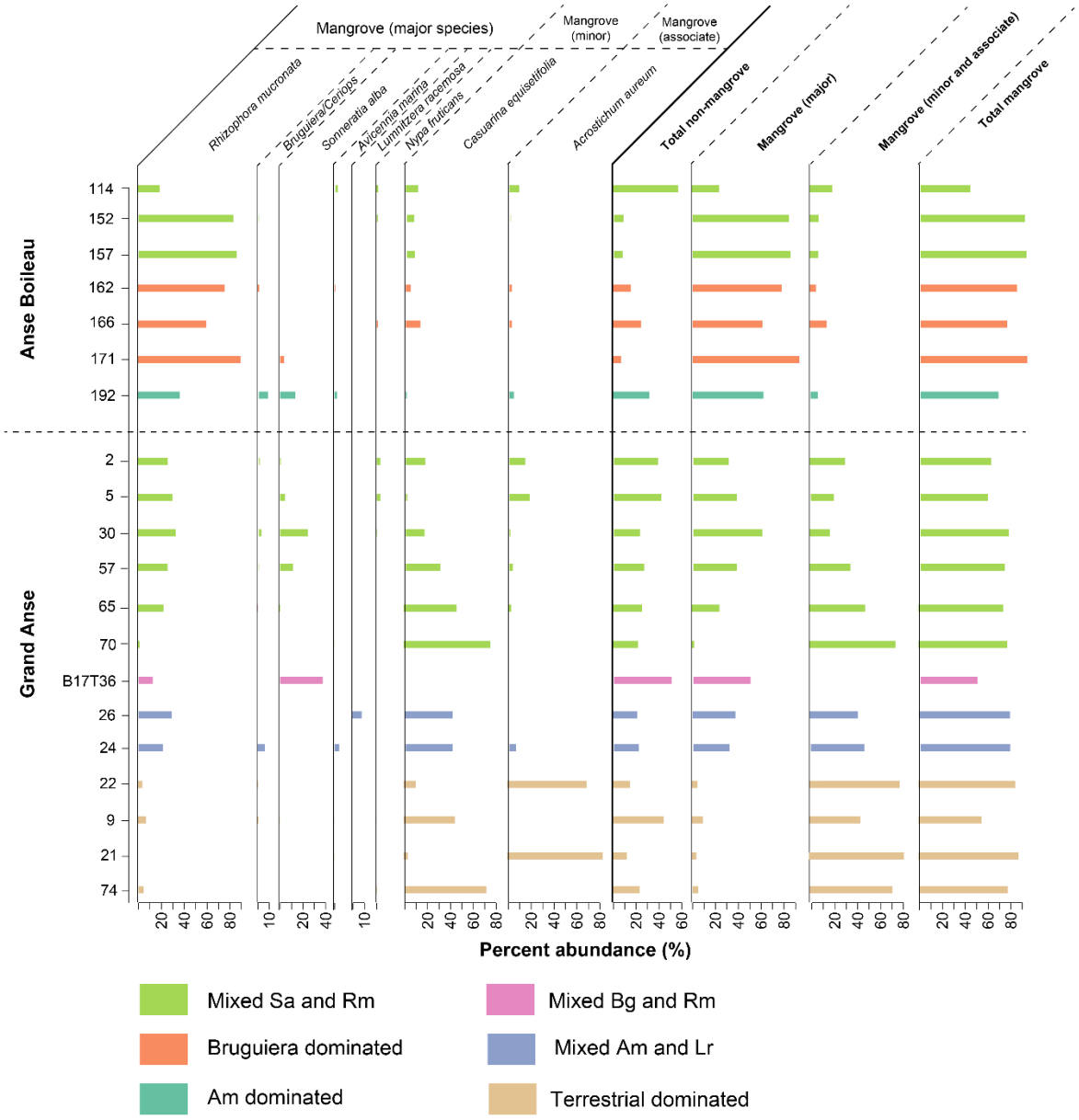

Figure 4.6: Pollen percent abundances separated by site locality and grouped by vegetation zone displayed in Figure 4.2. Grouping of mangrove species is consistent with categories in Mao et al. (2012).

The results of the pollen trap CCA are displayed in Figure 4.7. Environmental variables of distance from shore, TOC and TIC (which are surrogate proxies for other sediment composition and geomorphology) show longest axes and therefore display greatest amount of variance (TOC and TIC data and discussion available in Chapter 5:). Elevation is not a primary control of variance on pollen trap data.

4.4.3 *Surface sediment data*

Surface sediment samples contained very low abundances of pollen (e.g. typically five sample pollen, and similar number of *Lycopodium* marker pollen per microscope slide). Counts were so low that I decided that it was not practical to undertake any further analyses on the surface sediment samples as part of this study.

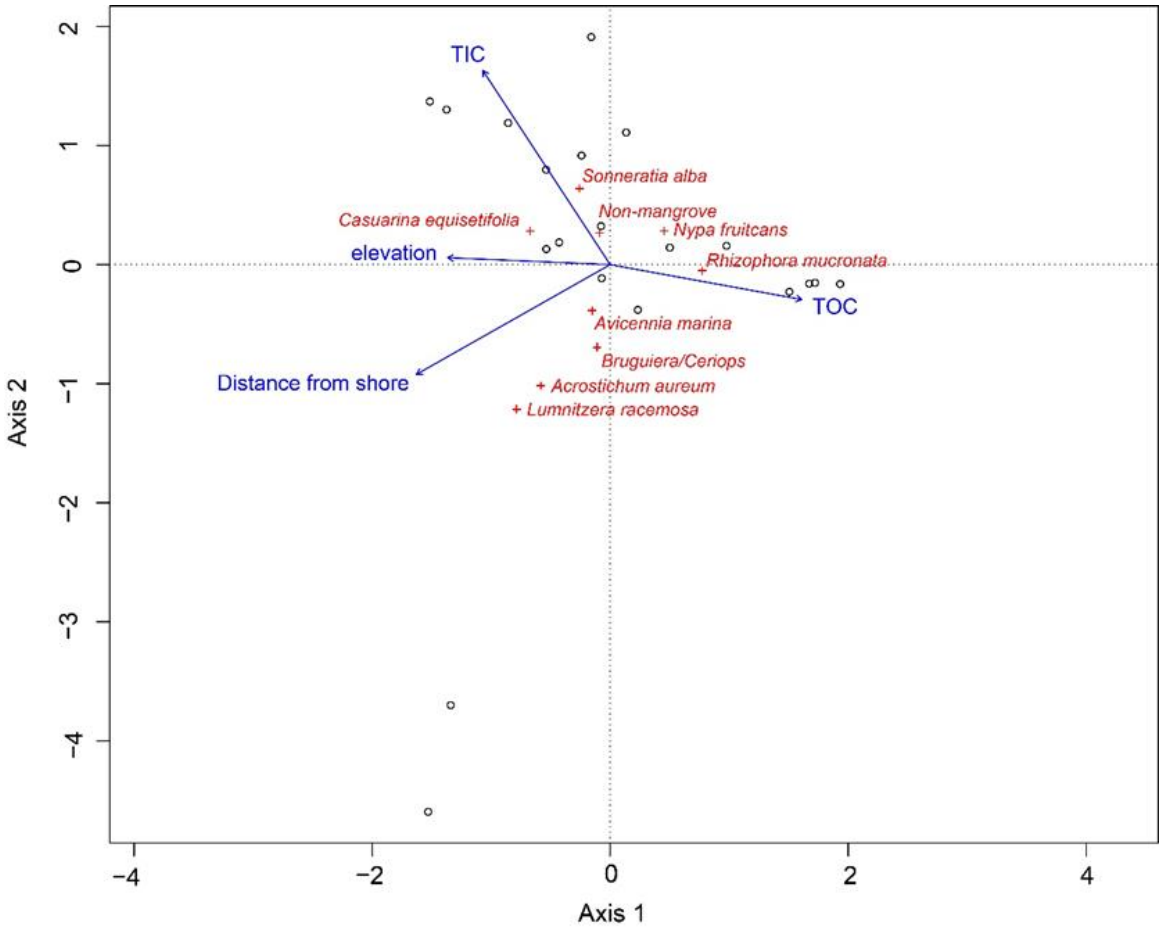

Figure 4.7: CCA on pollen trap assemblage data displaying first and second ordination axes. Environmental variables tested are elevation (m MTL), distance from shore, and TOC and total inorganic carbon (TIC). Pollen trap samples are displayed as black circles and pollen species are crosses and labels in red.

4.5 Discussion

4.5.1 *Pollen as a sea-level indicator in Seychelles mangrove sediments*

The results derived from the pollen traps and very low amounts of surface sediment pollen found in our samples do not provide sufficient justification for the use of pollen to improve

the resolution of quantitative RSL reconstructions in Seychelles mangrove sediments. While modern vegetation zones do show a relationship with elevation (Figure 4.2), the pollen trap data do not accurately reflect species abundance across the mangrove zone. *Rhizophora mucronata* pollen is well associated with the presence and abundance of its parent plant (Table 4.2), and this species has relatively higher levels of pollen production and efficient dispersal, an observation consistent with other mangroves worldwide (Behling et al., 2001; Engelhart et al., 2007; Li et al., 2008; Urrego et al., 2010, 2009). However in Seychelles, *Rhizophora mucronata* lives over the largest elevation range of all species in the mangrove zone (Figure 4.2). Species that live in the narrowest elevation ranges in the mangrove zone (e.g. *Avicennia marina* and *Lumnitzera racemosa*) have relatively low pollen production and therefore very low average abundances. A plant of this type can be a dominant species within any particular mangrove zone, but may at the same time be poorly represented or entirely absent in pollen trap samples. This characteristic makes it difficult to interpret whether the presence or absence of these pollen species indicates the presence or absence of the parent plant, and these species are therefore not suitable for quantitative palaeoenvironmental reconstructions.

Poor plant-pollen association of other key elevation-limited species like *Avicennia marina* means that it is unlikely pollen can improve upon the vertical resolution of using the upper and lower limits of mangrove vegetation as an indicative meaning for Seychelles coastal sediments (Figure 4.6). Despite this, the abundance of major mangrove species decreases with increasing elevation (Figure 4.5), and the abundance of minor and associate mangrove species (e.g. *Casuarina equisetifolia*) increases. While this apparent elevation relationship is evident on a qualitative basis, the CCA results suggest that elevation is not the primary control on the variance in the pollen trap data (Figure 4.7). Rather, pollen trap assemblages appear to reflect more closely variance associated with geomorphological factors such as distance from open shore and sediment composition (which is a surrogate proxy for relative influences of riverine versus tidal and wave sedimentation, see Chapter 5:). It is possible that in mangroves with a small present-day extent like those at the studied sites in Seychelles, local hydro-geomorphological processes drive vegetation and pollen patterns rather than elevation, making the use of pollen as a quantitative proxy challenging. The utility of mangrove pollen is therefore its highly localised dispersal (Ellison, 1989; Grindrod, 1985). Its presence in a sediment sequence could potentially be used to distinguish a mangrove depositional environment from other organic sediments (e.g. a freshwater wetland or salt marsh) that may be difficult to distinguish on sedimentology and visual description alone.

While there are very few areas of freshwater wetlands and no salt marshes in Seychelles to test this hypothesis, this may be a useful technique to identify mangrove deposits in other small island, microtidal sites and should be tested by observing modern pollen rain across the transition between freshwater and mangrove environments.

The pollen trap data from Seychelles mangroves (in the absence of comparative surface sediment data) are in contrast with other studies that have used surface sediment pollen assemblages to justify use of pollen for quantitative RSL and/or palaeoenvironmental reconstructions. Engelhart et al. (2007) and Punwong et al., (2018, 2013a, 2013b) found good association of plant presence with pollen presence in surface sediment, which enabled the use of pollen transfer functions and improved the vertical resolution of RSL reconstructions (Table 2.1). However, Seychelles mangrove sites differ from those of the above studies in that: 1) they are much smaller in lateral extent and therefore have less developed and extensive mangrove zonation and/or 2) are less connected to the open shoreline and are more dominated by riverine processes and sedimentation. Another key difference between these studies and the Seychelles sites is that presence of *Avicennia* pollen species appear to be better associated with presence of parent plants than I find in this study. High *Avicennia* pollen-plant association is also found in other surface sediment and pollen trap studies in Brazil, New Zealand and Colombia (Behling et al., 2001; Deng et al., 2006; Urrego et al., 2010). Therefore, it is possible that if the pollen monitoring was conducted over several years (rather than only one as in this study) the traps would have been able to capture multi-year mangrove flowering cycles (Tomlinson, 2016). It is also possible that had sufficient numbers of pollen been detected in surface sediment samples, there could have been better plant-pollen association as surface sediment is considered a multi-year pollen flux average (Engelhart et al., 2007).

4.5.2 Preservation of pollen in mangrove sediments

Despite the relatively good preservation of pollen in pollen trap samples, an assessment of the transport of pollen from tree to sediment surface is not possible due to the lack of pollen detected in the Grand Anse and Anse Boileau surface sediment samples. These extremely low pollen counts suggest either: 1) the laboratory process did not sufficiently isolate pollen grains for light microscopy analysis or 2) pollen has been degraded or transported by post-depositional processes. I followed standard pollen isolation procedures (Moore et al., 1991) which has been used extensively in other mangrove settings, although counts were low for both *Lycopodium* marker pollen and for sample pollen. This suggests the pollen residues

contain too much non-pollen material which meant that it was not possible to find enough marker and sample pollen within a practical time limit per sample. Other pollen isolation procedures use heavy liquid separation rather than chemical dissolution (Campbell et al., 2016). However it is unlikely that a different preparation method would have improved pollen counts, as a modified heavy-liquid separation method yielded very low pollen abundances in sediment core samples intended for radiocarbon measurements (see Section 3.6.3). Low pollen concentrations have been reported in other mangrove sediment studies where multiple microscope slides were needed to obtain statistically robust counts from both surface and fossil sediment samples (Behling et al., 2004; Engelhart, 2007; Punwong, 2013; Woodroffe et al., 2015b).

Pollen is one of the most widely used palaeoenvironmental proxies in mangrove sediments largely due to the prevailing sediment conditions that enhance pollen preservation. However, when certain sediment conditions are not met, pollen grains can be degraded post-deposition. Coarser-grained sediments (sand-sized and larger) have greater interstitial pore space that can be filled by incoming tidal or river waters, which can abrade pollen grains (Fægri, 1971; Grindrod, 1988). Similarly, greater interstitial pore space allows oxidation of pollen grains to occur when sediments are not inundated and/or saturated (Grindrod, 1988; Havinga, 1967). The wetting and drying of mangrove sediments with tidal inundation and seasonal rainfall patterns can expand and contract pollen grain walls, which can weaken pollen grains over time (Campbell and Campbell, 1994). Variable salinity conditions in sediments overtime due to seasonal rainfall and river discharge may also affect the preservation of pollen grains (Campbell and Campbell, 1994). In an experimental study, Phuphumirat et al. (2015) found that pollen degradation rates in mangrove sediments in Thailand were lessened in fine-grained sediments that were saturated and/or inundated for greater time periods. Phuphumirat et al. (2015) also found that pollen degradation was enhanced in sediments with relatively low salinity and less acidic conditions. Bacterial and fungal activity can also degrade pollen grains (Bryant et al., 1994; Phuphumirat et al., 2011).

A number of the processes suggested above could have resulted in post-depositional degradation of pollen grains at Grand Anse and Anse Boileau, creating a situation of extremely low pollen preservation in surface sediments that I found in this study. The mangrove sediments at both Grand Anse and Anse Boileau are relatively coarse-grained, characterised by high percentages of coarse sands and gravels likely deposited by fluvial processes (see Chapter 5:). The greater interstitial space in coarser sediments may lead to progressive abrasion of pollen grains through tidal and river pumping and/or oxidation over

the time, leaving very low concentrations in surface and fossil sediments to utilise for RSL or palaeoenvironmental reconstructions. Measured salinities of surface waters at Grand Anse varies from freshwater to marine levels within daily tidal inundation cycles, and also with seasonal rainfall patterns (wet and dry seasons associated with the shift of the Intertropical Convergence Zone). These highly variable salinity conditions in the mangrove sediments at Grand Anse and Anse Boileau may also impact the preservation of pollen grains. Other factors that also apply to sediment organic matter in general (see Section 3.6.1) may have led to loss of pollen grains in surface sediments. Bioturbation by crabs and mangrove roots that increase oxidation levels, and combined with low sedimentation rates and limited sediment accommodation space (see Section 3.6.4) reduces the preservation potential of pollen grains in the particular mangrove setting of the Seychelles. Degradation by microbial activity may have also led to loss of pollen grains in the Grand Anse and Anse Boileau surface sediments, as evidence of such microbial attack can be seen on organic matter collected from sediment cores under light microscopy (Figure 3.5).

4.6 Conclusions

I find that pollen collected in traps deployed over the whole elevation range of mangrove environments in the Seychelles for a year show that overall mangrove pollen production is relatively low compared to temperate intertidal settings (Long et al., 1999; Neulieb et al., 2013). While modern vegetation zonation is related to elevation, the association between plant and pollen trap data is not consistent between mangrove species. Additionally, very low pollen concentrations are detected in surface sediments which do not enable the assessment of pollen transport mechanisms or for use in fossil sediment sequences. These results suggest that the Seychelles mangroves, with their small lateral extent and narrow connections to open marine environments, are not suitable for pollen-based quantitative RSL reconstructions as elevation is not the primary driving variable for vegetation and pollen zonation. Sediment grainsize, variable sediment saturation levels, and low sedimentation rates may have contributed to degradation of pollen post-deposition leading to very low pollen preservation. Increased abundances of mangrove pollen in a sediment sequence is indicative of a mangrove zone (and therefore an intertidal) depositional environment. Mangrove pollen abundances can therefore aid interpretation where depositional environment may be unclear from sedimentological descriptions (e.g. mangrove vs. freshwater peat).

Palynological approaches are not able to provide suitable improvements to existing vertical uncertainties on RSL reconstructions from Seychelles mangroves. This study suggests that it is unlikely pollen will improve reconstructions at other similar small island mangroves too, and will therefore not aid in constraining late Holocene eustasy which focuses on obtaining records from low latitude sites away from major continent margins (Milne and Mitrovica, 2008). However, pollen may still be useful at other sites where: 1) mangrove vegetation and pollen zonation is more laterally extensive and is distributed according to elevation, 2) there is good plant-pollen association, and 3) sedimentological conditions allow for the preservation of pollen in sedimentary sequences (e.g. fine-grained and anoxic).

Chapter 5: Testing the use of total organic carbon, inorganic carbon, and lipid biomarker analyses as quantitative sea-level indicators from Seychelles mangrove sediments

5.1 Introduction

Geological records of relative sea-level (RSL) change are important archives that improve our understanding of ice sheet dynamics and climate processes on longer timescales than satellite and historical observations can provide (Barlow et al., 2013; Horton et al., 2018). RSL records from low-latitude sites are particularly useful as RSL in these locations is modelled to be closer to global eustatic sea level (i.e. sea level change from ice sheet volume change) than in the mid- or high latitudes (Milne and Mitrovica, 2008). Most RSL records in the low latitudes are derived from corals (Chappell and Polach, 1991; Hibbert et al., 2016; Peltier and Fairbanks, 2006), but because coral sea-level indicators live in a large depth range (at least ± 5 metres) (Hibbert et al., 2016; Lighty et al., 1982), the precision they provide for Late Holocene to present RSL reconstructions is limited as the uncertainties exceed the amplitude of likely RSL changes (Woodroffe and Horton, 2005).

Mangroves are salt-tolerant trees than inhabit a narrow ecological niche along low-latitude coastlines (Tomlinson, 2016). Generally, mangroves occupy the upper half of the intertidal zone and their sediments record changes in RSL over time (Bird et al., 2010; Culver et al., 2015; Ellison and Stoddart, 1991; Horton et al., 2005a; Tam et al., 2018; Woodroffe, 1981; Woodroffe et al., 2015a). However, it remains challenging to produce quantitative RSL reconstructions from mangrove sediments. Common approaches such as microfossil transfer functions are often not applicable because foraminifera and diatoms may be poorly preserved in mangrove sediments due to dissolution. Pollen-derived reconstructions can be successful as pollen are more resistant to degradation (Ellison, 1989; Engelhart et al., 2007; Punwong et al., 2013a), however these approaches are largely dependent on highly-localised factors such as mangrove species zoning, mangrove extent and pollen production rates (see Chapter 4:). More recently, sea-level researchers have tested geochemical methods (stable carbon isotopes, carbon/nitrogen ratios, and total organic carbon) for quantitative RSL reconstructions as an alternative approach (Engelhart et al., 2013; Kemp et al., 2019, 2010; Khan et al., 2019b, 2015b; Lamb et al., 2006; Mackie et al., 2005; Sen and Bhadury, 2017). These studies operate under the assumption that geochemical properties of mangrove

sediments reflect environmental conditions such as vegetation type, salinity, and geomorphological conditions such as elevation in the tidal range and distance from the open shoreline.

Previous studies using bulk-sediment stable carbon isotopes ($\delta^{13}C$), carbon/nitrogen ratios (C:N) and total organic carbon (TOC) for quantitative RSL reconstructions in salt marsh and mangrove environments have found it challenging to distinguish different vegetation zones present in the modern environment. In particular, mangroves are exclusively C3 plants which means their compositional range in $\delta^{13}C$ and C:N space is limited and indistinguishable from other terrestrial freshwater plants (Kemp et al., 2019; Khan et al., 2019b). C3 and C4 plants commonly coexist in temperate region salt marshes, but bulk sediment $\delta^{13}C$ measurements on surface sediments are not always able to capture this variability (Kemp et al., 2017). Similar studies show that bulk sediment C:N values, again in salt marshes are particularly influenced by post-depositional processes (Kemp et al., 2010; Khan et al., 2015b). These studies suggest that further analyses should test more specific sediment fractions (Kemp et al., 2010) or specific organic compounds.

Biomarkers are lipid molecules which are synthesized by plants, animals and microorganisms. They are present in a wide array of modern environments, and are also preserved in the geological record (Castañeda and Schouten, 2011; Eglinton and Eglinton, 2008; Naafs et al., 2019). Organisms that synthesize biomarkers in mangrove environments — and that are preserved in their sedimentary sequences — have the potential to be proxy sea-level indicators, if biomarkers and their parent organisms can be found within different elevation zones. Biomarkers, and in particular the compound taraxerol, have been used to understand past mangrove dynamics and organic matter cycling (He et al., 2014; Koch et al., 2011; Kumar et al., 2019; Versteegh et al., 2004), and compound specific isotopes in mangroves have been identified as potential salinity proxies (He et al., 2017; Ladd and Sachs, 2015a, 2013). Further testing of biomarker distributions in mangrove environments is required to evaluate their potential as sea-level indicators.

Therefore, to further test the use of geochemical properties of mangrove sediment for RSL reconstructions, I present a surface sediment sample dataset of TOC, TIC, and lipid biomarker distributions from two mangrove locations from Mahé, Seychelles (Figure 1.3). These properties are tested against observed and measured environmental characteristics of vegetation type, elevation, distance from open shore, and sediment grain size, which will help assess sedimentation sources, patterns, and transport mechanisms in the Seychelles

mangrove environment. To my knowledge, this study is the first to test the relationship between biomarker distributions and elevation in a mangrove environment for the purpose of quantitative RSL reconstructions.

5.2 Study site

Two mangrove areas were selected for this study: Grand Anse and Anse Boileau (Figure 5.1 and Figure 5.2) on the west coast of the island of Mahé, Seychelles (Figure 1.3). Mahé is a granitic and topographically steep island, vegetated with dense tropical rainforest (see Section 1.3.2). Mahé has a fringing coral reef, which is best developed on the east coast. The mangroves of Mahé typically occupy river channels that have eroded into the coastal plain that surrounds the island, which is mostly comprised of supratidal beach sediments that formed during the Late Holocene as sediment supply from the fringing reef system moved onshore as RSL stabilised (Woodroffe et al., 2015a). Generally, mangrove forests on Mahé are characterised by five species: *Rhizophora mucronata*, *Sonneratia alba*, *Bruguiera gymnorrhiza*, *Avicennia marina* and *Lumnitzera racemosa*. *Rhizophora mucronata* and *Sonneratia alba* typically occupy more seaward locations and *Avicennia marina* and *Lumnitzera racemosa* occupy more landward locations (see Section 4.2).

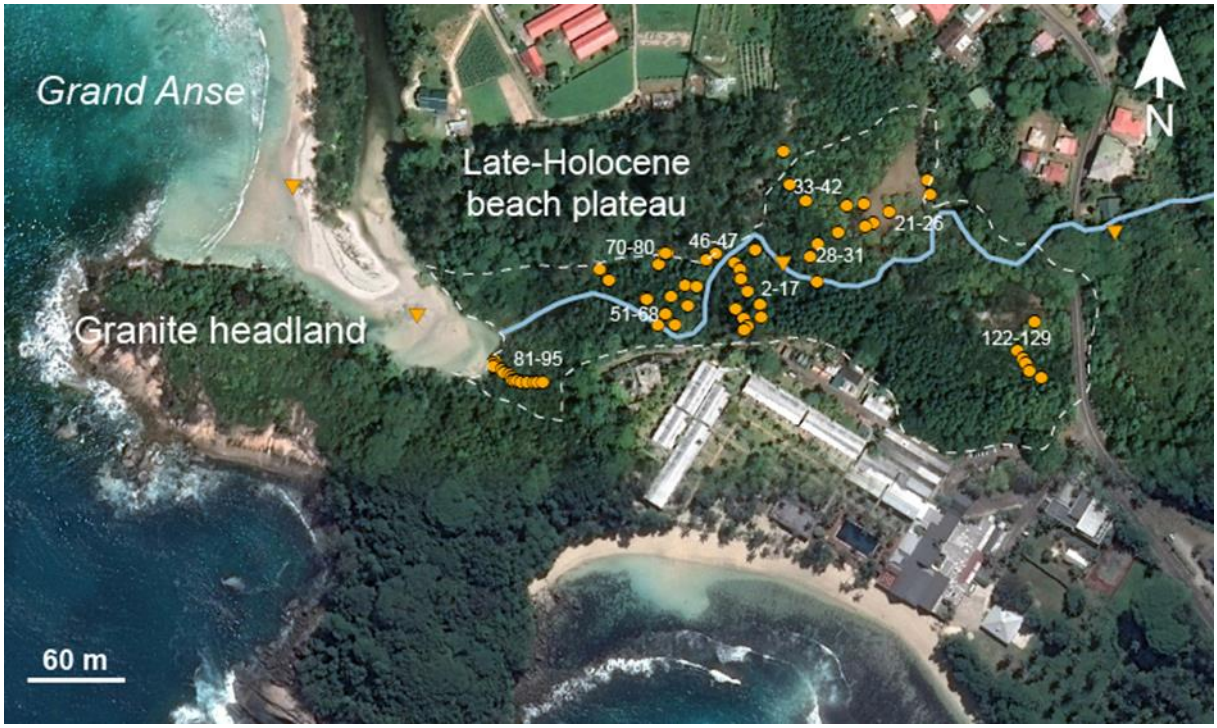

Figure 5.1: Surface sediment sample sites across the Grand Anse mangrove. All sites marked are for grainsize, TOC and TIC with grouped sample numbers (see Appendix Table A4). Sites that were analysed for biomarkers are shown in Appendix Figure A1. Samples to characterise beach and river

sediments are marked using triangle shapes. White dashed line is the approximate extent of the mangrove zone, and the light blue line is the River Dauban.

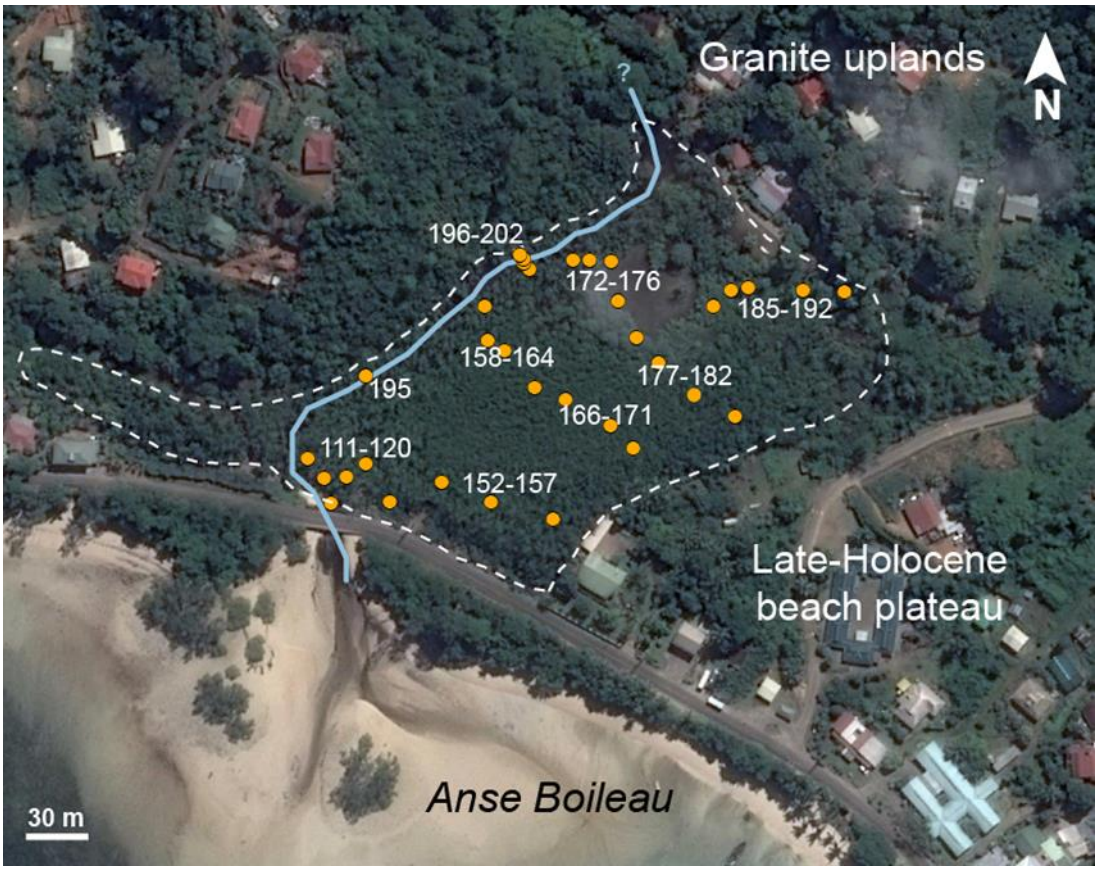

Figure 5.2: Surface sediment sample sites across the Anse Boileau mangrove. All sites marked are for grainsize, TOC and TIC with grouped sample site numbers (see Appendix Table A5). White dotted line is the approximate extent of the mangrove zone, and the light blue line is the River Cayman.

5.3 Methods

5.3.1 Field methods

At the two mangrove sites (Figure 5.1 and Figure 5.2), surface sediment samples (top 1 cm of sediment) were collected for grain size (Grand Anse, n = 60 ; Anse Boileau, n = 40), TOC and TIC (Grand Anse, n = 60 ; Anse Boileau, n = 40), and lipid biomarker analyses (Grand Anse, n = 12, Appendix Figure A1). Sample sites were selected to cover a range of geomorphological, sedimentological and plant species compositions within each of the mangrove sites. Site elevations were surveyed using a theodolite and staff, and a Van Essen Instrument water level logger was deployed to characterise the tidal timings and amplitudes at the Grand Anse mangrove for a duration of ~15 days. Data collected from the water level logger was compared to observations from the Point La Rue tide gauge situated at Victoria on the eastern side of the island (UHSLC, 2019), and sample elevations were related to mean tide

level (MTL) from timed water level measurements in calm-water locations in the mangrove. While there is a minor timing offset between the tide gauge measurements and the logger data (~25 minutes later at the west coast Grand Anse site compared to the east coast Point La Rue tide gauge), after this was corrected for, the tidal amplitudes between Grand Anse and Point La Rue are comparable and within the 0.1 metre error resulting from the predicted tidal amplitudes (*Admiralty Tide Tables*, 2017). Given the proximity of the two sampled locations of Anse Boileau and Grand Anse (~3 km), the tidal logger data from Grand Anse is considered representative of both sites.

5.3.2 Laboratory methods

5.3.2.1 Grain size

Grainsize samples (0–2000 µm) were treated with excess hydrogen peroxide to oxidize organic matter. To deflocculate fine sediments, sodium hexametaphosphate was added to the samples. Samples were then sieved at 2000 µm immediately prior to analysis with a Beckman Coulter LS 13 320 Laser Diffraction Particle Size Analyser.

5.3.2.2 TOC and TIC

TC and TIC were measured on an elemental analyser Analytic Jena 3000 using 10 mg of powdered sample (n = 100), and combusted at 1100°C. TIC samples were acidified with 40% phosphoric acid prior to combustion. TOC concentrations were calculated by the difference between TC and TIC concentrations. Samples were measured alongside two certified reference materials to determine measurement uncertainty as well as sample replicates (which is <1 % of reported values).

5.3.2.3 Biomarker solvent extraction

Approximately 1 g of each freeze-dried and powdered surface sample — selected to characterise a variety of elevations and sub-environments — was prepared for lipid extraction. An internal standard of known concentration was added to the dried samples (40 µL); 5α-cholestane (for the apolar fraction) and 5α-androstanol (for the polar fraction). Samples were sonicated four times for 15 minutes in 6 mL of a mixture of CH_2Cl_2/MeOH (3:1, v/v). The extracted total lipid fraction was saponified by adding an 8% KOH solution (in 95% MeOH, 5% Ω18M water) and heated for 1 hour at 70°C. The neutral lipid fraction was extracted with hexane. Apolar and polar compounds were separated using activated SiO_2

columns which were eluted with hexane and CH_2Cl_2/MeOH (1:1, v/v) respectively. The polar fraction was derivatised by adding Bis(trimethylsilyl)trifluoroacetamide (BSTFA) and heated for 1 hour at 70°C.

5.3.2.4 Gas-chromatograph-mass spectrometry (GC-MS)

Apolar and polar fractions were analysed using a Thermo Scientific Trace 1310 GC-MS. The GC-MS was equipped with a programmable temperature vaporizer (PTV) injector and helium gas was used as the carrier flow. The oven temperature was set at 40°C for 2 minutes, then increased to 170°C at 12°C per minute, then increased to 310°C at 6°C per minute, which was then held for 35 minutes.

Compounds were identified by comparing mass spectra data with those published in the literature (Goad and Akihisa, 1997; He et al., 2018; Killops and Frewin, 1994; Tulipani et al., 2017). Compounds were quantified through the comparison of compound and internal standard integrated peak areas. Unfortunately, 5α-cholestane appears to coelute with the C_{29}-alkane which adds uncertainty to the quantification of the apolar lipid fraction. Additionally, derivatisation of polar compounds was incomplete, likely due to high lipid concentrations, thus meaning increased uncertainty in the quantification of the polar lipid fraction. Biomarker concentrations are presented as either absolute concentrations (μg per gram of dried sediment) or as concentration per gram of TOC.

5.3.2.5 Statistical analyses

Linear regression and principle component analysis (PCA) were used to test the relationships between grainsize, TOC, TIC, total carbon (TOC + TIC) and biomarker distributions with the environmental variables of elevation (m MTL), distance from shore (m) and mapped vegetation zone. These analyses were computed and plotted in *R*, using base functions. Datasets were transformed for PCA analysis (using the *prcomp* function) to account for unit variance.

5.4 Results

5.4.1 Grain size

The grainsize distributions of both Grand Anse and Anse Boileau surface sediment samples are presented in Figure 5.3. At Grand Anse, samples across the mangrove surface are

distributed in a dominantly bi-modal pattern (a peak indicating well-sorted sediment at ~200 µm, and broader peak >500 µm). The Anse Boileau samples demonstrate similar characteristics but the peak at ~200 µm is of smaller magnitude and samples are typically more dominated by larger grainsizes >500 µm. Four sediment samples collected outside of mangrove-covered areas at Grand Anse (shown in Figure 5.1 as triangles), intended to represent 'end-member' grainsizes (beach versus riverine) are shown in Figure 5.3C. Samples collected at the beach facing sites are distinctly well-sorted and are dominantly fine sand-sized, whereas riverine samples are poorly-sorted and are dominantly coarse sand (>500 µm). This is further evidenced by a significant (R^2 >0.5) relationship between distance from shore and percent fine sand at Grand Anse, and at Anse Boileau (R^2 = 0.49) (Figure 5.6 and Figure 5.7).

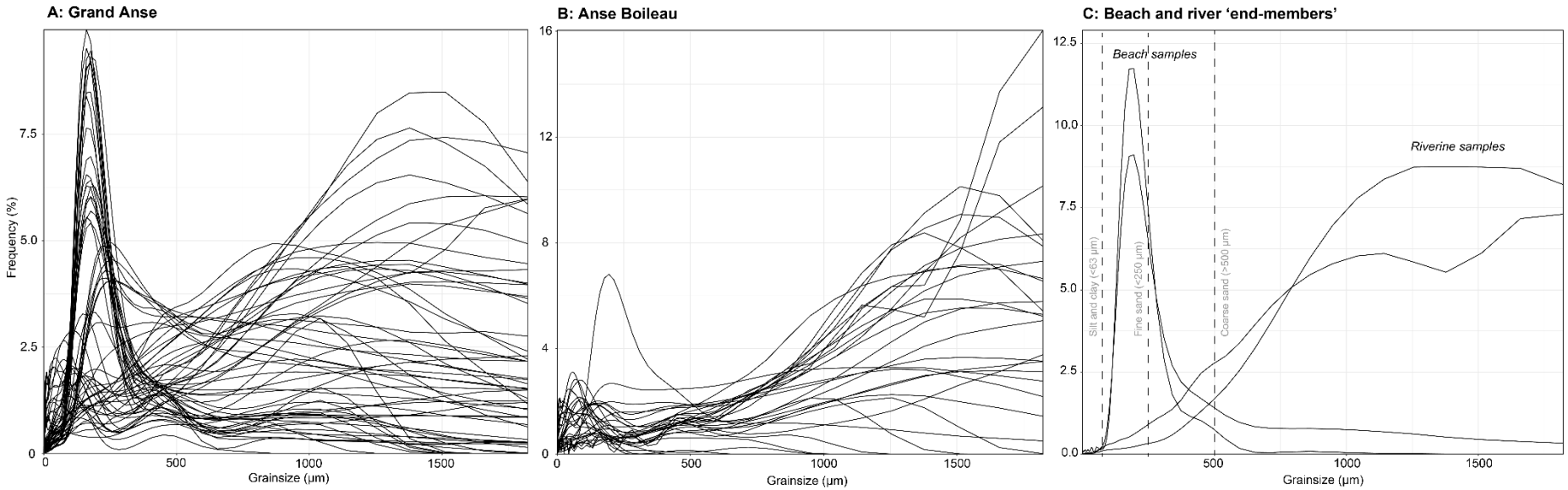

Figure 5.3: Grainsize distributions for surface sediment samples collected at A) Grand Anse B) Anse Boileau and C) 'end-member' samples collected from adjacent beach and river environments (see Figure 5.1) . Frequency values are the fraction (%) of each sample as binned grainsize ranges. Note the y-axis on each plot varies.

5.4.2 TOC and TIC

TOC and TIC compositions of surface sediment sample at both mangrove sites are wide ranging. TOC values range between 0–25.5 % (with a mean value of 6.9 %) at Grand Anse, and between 0–18.6 % (with a mean value of 7.5 %) at Anse Boileau. TIC ranges between 0–10.8 % (with a mean value of 4.5 %) at Grand Anse, and between 0–10.5 % (with a mean value of 0.9 %) at Anse Boileau. The spatial variation with elevation, distance from shore, and vegetation zone of TOC and TIC at both Grand Anse and Anse Boileau are displayed in Figures 5.4–5.7. At Grand Anse, percent TIC has a significant relationship with distance from shore (R^2 >0.5) (Figure 5.6), i.e. the closer to the open shore, the higher the percentage of TIC. No other combination of observations and environmental variables display significant relationships.

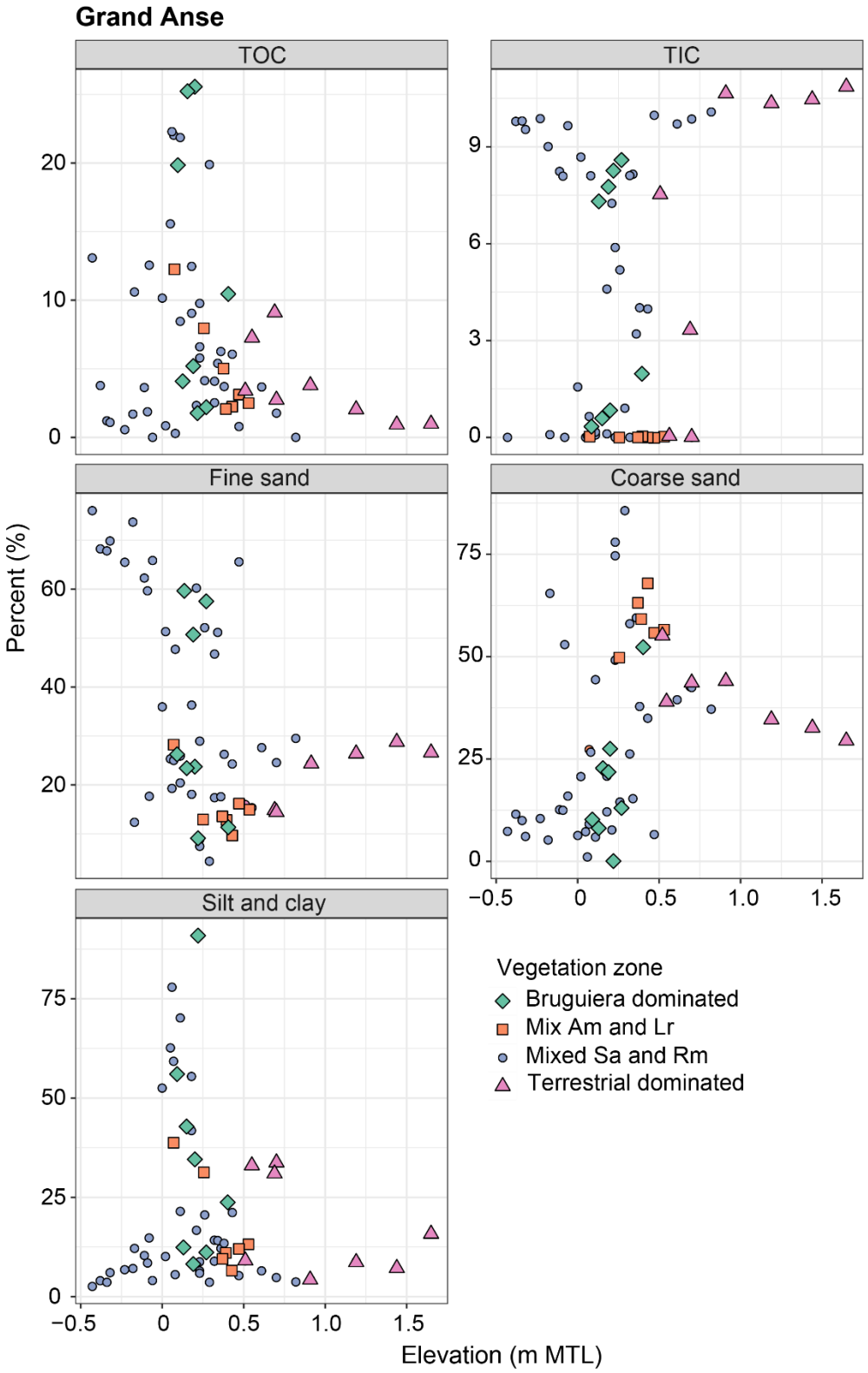

Figure 5.4: Variables TOC (%), TIC (%), percent fine sand (63–250 µm), coarse sand (500–1000 µm), and silt and clay (<63 µm) with elevation (metres above mean tide level) at Grand Anse (data in Appendix Table A4). TC, TOC, and TIC uncertainty not plotted as error bars are smaller than sample points. Mapped vegetation zone at each sample site is shown in the colour legend, where Bg or Bruguiera is Bruguiera gymnorrhiza, Am is Avicennia marina, Lr is Lumniztera racemosa, Sa is Sonneratia alba, and Rm is Rhizophora mucronata.

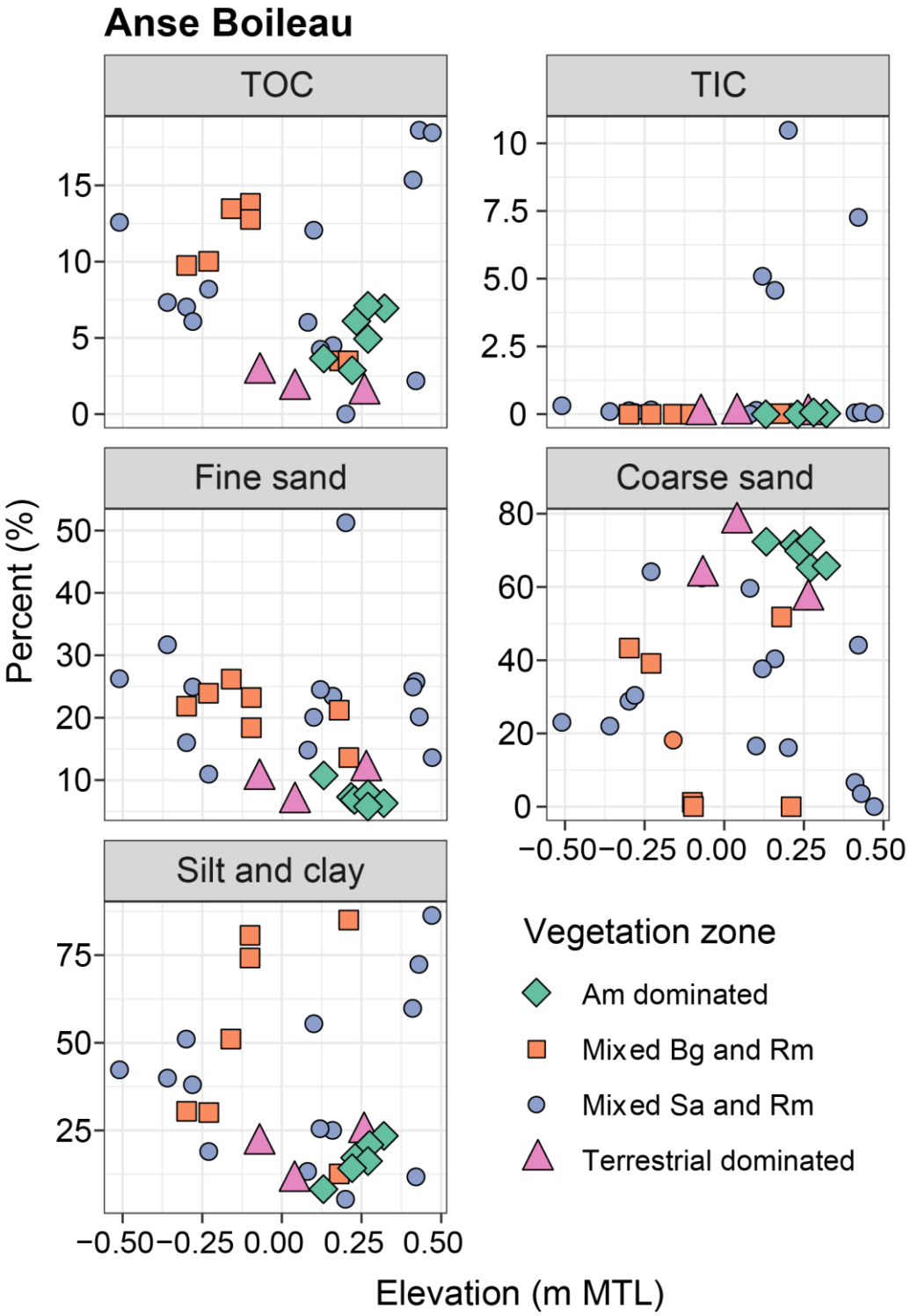

Figure 5.5: Variables TOC (%), TIC (%), percent fine sand (63–250 µm), coarse sand (500–1000 µm), and silt and clay (<63 µm) with elevation (metres above mean tide level) at Anse Boileau (data in Appendix Table A5). TC, TOC, and TIC uncertainty not plotted as error bars are smaller than sample points Mapped vegetation zone at each sample site is shown in the colour legend, where Bg or Bruguiera is Bruguiera gymnorrhiza, Am is Avicennia marina, Lr is Lumniztera racemosa, Sa is Sonneratia alba, and Rm is Rhizophora mucronata.

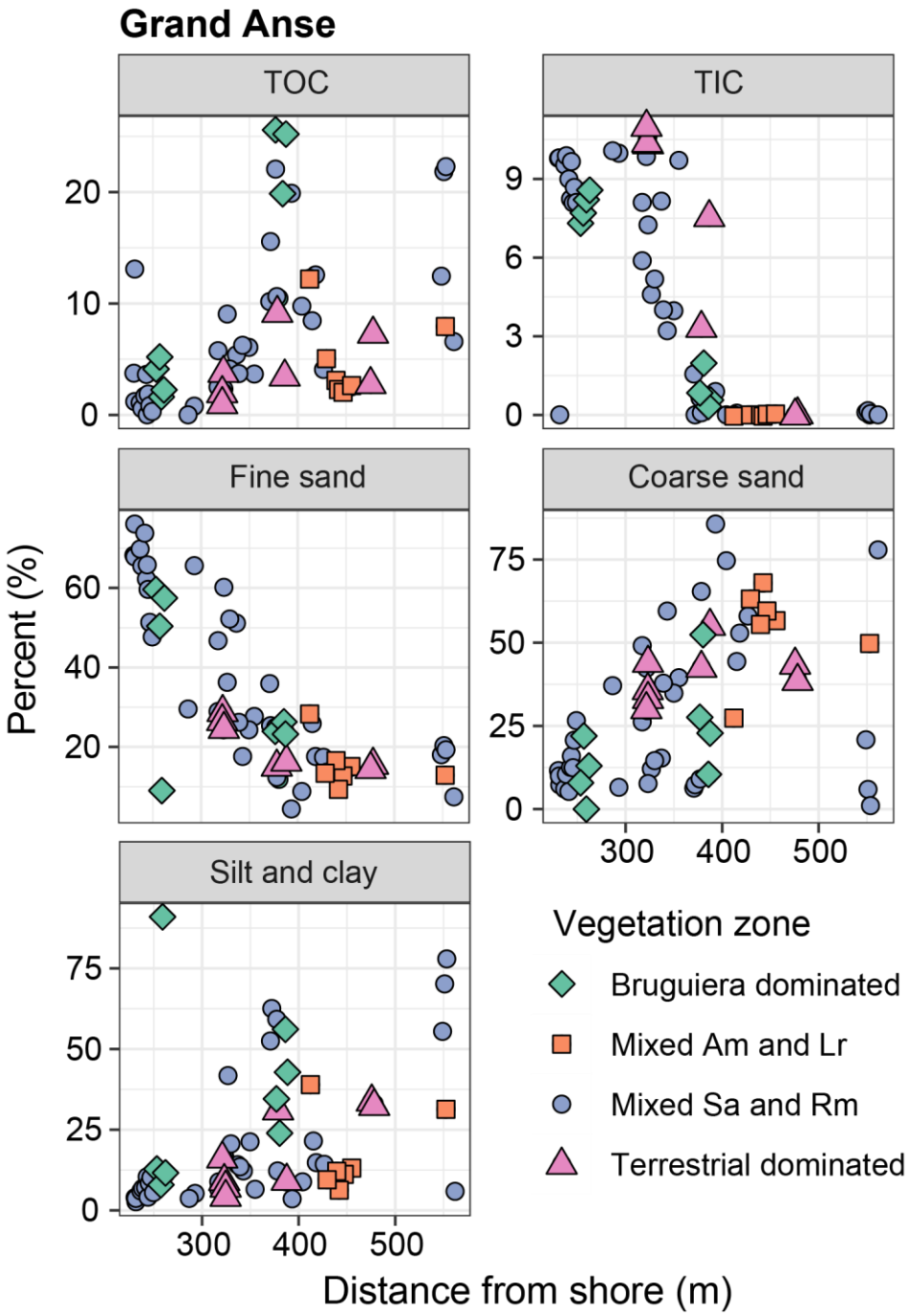

Figure 5.6: Variables TOC (%), TIC (%), percent fine sand (63–250 µm), coarse sand (500–1000 µm), and silt and clay (<63 µm) with distance from shore (m) at Grand Anse. TC, TOC, and TIC uncertainty not plotted as error bars are smaller than sample points Mapped vegetation zone at each sample site is shown in the colour legend, where Bg or Bruguiera is Bruguiera gymnorrhiza, Am is Avicennia marina, Lr is Lumniztera racemosa, Sa is Sonneratia alba, and Rm is Rhizophora mucronata. Distance from shore calculation details are available in Appendix Figure A2.

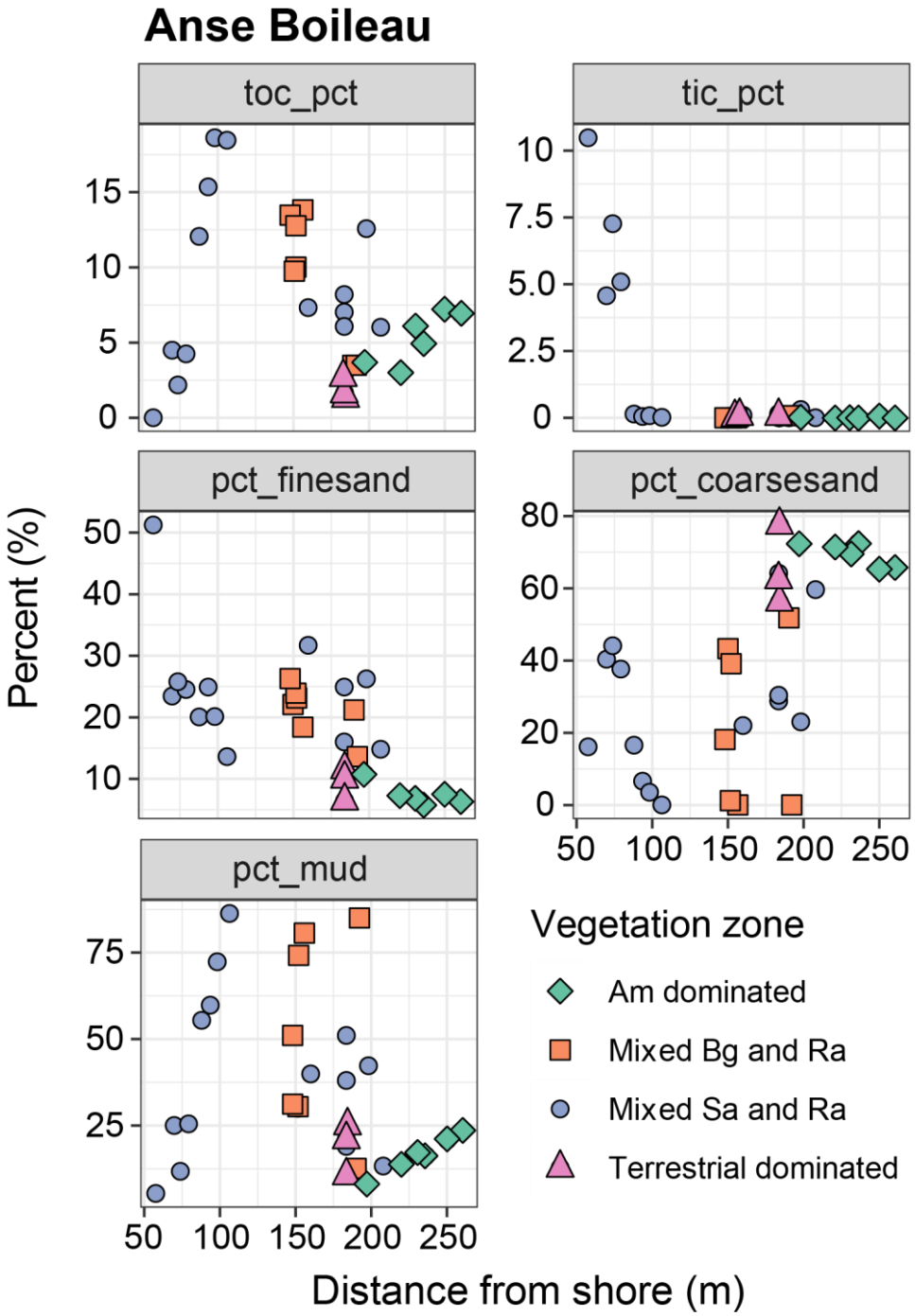

Figure 5.7: Variables TOC (%), TIC (%), percent fine sand (63–250 µm), coarse sand (500–1000 µm), and silt and clay (<63 µm) with distance from shore (m) at Anse Boileau. TC, TOC, and TIC uncertainty not plotted as error bars are smaller than sample points Mapped vegetation zone at each sample site is shown in the colour legend, where Bg or Bruguiera is Bruguiera gymnorrhiza, Am is Avicennia marina, Lr is Lumniztera racemosa, Sa is Sonneratia alba, and Rm is Rhizophora mucronata. Distance from shore calculation details are available in Appendix Figure A3.

The results of the PCA analyses of the combined Grand Anse and Anse Boileau datasets are displayed in Figure 5.8. The first and second principal components describe, cumulatively, 58.34 % of the variance. TIC and TOC as well as silt and clay show the largest amount of variance along the first dimension, and grainsize characteristics (fine sand and coarse sand) show the largest amount of variance in the second dimension. Elevation, distance from shore, and vegetation zone have shorter eigenvectors than other variables and therefore appear less responsible for the variance in the dataset.

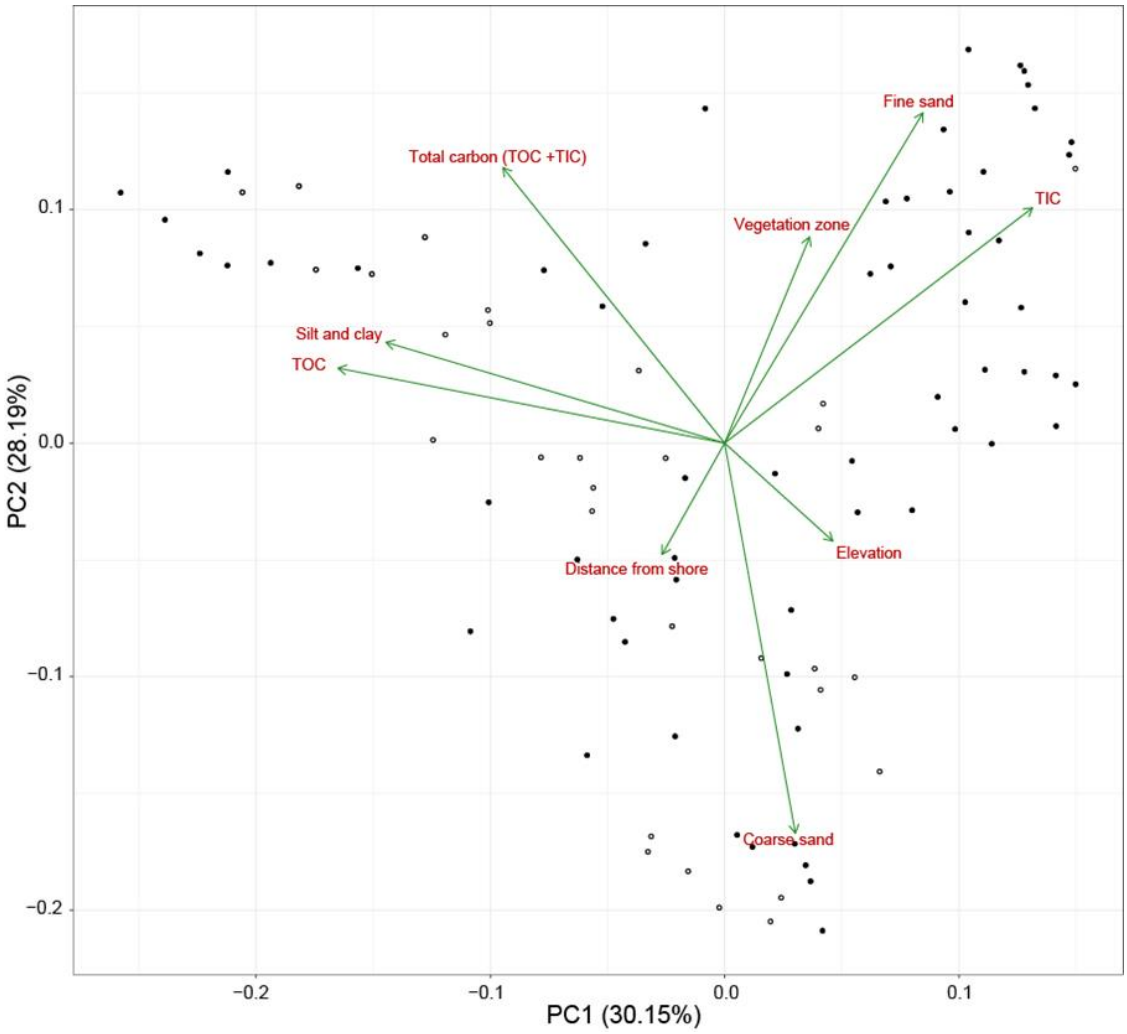

Figure 5.8: PCA results (PCA1 and PCA2) for combined Grand Anse and Anse Boileau datasets of surface sediment sample and environmental variables. Filled circles are Grand Anse samples, non-filled circles are Anse Boileau samples.

5.4.3 Biomarkers

The spatial patterns of biomarker concentrations per gram of dry sediment in the Grand Anse samples are heavily influenced by sample TOC, and thus both apolar and polar compounds peak where TOC peaks in the middle elevation in the mangrove zone (Figure 5.4). Therefore, all biomarker concentrations and distributions are plotted and discussed as normalised to TOC (i.e. in μg per gram of TOC).

5.4.3.1 Polar fraction

The polar fraction of the Grand Anse surface sediment samples is dominated by triterpene alcohols and sterols (Appendix Figure A4). The most abundant compounds found in all samples are (listed first is the common name and then the chemical nomenclature): taraxerol (taraxer-14-en-3β-ol), β-amyrin (olean-12-en-3β-ol), germanicol (olean-18-en-3β-ol) and lupeol (lup-20(29)-en-3β-ol) (Appendix Figure A6). Other compounds were found in some or all of the samples in varying abundances, including sitosterol (stigmast-5-en-3β-ol), β-stigmasterol (24*E*-stigmasta-5,22-dien-3β-ol), cholesterol (choles-5-en-3β-ol), poriferasterol (24*E*-poriferasta-5,22-dien-3β-ol), campesterol (campest-5-en-3β-ol), α-amyrin (5α-urs-12-en-3β-ol), and lanosterol (5α-lanosta-8,24-diene-3β-ol). Phytol (3,7,11,15-tetramethyl-hexadec-2-en-1-ol) was also found in most samples (Appendix Table A9). The polar fraction also contained *n*-alcohols, however I could not define chain lengths from the mass spectra data and thus only a total *n*-alcohol concentration per sample was determined (Appendix Table A9). Sterols and triterpene alcohols are compared with elevation, distance from shore, and vegetation zone variables in Figure 5.9 and Figure 5.10.

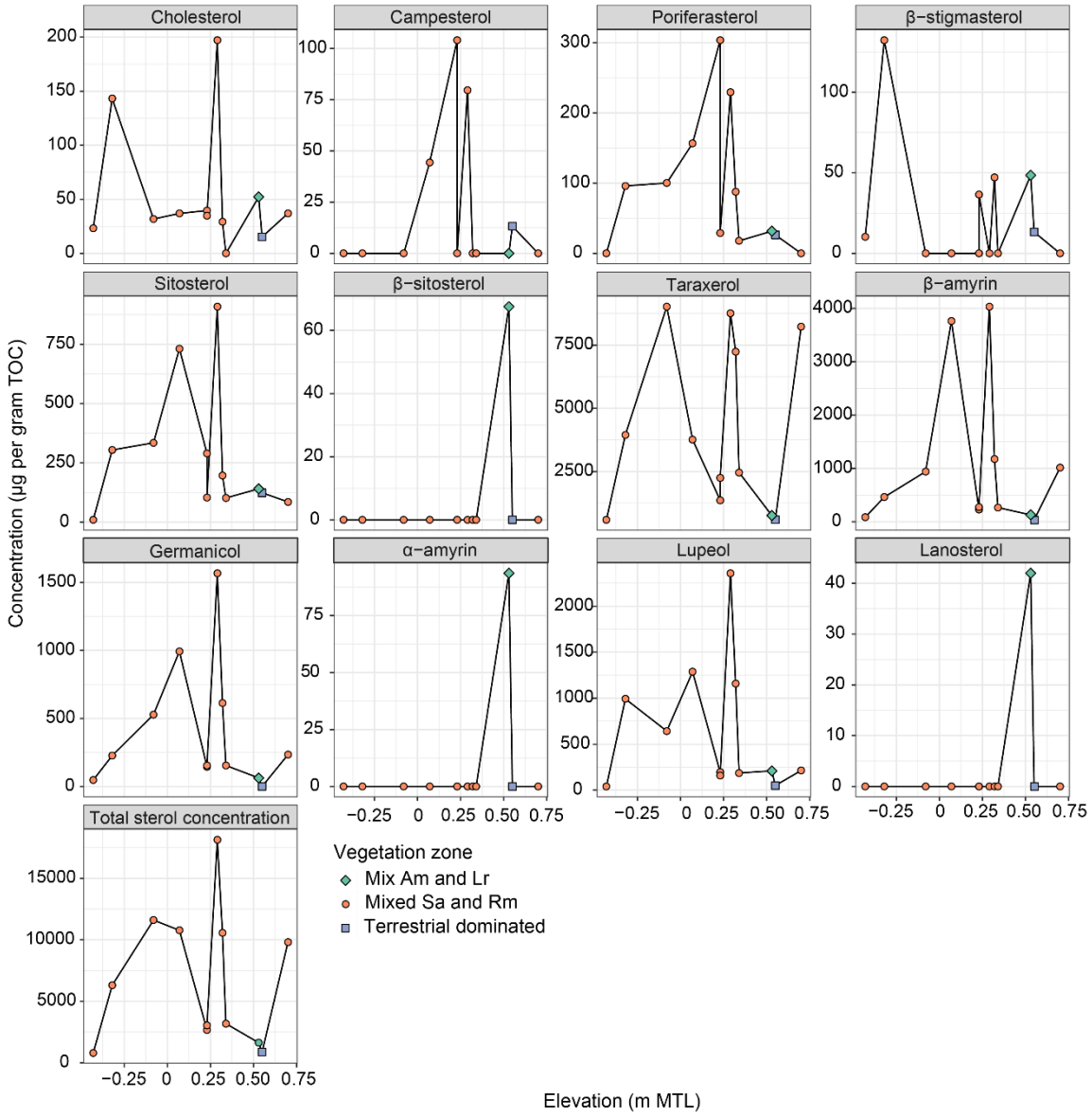

Figure 5.9: Sterol and triterpene alcohol concentrations (µg per gram of TOC) for surface sediment samples in the Grand Anse mangrove against elevation. Sample circles are coloured by mapped vegetation zone, where: Am is Avicennia marina, Lr is Lumnitzera racemosa, Sa is Sonneratia alba and Rm is Rhizophora mucronata.

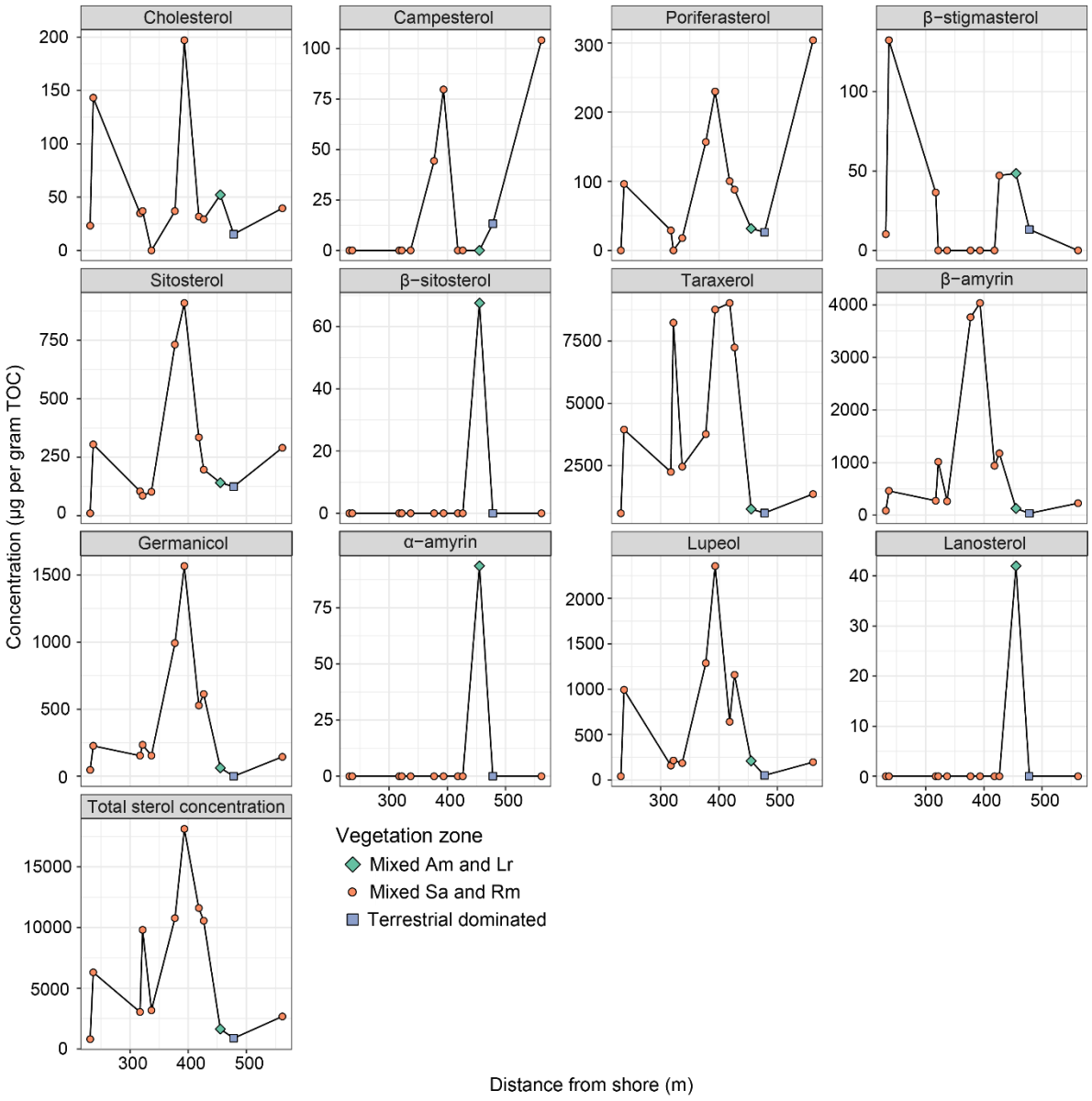

Figure 5.10: Sterol and triterpene alcohol concentrations (µg per gram of TOC) for surface sediment samples in the Grand Anse mangrove against elevation. Sample circles are coloured by mapped vegetation zone, where: Am is Avicennia marina, Lr is Lumnitzera racemosa, Sa is Sonneratia alba and Rm is Rhizophora mucronata.

5.4.3.2 Apolar fraction

The apolar fraction is dominated by *n*-alkanes and terpenoid hydrocarbons (Appendix Figure A5). A number of indices to describe the distributions of the *n*-alkane data are presented in Figure 5.11: a) the Carbon Preference Index (CPI) which determines the degree of odd-over-even preference of *n*-alkane distributions (Andersson and Meyers, 2012; Bray and Evans, 1961), b) the Average Chain Length (ACL) which describes the dominant chain length of *n*-alkane distributions (Poynter et al., 1989), and c) the P_{aq} index which evaluates the input of aquatic vegetation in peats (Ficken et al., 2000). The CPI indices of the surface sediment

samples vary between 0–22.5, the ACL indices vary from 25–29, and P_{aq} indices vary between 0.05–1.

A number of terpenoid hydrocarbons were also tentatively identified in the apolar fraction (Appendix Figure A8). Hopanoids with retention times between 36-38 minutes were noted but are not present in sufficient quantities for quantification. There is an additional unidentified compound group eluting between 26–30 minutes which has a distinctive mass spectra characterised by fragments at *m/z* 91 + 14*n*, which potentially classes these compounds as chlorinated hydrocarbons (Tulipani et al., 2017; Zhang et al., 2013). However as larger molecular ions were not identified in these mass spectra, confident identification could not be completed.

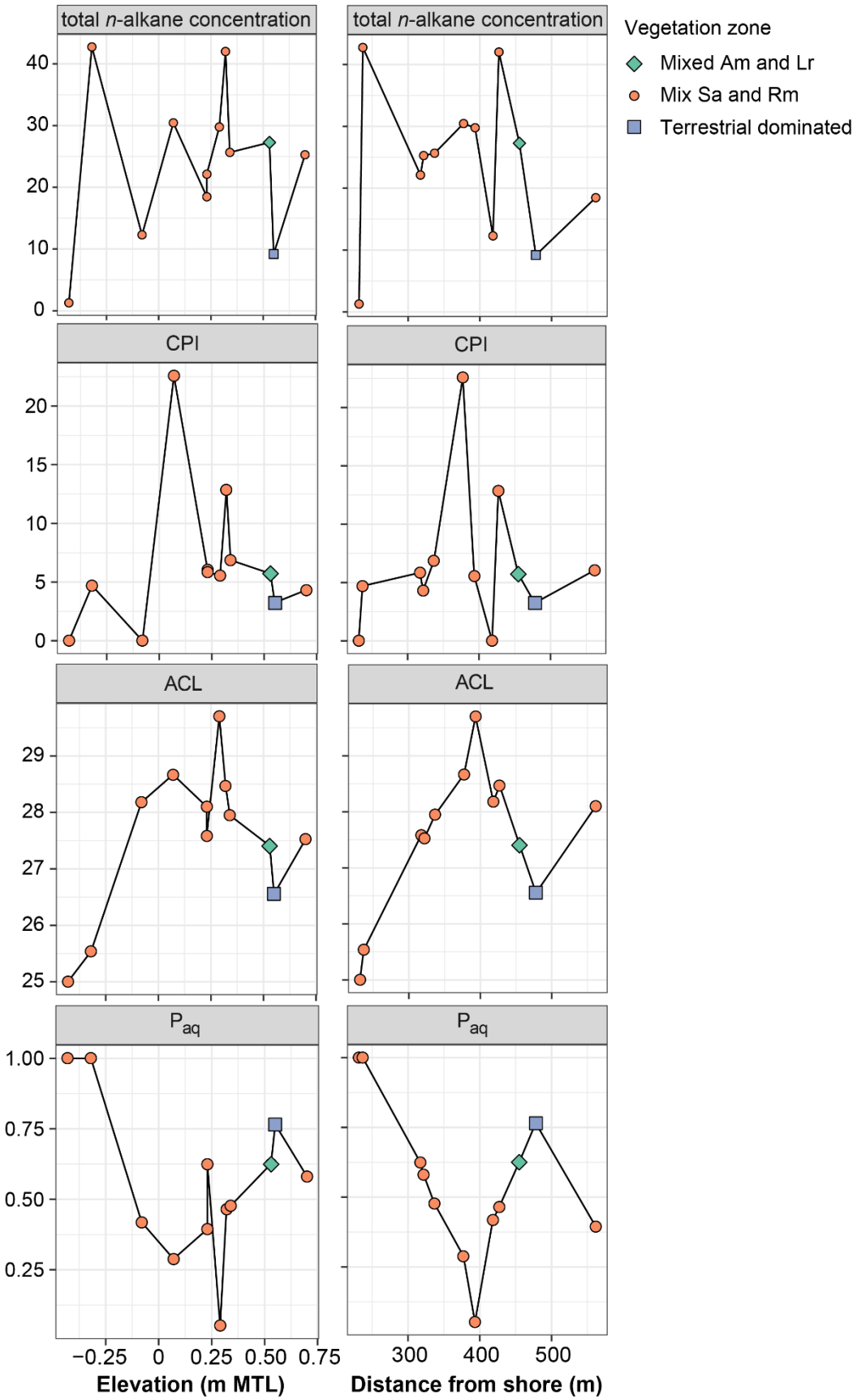

Figure 5.11: Total n-alkane concentrations (in µg per gram of TOC) and n-alkane indices with elevation and distance from shore.

5.4.3.3 Biomarker distribution across environmental gradients

The results of PCA for all identified biomarkers compared with environmental variables (and including totals, ratios and indices), are presented in Figure 5.12. The first and second principle components describe, cumulatively, 61.73% of the variance in the dataset. One sample (sample 37, with an PC1 eigenvalue of >0.75) in the same direction as the sterol eigenvectors accounts for the largest amount of variance along the first dimension (Figure 5.12A), and fine sand, TIC and distance from shore variable eigenvectors account for the largest amount of variance along the second dimension (Figure 5.8). To test the influence of the sample 37 outlier on the variance in the dataset, I also performed a PCA excluding this sample (Figure 5.12B). While there is some alteration to eigenvector directions (e.g. for variables for phytol concentrations and for silt and clay), the variance amongst the dataset is largely similar to that of the entire dataset.

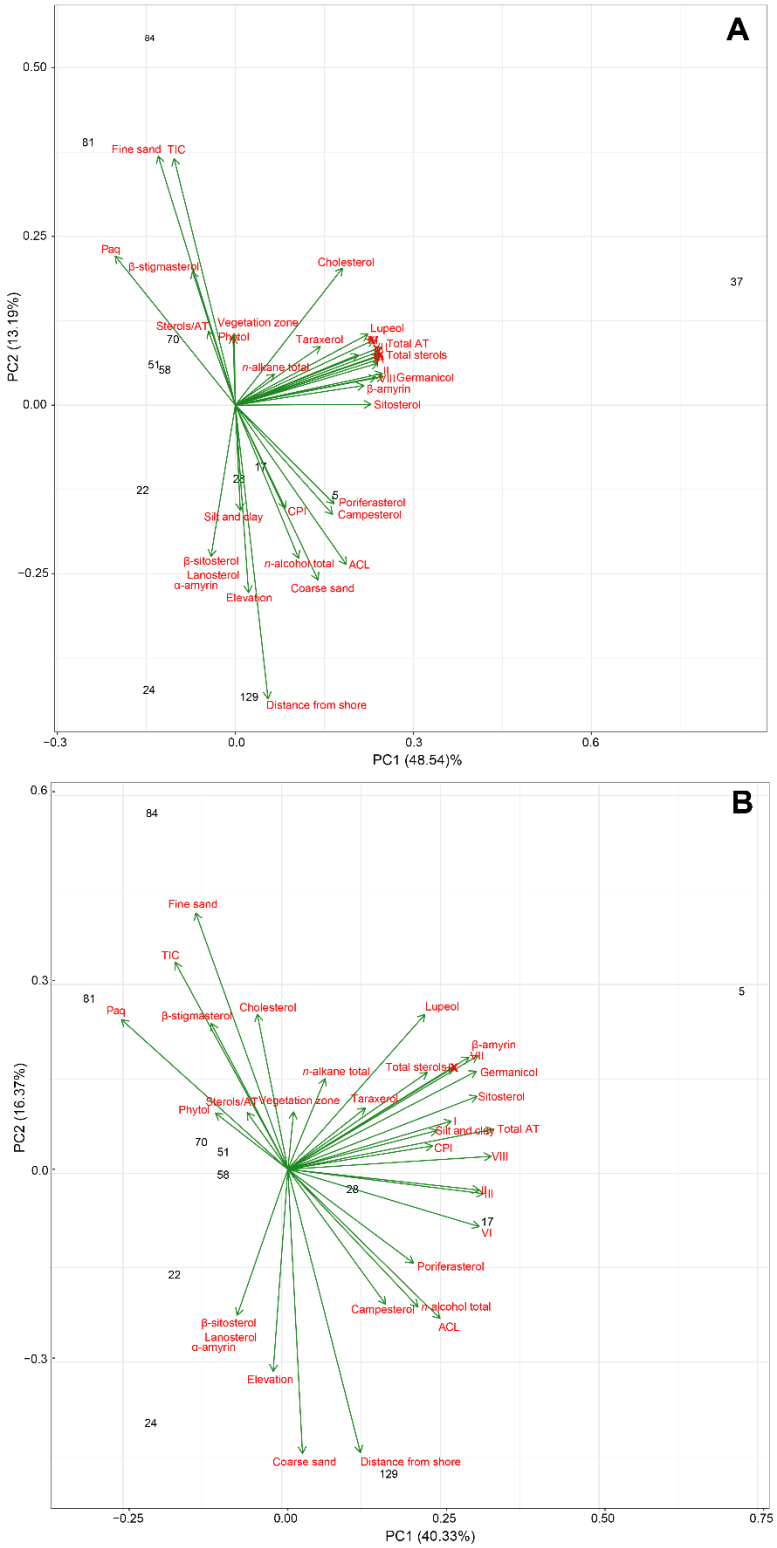

Figure 5.12: PCA results for all apolar and polar biomarkers, and environmental variables of elevation, distance from shore, and vegetation zone. Also included are n-alkane indices (CPI, ACL, P_{aq}), grouped totals: n-alkanes, sterols, n-alcohols, terpenoid hydrocarbons (Total AT), and the ratio of sterols to terpenoid hydrocarbons (Total ST). Roman numerals I–XI relate to the terpenoid hydrocarbon compounds displayed in Appendix Figure A8 and Table A7. A) includes the whole dataset, whereas B) excludes sample 37 which is a clear outlier in A) and dominates variance in the first dimension.

5.5 Discussion

5.5.1 Grain size, TOC and TIC

At Grand Anse, sediment at the seaward edge of the mangrove (e.g. samples 81-95, Figure 5.1) contains carbonate and minerogenic material derived from the nearby (seaward) beach and fringing reef flat environments. Generally, the sediment is fine sand-sized, well-sorted, and contains shell and coral fragments reworked from the nearby beach and fringing reef. The most seaward mangrove sediments generally have high % TIC and relatively low % TOC values (up to 10 % TIC, and 0 % TOC). The grain size distribution of these samples is also similar to those taken from the beach at Grand Anse (see Figure 5.1). Sections of the mangrove that are closest to the seaward edge likely undergo deposition of fine carbonate sand from the Grand Anse beach and reef flat via incoming flood tides and wave currents. Although there is a general trend for this fine carbonate sand to be present in the most seaward samples, when the whole Grand Anse dataset is analysed fine sand and TIC composition of surface sediment is only weakly correlated with distance from shore (Figure 5.6).

At the other end of the mangrove system, mangrove environments furthest from the influence of flood tide and wave action at Grand Anse have similar sediments to those taken from the stream of the River Dauban in its freshwater reach (Figure 5.3C). These are composed of poorly-sorted coarse sands, with low % TIC and variable % TOC values (e.g. samples 21-26, Figure 5.1). These river sediments are quartz-rich and are derived from erosion of granite bedrock and transported to the mangrove by the River Dauban. This pattern is repeated at Anse Boileau where the River Cayman transports coarse quartz-rich sand to the rear of this mangrove system.

Surface sediments with the highest TOC and silt/clay values are found in the middle section of the mangrove at both Grand Anse (samples 2-17, Figure 5.1) and Anse Boileau (e.g. samples 166-171, Figure 5.2), where geomorphology (e.g. a meander as at Grand Anse) reduces the relative influence of both marine (tidal and wave) and terrestrial (fluvial) sedimentation. In island locations elsewhere in the tropics such as Micronesia and Puerto Rico, recent sedimentation in mangroves is dominated by fluvial processes which respond to rainfall events and recent upstream land-use changes such as deforestation and agriculture (Khan et al., 2019b; Victor et al., 2006). The results of the work at Grand Anse and Anse Boileau suggest that upstream events do drive sedimentation in the landward portion of the

mangroves, and that tidal and wave energy is also an important mechanism that deposits marine-derived sediment in the seaward portion of the mangroves.

This spatial pattern of grainsize, TOC and TIC observations at Grand Anse and Anse Boileau suggests local hydrogeomorphological conditions strongly influence surface sediment composition. Seychelles mangroves typically occupy river channels that have eroded into a widely observed carbonate-sand beach plateau (see Section 1.3.2 and Figure 5.1) that prograded across the coastal plain as RSL stabilised around ~3,000 years before present (Woodroffe et al., 2015a). This beach plateau provides a further source of sediment to the mangrove zones at Grand Anse and Anse Boileau, in addition to that supplied by tidal, wave, fluvial, and biological processes. The beach plateau itself is composed of fine carbonate sand and shell material with some organic material similar to the modern beach material. This additional sediment source complicates the relationship between grainsize, TOC and TIC and elevation and distance from shore. The beach plateau sediment mainly influences the middle section of the mangrove at Grand Anse (samples 70-80, Figure 5.1) where the River Dauban meanders through this plateau. A range of environmental variables including tidal and wave energy, river floods, and erosion of plateau material by the estuarine section of the river, and others not analysed as part of this study such as water flow velocity and turbulence (Furukawa and Wolanski, 1996) appear to control modern sedimentation in Seychelles mangroves rather than explicitly elevation or distance from shore (Figure 5.8). This finding demonstrates that although it is important to analyse grainsize, TOC and TIC in the interpretation of fossil sedimentary records that are to be used for RSL reconstructions to provide additional environmental information, they should not be used as quantitative RSL proxies themselves in small, island mangroves like those of Seychelles.

5.5.2 Biomarkers

Generally, when biomarker concentrations are considered in µg per gram dry sediment (rather than µg per gram TOC), concentrations strongly peak where TOC values are high (e.g. sample 5, Appendix Table A4). This result is in agreement with the TOC data in that organic matter accumulation is highest in the section of the mangrove that is more protected from both fluvial and marine (tidal and wave) water flows. These high-TOC samples are also where surface sediment compositions have increased silt and clay (which is correlated with TOC in Figure 5.8). Organic matter, as evidenced by the biomarker concentrations, may accumulate preferentially in this zone of the Grand Anse mangrove because: a) the hydraulic conditions (i.e. quieter water flow) allow for deposition of organic matter particulates and fine-grained

minerogenic grains, b) there may be higher rates of mangrove organic carbon production in this zone as an ecological response to environmental conditions, or c) greater biomarker preservation at the sediment surface, as fine-grained sediments stay waterlogged and anoxic more readily than coarser sediments (Adame et al., 2015; Ezcurra et al., 2016; Furukawa and Wolanski, 1996; Owers et al., 2020). Therefore, to examine the biomarker distributions without the TOC influence, from here on I discuss biomarker data with respect to µg per gram of TOC rather than µg per gram of dry sediment.

The presence of *n*-alkanes in the Grand Anse surface sediments indicates input of organic matter by plant waxes (Eglinton and Hamilton, 1967). The distribution of *n*-alkanes and indices CPI, ACL and P_{aq} suggest that a) organic matter is likely derived from fresh/immature plant material as CPI values are generally >4, b) organic matter is likely from a higher plant source as ACL values are generally >27, and c) aquatic vegetation input is variable but not significant as P_{aq} values are generally <0.7 (Figure 5.11). The presence of *n*-alkanes does not solely determine a mangrove source, as *n*-alkanes are produced by many higher plants (Eglinton and Hamilton, 1967). However, other studies examining biomarkers in both fresh mangrove plant material and surface sediments find apolar lipid fractions dominated by *n*-alkanes (He et al., 2017; Kumar et al., 2019; Ladd and Sachs, 2015b; Ranjan et al., 2015). Spatial variability is evident in the samples analysed here, in that two samples at the lowest elevations and closest to the open shore demonstrate organic matter inputs from shorter chain *n*-alkanes (ACL <26) and likely some aquatic plant species (P_{aq} = 1) (Figure 5.11). Mangrove sediments are known to contain a mix of organic matter derived from multiple marine and terrestrial sources (Bouillon and Boschker, 2006; He et al., 2014; Kumar et al., 2019; Mead et al., 2005), and these results demonstrate that the distribution of *n*-alkanes may help differentiate different zones within a mangrove e.g. those more dominated by aquatic plant species rather than dominantly mangrove (which have a higher plant signature). Algae was observed on the outside of aerial roots of the mangroves at Grand Anse, however short chain *n*-alkanes can be derived from marine or brackish/freshwater algae. Brassicasterol ((22*E*)-Ergosta-5,22-dien-3β-ol) and dinosterol ((3β,4α,5α,22*E*)-4,23-Dimethylergost-22-en-3-ol) are indicators of marine sources but these were not detected in the polar fraction, which therefore does not help isolate the likely source(s) of the short chain *n*-alkane inputs. The PCA analysis (Figure 5.12) does not suggest a strong co-variance between *n*-alkane indices and environmental variables, however a larger dataset may help determine any spatial patterns (in particular relating to elevation).

The most abundant group of compounds in the Grand Anse surface sediments are the triterpenoid alcohols (Figure 5.9 and Figure 5.10), which is consistent with other measurements of mangrove plant material and sediments (Basyuni et al., 2007; Killops and Frewin, 1994; Koch et al., 2011; Koch et al., 2003; Ranjan et al., 2015). Taraxerol is the most abundant compound in all samples (Figure 5.9 and Figure 5.10), which is produced in mangrove leaves and roots (Koch et al., 2003). This result alone demonstrates a large component of organic matter input to the surface sediments is mangrove derived, as mangroves are unique among higher plants in that they synthesize larger quantities of taraxerol (Koch et al., 2011; Versteegh et al., 2004). Taraxerol abundances in the Grand Anse sediments therefore support the use of this compound as a mangrove-derived organic matter indicator in sedimentary sequences. However, this interpretation is based on the very high concentrations of taraxerol found in mangrove plants (Killops and Frewin, 1994), when it is known that taraxerol can be synthesized in lower concentrations in other higher plants (Johns et al., 1994; Versteegh et al., 2004). To confidently assign taraxerol as a mangrove organic matter proxy, analysis of biomarker distributions in samples from adjacent depositional environments or vegetation zones could be useful. Regardless of these concerns, all of the samples analysed in this study are located within the mangrove zone across and environmental gradient, and yet no relationship to any measured environmental variable was found (Figure 5.12).

Other triterpenoid alcohols that are abundant in the Grand Anse surface sediments are consistent with a mangrove origin (e.g. β-amyrin, lupeol, and germanicol) (Basyuni et al., 2007; Koch et al., 2011). The presence and concentrations of the majority of polar compounds does not appear to co-vary with either elevation, distance from shore or vegetation zone (Figure 5.12), with the exception of β-sitosterol, lanosterol and α-amyrin, which are only present in one sample (Figure 5.9 and Figure 5.10). This suggests that these compounds could be indicators of the *Avicennia marina* and *Lumnitzera racemosa* vegetation zone, although further sampling is required to validate this finding. Koch et al. (2011) demonstrated that different mangrove species produce different concentrations and distributions of triterpenoid alcohols. In particular, *Rhizophora* sp. produces the largest quantities of taraxerol, β-amyrin and germanicol in comparison to other species, and because of their high leaf litter production (Koch et al., 2005), these compounds are well distributed across mangrove surface sediments despite changes in vegetation zone (Koch et al., 2011). Further testing of surface sediments across a larger range of vegetation zones and of fresh plant material from different species may help identify whether particular

triterpenoid alcohols can indicate different vegetation zones in mangrove sedimentary sequences.

The terpenoid hydrocarbons present in the apolar fraction (Appendix Figure A8) are likely degradation products of sterols and triterpenoid alcohols produced by mangroves (He et al., 2018). The alteration of the triterpenoid alcohols to unsaturated terpenoid hydrocarbons is thought to occur relatively rapidly as these compounds have been found in fresh mangrove leaves, but are considered stable over centennial timescales as they have been found in both surface and core sediments (He et al., 2018). The mechanisms for the alteration of the parent compounds are not entirely clear but are likely to be a result of (or a combination of) photodegradation, bacterial or fungal attack, anaerobic alteration or oxidation (He et al., 2018). The spatial distribution of these degradation compounds across the Grand Anse surface sediments can therefore be attributed to the distribution and concentration of triterpenoid alcohol compounds (in particular taraxerol, which is a parent compound to multiple compounds displayed in Appendix Figure A8). However, in one sample (sample 37, at +0.29 m MTL, see Appendix Table A7) the total concentration (per gram TOC) of terpenoid hydrocarbons is an order of magnitude higher than other samples. The reasons for this outlier are not apparent in any patterns in measured environmental variables, but observations at the sample site during field sampling indicate that this sample was collected in a small topographic depression where surface water remained even during low tide (which did not occur elsewhere in the mangrove zone). It is possible that this surface water creates a unique and localised anaerobic environment at the sediment surface where either anaerobic degradation processes enhance triterpenoid alcohol alteration or increase preservation potential. To better determine the fate of triterpenoid alcohols in mangrove sediments, further analysis should increase spatial distribution of surface sediment sampling, as well as look to analyse fresh plant materials and down-core samples.

Phytol, a derivative of the chlorophyll molecule and commonly interpreted as an indicator of fresh plant material, was detected in a majority of the surface sediments at Grand Anse (Appendix Table A9). Notably, I did not detect common diagenetic products of phytol found in sediments: phytane and pristane, which can provide information on the whether oxidation or reduction of organic matter (Didyk et al., 1978). In the polar fraction, I also detect hopanoids, which are a compound group produced by bacteria, but are of insufficient abundances to quantify. Stanols are anaerobic degradation products of sterols commonly found in peats (Gaskell and Eglinton, 1976), but no stanol compounds were identified in the Grand Anse surface sediments. Further analysis on surface and core sediments may help to

identify whether the absence of degradation compounds is a result of either slow degradation processes, or through aerobic rather than anaerobic degradation.

5.6 Summary

The grainsize, TOC and TIC observations suggest that inorganic and organic sedimentation at both Grand Anse and Anse Boileau are strongly controlled by local hydrogeomorphological variables, rather than measured elevation and distance from shore. Sediment composition may be determined by river channel shape, in particular where river meanders provide suitable buffers from tidal, wave, and fluvial flow, so that organic sedimentation is enhanced (i.e. TOC values and biomarker concentrations are higher). This detailed study of mangrove surface sediments highlights that despite clear spatial differences in sediment compositions, elevation (and by proxy inundation and mean sea level variability) are not key drivers of sedimentation in the Seychelles mangrove systems. Therefore, I cannot justify the use of grain size data, % TOC or % TIC as quantitative sea-level indicators in Seychelles mangroves, but I can recommend their usefulness in interpreting sedimentation patterns and palaeogeography over time.

The biomarker observations show organic matter in the Seychelles mangrove surface sediments is likely derived from mangroves, and the high concentrations of taraxerol provide strong evidence for this. The distribution of *n*-alkanes possibly show a spatial pattern particularly with distance from shore, and a number of sterols may be indicative of the *Avicennia marina* and *Lumnitzera racemosa* vegetation zone. Despite this, the utility of biomarkers as quantitative sea-level indicators in mangroves is unclear from the Seychelles observations. This partly reflects the dominance of the taraxerol biomarker wherever mangroves are present, and the important influences of hydrogeomorphological factors on organic matter distribution. Although excellent preservation of mangrove biomarkers was determined in the surface samples, consideration of their lability through time will also be important for their proxy potential. Thus, further work is required to consider both how specific the mangrove compounds might be to environmental variables, and their down-core preservation in order to reconstruction past environmental changes in a mangrove setting. Increasing the datasets size and extending the sampling range outside of the mangrove zone will help determine whether particular compounds are exceptionally abundant or only present in mangrove zones. Analysing fresh plant material and core sediments will tell us more about species-specific compounds and core sediments will provide insight into the preservation of compounds in mangrove sediments over time.

Chapter 6: Lessons from Seychelles mangroves: summary and conclusions

The aim of this research was to evaluate the utility of mangrove proxies in quantitative RSL reconstructions, using a case study of mangrove environments in Seychelles. This chapter concludes this thesis by briefly summarising the initial research questions outlined in Chapter One. This chapter then outlines recommendations for future studies using mangrove proxies for RSL reconstructions and considers future research avenues.

6.1 Thesis summary

1) What materials in mangrove sediments are best suited for constructing radiocarbon age models?

In Chapter Three, I was able to evaluate the utility of different materials for radiocarbon measurements using a series of cores from the Grand Anse mangrove in Seychelles. I tested the use of bulk sediments, organic concentrates, above-ground macrofossils, and pollen concentrates collected from the same sediment depths in four different cores, and compared these results to radiocarbon ages measured in a previous study at the same mangrove (Woodroffe et al., 2015a).

In the Grand Anse cores, there were limited above-ground macrofossils (leaves, seeds etc.) available for analysis, and I attribute this to low sedimentation rates at the Grand Anse mangrove which has limited the preservation potential of above-ground organic macrofossils in sedimentary sequences. I developed a method to concentrate pollen from Seychelles mangrove sediments, but pollen concentrations were too low to consider these samples for radiocarbon measurements.

A majority of the radiocarbon measurement comparisons are between bulk sediment and organic concentrate samples (sediment size fraction 10-63 μm). Unlike a previous study which reported consistently older radiocarbon ages for organic concentrate samples (Woodroffe et al., 2015b), results from the Grand Anse mangrove cores show that bulk sediment and organic concentrate radiocarbon ages are indistinguishable, and thus likely sample the same carbon source (of the same age). Organic concentrate-derived radiocarbon ages probably sample younger carbon despite separation of coarser and finer sediment fractions, and therefore are not entirely representative of the 'true' depositional age at a given sediment depth. This is likely due to inputs from penetrating roots, bioturbation,

porewater exchange, and decomposition. The degree to which these processes influence mangrove sediment sequences likely varies greatly depending on sedimentation rates, bioturbation rates, sedimentology, and local hydrology.

2) **Does mangrove pollen provide a reliable alternative to other microfossils for quantitative RSL reconstructions in Seychelles mangroves?**

In Chapter Four I tested the use of mangrove pollen for quantitative RSL reconstructions by examining vegetation and pollen distributions in two Seychelles mangroves, Grand Anse and Anse Boileau. Detailed surveying in both mangrove areas showed that mangrove species zonation is broadly related to elevation in the mangrove zone. *Sonneratia alba* and *Rhizophora mucronata* occupy lower elevations closer to the open shore and rivers, and *Avicennia marina* and *Lumnitzera racemosa* occupy higher elevations closer to the terrestrial margin.

I constructed pollen traps which recorded modern pollen rain above tidal inundation for a period of one year in the mangrove zone. The pollen trap data show that pollen assemblages are not necessarily representative of vegetation cover at a sample site, due to some mangrove species producing low quantities of pollen such as *Lumnitzera racemosa* and *Avicennia marina*, which are characteristic species of particular elevation zones. Despite this lack of association, total mangrove pollen abundances generally peak in the mangrove zone and decrease immediately at higher elevations.

To evaluate the process by which mangrove pollen is transported from trees to the sediment surface, I also examined surface sediment samples at the same sites as the deployed pollen traps. However, very low pollen concentrations were detected in the surface sediments. Sedimentology, saturation and low sedimentation rates may have impacted the preservation of pollen in the Grand Anse and Anse Boileau surface sediments.

The results of pollen trap and surface sediment samples from at the Grand Anse and Anse Boileau mangroves suggest that it is unlikely pollen-based proxies will improve existing vertical uncertainties on mangrove-derived RSL reconstructions in Seychelles. However, the pollen traps data suggests that mangrove pollen, if preserved, could aid interpretation of sedimentary sequences where depositional environments may be unclear from sedimentological descriptions alone, as modern mangrove pollen abundance is closely linked with position in the mangrove zone. Palynological approaches may still be useful at locations where there is better plant and pollen association, and where sedimentological conditions allow for better pollen preservation.

3) Are geochemical properties potential proxies for quantitative RSL reconstructions in Seychelles mangroves?

In Chapter Five, I characterised the TOC, TIC and lipid biomarker compositions in surface sediments at the Grand Anse and Anse Boileau mangrove areas. TOC and TIC vary greatly across both study areas and reflect the variable processes and sources of sedimentation in Seychelles mangroves. Fine-sand sized, well-sorted and carbonate-rich sediment is supplied to the mangrove via tidal and wave currents which characterises the section of the mangrove closest the marine environment. Coarse-grained, poorly-sorted and quartz-rich sediment is supplied to the mangrove via the River Dauban and River Cayman (at Grand Anse and Anse Boileau respectively), which both drain granitic rivers catchments on Mahé. The relative contributions of both sediment sources in a given surface sediment sample is complicated by river channel morphology. This is demonstrated by the interior section of the Grand Anse mangrove, which is along a river channel meander and has lower TIC values, higher TOC values and finer-grained sediments (higher % silt and clay). Sediment provenance is further complicated by sediment derived from the Mid- to Late Holocene coastal plain deposits, as both mangrove zones occupy river channels which erode into this coastal feature composed of carbonate sands. Surface sediment composition therefore has a complicated relationship with measured environmental variables of elevation, distance from shore, and vegetation zone, as sedimentation is strongly controlled by hydrogeomorphological processes. Therefore, I cannot justify the use of TOC or TIC as a quantitative RSL indicator in Seychelles mangroves.

The lipid biomarker concentrations in the surface sediments at Grand Anse strongly reflect the pattern of TOC distribution across the mangrove zone. The biomarkers indicate that organic matter is most likely derived from mangroves, evidenced by the high concentrations of the triterpene alcohol taraxerol. *N*-alkane distributions and sterols may be indicative of different elevation and vegetation zones, however further work on both fresh plant material and surface sediments is needed to fully assess the nature of any spatial relationships. Terpenoid hydrocarbons that are likely derived from the degradation of mangrove-derived taraxerol are present in the surface sediments at Grand Anse, which suggests degradation of organic matter happens rapidly. Further work is needed to examine how biomarkers are preserved in fossil sedimentary sequences to evaluate their potential as RSL proxies.

6.2 Future recommendations

Based on the finding of this thesis and a review of the literature, I provide below some broad recommendations for future mangrove-derived RSL research:

6.2.1 Mangrove sediments and proxy indicators

Sedimentological descriptions should be complimented with further analyses to confidently determine mangrove depositional environments (e.g. palynology or taraxerol concentrations), as freshwater and mangrove 'peat' deposits can be indistinguishable from physical properties alone. My research has demonstrated that total mangrove pollen abundances (of the major species category) peak within the mangrove zone and decline at higher elevations, even in short horizontal distances. My research has also demonstrated the potential for taraxerol being an indicator of a mangrove depositional environment, although further work is required to test taraxerol abundances in adjacent terrestrial environments.

Micropalaeontological approaches (foraminifera, diatoms, pollen etc.) can provide precise, high-resolution sea-level indicators. These can be used to reconstruct RSL if modern distributions are related to elevation in the intertidal zone. Additionally, this requires that a) microfossils preserve well down-core, and that the fossil assemblages reflect patterns present in the modern environments and b) have not been considerably altered by post-depositional processes such as test dissolution. Particular consideration is needed of infaunal microfossil production, and also when considering pollen of the potential for redistribution by winds, tides and other water currents. My research demonstrated that despite a good relationship between mangrove species zonation and elevation, pollen assemblages are not necessarily representative of the depositional environment and do not always preserve well in sedimentary sequences.

Organic geochemical techniques are showing promise in mangrove RSL research, but generally these are currently applied in a multi-proxy context. Further studies should tackle specific sediment fractions or biomarkers (rather than bulk sediments) to evaluate the environmental controls on specific sediment and/or carbon sources. Future work may also investigate whether biomarkers that can be linked to specific mangrove species or particular macrofossils (e.g. distinctly leaves) can be identified and isolated for leverage in RSL studies.

Because of the challenge using proxy indicators, RSL reconstructions from mangroves should use multi-proxy approaches to assess the drivers of sedimentation in the depositional

setting. Additionally, the researcher should consider the likely precision obtained from different techniques alongside the amount of time it takes to do the analysis.

6.2.2 Dating

Radiocarbon is the most widely applied chronological technique as mangroves provide an abundance of organic carbon. The researcher should interpret radiocarbon measurements on bulk sediment samples cautiously. Samples which are more easily related to specific carbon sources (e.g. an above-ground macrofossil) can be more readily linked to depositional processes and therefore RSL. Where macrofossils are not readily available, future studies should investigate the potential for mangrove-specific biomarkers for compound-specific radiocarbon measurements.

Researchers could consider chronological methods independent of radiocarbon for <100 year records e.g. ^{210}Pb, ^{137}Cs, pollution markers and anthropogenic pollen markers. Tephrochronology could be a useful approach if tephra is available and it can be readily linked to known and dated eruptions, but such sites are likely rare.

References

Adame, M.F., Lovelock, C.E., 2011. Carbon and nutrient exchange of mangrove forests with the coastal ocean. Hydrobiologia 663, 23–50. https://doi.org/10.1007/s10750-010-0554-7

Adame, M.F., Neil, D., Wright, S.F., Lovelock, C.E., 2010. Sedimentation within and among mangrove forests along a gradient of geomorphological settings. Estuarine, Coastal and Shelf Science 86, 21–30. https://doi.org/10.1016/j.ecss.2009.10.013

Adame, M.F., Santini, N.S., Tovilla, C., Vázquez-Lule, A., Castro, L., Guevara, M., 2015. Carbon stocks and soil sequestration rates of tropical riverine wetlands. Biogeosciences 12, 3805–3818. https://doi.org/10.5194/bg-12-3805-2015

Admiralty Tide Tables (No. Volume 3), 2017. United Kingdom Hydrographic Office.

Alongi, D.M., 2014. Carbon Cycling and Storage in Mangrove Forests. Annual Review of Marine Science 6, 195–219. https://doi.org/10.1146/annurev-marine-010213-135020

Andersson, R.A., Meyers, P.A., 2012. Effect of climate change on delivery and degradation of lipid biomarkers in a Holocene peat sequence in the Eastern European Russian Arctic. Organic Geochemistry, Advances in Organic Geochemistry 2011: Proceedings of the 25th International Meeting on Organic Geochemistry 53, 63–72. https://doi.org/10.1016/j.orggeochem.2012.05.002

Angulo, R.J., Lessa, G.C., Souza, M.C., 2006. A critical review of mid- to late-Holocene sea-level fluctuations on the eastern Brazilian coastline. Quaternary Science Reviews 25, 486–506. https://doi.org/10.1016/j.quascirev.2005.03.008

Badyukov, D.D., Demidenko, E.L., Kaplin, P.A., 1989. Paleogeography of the Seychelles Bank and the northwest Madagascar Shelf during the last glacio-eustatic regression (18,000 a B.P.). Chin. J. Ocean. Limnol. 7, 89–92. https://doi.org/10.1007/BF02842661

Barbosa, C.F., Scott, D.B., Seoane, J.C.S., Turcq, B.J., 2005. Formainifera zonations as base lines for Quaternary sea-level fluctuations in south-southeast Brazilian mangroves and marshes. Journal of Foraminiferal Research 35, 22–43. https://doi.org/10.2113/35.1.22

Bard, E., Hamelin, B., Arnold, M., Montaggioni, L., Cabioch, G., Faure, G., Rougerie, F., 1996. Deglacial sea-level record from Tahiti corals and the timing of global meltwater discharge. Nature 382, 241–244. https://doi.org/10.1038/382241a0

Barker, P., Fontes, J.C., Gasse, F., Druart, J.C., 1994. Experimental Dissolution of Diatom Silica in Concentrated Salt Solutions and Implications for Paleoenvironmental Reconstruction. Limnology and Oceanography 39, 99–110.

Barlow, N.L.M., Long, A.J., Saher, M.H., Gehrels, W.R., Garnett, M.H., Scaife, R.G., 2014. Salt-marsh reconstructions of relative sea-level change in the North Atlantic during the last 2000 years. Quaternary Science Reviews 99, 1–16. https://doi.org/10.1016/j.quascirev.2014.06.008

Barlow, N.L.M., Shennan, I., Long, A.J., Gehrels, W.R., Saher, M.H., Woodroffe, S.A., Hillier, C., 2013. Salt marshes as late Holocene tide gauges. Global and Planetary Change 106, 90–110. https://doi.org/10.1016/j.gloplacha.2013.03.003

Barnett, R.L., Bernatchez, P., Garneau, M., Brain, M.J., Charman, D.J., Stephenson, D.B., Haley, S., Sanderson, N., 2019. Late Holocene sea-level changes in eastern Québec and potential drivers. Quaternary Science Reviews 203, 151–169. https://doi.org/10.1016/j.quascirev.2018.10.039

Bartlett, A., Barghoorn, E.S., 1973. Phytogeographic history of the isthmus of Panama during the past 12,000 years (A history of vegetation, climate and sea level change), in:

Vegetation and Vegetational History of Northern Latin America. Elsevier, Amsterdam, pp. 203–299.
Baskaran, M., 2011. Po-210 and Pb-210 as atmospheric tracers and global atmospheric Pb-210 fallout: a Review. Journal of Environmental Radioactivity, International Topical Meeting on Polonium and Radioactive Lead Isotopes 102, 500–513. https://doi.org/10.1016/j.jenvrad.2010.10.007
Basyuni, M., Oku, H., Baba, S., Takara, K., Iwasaki, H., 2007. Isoprenoids of Okinawan mangroves as lipid input into estuarine ecosystem. J Oceanogr 63, 601–608. https://doi.org/10.1007/s10872-007-0053-2
Beaman, R., Larcombe, P., Carter, R.M., 1994. New evidence for the Holocene sea-level high from the inner shelf, central Great Barrier Reef, Australia. Journal of Sedimentary Research 64, 881–885. https://doi.org/10.1306/D4267EF1-2B26-11D7-8648000102C1865D
Behling, H., Cohen, M.C.L., Lara, R.J., 2004. Late Holocene mangrove dynamics of Marajó Island in Amazonia, northern Brazil. Veget Hist Archaeobot 13, 73–80. https://doi.org/10.1007/s00334-004-0031-1
Behling, H., Cohen, M.C.L., Lara, R.J., 2001. Studies on Holocene mangrove ecosystem dynamics of the Bragança Peninsula in north-eastern Pará, Brazil. Palaeogeography, Palaeoclimatology, Palaeoecology 167, 225–242. https://doi.org/10.1016/S0031-0182(00)00239-X
Berdin, R.D., Siringan, F.P., Maeda, Y., 2003. Holocene Relative Sea-Level Changes and Mangrove Response in Southwest Bohol, Philippines. Journal of Coastal Research 19, 304–313.
Berkeley, A., Perry, C.T., Smithers, S.G., Hoon, S., 2014. Towards a formal description of foraminiferal assemblage formation in shallow-water environments: Qualitative and quantitative concepts. Marine Micropaleontology 112, 27–38. https://doi.org/10.1016/j.marmicro.2014.08.005
Berkeley, A., Perry, C.T., Smithers, S.G., Horton, B.P., 2008. The spatial and vertical distribution of living (stained) benthic foraminifera from a tropical, intertidal environment, north Queensland, Australia. Marine Micropaleontology 69, 240–261. https://doi.org/10.1016/j.marmicro.2008.08.002
Berkeley, A., Perry, C.T., Smithers, S.G., Horton, B.P., Cundy, A.B., 2009a. Foraminiferal biofacies across mangrove-mudflat environments at Cocoa Creek, north Queensland, Australia. Marine Geology 263, 64–86. https://doi.org/10.1016/j.margeo.2009.03.019
Berkeley, A., Perry, C.T., Smithers, S.G., Horton, B.P., Cundy, A.B., 2009b. Foraminiferal biofacies across mangrove-mudflat environments at Cocoa Creek, north Queensland, Australia. Marine Geology 263, 64–86. https://doi.org/10.1016/j.margeo.2009.03.019
Berkeley, A., Perry, C.T., Smithers, S.G., Horton, B.P., Taylor, K.G., 2007. A review of the ecological and taphonomic controls on foraminiferal assemblage development in intertidal environments. Earth-Science Reviews 83, 205–230. https://doi.org/10.1016/j.earscirev.2007.04.003
Bernhardt, C.E., Willard, D.A., 2015. Pollen and spores of terrestrial plants, in: Shennan, I., Long, A.J., Horton, B.P. (Eds.), Handbook of Sea-Level Research. Wiley, pp. 218–232.
Bird, M.I., Austin, W.E.N., Wurster, C.M., Fifield, L.K., Mojtahid, M., Sargeant, C., 2010. Punctuated eustatic sea-level rise in the early mid-Holocene. Geology 38, 803–806. https://doi.org/10.1130/G31066.1
Bird, M.I., Fifield, L.K., Teh, T.S., Chang, C.H., Shirlaw, N., Lambeck, K., 2007. An inflection in the rate of early mid-Holocene eustatic sea-level rise: A new sea-level curve from Singapore. Estuarine, Coastal and Shelf Science 71, 523–536. https://doi.org/10.1016/j.ecss.2006.07.004

Blanchon, P., Shaw, J., 1995. Reef drowning during the last deglaciation: Evidence for catastrophic sea-level rise and ice-sheet collapse. Geology 23, 4–8. https://doi.org/10.1130/0091-7613(1995)023<0004:RDDTLD>2.3.CO;2

Blasco, F., Saenger, P., Janodet, E., 1996. Mangroves as indicators of coastal change. CATENA 27, 167–178. https://doi.org/10.1016/0341-8162(96)00013-6

Bloemendaal, N., Haigh, I.D., de Moel, H., Muis, S., Haarsma, R.J., Aerts, J.C.J.H., 2020. Generation of a global synthetic tropical cyclone hazard dataset using STORM. Scientific Data 7, 1–12. https://doi.org/10.1038/s41597-020-0381-2

Bocanegra Ramírez, D.M., Li, H.-C., Vázquez, G.D., Alcantara, I.I., Bischoff, J.L., 2019. Holocene climate change and sea level oscillations in the pacific coast of Mexico. Quaternary International. https://doi.org/10.1016/j.quaint.2019.01.003

Boski, T., Bezerra, F.H.R., de Fátima Pereira, L., Souza, A.M., Maia, R.P., Lima-Filho, F.P., 2015. Sea-level rise since 8.2 ka recorded in the sediments of the Potengi–Jundiai Estuary, NE Brasil. Marine Geology 365, 1–13. https://doi.org/10.1016/j.margeo.2015.04.003

Bouillon, S., Boschker, H.T.S., 2006. Bacterial carbon sources in coastal sediments: a cross-system analysis based on stable isotope data of biomarkers. Biogeosciences.

Bouillon, S., Connolly, R.M., Lee, S.Y., 2008. Organic matter exchange and cycling in mangrove ecosystems: Recent insights from stable isotope studies. Journal of Sea Research, Mangrove Macrobenthos Special IssueProceedings of the Mangrove Macrobenthos Meeting II 59, 44–58. https://doi.org/10.1016/j.seares.2007.05.001

Bouillon, S., Middelburg, J.J., Dehairs, F., Borges, A.V., Abril, G., Flindt, M.R., Ulomi, S., Kristensen, E., 2007. Importance of intertidal sediment processes and porewater exchange on the water column biogeochemistry in a pristine mangrove creek (Ras Dege, Tanzania). Biogeosciences 4, 311–322. https://doi.org/10.5194/bg-4-311-2007

Bourgeois, C., Alfaro, A.C., Leopold, A., Andréoli, R., Bisson, E., Desnues, A., Duprey, J.L., Marchand, C., 2019. Sedimentary and elemental dynamics as a function of the elevation profile in a semi-arid mangrove toposequence. CATENA 173, 289–301. https://doi.org/10.1016/j.catena.2018.10.025

Bradley, S.L., Milne, G.A., Horton, B.P., Zong, Y., 2016. Modelling sea level data from China and Malay-Thailand to estimate Holocene ice-volume equivalent sea level change. Quaternary Science Reviews 137, 54–68. https://doi.org/10.1016/j.quascirev.2016.02.002

Bradley, S.L., Milne, G.A., Shennan, I., Edwards, R., 2011. An improved glacial isostatic adjustment model for the British Isles. Journal of Quaternary Science 26, 541–552. https://doi.org/10.1002/jqs.1481

Braithwaite, C.J.R., Montaggioni, L.F., Camoin, G.F., Dalmasso, H., Dullo, W.C., Mangini, A., 2000. Origins and development of Holocene coral reefs: a revisited model based on reef boreholes in the Seychelles, Indian Ocean. Int Journ Earth Sciences 89, 431–445. https://doi.org/10.1007/s005310000078

Bray, E.E., Evans, E.D., 1961. Distribution of n-paraffins as a clue to recognition of source beds. Geochimica et Cosmochimica Acta 22, 2–15. https://doi.org/10.1016/0016-7037(61)90069-2

Bronk Ramsey, C., 2009. Bayesian Analysis of Radiocarbon Dates. Radiocarbon 51, 337–360. https://doi.org/10.1017/S0033822200033865

Bryant Jr, V.M., Holloway, R.G., Jones, J.G., Carlson, D.L., 1994. Pollen preservation in alkaline soils of the American Southwest, in: Traverse, A. (Ed.), Sedimentation of Organic Particles. Cambridge University Press, pp. 47–58.

Cahoon, D.R., Lynch, J.C., 1997. Vertical accretion and shallow subsidence in a mangrove forest of southwestern Florida, U.S.A. Mangroves and Salt Marshes 1, 173–186. https://doi.org/10.1023/A:1009904816246

Camoin, G.F., Montaggioni, L.F., Braithwaite, C.J.R., 2004. Late glacial to post glacial sea levels in the Western Indian Ocean. Marine Geology 206, 119–146. https://doi.org/10.1016/j.margeo.2004.02.003

Campbell, I.D., Campbell, C., 1994. Pollen Preservation: Experimental Wet-Dry Cycles in Saline and Desalinated Sediments. Palynology 18, 5–10.

Campbell, J.F.E., Fletcher, W.J., Hughes, P.D., Shuttleworth, E.L., 2016. A comparison of pollen extraction methods confirms dense-media separation as a reliable method of pollen preparation. Journal of Quaternary Science 31, 631–640. https://doi.org/10.1002/jqs.2886

Caratini, C., Fontugne, M., 1992. A high sea level stand assigned to C. 125,000 years BP on the western coast of India, in: Desai, B.N. (Ed.), Oceanography of the Indian Ocean. New Dehli: Oxford and IBH, pp. 439–445.

Castañeda, I.S., Schouten, S., 2011. A review of molecular organic proxies for examining modern and ancient lacustrine environments. Quaternary Science Reviews 30, 2851–2891. https://doi.org/10.1016/j.quascirev.2011.07.009

Castañeda-Moya, E., Twilley, R.R., Rivera-Monroy, V.H., Marx, B.D., Coronado-Molina, C., Ewe, S.M.L., 2011. Patterns of Root Dynamics in Mangrove Forests Along Environmental Gradients in the Florida Coastal Everglades, USA. Ecosystems 14, 1178–1195. https://doi.org/10.1007/s10021-011-9473-3

Chappell, J., 1983. Evidence for smoothly falling sea level relative to north Queensland, Australia, during the past 6,000 yr. Nature 302, 406–408. https://doi.org/10.1038/302406a0

Chappell, J., Grindrod, J., 1984. Chenier plain formation in northern Australia, in: Thom, B.G. (Ed.), Coastal Geomorphology in Australia. Academic Press, New York, pp. 197–231.

Chappell, J., Polach, H., 1991. Post-glacial sea-level rise from a coral record at Huon Peninsula, Papua New Guinea. Nature 349, 147–149. https://doi.org/10.1038/349147a0

Chappell, J., Rhodes, E.G., Thom, B.G., Wallensky, E., 1982. Hydro-isostasy and the sea-level isobase of 5500 B.P. in north Queensland, Australia. Marine Geology 49, 81–90. https://doi.org/10.1016/0025-3227(82)90030-5

Chmura, G.L., Aharon, P., 1995. Stable Carbon Isotope Signatures of Sedimentary Carbon in Coastal Wetlands as Indicators of Salinity Regime. Journal of Coastal Research 11, 124–135.

Chmura, G.L., Aharon, P., Socki, R.A., Abernethy, R., 1987. An inventory of <Superscript>13</Superscript>C abundances in coastal wetlands of Louisiana, USA: vegetation and sediments. Oecologia 74, 264–271. https://doi.org/10.1007/BF00379369

Church, J.A., Clark, P.U., Cazenave, A., Gregory, J.M., Jevrejeva, S., Levermann, A., Merrifield, M.A., Milne, G.A., Nerem, R.S., Nunn, P.D., Payne, A.J., Pfeffer, W.T., Stammer, D., Unnikrishnan, A.S., 2013. Sea Level Change, in: Stocker, T.F., Qin, D., Plattner, G.K., Tignor, M., Allen, S.K., Boschung, J., Nauels, A., Xia, Y., Bex, V., Midgley, P.M. (Eds.), Climate Change 2013: The Physical Science Basis. Contribution of Working Group I to the Fifth Assessment Report of the Intergovernmental Panel on Climate Change. Cambridge University Press, Cambridge, United Kingdom and New York, NY, USA.

Clark, J.A., Farrell, W.E., Peltier, W.R., 1978. Global changes in postglacial sea level: A numerical calculation. Quaternary Research 9, 265–287. https://doi.org/10.1016/0033-5894(78)90033-9

Cohen, M.C.L., Lara, R.J., Smith, C.B., Angélica, R.S., Dias, B.S., Pequeno, T., 2008. Wetland dynamics of Marajó Island, northern Brazil, during the last 1000 years. CATENA 76, 70–77. https://doi.org/10.1016/j.catena.2008.09.009

Corbett, D.R., Walsh, J.P., 2015. 210Lead and 137Cesium: establishing a chronology for the last century, in: The Handbook of Sea-Level Research. Wiley, pp. 361–372.

Crase, B., Liedloff, A., Vesk, P.A., Burgman, M.A., Wintle, B.A., 2013. Hydroperiod is the main driver of the spatial pattern of dominance in mangrove communities. Global Ecology and Biogeography 22, 806–817. https://doi.org/10.1111/geb.12063

Culver, S.J., 1990. Benthic Foraminifera of Puerto Rican Mangrove-Lagoon Systems: Potential for Paleoenvironmental Interpretations. PALAIOS 5, 34–51. https://doi.org/10.2307/3514995

Culver, S.J., Leorri, E., Corbett, D.R., Mallinson, D.J., Shazili, N.A.M., Mohammad, M.N., Parham, P.R., Yaacob, R., 2013. Infaunal mangrove swamp foraminifera in the Setiu wetland, Terengganu, Malaysia. Journal of Foraminiferal Research 43, 262–279. https://doi.org/10.2113/gsjfr.43.3.262

Culver, S.J., Leorri, E., Mallinson, D.J., Corbett, D.R., Shazili, N.A.M., 2015. Recent coastal evolution and sea-level rise, Setiu Wetland, Peninsular Malaysia. Palaeogeography, Palaeoclimatology, Palaeoecology 417, 406–421. https://doi.org/10.1016/j.palaeo.2014.10.001

Cuzzone, J.K., Clark, P.U., Carlson, A.E., Ullman, D.J., Rinterknecht, V.R., Milne, G.A., Lunkka, J., Wohlfarth, B., Marcott, S.A., Caffee, M., 2016. Final deglaciation of the Scandinavian Ice Sheet and implications for the Holocene global sea-level budget. Earth and Planetary Science Letters 448, 34–41. https://doi.org/10.1016/j.epsl.2016.05.019

Dahdouh-Guebas, F., Koedam, N., 2008. Long-term retrospection on mangrove development using transdisciplinary approaches: A review. Aquatic Botany, Mangrove Ecology – Applications in Forestry and Costal Zone Management 89, 80–92. https://doi.org/10.1016/j.aquabot.2008.03.012

Dahl, J., 2019. A High-Resolution Chronology of Human Arrival and Environmental Impact in Northland, New Zealand (MSc thesis). University of Otago.

Davis, K.O., 1984. Pollen frequencies reflect vegetation patterns in a great basin (U.S.A.) mountain range. Review of Palaeobotany and Palynology 40, 295–315. https://doi.org/10.1016/0034-6667(84)90013-7

de Souza, J.R.B., do Rosário Zucchi, M., Costa, A.B., de Azevedo, A.E.G., Spano, S., 2017. Geochemical markers of sedimentary organic matter in Todos os Santos Bay, Bahia - Brazil. Indicators of sources and preservation. Mar. Pollut. Bull. 119, 239–246. https://doi.org/10.1016/j.marpolbul.2017.04.020

De Vries, H., Barendsen, G.W., 1954. Measurements of Age by the Carbon-14 Technique. Nature 174, 1138–1141. https://doi.org/10.1038/1741138a0

Debenay, J., Guiral, D., Parra, M., 2004. Behaviour and taphonomic loss in foraminiferal assemblages of mangrove swamps of French Guiana. Marine Geology, Material Exchange Between the Upper Continental Shelf and Mangrove Fringed Coasts with Special Reference to the N. Amazon-Guianas Coast 208, 295–314. https://doi.org/10.1016/j.margeo.2004.04.013

Debenay, J., Guiral, D., Parra, M., 2002. Ecological Factors Acting on the Microfauna in Mangrove Swamps. The Case of Foraminiferal Assemblages in French Guiana. Estuarine, Coastal and Shelf Science 55, 509–533. https://doi.org/10.1006/ecss.2001.0906

Debenay, J.-P., Guillou, J.-J., Redois, F., Geslin, E., 2000. Distribution Trends of Foraminiferal Assemblages in Paralic Environments, in: Environmental Micropaleontology, Topics in Geobiology. Springer, Boston, MA, pp. 39–67. https://doi.org/10.1007/978-1-4615-4167-7_3

Deng, Y., Horrocks, M., Ogden, J., Anderson, S., 2006. Modern pollen–vegetation relationships along transects on the Whangapoua Estuary, Great Barrier Island, northern New Zealand. Journal of Biogeography 33, 592–608. https://doi.org/10.1111/j.1365-2699.2005.01417.x

Dey, M., Ganguly, D., Chowdhury, C., Majumder, N., Jana, T.K., 2012. Intra-Annual Variation of Modern Foraminiferal Assemblage in a Tropical Mangrove Ecosystem in India. Wetlands 32, 813–826. https://doi.org/10.1007/s13157-012-0312-x

Didyk, B.M., Simoneit, B.R.T., Brassell, S.C., Eglinton, G., 1978. Organic geochemical indicators of palaeoenvironmental conditions of sedimentation. Nature 272, 216–222. https://doi.org/10.1038/272216a0

Dittmar, T., Hertkorn, N., Kattner, G., Lara, R.J., 2006. Mangroves, a major source of dissolved organic carbon to the oceans. Global Biogeochemical Cycles 20. https://doi.org/10.1029/2005GB002570

Dunbar, E., Cook, G.T., Naysmith, P., Tripney, B.G., Xu, S., 2016. AMS 14C Dating at the Scottish Universities Environmental Research Centre (SUERC) Radiocarbon Dating Laboratory. Radiocarbon 58, 9–23. https://doi.org/10.1017/RDC.2015.2

Dutton, A., Carlson, A.E., Long, A.J., Milne, G.A., Clark, P.U., DeConto, R., Horton, B.P., Rahmstorf, S., Raymo, M.E., 2015a. Sea-level rise due to polar ice-sheet mass loss during past warm periods. Science 349, aaa4019. https://doi.org/10.1126/science.aaa4019

Dutton, A., Webster, J.M., Zwartz, D., Lambeck, K., Wohlfarth, B., 2015b. Tropical tales of polar ice: evidence of Last Interglacial polar ice sheet retreat recorded by fossil reefs of the granitic Seychelles islands. Quaternary Science Reviews 107, 182–196. https://doi.org/10.1016/j.quascirev.2014.10.025

Edwards, R.J., Wright, A., 2015. Foraminifera, in: Shennan, I., Long, A.J., Horton, B.P. (Eds.), Handbook of Sea-Level Research. Wiley, UK, pp. 191–217.

Eglinton, G., Hamilton, R.J., 1967. Leaf Epicuticular Waxes. Science 156, 1322–1335. https://doi.org/10.1126/science.156.3780.1322

Eglinton, T.I., Eglinton, G., 2008. Molecular proxies for paleoclimatology. Earth and Planetary Science Letters 275, 1–16. https://doi.org/10.1016/j.epsl.2008.07.012

Ellison, J.C., 2008. Long-term retrospection on mangrove development using sediment cores and pollen analysis: A review. Aquatic Botany, Mangrove Ecology – Applications in Forestry and Costal Zone Management 89, 93–104. https://doi.org/10.1016/j.aquabot.2008.02.007

Ellison, J.C., 2005. Holocene palynology and sea-level change in two estuaries in Southern Irian Jaya. Palaeogeography, Palaeoclimatology, Palaeoecology 220, 291–309. https://doi.org/10.1016/j.palaeo.2005.01.008

Ellison, J.C., 1989. Pollen analysis of mangrove sediments as a sea-level indicator: assessment from Tongatapu, Tonga. Palaeogeography, Palaeoclimatology, Palaeoecology 74, 327–341. https://doi.org/10.1016/0031-0182(89)90068-0

Ellison, J.C., Stoddart, D.R., 1991. Mangrove Ecosystem Collapse during Predicted Sea-Level Rise: Holocene Analogues and Implications. Journal of Coastal Research 7, 151–165.

Ellison, J.C., Strickland, P., 2015. Establishing relative sea level trends where a coast lacks a long term tide gauge. Mitig Adapt Strateg Glob Change 20, 1211–1227. https://doi.org/10.1007/s11027-013-9534-3

Emery, K.O., Wigley, R.L., Bartlett, A.S., Rubin, M., Barghoorn, E.S., 1967. Freshwater Peat on the Continental Shelf. Science 158, 1301–1307. https://doi.org/10.1126/science.158.3806.1301

Engelhart, S.E., 2007. Mangrove pollen of Indonesia and its suitability as a sea-level indicator (Masters). Durham University.

Engelhart, S.E., Horton, B.P., Roberts, D.H., Bryant, C.L., Corbett, D.R., 2007. Mangrove pollen of Indonesia and its suitability as a sea-level indicator. Marine Geology, Quaternary Land-Ocean Interactions: Sea-Level Change, Sediments and Tsunami 242, 65–81. https://doi.org/10.1016/j.margeo.2007.02.020

Engelhart, S.E., Horton, B.P., Vane, C.H., Nelson, A.R., Witter, R.C., Brody, S.R., Hawkes, A.D., 2013. Modern foraminifera, δ13C, and bulk geochemistry of central Oregon tidal

marshes and their application in paleoseismology. Palaeogeography, Palaeoclimatology, Palaeoecology 377, 13–27. https://doi.org/10.1016/j.palaeo.2013.02.032
Escobar, J., Brenner, M., Whitmore, T.J., Kenney, W.F., Curtis, J.H., 2008. Ecology of testate amoebae (thecamoebians) in subtropical Florida lakes. J Paleolimnol 40, 715–731. https://doi.org/10.1007/s10933-008-9195-5
Ezcurra, P., Ezcurra, E., Garcillán, P.P., Costa, M.T., Aburto-Oropeza, O., 2016. Coastal landforms and accumulation of mangrove peat increase carbon sequestration and storage. PNAS 113, 4404–4409. https://doi.org/10.1073/pnas.1519774113
Fægri, K., 1971. Preservation of sporopollenin membranes under natural conditions, in: Brooks, J., Grant, P.R., Muir, M., van Gijzel, P., Shaw, G. (Eds.), Sporopollenin. pp. 256–272.
Fairbanks, R.G., 1989. A 17,000-year glacio-eustatic sea level record: influence of glacial melting rates on the Younger Dryas event and deep-ocean circulation. Nature 342, 637–642. https://doi.org/10.1038/342637a0
Ficken, K.J., Li, B., Swain, D.L., Eglinton, G., 2000. An n-alkane proxy for the sedimentary input of submerged/floating freshwater aquatic macrophytes. Organic Geochemistry 31, 745–749. https://doi.org/10.1016/S0146-6380(00)00081-4
Figueroa-Rangel, B.L., Valle-Martínez, A., Olvera-Vargas, M., Liu, K., 2016. Environmental History of Mangrove Vegetation in Pacific West-Central Mexico during the Last 1300 Years. Front. Ecol. Evol. 4. https://doi.org/10.3389/fevo.2016.00101
Fleming, K., Johnston, P., Zwartz, D., Yokoyama, Y., Lambeck, K., Chappell, J., 1998. Refining the eustatic sea-level curve since the Last Glacial Maximum using far- and intermediate-field sites. Earth and Planetary Science Letters 163, 327–342. https://doi.org/10.1016/S0012-821X(98)00198-8
Friess, D.A., Rogers, K., Lovelock, C.E., Krauss, K.W., Hamilton, S.E., Lee, S.Y., Lucas, R., Primavera, J., Rajkaran, A., Shi, S., 2019. The State of the World's Mangrove Forests: Past, Present, and Future. Annual Review of Environment and Resources 44, null. https://doi.org/10.1146/annurev-environ-101718-033302
Fry, B., Ewel, K.C., 2003. Using stable isotopes in mangrove fisheries research — A review and outlook. Isotopes in Environmental and Health Studies 39, 191–196. https://doi.org/10.1080/10256010310001601067
Fry, B., Scalan, R.S., Winters, J.K., Parker, P.L., 1982. Sulphur uptake by salt grasses, mangroves, and seagrasses in anaerobic sediments. Geochimica et Cosmochimica Acta 46, 1121–1124. https://doi.org/10.1016/0016-7037(82)90063-1
Fujimoto, K., Miyagi, T., 1993. Development process of tidal-flat type mangrove habitats and their zonation in the Pacific Ocean. Vegetatio 106, 137–146. https://doi.org/10.1007/BF00045067
Furukawa, K., Wolanski, E., 1996. Sedimentation in Mangrove Forests. Mangroves and Salt Marshes 1, 3–10. https://doi.org/10.1023/A:1025973426404
Furukawa, K., Wolanski, E., Mueller, H., 1997. Currents and Sediment Transport in Mangrove Forests. Estuarine, Coastal and Shelf Science 44, 301–310. https://doi.org/10.1006/ecss.1996.0120
Gaskell, S.J., Eglinton, G., 1976. Sterols of a contemporary lacustrine sediment. Geochimica et Cosmochimica Acta 40, 1221–1228. https://doi.org/10.1016/0016-7037(76)90157-5
Gehrels, W.R., 2013. Microfossil-based reconstructions of Holocene relative sea-level change, in: Encyclopedia of Quaternary Science. Elsevier.
Gehrels, W.R., 2000. Using foraminiferal transfer functions to produce high-resolution sea-level records from salt-marsh deposits, Maine, USA. The Holocene 10, 367–376. https://doi.org/10.1191/095968300670746884

Gehrels, W.R., Kirby, J.R., Prokoph, A., Newnham, R.M., Achterberg, E.P., Evans, H., Black, S., Scott, D.B., 2005. Onset of recent rapid sea-level rise in the western Atlantic Ocean. Quaternary Science Reviews, Quaternary coastal morphology and sea-level changes 24, 2083–2100. https://doi.org/10.1016/j.quascirev.2004.11.016

Gehrels, W.R., Roe, H.M., Charman, D.J., 2001. Foraminifera, testate amoebae and diatoms as sea-level indicators in UK saltmarshes: a quantitative multiproxy approach. J. Quaternary Sci. 16, 201–220. https://doi.org/10.1002/jqs.588

Gehrels, W.R., Woodworth, P.L., 2013. When did modern rates of sea-level rise start? Global and Planetary Change 100, 263–277. https://doi.org/10.1016/j.gloplacha.2012.10.020

Geyh, M.A., Streif, H., Kudrass, H.-R., 1979. Sea-level changes during the late Pleistocene and Holocene in the Strait of Malacca. Nature 278, 441–443. https://doi.org/10.1038/278441a0

Gill, A.M., Tomlinson, P.B., 1977. Studies on the Growth of Red Mangrove (Rhizophora mangle L.) 4. The Adult Root System. Biotropica 9, 145–155. https://doi.org/10.2307/2387877

Gillis, L.G., Snavely, E., Lovelock, C., Zimmer, M., 2019. Effects of crab burrows on sediment characteristics in a Ceriops australis-dominated mangrove forest. Estuarine, Coastal and Shelf Science 218, 334–339. https://doi.org/10.1016/j.ecss.2019.01.008

Giri, C., Ochieng, E., Tieszen, L.L., Zhu, Z., Singh, A., Loveland, T., Masek, J., Duke, N., 2011. Status and distribution of mangrove forests of the world using earth observation satellite data. Global Ecology and Biogeography 20, 154–159. https://doi.org/10.1111/j.1466-8238.2010.00584.x

Gischler, E., 2006. Comment on "Corrected western Atlantic sea-level curve for the last 11,000 years based on calibrated 14C dates from Acropora palmata framework and intertidal mangrove peat" by Toscano and Macintyre. Coral Reefs 22:257–270 (2003), and their response in Coral Reefs 24:187–190 (2005). Coral Reefs 25, 273–279. https://doi.org/10.1007/s00338-006-0101-1

Gleeson, J., Santos, I.R., Maher, D.T., Golsby-Smith, L., 2013. Groundwater–surface water exchange in a mangrove tidal creek: Evidence from natural geochemical tracers and implications for nutrient budgets. Marine Chemistry, Radium and Radon Tracers in Aquatic Systems 156, 27–37. https://doi.org/10.1016/j.marchem.2013.02.001

Goad, L.J., Akihisa, T., 1997. Analysis of sterols. Chapman and Hall.

Gonneea, M.E., Paytan, A., Herrera-Silveira, J.A., 2004. Tracing organic matter sources and carbon burial in mangrove sediments over the past 160 years. Estuarine, Coastal and Shelf Science 61, 211–227. https://doi.org/10.1016/j.ecss.2004.04.015

González, C., Urrego, L.E., Martínez, J.I., Polanía, J., Yokoyama, Y., 2010. Mangrove dynamics in the southwestern Caribbean since the 'Little Ice Age': A history of human and natural disturbances. The Holocene 20, 849–861. https://doi.org/10.1177/0959683610365941

Grand Pre, C.A., Horton, B.P., Kelsey, H.M., Rubin, C.M., Hawkes, A.D., Daryono, M.R., Rosenberg, G., Culver, S.J., 2012. Stratigraphic evidence for an early Holocene earthquake in Aceh, Indonesia. Quaternary Science Reviews, Coastal Change during the Late Quaternary 54, 142–151. https://doi.org/10.1016/j.quascirev.2012.03.011

Grindrod, J., 1988. The palynology of holocene mangrove and saltmarsh sediments, particularly in Northern Australia. Review of Palaeobotany and Palynology, Quaternary Palynology of Tropical Areas 55, 229–245. https://doi.org/10.1016/0034-6667(88)90088-7

Grindrod, J., 1985. The Palynology of Mangroves on a Prograded Shore, Princess Charlotte Bay, North Queensland, Australia. Journal of Biogeography 12, 323–348. https://doi.org/10.2307/2844865

Grindrod, J., Moss, P., Kaars, S.V., 1999. Late Quaternary cycles of mangrove development and decline on the north Australian continental shelf. J. Quaternary Sci. 14, 465–470. https://doi.org/10.1002/(SICI)1099-1417(199908)14:5<465::AID-JQS473>3.0.CO;2-E

Grindrod, J., Rhodes, E.G., 1984. Holocene sea level history of a tropical estuary: Missionary Bay, north Queensland., in: Thom, B.G. (Ed.), Coastal Geomorphology in Australia. Academic Press, Australia, pp. 151–178.

Haines, E.B., 1976. Relation between the stable carbon isotope composition of fiddler crabs, plants, and soils in a salt marsh1. Limnol. Oceanogr. 21, 880–883. https://doi.org/10.4319/lo.1976.21.6.0880

Hanebuth, T.J.J., Stattegger, K., Grootes, P.M., 2000. Rapid Flooding of the Sunda Shelf: A Late-Glacial Sea-Level Record. Science 288, 1033–1035. https://doi.org/10.1126/science.288.5468.1033

Havinga, A.J., 1967. Palynology and pollen preservation. Review of Palaeobotany and Palynology 2, 81–98. https://doi.org/10.1016/0034-6667(67)90138-8

Hawkes, A.D., Horton, B.P., Nelson, A.R., Vane, C.H., Sawai, Y., 2011. Coastal subsidence in Oregon, USA, during the giant Cascadia earthquake of AD 1700. Quaternary Science Reviews 30, 364–376. https://doi.org/10.1016/j.quascirev.2010.11.017

Hayward, B.W., Grenfell, H.R., Reid, C.M., Hayward, K.A., 1999. Recent New Zealand shallow water benthic foraminifera : taxonomy, ecologic distribution, biogeography, and use in paleoenvironmental assessment, Institute of Geological and Nuclear Sciences monograph. Institute of Geological and Nuclear Sciences, Lower Hutt, New Zealand.

Hayward, B.W., Scott, G.H., Grenfell, H.R., Carter, R., Lipps, J.H., 2004. Techniques for estimation of tidal elevation and confinement (approximately salinity) histories of sheltered harbours and estuaries using benthic Foraminifera; examples from New Zealand. The Holocene 14, 218–232. https://doi.org/10.1191/0959683604hl678

He, D., Ladd, S.N., Sachs, J.P., Jaffé, R., 2017. Inverse relationship between salinity and 2H/1H fractionation in leaf wax n-alkanes from Florida mangroves. Organic Geochemistry 110, 1–12. https://doi.org/10.1016/j.orggeochem.2017.04.007

He, D., Mead, R.N., Belicka, L., Pisani, O., Jaffé, R., 2014. Assessing source contributions to particulate organic matter in a subtropical estuary: A biomarker approach. Organic Geochemistry 75, 129–139. https://doi.org/10.1016/j.orggeochem.2014.06.012

He, D., Simoneit, B.R.T., Cloutier, J.B., Jaffé, R., 2018. Early diagenesis of triterpenoids derived from mangroves in a subtropical estuary. Organic Geochemistry 125, 196–211. https://doi.org/10.1016/j.orggeochem.2018.09.005

Hendy, I.L., Minckley, T.A., Whitlock, C., 2016. Eastern tropical Pacific vegetation response to rapid climate change and sea level rise: A new pollen record from the Gulf of Tehuantepec, southern Mexico. Quaternary Science Reviews 145, 152–160. https://doi.org/10.1016/j.quascirev.2016.05.039

Hernandez, M.E., Mead, R., Peralba, M.C., Jaffé, R., 2001. Origin and transport of n-alkane-2-ones in a subtropical estuary: potential biomarkers for seagrass-derived organic matter. Organic Geochemistry 32, 21–32. https://doi.org/10.1016/S0146-6380(00)00157-1

Hibbert, F.D., Rohling, E.J., Dutton, A., Williams, F.H., Chutcharavan, P.M., Zhao, C., Tamisiea, M.E., 2016. Coral indicators of past sea-level change: A global repository of U-series dated benchmarks. Quaternary Science Reviews 145, 1–56. https://doi.org/10.1016/j.quascirev.2016.04.019

Hijma, M.P., Engelhart, S.E., Törnqvist, T.E., Horton, B.P., Hu, P., Hill, D.F., 2015. A protocol for a geological sea-level database, in: Handbook of Sea-Level Research. Wiley, pp. 536–553.

Hogarth, P.J., 2015. The Biology of Mangroves and Seagrasses. Oxford University Press.

Hogg, A.G., Hua, Q., Blackwell, P.G., Niu, M., Buck, C.E., Guilderson, T.P., Heaton, T.J., Palmer, J.G., Reimer, P.J., Reimer, R.W., Turney, C.S.M., Zimmerman, S.R.H., 2013. SHCal13

Southern Hemisphere Calibration, 0–50,000 Years cal BP. Radiocarbon 55, 1889–1903. https://doi.org/10.2458/azu_js_rc.55.16783
Horton, B.P., 1999. The distribution of contemporary intertidal foraminifera at Cowpen Marsh, Tees Estuary, UK: implications for studies of Holocene sea-level changes. Palaeogeography, Palaeoclimatology, Palaeoecology 149, 127–149. https://doi.org/10.1016/S0031-0182(98)00197-7
Horton, B.P., Culver, S.J., Hardbattle, M.I.J., Larcombe, P., Milne, G.A., Morigi, C., Whittaker, J.E., Woodroffe, S.A., 2007a. Reconstructing Holocene Sea-Level Change for the Central Great Barrier Reef (australia) Using Subtidal Foraminifera. Journal of Foraminiferal Research 37, 327–343. https://doi.org/10.2113/gsjfr.37.4.327
Horton, B.P., Gibbard, P.L., Mine, G.M., Morley, R.J., Purintavaragul, C., Stargardt, J.M., 2005a. Holocene sea levels and palaeoenvironments, Malay-Thai Peninsula, southeast Asia. The Holocene 15, 1199–1213. https://doi.org/10.1191/0959683605hl891rp
Horton, B.P., Kopp, R.E., Garner, A.J., Hay, C.C., Khan, N.S., Roy, K., Shaw, T.A., 2018. Mapping Sea-Level Change in Time, Space, and Probability. Annual Review of Environment and Resources 43, 481–521. https://doi.org/10.1146/annurev-environ-102017-025826
Horton, B.P., Whittaker, J.E., Thomson, K.H., Hardbattle, M.I.J., Kemp, A., Woodroffe, S.A., Wright, M.R., 2005b. The Development of a Modern Foraminiferal Data Set for Sea-Level Reconstructions, Wakatobi Marine National Park, Southeast Sulawesi, Indonesia. Journal of Foraminiferal Research 35, 1–14. https://doi.org/10.2113/35.1.1
Horton, B.P., Zong, Y., Hillier, C., Engelhart, S., 2007b. Diatoms from Indonesian mangroves and their suitability as sea-level indicators for tropical environments. Marine Micropaleontology 63, 155–168. https://doi.org/10.1016/j.marmicro.2006.11.005
Howarth, J.D., Fitzsimons, S.J., Jacobsen, G.E., Vandergoes, M.J., Norris, R.J., 2013. Identifying a reliable target fraction for radiocarbon dating sedimentary records from lakes. Quaternary Geochronology 17, 68–80. https://doi.org/10.1016/j.quageo.2013.02.001
Hua, Q., Barbetti, M., Rakowski, A.Z., 2013. Atmospheric Radiocarbon for the Period 1950–2010. Radiocarbon 55, 2059–2072.
Hussain, S.M., Ganesan, P., Ravi, G., Mohan, S.P., Sridhar, S.G.D., 2007. Distribution of Ostracoda in marine and marginal marine habitats off Tamil Nadu and adjoining areas, southern east coast of India and Andaman Islands: Environmental implications. IJMS Vol.36(4) [December 2007].
Huxham, M., Langat, J., Tamooh, F., Kennedy, H., Mencuccini, M., Skov, M.W., Kairo, J., 2010. Decomposition of mangrove roots: Effects of location, nutrients, species identity and mix in a Kenyan forest. Estuarine, Coastal and Shelf Science 88, 135–142. https://doi.org/10.1016/j.ecss.2010.03.021
IPCC, 2019. IPCC Special Report on the Ocean and Cryosphere in a Changing Climate. Intergovernmental Panel on Climate Change.
Ish-Shalom-Gordon, N., Lin, G., da Silveira Lobo Sternberg, L., 1992. Isotopic fractionation during cellulose synthesis in two mangrove species: Salinity effects. Phytochemistry, The International Journal of Plant Biochemistry 31, 2623–2626. https://doi.org/10.1016/0031-9422(92)83598-S
Israelson, C., Wohlfarth, B., 1999. Timing of the Last-Interglacial High Sea Level on the Seychelles Islands, Indian Ocean. Quaternary Research 51, 306–316. https://doi.org/10.1006/qres.1998.2030
Jaffé, R., Mead, R., Hernandez, M.E., Peralba, M.C., DiGuida, O.A., 2001. Origin and transport of sedimentary organic matter in two subtropical estuaries: a comparative,

biomarker-based study. Organic Geochemistry 32, 507–526. https://doi.org/10.1016/S0146-6380(00)00192-3
Jantz, N., Homeier, J., León-Yánez, S., Moscoso, A., Behling, H., 2013. Trapping pollen in the tropics — Comparing modern pollen rain spectra of different pollen traps and surface samples across Andean vegetation zones. Review of Palaeobotany and Palynology 193, 57–69. https://doi.org/10.1016/j.revpalbo.2013.01.011
Johns, R.B., Brady, B.A., Butler, M.S., Dembitsky, V.M., Smith, J.D., 1994. Organic geochemical and geochemical studies of Inner Great Barrier Reef sediments—IV. Identification of terrigenous and marine sourced inputs. Organic Geochemistry 21, 1027–1035. https://doi.org/10.1016/0146-6380(94)90066-3
Juggins, S., 2017. rioja: Analysis of Quaternary Science Data. R package version 0.9-21.
Kemp, A.C., Horton, B.P., Culver, S.J., Corbett, D.R., Plassche, O., Gehrels, W.R., Douglas, B.C., Parnell, A.C., 2009. Timing and magnitude of recent accelerated sea-level rise (North Carolina, United States). Geology 37, 1035–1038. https://doi.org/10.1130/G30352A.1
Kemp, A.C., Horton, B.P., Donnelly, J.P., Mann, M.E., Vermeer, M., Rahmstorf, S., 2011. Climate related sea-level variations over the past two millennia. PNAS 108, 11017–11022. https://doi.org/10.1073/pnas.1015619108
Kemp, A.C., Vane, C.H., Horton, B.P., Culver, S.J., 2010. Stable carbon isotopes as potential sea-level indicators in salt marshes, North Carolina, USA. The Holocene 20, 623–636. https://doi.org/10.1177/0959683609354302
Kemp, A.C., Vane, C.H., Horton, B.P., Engelhart, S.E., Nikitina, D., 2012. Application of stable carbon isotopes for reconstructing salt-marsh floral zones and relative sea level, New Jersey, USA. Journal of Quaternary Science 27, 404–414. https://doi.org/10.1002/jqs.1561
Kemp, A.C., Vane, C.H., Khan, N.S., Ellison, J.C., Engelhart, S.E., Horton, B.P., Nikitina, D., Smith, S.R., Rodrigues, L.J., Moyer, R.P., 2019. Testing the Utility of Geochemical Proxies to Reconstruct Holocene Coastal Environments and Relative Sea Level: A Case Study from Hungry Bay, Bermuda. Open Quaternary 5, 1. https://doi.org/10.5334/oq.49
Kemp, A.C., Wright, A.J., Barnett, R.L., Hawkes, A.D., Charman, D.J., Sameshima, C., King, A.N., Mooney, H.C., Edwards, R.J., Horton, B.P., van de Plassche, O., 2017. Utility of salt-marsh foraminifera, testate amoebae and bulk-sediment δ13C values as sea-level indicators in Newfoundland, Canada. Marine Micropaleontology 130, 43–59. https://doi.org/10.1016/j.marmicro.2016.12.003
Kemp, A.C., Wright, A.J., Edwards, R.J., Barnett, R.L., Brain, M.J., Kopp, R.E., Cahill, N., Horton, B.P., Charman, D.J., Hawkes, A.D., Hill, T.D., van de Plassche, O., 2018. Relative sea-level change in Newfoundland, Canada during the past ∼3000 years. Quaternary Science Reviews 201, 89–110. https://doi.org/10.1016/j.quascirev.2018.10.012
Khan, N.S., Ashe, E., Horton, B.P., Dutton, A., Kopp, R.E., Brocard, G., Engelhart, S.E., Hill, D.F., Peltier, W.R., Vane, C.H., Scatena, F.N., 2017. Drivers of Holocene sea-level change in the Caribbean. Quaternary Science Reviews 155, 13–36. https://doi.org/10.1016/j.quascirev.2016.08.032
Khan, N.S., Horton, B.P., Engelhart, S., Rovere, A., Vacchi, M., Ashe, E.L., Törnqvist, T.E., Dutton, A., Hijma, M.P., Shennan, I., 2019a. Inception of a global atlas of sea levels since the Last Glacial Maximum. Quaternary Science Reviews 220, 359–371. https://doi.org/10.1016/j.quascirev.2019.07.016
Khan, N.S., Vane, C., Horton, B.P., 2015a. Stable carbon isotope and C/N geochemistry of coastal wetland sediments a sea-level indicator, in: Shennan, I., Long, A.J., Horton, B.P. (Eds.), Handbook of Sea-Level Research. Wiley, pp. 295–311.
Khan, N.S., Vane, C.H., Engelhart, S.E., Kendrick, C.P., Horton, B.P., 2019b. The application of δ13C, TOC and C/N geochemistry of mangrove sediments to reconstruct Holocene

paleoenvironments and relative sea levels, Puerto Rico. Marine Geology 415, 105963. https://doi.org/10.1016/j.margeo.2019.105963
Khan, N.S., Vane, C.H., Horton, B.P., Hillier, C., Riding, J.B., Kendrick, C.P., 2015b. The application of δ13C, TOC and C/N geochemistry to reconstruct Holocene relative sea levels and paleoenvironments in the Thames Estuary, UK. J. Quaternary Sci. 30, 417–433. https://doi.org/10.1002/jqs.2784
Kilian, M.R., van der Plicht, J., van Geel, B., Goslar, T., 2002. Problematic 14C-AMS dates of pollen concentrates from Lake Gosciaz (Poland). Quaternary International, The Value of Annually Laminated Sediments in Palaeoenvironment Re constructions: Dedicated to Bjorn E. Berglund 88, 21–26. https://doi.org/10.1016/S1040-6182(01)00070-2
Killops, S.D., Frewin, N.L., 1994. Triterpenoid diagenesis and cuticular preservation. Organic Geochemistry 21, 1193–1209. https://doi.org/10.1016/0146-6380(94)90163-5
Koch, B.P., Harder, J., Lara, R.J., Kattner, G., 2005. The effect of selective microbial degradation on the composition of mangrove derived pentacyclic triterpenols in surface sediments. Organic Geochemistry 36, 273–285. https://doi.org/10.1016/j.orggeochem.2004.07.019
Koch, B.P., Rullkötter, J., Lara, R.J., 2003. Evaluation of triterpenols and sterols as organic matter biomarkers in a mangrove ecosystem in northern Brazil. Wetlands Ecology and Management 11, 257–263. https://doi.org/10.1023/A:1025063516054
Koch, B.P., Souza Filho, P.W.M., Behling, H., Cohen, M.C.L., Kattner, G., Rullkötter, J., Scholz-Böttcher, B., Lara, R.J., 2011. Triterpenols in mangrove sediments as a proxy for organic matter derived from the red mangrove (Rhizophora mangle). Organic Geochemistry 42, 62–73. https://doi.org/10.1016/j.orggeochem.2010.10.007
Koch, B.P., Souza Filho, P.W.M., Behling, H., Cohen, M.C.L., Kattner, G., Rullkötter, J., Scholz-Böttcher, B., Lara, R.J., 2011. Triterpenols in mangrove sediments as a proxy for organic matter derived from the red mangrove (Rhizophora mangle). Organic Geochemistry 42, 62–73. https://doi.org/10.1016/j.orggeochem.2010.10.007
Kozlowski, T.T., 1999. Soil Compaction and Growth of Woody Plants. Scandinavian Journal of Forest Research 14, 596–619. https://doi.org/10.1080/02827589908540825
Krauss, K.W., Cahoon, D.R., Allen, J.A., Ewel, K.C., Lynch, J.C., Cormier, N., 2010. Surface Elevation Change and Susceptibility of Different Mangrove Zones to Sea-Level Rise on Pacific High Islands of Micronesia. Ecosystems 13, 129–143. https://doi.org/10.1007/s10021-009-9307-8
Krauss, K.W., McKee, K.L., Lovelock, C.E., Cahoon, D.R., Saintilan, N., Reef, R., Chen, L., 2014. How mangrove forests adjust to rising sea level. New Phytol 202, 19–34. https://doi.org/10.1111/nph.12605
Kristensen, E., 2008. Mangrove crabs as ecosystem engineers; with emphasis on sediment processes. Journal of Sea Research, Mangrove Macrobenthos Special IssueProceedings of the Mangrove Macrobenthos Meeting II 59, 30–43. https://doi.org/10.1016/j.seares.2007.05.004
Kumar, M., Boski, T., Lima-Filho, F.P., Bezerra, F.H.R., González -Vila, F.J., Alam Bhuiyan, M.K., González-Pérez, J.A., 2019. Biomarkers as indicators of sedimentary organic matter sources and early diagenetic transformation of pentacyclic triterpenoids in a tropical mangrove ecosystem. Estuarine, Coastal and Shelf Science 229, 106403. https://doi.org/10.1016/j.ecss.2019.106403
Ladd, S.N., 2014. Tropical paleoclimate reconstructions from stable isotopes of mangrove lipid biomarkers. (PhD Thesis). University of Washington, USA.
Ladd, S.N., Sachs, J.P., 2017. 2H/1H fractionation in lipids of the mangrove Bruguiera gymnorhiza increases with salinity in marine lakes of Palau. Geochimica et Cosmochimica Acta 204, 300–312. https://doi.org/10.1016/j.gca.2017.01.046

Ladd, S.N., Sachs, J.P., 2015a. Hydrogen isotope response to changing salinity and rainfall in Australian mangroves. Plant Cell Environ 38, 2674–2687. https://doi.org/10.1111/pce.12579
Ladd, S.N., Sachs, J.P., 2015b. Influence of salinity on hydrogen isotope fractionation in Rhizophora mangroves from Micronesia. Geochimica et Cosmochimica Acta 168, 206–221. https://doi.org/10.1016/j.gca.2015.07.004
Ladd, S.N., Sachs, J.P., 2013. Positive correlation between salinity and n-alkane δ13C values in the mangrove Avicennia marina. Organic Geochemistry 64, 1–8. https://doi.org/10.1016/j.orggeochem.2013.08.011
Ladd, S.N., Sachs, J.P., 2012. Inverse relationship between salinity and n-alkane δD values in the mangrove Avicennia marina. Organic Geochemistry 48, 25–36. https://doi.org/10.1016/j.orggeochem.2012.04.009
Lamb, A.L., Vane, C.H., Wilson, G.P., Rees, J.G., Moss-Hayes, V.L., 2007. Assessing δ13C and C/N ratios from organic material in archived cores as Holocene sea level and palaeoenvironmental indicators in the Humber Estuary, UK. Marine Geology 244, 109–128. https://doi.org/10.1016/j.margeo.2007.06.012
Lamb, A.L., Wilson, G.P., Leng, M.J., 2006. A review of coastal palaeoclimate and relative sea-level reconstructions using δ13C and C/N ratios in organic material. Earth-Science Reviews, ISOtopes in PALaeoenvironmental reconstruction (ISOPAL) 75, 29–57. https://doi.org/10.1016/j.earscirev.2005.10.003
Lambeck, K., Rouby, H., Purcell, A., Sun, Y., Sambridge, M., 2014. Sea level and global ice volumes from the Last Glacial Maximum to the Holocene. PNAS 111, 15296–15303. https://doi.org/10.1073/pnas.1411762111
Larcombe, P., Carter, R.M., Dye, J., Gagan, M.K., Johnson, D.P., 1995. New evidence for episodic post-glacial sea-level rise, central Great Barrier Reef, Australia. Marine Geology 127, 1–44. https://doi.org/10.1016/0025-3227(95)00059-8
Lecavalier, B.S., Milne, G.A., Simpson, M.J.R., Wake, L., Huybrechts, P., Tarasov, L., Kjeldsen, K.K., Funder, S., Long, A.J., Woodroffe, S., Dyke, A.S., Larsen, N.K., 2014. A model of Greenland ice sheet deglaciation constrained by observations of relative sea level and ice extent. Quaternary Science Reviews 102, 54–84. https://doi.org/10.1016/j.quascirev.2014.07.018
Leng, M.J., Lewis, J.P., 2017. C/N ratios and Carbon Isotope Composition of Organic Matter in Estuarine Environments, in: Applications of Paleoenvironmental Techniques in Estuarine Studies: Developments in Paleoenvironmental Research. Springer Netherlands, pp. 213–238.
Leong, R.C., Friess, D.A., Crase, B., Lee, W.K., Webb, E.L., 2018. High-resolution pattern of mangrove species distribution is controlled by surface elevation. Estuarine, Coastal and Shelf Science. https://doi.org/10.1016/j.ecss.2017.12.015
Li, C., Li, Y., Burr, G.S., 2014. Testing the Accuracy of 14C Age Data from Pollen Concentrates in the Yangtze Delta, China. Radiocarbon 56, 181–187. https://doi.org/10.2458/56.16920
Li, Z., Zhang, Z., Li, J., Zhang, Y., Li, Z., Liu, L., Fan, H., Li, G., 2008. Pollen distribution in surface sediments of a mangrove system, Yingluo Bay, Guangxi, China. Review of Palaeobotany and Palynology 152, 21–31. https://doi.org/10.1016/j.revpalbo.2008.04.001
Lighty, R.G., Macintyre, I.G., Stuckenrath, R., 1982. Acropora palmata reef framework: A reliable indicator of sea level in the western atlantic for the past 10,000 years. Coral Reefs 1, 125–130. https://doi.org/10.1007/BF00301694
Long, A.J., Barlow, N.L.M., Gehrels, W.R., Saher, M.H., Woodworth, P.L., Scaife, R.G., Brain, M.J., Cahill, N., 2014. Contrasting records of sea-level change in the eastern and western North Atlantic during the last 300 years. Earth and Planetary Science Letters 388, 110–122. https://doi.org/10.1016/j.epsl.2013.11.012

Long, A.J., Scaife, R.G., Edwards, R.J., 1999. Pine pollen in intertidal sediments from Poole Harbour, UK; implications for late-Holocene sediment accretion rates and sea-level rise. Quaternary International 55, 3–16. https://doi.org/10.1016/S1040-6182(98)00017-2

Long, A.J., Woodroffe, S.A., Milne, G.A., Bryant, C.L., Simpson, M.J.R., Wake, L.M., 2012. Relative sea-level change in Greenland during the last 700yrs and ice sheet response to the Little Ice Age. Earth and Planetary Science Letters, Sea Level and Ice Sheet Evolution: A PALSEA Special Edition 315–316, 76–85. https://doi.org/10.1016/j.epsl.2011.06.027

Lovelock, C.E., Feller, I.C., Ellis, J., Schwarz, A.M., Hancock, N., Nichols, P., Sorrell, B., 2007. Mangrove growth in New Zealand estuaries: the role of nutrient enrichment at sites with contrasting rates of sedimentation. Oecologia 153, 633–641. https://doi.org/10.1007/s00442-007-0750-y

Lugo, A.E., Snedaker, and S.C., 1974. The Ecology of Mangroves. Annual Review of Ecology and Systematics 5, 39–64. https://doi.org/10.1146/annurev.es.05.110174.000351

Lynch, J.C., Meriwether, J.R., McKee, B.A., Vera-Herrera, F., Twilley, R.R., 1989. Recent accretion in mangrove ecosystems based on<Superscript>137</Superscript>Cs and<Superscript>210</Superscript>Pb. Estuaries 12, 284–299. https://doi.org/10.2307/1351907

Mackie, E.A.V., Leng, M.J., Lloyd, J.M., Arrowsmith, C., 2005. Bulk organic δ13C and C/N ratios as palaeosalinity indicators within a Scottish isolation basin. J. Quaternary Sci. 20, 303–312. https://doi.org/10.1002/jqs.919

Mackie, E.A.V., Lloyd, J.M., Leng, M.J., Bentley, M.J., Arrowsmith, C., 2007. Assessment of δ13C and C/N ratios in bulk organic matter as palaeosalinity indicators in Holocene and Lateglacial isolation basin sediments, northwest Scotland. J. Quaternary Sci. 22, 579–591. https://doi.org/10.1002/jqs.1081

Maechler, M., Rousseeuw, P., Struyf, A., Hubert, M., Hornik, K., 2019. cluster: Cluster Analysis Basics and Extensions. R package version 2.1.0.

Maher, D.T., Santos, I.R., Schulz, K.G., Call, M., Jacobsen, G.E., Sanders, C.J., 2017. Blue carbon oxidation revealed by radiogenic and stable isotopes in a mangrove system. Geophysical Research Letters 44, 4889–4896. https://doi.org/10.1002/2017GL073753

Mallinson, D.J., Culver, S.J., Corbett, D.R., Parham, P.R., Shazili, N.A.M., Yaacob, R., 2014. Holocene coastal response to monsoons and relative sea-level changes in northeast peninsular Malaysia. Journal of Asian Earth Sciences 91, 194–205. https://doi.org/10.1016/j.jseaes.2014.05.005

Mao, L., Batten, D.J., Fujiki, T., Li, Z., Dai, L., Weng, C., 2012. Key to mangrove pollen and spores of southern China: an aid to palynological interpretation of Quaternary deposits in the South China Sea. Review of Palaeobotany and Palynology 176–177, 41–67. https://doi.org/10.1016/j.revpalbo.2012.03.004

Mao, L., Zhang, Y., Bi, H., 2006. Modern Pollen Deposits in Coastal Mangrove Swamps from Northern Hainan Island, China. Journal of Coastal Research 1423–1436. https://doi.org/10.2112/05-0516.1

Mart, Y., 1988. The tectonic setting of the Seychelles, Mascarene and Amirante plateaus in the western equatorial Indian Ocean. Marine Geology 79, 261–274. https://doi.org/10.1016/0025-3227(88)90042-4

McArthur, A.D., Gamberi, F., Kneller, B.C., Wakefield, M.I., Souza, P.A., Kuchle, J., 2017. Palynofacies classification of submarine fan depositional environments: Outcrop examples from the Marnoso-Arenacea Formation, Italy. Marine and Petroleum Geology 88, 181–199. https://doi.org/10.1016/j.marpetgeo.2017.08.018

McKee, K.L., 2011. Biophysical controls on accretion and elevation change in Caribbean mangrove ecosystems. Estuarine, Coastal and Shelf Science 91, 475–483. https://doi.org/10.1016/j.ecss.2010.05.001
McKee, K.L., 2001. Root proliferation in decaying roots and old root channels: a nutrient conservation mechanism in oligotrophic mangrove forests? Journal of Ecology 89, 876–887. https://doi.org/10.1046/j.0022-0477.2001.00606.x
McKee, K.L., Cahoon, D.R., Feller, I., 2007. Caribbean mangroves adjust to rising sea level through biotic controls on soil elevation change. Global Ecol. Biogeogr 16, 545–556. https://doi.org/DOI: 10.1111/j.1466-8238.2007.00317.x
McKee, K.L., Faulkner, P.L., 2000. Mangrove peat analysis and reconstruction of vegetation history at the Pelican Cays, Belize. Atoll Research Bulletin 12.
McKee, K.L., Feller, I.C., Popp, M., Wanek, W., 2002. Mangrove isotopic (δ15N AND δ13C) fractionation across a nitrogen vs. phosphorus limitation gradient. Ecology 83, 1065–1075. https://doi.org/10.1890/0012-9658(2002)083[1065:MINACF]2.0.CO;2
McKee, K.L., Rogers, K., Saintilan, N., 2012. Response of Salt Marsh and Mangrove Wetlands to Changes in Atmospheric CO2, Climate, and Sea Level, in: Middleton, B.A. (Ed.), Global Change and the Function and Distribution of Wetlands, Global Change Ecology and Wetlands. Springer Netherlands, pp. 63–96. https://doi.org/10.1007/978-94-007-4494-3_2
Mead, R., Xu, Y., Chong, J., Jaffé, R., 2005. Sediment and soil organic matter source assessment as revealed by the molecular distribution and carbon isotopic composition of n-alkanes. Organic Geochemistry 36, 363–370. https://doi.org/10.1016/j.orggeochem.2004.10.003
Mengel, M., Nauels, A., Rogelj, J., Schleussner, C.-F., 2018. Committed sea-level rise under the Paris Agreement and the legacy of delayed mitigation action. Nature Communications 9, 1–10. https://doi.org/10.1038/s41467-018-02985-8
Meyers, P.A., 2003. Applications of organic geochemistry to paleolimnological reconstructions: a summary of examples from the Laurentian Great Lakes. Organic Geochemistry 34, 261–289. https://doi.org/10.1016/S0146-6380(02)00168-7
Middleton, B.A., McKee, K.L., 2001. Degradation of mangrove tissues and implications for peat formation in Belizean island forests. Journal of Ecology 89, 818–828. https://doi.org/10.1046/j.0022-0477.2001.00602.x
Milker, Y., Horton, B.P., Vane, C.H., Engelhart, S.E., Nelson, A.R., Witter, R.C., Khan, N.S., Bridgeland, W.T., 2015. Annual and seasonal distribution of intertidal foraminifera and stable carbon isotope geochemistry, Bandon Marsh, Oregon, USA. Journal of Foraminiferal Research 45, 146–155. https://doi.org/10.2113/gsjfr.45.2.146
Milne, G.A., Gehrels, W.R., Hughes, C.W., Tamisiea, M.E., 2009. Identifying the causes of sea-level change. Nature Geosci 2, 471–478. https://doi.org/10.1038/ngeo544
Milne, G.A., Long, A.J., Bassett, S.E., 2005. Modelling Holocene relative sea-level observations from the Caribbean and South America. Quaternary Science Reviews 24, 1183–1202. https://doi.org/10.1016/j.quascirev.2004.10.005
Milne, G.A., Mitrovica, J.X., 2008. Searching for eustasy in deglacial sea-level histories. Quaternary Science Reviews 27, 2292–2302. https://doi.org/10.1016/j.quascirev.2008.08.018
Mitrovica, J.X., Tamisiea, M.E., Davis, J.L., Milne, G.A., 2001. Recent mass balance of polar ice sheets inferred from patterns of global sea-level change. Nature 409, 1026–1029. https://doi.org/10.1038/35059054
Monacci, N.M., Meier-Grünhagen, U., Finney, B.P., Behling, H., Wooller, M.J., 2009. Mangrove ecosystem changes during the Holocene at Spanish Lookout Cay, Belize. Palaeogeography, Palaeoclimatology, Palaeoecology 280, 37–46. https://doi.org/10.1016/j.palaeo.2009.05.013

Montaggioni, L.F., Cabioch, G., Camoin, G.F., Bard, E., Laurenti, A.R., Faure, G., Déjardin, P., Récy, J., 1997. Continuous record of reef growth over the past 14 k.y. on the mid-Pacific island of Tahiti. Geology 25, 555–558. https://doi.org/10.1130/0091-7613(1997)025<0555:CRORGO>2.3.CO;2

Moore, P.D., Webb, J.A., Collinson, M.E., 1991. Pollen analysis. Blackwell Scientific Publications.

Murray-Wallace, C.V., Banerjee, D., Bourman, R.P., Olley, J.M., Brooke, B.P., 2002. Optically stimulated luminescence dating of Holocene relict foredunes, Guichen Bay, South Australia. Quaternary Science Reviews 21, 1077–1086. https://doi.org/10.1016/S0277-3791(01)00060-9

Murray-Wallace, C.V., Woodroffe, C.D., 2014. Quaternary Sea-Level Changes: A Global Perspective. Cambridge University Press.

Naafs, B.D.A., Inglis, G.N., Blewett, J., McClymont, E.L., Lauretano, V., Xie, S., Evershed, R.P., Pancost, R.D., 2019. The potential of biomarker proxies to trace climate, vegetation, and biogeochemical processes in peat: A review. Global and Planetary Change 179, 57–79. https://doi.org/10.1016/j.gloplacha.2019.05.006

Nakada, M., Lambeck, K., 1989. Late Pleistocene and Holocene sea-level change in the Australian region and mantle rheology. Geophysical Journal International 96, 497–517. https://doi.org/10.1111/j.1365-246X.1989.tb06010.x

Nelson, D.B., Sachs, J.P., 2016. Galápagos hydroclimate of the Common Era from paired microalgal and mangrove biomarker 2H/1H values. PNAS 113, 3476–3481. https://doi.org/10.1073/pnas.1516271113

Neulieb, T., Levac, E., Southon, J., Lewis, M., Pendea, I.F., Chmura, G.L., 2013. Potential Pitfalls of Pollen Dating. Radiocarbon 55, 1142–1155. https://doi.org/10.1017/S0033822200048050

Newnham, R.M., Vandergoes, M.J., Garnett, M.H., Lowe, D.J., Prior, C., Almond, P.C., 2007. Test of AMS 14C dating of pollen concentrates using tephrochronology. Journal of Quaternary Science 22, 37–51. https://doi.org/10.1002/jqs.1016

Ohkouchi, N., Eglinton, T.I., 2008. Compound-specific radiocarbon dating of Ross Sea sediments: A prospect for constructing chronologies in high-latitude oceanic sediments. Quaternary Geochronology, Prospects for the New Frontiers of earth and Environmental Sciences 3, 235–243. https://doi.org/10.1016/j.quageo.2007.11.001

Oksanen, J., 2019. Vegan: an introduction to ordination. R package version 2.5-6.

Owers, C.J., Rogers, K., Mazumder, D., Woodroffe, C.D., 2020. Temperate coastal wetland near-surface carbon storage: Spatial patterns and variability. Estuarine, Coastal and Shelf Science 235, 106584. https://doi.org/10.1016/j.ecss.2020.106584

Palmer, A.J.M., Abbott, W.H., 1986. Diatoms as indicators of sea-level change, in: Sea Level Reseach: A Manual for the Collection and Evaluation of Data. Geo Books, Norwich.

Pancost, R.D., Geel, B., Baas, M., Damsté, J.S.S., 2000. δ13C values and radiocarbon dates of microbial biomarkers as tracers for carbon recycling in peat deposits. Geology 28, 663–666. https://doi.org/10.1130/0091-7613(2000)28<663:CVARDO>2.0.CO;2

Parkinson, R.W., DeLaune, R.D., White, J.R., 1994. Holocene Sea-Level Rise and the Fate of Mangrove Forests within the Wider Caribbean Region. Journal of Coastal Research 10, 1077–1086.

Peltier, W.R., 2004. Global glacial isostasy and the surface of the Ice-Age Earth: the ICE-5G (VM2) Model and GRACE. Annual Review of Earth and Planetary Sciences 32, 111–149. https://doi.org/10.1146/annurev.earth.32.082503.144359

Peltier, W.R., 2002. On eustatic sea level history: Last Glacial Maximum to Holocene. Quaternary Science Reviews, EPILOG 21, 377–396. https://doi.org/10.1016/S0277-3791(01)00084-1

Peltier, W.R., Argus, D.F., Drummond, R., 2015. Space geodesy constrains ice age terminal deglaciation: The global ICE-6G_C (VM5a) model. Journal of Geophysical Research: Solid Earth 120, 450–487. https://doi.org/10.1002/2014JB011176

Peltier, W.R., Fairbanks, R.G., 2006. Global glacial ice volume and Last Glacial Maximum duration from an extended Barbados sea level record. Quaternary Science Reviews, Critical Quaternary Stratigraphy 25, 3322–3337. https://doi.org/10.1016/j.quascirev.2006.04.010

Perry, C.T., Berkeley, A., Smithers, S.G., 2008. Microfacies Characteristics of a Tropical, Mangrove-Fringed Shoreline, Cleveland Bay, Queensland, Australia: Sedimentary and Taphonomic Controls on Mangrove Facies Development. Journal of Sedimentary Research 78, 77–97. https://doi.org/10.2110/jsr.2008.015

Pfeiffer, M., Dullo, W.-C., 2006. Monsoon-induced cooling of the western equatorial Indian Ocean as recorded in coral oxygen isotope records from the Seychelles covering the period of 1840–1994AD. Quaternary Science Reviews 25, 993–1009. https://doi.org/10.1016/j.quascirev.2005.11.005

Phillips, S., Bustin, R.M., Lowe, L.E., 1994. Earthquake-induced flooding of a tropical coastal peat swamp: A modern analogue for high-sulfur coals? Geology 22, 929–932. https://doi.org/10.1130/0091-7613(1994)022<0929:EIFOAT>2.3.CO;2

Phuphumirat, W., Gleason, F.H., Phongpaichit, S., Mildenhall, D.C., 2011. The infection of pollen by zoosporic fungi in tropical soils and its impact on pollen preservation: A preliminary study [WWW Document]. URL https://www.ingentaconnect.com/content/schweiz/novh/2011/00000092/f0020001/art00015 (accessed 1.10.20).

Phuphumirat, W., Zetter, R., Hofmann, C.-C., Ferguson, D.K., 2015. Pollen degradation in mangrove sediments: A short-term experiment. Review of Palaeobotany and Palynology 221, 106–116. https://doi.org/10.1016/j.revpalbo.2015.06.004

Plater, A.J., Kirby, J.R., Boyle, J.F., Shaw, T., Mills, H., 2015. Loss on ignition and organic content, in: The Handbook of Sea-Level Research. Wiley, pp. 312–330.

Plaziat, J.-C., 1995. Modern and fossil mangroves and mangals: their climatic and biogeographic variability. Geological Society, London, Special Publications 83, 73–96. https://doi.org/10.1144/GSL.SP.1995.083.01.05

Plaziat, J.-C., Cavagnetto, C., Koeniguer, J.-C., Baltzer, F., 2001. History and biogeography of the mangrove ecosystem, based on a critical reassessment of the paleontological record. Wetlands Ecology and Management 9, 161–180. https://doi.org/10.1023/A:1011118204434

Poret, N., Twilley, R.R., Rivera-Monroy, V.H., Coronado-Molina, C., 2007. Belowground decomposition of mangrove roots in Florida coastal everglades. Estuaries and Coasts: J ERF 30, 491–496. https://doi.org/10.1007/BF02819395

Poynter, J.G., Farrimond, P., Robinson, N., Eglinton, G., 1989. Aeolian-Derived Higher Plant Lipids in the Marine Sedimentary Record: Links with Palaeoclimate, in: Leinen, M., Sarnthein, M. (Eds.), Paleoclimatology and Paleometeorology: Modern and Past Patterns of Global Atmospheric Transport, NATO ASI Series. Springer Netherlands, Dordrecht, pp. 435–462. https://doi.org/10.1007/978-94-009-0995-3_18

Punwong, P., 2013. Holocene mangrove dynamics and sea level changes: records from the Tanzanian coast. University of York.

Punwong, P., Marchant, R., Selby, K., 2013a. Holocene mangrove dynamics in Makoba Bay, Zanzibar. Palaeogeography, Palaeoclimatology, Palaeoecology 379–380, 54–67. https://doi.org/10.1016/j.palaeo.2013.04.004

Punwong, P., Marchant, R., Selby, K., 2013b. Holocene mangrove dynamics from Unguja Ukuu, Zanzibar. Quaternary International, Zanzibar to the Yellow Sea: A transect of Quaternary Studies from 6°S, 39°E to 35°N, 127°E 298, 4–19. https://doi.org/10.1016/j.quaint.2013.02.007

Punwong, P., Selby, K., Marchant, R., 2018. Holocene mangrove dynamics and relative sea-level changes along the Tanzanian coast, East Africa. Estuarine, Coastal and Shelf Science 212, 105–117. https://doi.org/10.1016/j.ecss.2018.07.004

Punwong, P., Sritrairat, S., Selby, K., Marchant, R., Pumijumnong, N., Traiperm, P., 2017. An 800 year record of mangrove dynamics and human activities in the upper Gulf of Thailand. Veget Hist Archaeobot 1–15. https://doi.org/10.1007/s00334-017-0651-x

Ranjan, R.K., Routh, J., Val Klump, J., Ramanathan, AL., 2015. Sediment biomarker profiles trace organic matter input in the Pichavaram mangrove complex, southeastern India. Marine Chemistry 171, 44–57. https://doi.org/10.1016/j.marchem.2015.02.001

Rashid, T., Suzuki, S., Sato, H., Monsur, M.H., Saha, S.K., 2013. Relative sea-level changes during the Holocene in Bangladesh. Journal of Asian Earth Sciences 64, 136–150. https://doi.org/10.1016/j.jseaes.2012.12.007

Roberts, D.L., Neumann, F.H., Cawthra, H.C., Carr, A.S., Scott, L., Durugbo, E.U., Humphries, M.S., Cowling, R.M., Bamford, M.K., Musekiwa, C., MacHutchon, M., 2017. Palaeoenvironments during a terminal Oligocene or early Miocene transgression in a fluvial system at the southwestern tip of Africa. Global and Planetary Change 150, 1–23. https://doi.org/10.1016/j.gloplacha.2017.01.007

Rogers, K., Kelleway, J.J., Saintilan, N., Megonigal, J.P., Adams, J.B., Holmquist, J.R., Lu, M., Schile-Beers, L., Zawadzki, A., Mazumder, D., Woodroffe, C.D., 2019. Wetland carbon storage controlled by millennial-scale variation in relative sea-level rise. Nature 567, 91. https://doi.org/10.1038/s41586-019-0951-7

Rogers, K., Saintilan, N., Heijnis, H., 2005. Mangrove encroachment of salt marsh in Western Port Bay, Victoria: The role of sedimentation, subsidence, and sea level rise. Estuaries 28, 551–559. https://doi.org/10.1007/BF02696066

Sachse, D., Billault, I., Bowen, G.J., Chikaraishi, Y., Dawson, T.E., Feakins, S.J., Freeman, K.H., Magill, C.R., McInerney, F.A., Meer, M.T.J., Polissar, P., Robins, R.J., Sachs, J.P., Schmidt, H., Sessions, A.L., White, J.W.C., West, J.B., Kahmen, A., 2012. Molecular Paleohydrology: Interpreting the Hydrogen-Isotopic Composition of Lipid Biomarkers from Photosynthesizing Organisms. Annual Review of Earth and Planetary Sciences 40, 221–249. https://doi.org/10.1146/annurev-earth-042711-105535

Saenger, P., Snedaker, S.C., 1993. Pantropical trends in mangrove above-ground biomass and annual litterfall. Oecologia 96, 293–299. https://doi.org/10.1007/BF00317496

Saintilan, N., Rogers, K., Mazumder, D., Woodroffe, C., 2013. Allochthonous and autochthonous contributions to carbon accumulation and carbon store in southeastern Australian coastal wetlands. Estuarine, Coastal and Shelf Science 128, 84–92. https://doi.org/10.1016/j.ecss.2013.05.010

Sanders, C.J., Santos, I.R., Maher, D.T., Breithaupt, J.L., Smoak, J.M., Ketterer, M., Call, M., Sanders, L., Eyre, B.D., 2016. Examining 239+240Pu, 210Pb and historical events to determine carbon, nitrogen and phosphorus burial in mangrove sediments of Moreton Bay, Australia. Journal of Environmental Radioactivity, South Pacific Environmental Radioactivity Association (SPERA): 2014 Conference 151, 623–629. https://doi.org/10.1016/j.jenvrad.2015.04.018

Sanders, C.J., Smoak, J.M., Sanders, L.M., Waters, M.N., Patchineelam, S.R., Ketterer, M.E., 2010. Intertidal mangrove mudflat 240+239Pu signatures, confirming a 210Pb geochronology on the southeastern coast of Brazil. J Radioanal Nucl Chem 283, 593–596. https://doi.org/10.1007/s10967-009-0418-7

Santos, G.M., Southon, J.R., Griffin, S., Beaupre, S.R., Druffel, E.R.M., 2007. Ultra small-mass AMS 14C sample preparation and analyses at KCCAMS/UCI Facility. Nuclear Instruments and Methods in Physics Research Section B: Beam Interactions with Materials and Atoms, Accelerator Mass Spectrometry 259, 293–302. https://doi.org/10.1016/j.nimb.2007.01.172

Scholl, D.W., 1964a. Recent sedimentary record in mangrove swamps and rise in sea level over the southwestern coast of Florida: Part 2. Marine Geology 2, 343–364. https://doi.org/10.1016/0025-3227(64)90047-7
Scholl, D.W., 1964b. Recent sedimentary record in mangrove swamps and rise in sea level over the southwestern coast of Florida: Part 1. Marine Geology 1, 344–366. https://doi.org/10.1016/0025-3227(64)90020-9
Scholl, D.W., Stuiver, M., 1967. Recent Submergence of Southern Florida: A Comparison with Adjacent Coasts and Other Eustatic Data. GSA Bulletin 78, 437–454. https://doi.org/10.1130/0016-7606(1967)78[437:RSOSFA]2.0.CO;2
Scott, D.S., Medioli, F.S., 1978. Vertical zonations of marsh foraminifera as accurate indicators of former sea-levels. Nature 272, 528–531. https://doi.org/10.1038/272528a0
Scourse, J., Marret, F., Versteegh, G.J.M., Jansen, J.H.F., Schefuß, E., van der Plicht, J., 2005. High-resolution last deglaciation record from the Congo fan reveals significance of mangrove pollen and biomarkers as indicators of shelf transgression. Quaternary Research 64, 57–69. https://doi.org/10.1016/j.yqres.2005.03.002
Sen, A., Bhadury, P., 2017. Intertidal foraminifera and stable isotope geochemistry from world's largest mangrove, Sundarbans: Assessing a multiproxy approach for studying changes in sea-level. Estuarine, Coastal and Shelf Science 192, 128–136. https://doi.org/10.1016/j.ecss.2017.05.010
Shennan, I., 1986. Flandrian sea-level changes in the Fenland. I: The geographical setting and evidence of relative sea-level changes. Journal of Quaternary Science 1, 119–153. https://doi.org/10.1002/jqs.3390010204
Simms, A.R., Lisiecki, L., Gebbie, G., Whitehouse, P.L., Clark, J.F., 2019. Balancing the last glacial maximum (LGM) sea-level budget. Quaternary Science Reviews 205, 143–153. https://doi.org/10.1016/j.quascirev.2018.12.018
Simms, A.R., Whitehouse, P.L., Simkins, L.M., Nield, G., DeWitt, R., Bentley, M.J., 2018. Late Holocene relative sea levels near Palmer Station, northern Antarctic Peninsula, strongly controlled by late Holocene ice-mass changes. Quaternary Science Reviews 199, 49–59. https://doi.org/10.1016/j.quascirev.2018.09.017
Skov, M.W., Hartnoll, R.G., 2002. Paradoxical selective feeding on a low-nutrient diet: why do mangrove crabs eat leaves? Oecologia 131, 1–7. https://doi.org/10.1007/s00442-001-0847-7
Slota, P.J., Jull, A.J.T., Linick, T.W., Toolin, L.J., 1987. Preparation of Small Samples for 14C Accelerator Targets by Catalytic Reduction of CO. Radiocarbon 29, 303–306. https://doi.org/10.1017/S0033822200056988
Smallwood, B.J., Wooller, M.J., Jacobson, M.E., Fogel, M.L., 2003. Isotopic and molecular distributions of biochemicals from fresh and buried Rhizophora mangle leaves†. Geochemical Transactions 4, 38. https://doi.org/10.1186/1467-4866-4-38
Smittenberg, R.H., Hopmans E. C., Schouten S., Hayes J. M., Eglinton T. I., Sinninghe Damsté J. S., 2004. Compound-specific radiocarbon dating of the varved Holocene sedimentary record of Saanich Inlet, Canada. Paleoceanography 19. https://doi.org/10.1029/2003PA000927
Spalding, M., Kainuma, M., Collins, L., 2010. World Atlas of Mangroves. Earthscan.
Stattegger, K., Tjallingii, R., Saito, Y., Michelli, M., Trung Thanh, N., Wetzel, A., 2013. Mid to late Holocene sea-level reconstruction of Southeast Vietnam using beachrock and beach-ridge deposits. Global and Planetary Change, Land-Ocean-Atmosphere interaction in the coastal zone of South Vietnam 110, Part B, 214–222. https://doi.org/10.1016/j.gloplacha.2013.08.014
Steffen, W., Rockström, J., Richardson, K., Lenton, T.M., Folke, C., Liverman, D., Summerhayes, C.P., Barnosky, A.D., Cornell, S.E., Crucifix, M., Donges, J.F., Fetzer, I., Lade, S.J., Scheffer, M., Winkelmann, R., Schellnhuber, H.J., 2018. Trajectories of the

Earth System in the Anthropocene. PNAS 115, 8252–8259. https://doi.org/10.1073/pnas.1810141115
Stieglitz, T., Ridd, P., Müller, P., 2000. Passive irrigation and functional morphology of crustacean burrows in a tropical mangrove swamp. Hydrobiologia 421, 69–76. https://doi.org/10.1023/A:1003925502665
Stieglitz, T.C., Clark, J.F., Hancock, G.J., 2013. The mangrove pump: The tidal flushing of animal burrows in a tropical mangrove forest determined from radionuclide budgets. Geochimica et Cosmochimica Acta 102, 12–22. https://doi.org/10.1016/j.gca.2012.10.033
Sukardjo, S., Alongi, D.M., Kusmana, C., 2013. Rapid litter production and accumulation in Bornean mangrove forests. Ecosphere 4, art79. https://doi.org/10.1890/ES13-00145.1
Swales, A., Bentley, S.J., Lovelock, C.E., 2015. Mangrove-forest evolution in a sediment-rich estuarine system: opportunists or agents of geomorphic change? Earth Surface Processes and Landforms 40, 1672–1687. https://doi.org/10.1002/esp.3759
Tait, D.R., Maher, D.T., Macklin, P.A., Santos, I.R., 2016. Mangrove pore water exchange across a latitudinal gradient. Geophysical Research Letters 43, 3334–3341. https://doi.org/10.1002/2016GL068289
Tam, C.-Y., Zong, Y., Hassan, K. bin, Ismal, H. bin, Jamil, H. binti, Xiong, H., Wu, P., Sun, Y., Huang, G., Zheng, Z., 2018. A below-the-present late Holocene relative sea level and the glacial isostatic adjustment during the Holocene in the Malay Peninsula. Quaternary Science Reviews 201, 206–222. https://doi.org/10.1016/j.quascirev.2018.10.009
Tamura, T., Saito, Y., Nguyen, V.L., Ta, T.K.O., Bateman, M.D., Matsumoto, D., Yamashita, S., 2012. Origin and evolution of interdistributary delta plains; insights from Mekong River delta. Geology 40, 303–306. https://doi.org/10.1130/G32717.1
Tamura, T., Saito, Y., Sieng, S., Ben, B., Kong, M., Sim, I., Choup, S., Akiba, F., 2009. Initiation of the Mekong River delta at 8 ka: evidence from the sedimentary succession in the Cambodian lowland. Quaternary Science Reviews, Special Theme: Modern Analogues in Quaternary Palaeoglaciological Reconstruction (pp. 181-260) 28, 327–344. https://doi.org/10.1016/j.quascirev.2008.10.010
Thanikaimoni, G., 1987. Mangrove palynology. UNDP/UNESCO Regional Project on Training and Research on Mangrove Ecosystems, RAS/79/002.
The Australasian Pollen and Spore Atlas, n.d. URL http://apsa.anu.edu.au/
Tomlinson, P.B., 2016. The Botany of Mangroves. Cambridge University Press.
Törnqvist, T.E., González, J.L., Newsom, L.A., Borg, K. van der, Jong, A.F.M. de, Kurnik, C.W., 2004. Deciphering Holocene sea-level history on the U.S. Gulf Coast: A high-resolution record from the Mississippi Delta. Geological Society of America Bulletin 116, 1026–1039. https://doi.org/10.1130/B2525478.1
Törnqvist, T.E., Rosenheim, B.E., Hu, P., Fernandez, A.B., 2015. Radiocarbon dating and calibration, in: Shennan, I., Long, A.J., Horton, B.P. (Eds.), Handbook of Sea-Level Research. Wiley, pp. 349–360.
Troels-Smith, J. 1955. Karakterisering af lose jordarter. Characterisation of unconsolidated sediments. Geological Survey of Denmark 4 (3), 1-73.
Tulipani, S., Schwark, L., Holman, A.I., Bush, R.T., Grice, K., 2017. 1-Chloro-n-alkanes: Potential mangrove and saltmarsh vegetation biomarkers. Organic Geochemistry 107, 54–58. https://doi.org/10.1016/j.orggeochem.2017.02.007
Tyson, R., 1995. Sedimentary Organic Matter: Organic facies and palynofacies. Springer.
Ullman, D.J., Carlson, A.E., Hostetler, S.W., Clark, P.U., Cuzzone, J., Milne, G.A., Winsor, K., Caffee, M., 2016. Final Laurentide ice-sheet deglaciation and Holocene climate-sea

level change. Quaternary Science Reviews 152, 49–59. https://doi.org/10.1016/j.quascirev.2016.09.014
University of Hawaii Sea Level Centre, 2019. https://uhslc.soest.hawaii.edu/
Urrego, L.E., Bernal, G., Polanía, J., 2009. Comparison of pollen distribution patterns in surface sediments of a Colombian Caribbean mangrove with geomorphology and vegetation. Review of Palaeobotany and Palynology 156, 358–375. https://doi.org/10.1016/j.revpalbo.2009.04.004
Urrego, L.E., Correa-Metrio, A., Gonzalez-Arango, C., Castaño, A.R., Yokoyama, Y., 2013. Contrasting responses of two Caribbean mangroves to sea-level rise in the Guajira Peninsula (Colombian Caribbean). Palaeogeography, Palaeoclimatology, Palaeoecology 370, 92–102. https://doi.org/10.1016/j.palaeo.2012.11.023
Urrego, L.E., Gonzalez-Arango, C., Urán, G., Polanía, J., 2010. Modern pollen rain in mangroves from San Andres Island, Colombian Caribbean. Review of Palaeobotany and Palynology 162, 168–182. https://doi.org/10.1016/j.revpalbo.2010.06.006
Van Campo, E., Bengo, M.D., 2004. Mangrove palynology in recent marine sediments off Cameroon. Marine Geology, Material Exchange Between the Upper Continental Shelf and Mangrove Fringed Coasts with Special Reference to the N. Amazon-Guianas Coast 208, 315–330. https://doi.org/10.1016/j.margeo.2004.04.014
Vandeputte, K., Moens, L., Dams, R., 1996. Improved Sealed-Tube Combustion of Organic Samples to CO2 for Stable Carbon Isotope Analysis, Radiocarbon Dating and Percent Carbon Determinations. Analytical Letters 29, 2761–2773. https://doi.org/10.1080/00032719608002279
Vandergoes, M.J., Prior, C.A., 2003. AMS Dating of Pollen Concentrates—A Methodological Study of Late Quaternary Sediments from South Westland, New Zealand. Radiocarbon 45, 479–491. https://doi.org/10.1017/S0033822200032823
Vane, C.H., Kim, A.W., Moss-Hayes, V., Snape, C.E., Diaz, M.C., Khan, N.S., Engelhart, S.E., Horton, B.P., 2013. Degradation of mangrove tissues by arboreal termites (Nasutitermes acajutlae) and their role in the mangrove C cycle (Puerto Rico): Chemical characterization and organic matter provenance using bulk δ13C, C/N, alkaline CuO oxidation-GC/MS, and solid-state 13C NMR. Geochem. Geophys. Geosyst. 14, 3176–3191. https://doi.org/10.1002/ggge.20194
Veerasingam, S., Vethamony, P., Mani Murali, R., Fernandes, B., 2015. Depositional record of trace metals and degree of contamination in core sediments from the Mandovi estuarine mangrove ecosystem, west coast of India. Marine Pollution Bulletin 91, 362–367. https://doi.org/10.1016/j.marpolbul.2014.11.045
Verheyden, A., Helle, G., Schleser, G.H., Dehairs, F., Beeckman, H., Koedam, N., 2004. Annual cyclicity in high-resolution stable carbon and oxygen isotope ratios in the wood of the mangrove tree Rhizophora mucronata. Plant, Cell & Environment 27, 1525–1536. https://doi.org/10.1111/j.1365-3040.2004.01258.x
Versteegh, G.J.M., Schefuß, E., Dupont, L., Marret, F., Sinninghe Damsté, J.S., Jansen, J.H.F., 2004. Taraxerol and Rhizophora pollen as proxies for tracking past mangrove ecosystems 1. Geochimica et Cosmochimica Acta 68, 411–422. https://doi.org/10.1016/S0016-7037(03)00456-3
Vesey-Fitzgerald, D., 1940. On the Vegetation of Seychelles. Journal of Ecology 28, 465–483. https://doi.org/10.2307/2256241
Victor, S., Neth, L., Golbuu, Y., Wolanski, E., Richmond, R.H., 2006. Sedimentation in mangroves and coral reefs in a wet tropical island, Pohnpei, Micronesia. Estuarine, Coastal and Shelf Science 66, 409–416. https://doi.org/10.1016/j.ecss.2005.07.025
Vyverberg, K., Dechnik, B., Dutton, A., Webster, J.M., Zwartz, D., Portell, R.W., 2018. Episodic reef growth in the granitic Seychelles during the Last Interglacial: Implications for polar ice sheet dynamics. Marine Geology 399, 170–187. https://doi.org/10.1016/j.margeo.2018.02.010

Wang, P., Chappell, J., 2001. Foraminifera as Holocene environmental indicators in the South Alligator River, Northern Australia. Quaternary International, Australian Quaternary Studies: A Tribute to Jim Bowler 83–85, 47–62. https://doi.org/10.1016/S1040-6182(01)00030-1

Whitehouse, P.L., 2018. Glacial isostatic adjustment modelling: historical perspectives, recent advances, and future directions. Earth Surface Dynamics 6, 401–429. https://doi.org/10.5194/esurf-6-401-2018

Whitehouse, P.L., Bentley, M.J., Milne, G.A., King, M.A., Thomas, I.D., 2012. A new glacial isostatic adjustment model for Antarctica: calibrated and tested using observations of relative sea-level change and present-day uplift rates. Geophys J Int 190, 1464–1482. https://doi.org/10.1111/j.1365-246X.2012.05557.x

Wickham, H., 2016. ggplot2: Elegant graphics for data analysis. Springer-Verlag, New York.

Wilson, G.P., Lamb, A.L., Leng, M.J., Gonzalez, S., Huddart, D., 2005. δ13C and C/N as potential coastal palaeoenvironmental indicators in the Mersey Estuary, UK. Quaternary Science Reviews, Quaternary coastal morphology and sea-level changes 24, 2015–2029. https://doi.org/10.1016/j.quascirev.2004.11.014

Woodroffe, C.D., 1992. Mangrove Sediments and Geomorphology, in: Robertson, A.I., Alongi, D.M. (Eds.), Tropical Mangrove Ecosystems. American Geophysical Union, pp. 7–41. https://doi.org/10.1029/CE041p0007

Woodroffe, C.D., 1990. The impact of sea-level rise on mangrove shorelines. Progress in Physical Geography 14, 483–520. https://doi.org/10.1177/030913339001400404

Woodroffe, C.D., 1981. Mangrove swamp stratigraphy and Holocene transgression, Grand Cayman Island, West Indies. Marine Geology 41, 271–294. https://doi.org/10.1016/0025-3227(81)90085-2

Woodroffe, C.D., McGregor, H.V., Lambeck, K., Smithers, S.G., Fink, D., 2012. Mid-Pacific microatolls record sea-level stability over the past 5000 yr. Geology 40, 951–954. https://doi.org/10.1130/G33344.1

Woodroffe, C.D., Rogers, K., McKee, K.L., Lovelock, C.E., Mendelssohn, I.A., Saintilan, N., 2016. Mangrove Sedimentation and Response to Relative Sea-Level Rise. Annual Review of Marine Science 8, 243–266. https://doi.org/10.1146/annurev-marine-122414-034025

Woodroffe, C.D., Thom, B.G., Chappell, J., 1985. Development of widespread mangrove swamps in mid-Holocene times in northern Australia. Nature 317, 711–713. https://doi.org/10.1038/317711a0

Woodroffe, S.A., 2009a. Recognising subtidal foraminiferal assemblages: implications for quantitative sea-level reconstructions using a foraminifera-based transfer function. J. Quaternary Sci. 24, 215–223. https://doi.org/10.1002/jqs.1230

Woodroffe, S.A., 2009b. Testing models of mid to late Holocene sea-level change, North Queensland, Australia. Quaternary Science Reviews 28, 2474–2488. https://doi.org/10.1016/j.quascirev.2009.05.004

Woodroffe, S.A., Horton, B.P., 2005. Holocene sea-level changes in the Indo-Pacific. Journal of Asian Earth Sciences 25, 29–43. https://doi.org/10.1016/j.jseaes.2004.01.009

Woodroffe, S.A., Horton, B.P., Larcombe, P., Whittaker, J.E., 2005. Intertidal Mangrove Foraminifera from the Central Great Barrier Reef Shelf, Australia: Implications for Sea-Level Reconstruction. Journal of Foraminiferal Research 35, 259–270. https://doi.org/10.2113/35.3.259

Woodroffe, S.A., Long, A.J., 2009. Salt marshes as archives of recent relative sea level change in West Greenland. Quaternary Science Reviews, Quaternary Ice Sheet-Ocean Interactions and Landscape Responses 28, 1750–1761. https://doi.org/10.1016/j.quascirev.2009.02.009

Woodroffe, S.A., Long, A.J., Milne, G.A., Bryant, C.L., Thomas, A.L., 2015a. New constraints on late Holocene eustatic sea-level changes from Mahé, Seychelles. Quaternary Science Reviews 115, 1–16. https://doi.org/10.1016/j.quascirev.2015.02.011

Woodroffe, S.A., Long, A.J., Punwong, P., Selby, K., Bryant, C.L., Marchant, R., 2015b. Radiocarbon dating of mangrove sediments to constrain Holocene relative sea-level change on Zanzibar in the southwest Indian Ocean. The Holocene 25, 820–831. https://doi.org/10.1177/0959683615571422

Wooller, M.J., Morgan, R., Fowell, S., Behling, H., Fogel, M., 2007. A multiproxy peat record of Holocene mangrove palaeoecology from Twin Cays, Belize. The Holocene 17, 1129–1139. https://doi.org/10.1177/0959683607082553

Wooller, M.J., Smallwood, B.J., Jacobson, M., Fogel, M., 2003a. Carbon and nitrogen stable isotopic variation in <Emphasis Type="Italic">Laguncularia racemosa</Emphasis> (L.) (white mangrove) from Florida and Belize: implications for trophic level studies. Hydrobiologia 499, 13–23. https://doi.org/10.1023/A:1026339517242

Wooller, M.J., Smallwood, B.J., Scharler, U., Jacobson, M., Fogel, M., 2003b. A taphonomic study of δ13C and δ15N values in Rhizophora mangle leaves for a multi-proxy approach to mangrove palaeoecology. Organic Geochemistry 34, 1259–1275. https://doi.org/10.1016/S0146-6380(03)00116-5

Xia, P., Meng, X., Li, Z., Feng, A., Yin, P., Zhang, Y., 2015. Mangrove development and its response to environmental change in Yingluo Bay (SW China) during the last 150years: Stable carbon isotopes and mangrove pollen. Organic Geochemistry 85, 32–41. https://doi.org/10.1016/j.orggeochem.2015.04.003

Yao, Q., Liu, K., 2017. Changes in modern pollen assemblages and soil geochemistry along coastal environmental gradients in the Everglades of south Florida. Front. Ecol. Evol. 5. https://doi.org/10.3389/fevo.2017.00178

Zhang, Z., Metzger, P., Sachs, J.P., 2013. Unprecedented long chain 1-chloroalkenes and 1-chloroalkanes in the Holocene sediments of Lake El Junco, Galápagos Islands. Organic Geochemistry 57, 1–6. https://doi.org/10.1016/j.orggeochem.2013.01.009

Zong, Y. 2004. Mid-Holocene sea-level highstand along the Southeast Coast of China. Quaternary International 117, 55-67.

Zong, Y., Hassan, K.B., 2004. Diatom Assemblages from Two Mangrove Tidal Flats in Peninsular Malaysia. Diatom Research 19, 329–344. https://doi.org/10.1080/0269249X.2004.9705878

Zong, Y., Horton, B.P., 1999. Diatom-based tidal-level transfer functions as an aid in reconstructing Quaternary history of sea-level movements in the UK. J. Quaternary Sci. 14, 153–167. https://doi.org/10.1002/(SICI)1099-1417(199903)14:2<153::AID-JQS425>3.0.CO;2-6

Zurbuchen, J., Simms, A.R., 2019. Late Holocene ice-mass changes recorded in a relative sea-level record from Joinville Island, Antarctica. Geology 47, 1064–1068. https://doi.org/10.1130/G46649.1

Appendix

Table A1: Grand Anse and Anse Boileau pollen trap data (percentage total counts). Rm is Rhizophora mucronata, B/C is group Bruguiera sp. and Ceriops sp., Sa is Sonneratia alba, Am is Avicennia marina, Lr is Lumnitzera racemosa, Aa is Acrostichum aureum, Ce is Casuarina equisetifolia. Mangrove species groupings are according to Mao et al. (2012), see Chapter three. Pollen concentrations calculated as per equation:

$$Concentration = \frac{\left(\frac{Taxa\ counts}{Lycopodium\ counts}\right) \times Total\ Lycopodium\ grains\ added}{Weight\ of\ sample\ (grams)}$$

Trap Sample	Rm	B/C	Sa	Am	Lr	Aa	Nf	Ce	Total non-mangrove	Mangrove (major species)	Mangrove (minor species)	Mangrove (associate species)	Total mangrove	Concentration
30	33.2	2.1	24.3	0.0	0.0	0.9	0.4	16.6	22.6	60.0	16.6	0.9	77.4	79734
57	26.1	0.4	11.4	0.0	0.0	2.9	0.0	30.2	26.1	38.0	33.1	2.9	73.9	38003
2	26.5	0.7	0.7	0.0	0.0	14.0	2.9	16.9	38.2	30.9	16.9	14.0	61.8	29301
24	21.6	5.9	0.0	3.9	0.0	5.9	0.0	41.2	21.6	31.4	41.2	5.9	78.4	7258
21	0.0	0.0	0.0	0.4	0.0	83.3	0.0	3.5	12.7	0.4	3.5	83.3	87.3	21703
74	4.6	0.0	0.0	0.0	0.0	0.4	0.4	71.4	22.9	5.0	71.8	0.4	77.1	108630
22	4.2	0.9	0.0	0.0	0.0	69.3	0.0	10.2	15.3	5.1	10.2	69.3	84.7	74317
5	30.4	0.0	4.4	0.0	0.0	17.7	3.2	1.3	41.1	38.0	3.2	17.7	58.9	36596
65	22.5	0.9	0.9	0.0	0.0	2.3	0.0	45.9	26.1	24.3	47.3	2.3	73.9	41723
9	7.1	1.3	0.4	0.4	0.0	0.0	0.4	44.5	45.0	9.7	44.5	0.8	55.0	57297
70	1.6	0.0	0.0	0.4	0.0	0.0	0.0	75.5	22.5	2.0	75.5	0.0	77.5	264851
26	29.2	0.0	0.0	0.0	8.3	0.0	0.0	41.7	20.8	37.5	41.7	0.0	79.2	3953
B17/T3/6	12.5	0.0	37.5	0.0	0.0	0.0	0.0	0.0	50.0	50.0	0.0	0.0	50.0	2195

Trap Sample	Rm	B/C	Sa	Am	Lr	Aa	Nf	Ce	Total non-mangrove	Mangrove (major species)	Mangrove (minor species)	Mangrove (associate species)	Total mangrove	Concentration
192	36.7	8.2	13.3	2.0	0.0	4.1	0.0	1.0	31.6	60.2	2.0	6.1	68.4	1949
162	76.1	1.3	0.0	0.4	0.0	2.1	0.0	4.3	15.4	77.8	4.3	2.6	84.6	15002
157	85.7	0.0	0.0	0.0	0.0	0.0	0.0	7.1	7.1	85.7	7.1	0.0	92.9	1186
152	82.8	0.4	0.0	0.0	0.0	0.4	0.8	6.7	8.4	84.1	6.7	0.8	91.6	115577
166	60.0	0.0	0.0	0.0	0.0	2.1	1.1	12.6	24.2	61.1	12.6	2.1	75.8	5937
114	19.6	0.0	0.0	2.2	0.0	8.7	2.2	10.9	56.5	23.9	10.9	8.7	43.5	1034
171	90.0	0.0	3.3	0.0	0.0	0.0	0.0	0.0	6.7	93.3	0.0	0.0	93.3	16379

Table A2: Grand Anse vegetation survey data. All sites displayed in Appendix Figure A2.

Site name	Elevation (m MTL)	Vegetation zone
1	-0.22	Mixed Sa and Ra
2	0	Mixed Sa and Ra
3	0.05	Mixed Sa and Ra
4	0.07	Mixed Sa and Ra
5	0.07	Mixed Sa and Ra
6	0.11	Bruguiera dominated
7	0.2	Bruguiera dominated
8	0.4	Bruguiera dominated
9	0.69	Terrestrial dominated
10	-0.17	Mixed Sa and Ra
11	0.11	Mixed Sa and Ra
12	0.07	Bruguiera dominated
13	0.09	Bruguiera dominated
14	0.09	Bruguiera dominated
15	0.15	Bruguiera dominated
16	0.33	Bruguiera dominated
17	-0.08	Mixed Sa and Ra
18	0.08	Bruguiera dominated
19	0.2	Bruguiera dominated
20	0.33	Bruguiera dominated
21	0.7	Terrestrial dominated
22	0.55	Terrestrial dominated
23	0.49	Mixed Am and Lr
24	0.53	Mixed Am and Lr
25	0.39	Mixed Am and Lr
26	0.43	Mixed Am and Lr
27	0.37	Mixed Sa and Ra
28	0.32	Mixed Sa and Ra
29	0.24	Mixed Sa and Ra
30	0.11	Mixed Sa and Ra
31	0.07	Mixed Sa and Ra
32	0.47	Mixed Am and Lr
33	0.37	Mixed Am and Lr
34	0.33	Mixed Am and Lr
35	0.23	Mixed Sa and Ra
36	0.22	Mixed Sa and Ra
37	0.29	Mixed Sa and Ra
38	0.38	Mixed Sa and Ra
39	0.68	Terrestrial dominated
40	0.58	Terrestrial dominated
41	1.81	Terrestrial dominated
42	0.51	Terrestrial dominated

Site name	Elevation (m MTL)	Vegetation zone
43	0.53	Terrestrial dominated
46	0.61	Mixed Sa and Ra
47	0.43	Mixed Sa and Ra
48	0.4	Mixed Sa and Ra
49	0.33	Mixed Sa and Ra
50	0.33	Mixed Sa and Ra
51	0.34	Mixed Sa and Ra
52	0.15	Mixed Sa and Ra
53	0.14	Mixed Sa and Ra
54	0.27	Mixed Sa and Ra
55	0.18	Mixed Sa and Ra
56	0.21	Mixed Sa and Ra
57	0.26	Mixed Sa and Ra
58	0.23	Mixed Sa and Ra
59	0.32	Mixed Sa and Ra
60	0.3	Mixed Sa and Ra
61	0.39	Mixed Sa and Ra
62	0.38	Mixed Sa and Ra
63	0.3	Mixed Sa and Ra
64	0.3	Mixed Sa and Ra
65	0.36	Mixed Sa and Ra
66	0.39	Mixed Sa and Ra
67	0.38	Mixed Sa and Ra
68	0.51	Mixed Sa and Ra
69	0.46	Mixed Sa and Ra
70	0.7	Mixed Sa and Ra
71	0.91	Terrestrial dominated
72	1.19	Terrestrial dominated
73	1.44	Terrestrial dominated
74	1.65	Terrestrial dominated
75	1.87	Terrestrial dominated
76	2.02	Terrestrial dominated
77	2.05	Terrestrial dominated
78	0.43	Terrestrial dominated
79	0.47	Mixed Sa and Ra
80	0.82	Mixed Sa and Ra
81	-0.43	Mixed Sa and Ra
82	-0.38	Mixed Sa and Ra
83	-0.34	Mixed Sa and Ra
84	-0.32	Mixed Sa and Ra
85	-0.23	Mixed Sa and Ra
86	-0.18	Mixed Sa and Ra
87	-0.11	Mixed Sa and Ra

Site name	Elevation (m MTL)	Vegetation zone
88	-0.06	Mixed Sa and Ra
89	-0.09	Mixed Sa and Ra
90	0.02	Mixed Sa and Ra
91	0.08	Mixed Sa and Ra
92	0.13	Bruguiera dominated
93	0.19	Bruguiera dominated
94	0.22	Bruguiera dominated
95	0.27	Bruguiera dominated
96	0.33	Bruguiera dominated
97	0.38	Bruguiera dominated
99	0.46	Bruguiera dominated
100	0.48	Bruguiera dominated
101	0.52	Terrestrial dominated
102	0.86	Terrestrial dominated
103	0.92	Terrestrial dominated
104	0.88	Terrestrial dominated
105	1.65	Terrestrial dominated
106	2.17	Terrestrial dominated
122	0.25	Mixed Am and Lr
123	0.37	Mixed Am and Lr
124	0.29	Mixed Am and Lr
125	0.22	Mixed Am and Lr
126	0.18	Rhizophora
127	0.11	Rhizophora
128	0.06	Rhizophora
129	0.23	Rhizophora
130	0.29	Bruguiera dominated
131	0.28	Bruguiera dominated
132	0.34	Bruguiera dominated
133	0.94	Terrestrial dominated
134	0.28	Mixed Am and Lr
135	0.32	Mixed Am and Lr
136	0.21	Mixed Am and Lr
137	0.19	Mixed Sa and Ra
139	0.37	Mixed Am and Lr
140	0.36	Mixed Am and Lr
141	0.38	Mixed Am and Lr
142	0.53	Mixed Am and Lr
143	0.4	Mixed Am and Lr
144	0.42	Mixed Am and Lr
145	0.48	Mixed Am and Lr
146	0.37	Mixed Am and Lr
147	0.36	Mixed Am and Lr

Table A3: Anse Boileau vegetation survey data. All sites displayed in Appendix Figure A3.

Site name	Elevation (m MTL)	Vegetation zone
111	0.2	Mixed Sa and Ra
112	0.26	Mixed Sa and Ra
113	0.13	Mixed Sa and Ra
114	0.16	Mixed Sa and Ra
115	0.12	Mixed Sa and Ra
116	0.1	Mixed Sa and Ra
117	0.31	Mixed Sa and Ra
118	0.32	Mixed Sa and Ra
119	0.32	Mixed Sa and Ra
120	0.42	Mixed Sa and Ra
150	0.41	Mixed Sa and Ra
151	0.42	Mixed Sa and Ra
152	0.43	Mixed Sa and Ra
153	0.45	Mixed Sa and Ra
154	0.45	Mixed Sa and Ra
155	0.47	Mixed Sa and Ra
156	0.51	Mixed Sa and Ra
157	0.51	Mixed Sa and Ra
158	-0.36	Mixed Sa and Ra
159	-0.32	Mixed Sa and Ra
160	-0.3	Mixed Bg and Ra
161	-0.25	Mixed Bg and Ra
162	-0.23	Mixed Bg and Ra
163	-0.2	Mixed Bg and Ra
164	-0.16	Mixed Bg and Ra
165	-0.13	Mixed Bg and Ra
166	-0.1	Mixed Bg and Ra
167	-0.08	Mixed Bg and Ra
168	-0.14	Mixed Bg and Ra
169	-0.1	Mixed Bg and Ra
170	-0.1	Mixed Bg and Ra
171	-0.1	Mixed Bg and Ra
172	-0.51	Mixed Sa and Ra
173	-0.58	Mixed Sa and Ra
174	0.08	Mixed Sa and Ra
175	0.13	Mixed Sa and Ra
176	0.13	Am dominated
177	0.15	Mixed Bg and Ra
178	0.12	Mixed Bg and Ra
179	0.18	Mixed Bg and Ra

Site name	Elevation (m MTL)	Vegetation zone
180	0.21	Mixed Bg and Ra
181	0.2	Mixed Bg and Ra
182	0.2	Mixed Bg and Ra
183	0.21	Mixed Bg and Ra
184	0.21	Mixed Bg and Ra
185	0.21	Mixed Bg and Ra
186	0.22	Am dominated
187	0.23	Am dominated
188	0.27	Am dominated
189	0.28	Am dominated
190	0.27	Am dominated
191	0.3	Am dominated
192	0.32	Am dominated
193	0.06	Am dominated
194	0.45	Am dominated
195	-0.23	Mixed Sa and Ra
196	-0.39	Mixed Sa and Ra
197	-0.3	Mixed Sa and Ra
198	-0.28	Mixed Sa and Ra
199	-0.23	Mixed Sa and Ra

Table A4: Surface sediment sample data for Grand Anse (see Chapter five for method details and uncertainties). Latitude and longitude are in decimal degrees, see Appendix Figure A2 for distance from shore calculations. Fine sand (63-250 µm), coarse sand (>500 µm), silt and clay (<63 µm). Vegetation codes: Sa is Sonneratia alba, Rm is Rhizophora mucronata, Bg is Bruguiera gymnorrhiza, Am is Avicennia marina, Lr is Lumnitzera racemosa.

Site name	Latitude	Longitude	Elevation (m MTL)	Distance from shore (m)	TOC %	TIC %	TC %	Vegetation zone	Fine sand %	Coarse sand %	Silt and clay %
2	-4.68218	55.45389	0	370.9	10.1	1.6	11.7	Mixed Sa and Rm	35.9	6.3	52.6
3	-4.68226	55.45401	0.05	372.1	15.6	0.0	15.6	Mixed Sa and Rm	25.3	7.2	62.7
5	-4.68233	55.45398	0.07	377.3	22.0	0.6	22.7	Mixed Sa and Rm	25.0	9.1	59.3
7	-4.6825	55.45401	0.2	377.3	25.6	0.8	26.4	Mixed Bg and Rm	23.9	27.5	34.6
8	-4.68251	55.45398	0.4	380.3	10.5	2.0	12.4	Mixed Bg and Rm	11.8	52.3	23.8
9	-4.68251	55.45405	0.69	378.7	9.1	3.3	12.4	Terrestrial dominated	14.7	42.6	31.0
10	-4.6821	55.45402	-0.17	378.3	10.6	0.1	10.7	Mixed Sa and Rm	12.3	65.5	12.2
14	-4.68237	55.45405	0.09	385.9	19.9	0.3	20.2	Mixed Bg and Rm	26.1	10.2	56.1
15	-4.6825	55.45406	0.15	387.8	25.2	0.6	25.7	Mixed Bg and Rm	23.4	22.8	42.8
17	-4.68227	55.45437	-0.08	418.2	12.5	0.0	12.5	Mixed Sa and Rm	17.7	52.9	14.8
21	-4.68178	55.45498	0.7	475.6	2.7	0.0	2.7	Terrestrial dominated	14.4	43.4	33.8
22	-4.68181	55.45499	0.55	478.1	7.3	0.0	7.3	Terrestrial dominated	15.3	39.0	33.0
24	-4.6819	55.45483	0.53	455.2	2.5	0.0	2.5	Mixed Am and Lr	14.9	56.6	13.0
25	-4.68195	55.45468	0.39	446.9	2.1	0.0	2.1	Mixed Am and Lr	12.9	59.2	11.0
26	-4.68197	55.45463	0.43	442.2	2.2	0.0	2.2	Mixed Am and Lr	9.5	67.9	6.4
28	-4.682	55.45448	0.32	426.6	4.1	0.0	4.1	Mixed Sa and Ra	17.4	58.0	14.2
30	-4.68207	55.45437	0.11	415.2	8.5	0.1	8.5	Mixed Sa and Ra	25.9	44.4	21.5
31	-4.68209	55.45434	0.07	412.2	12.2	0.0	12.2	Mixed Am and Lr	28.2	27.3	39.0
32	-4.68186	55.45467	0.47	439.5	3.1	0.0	3.1	Mixed Am and Lr	16.1	55.8	12.1
33	-4.68186	55.45453	0.37	429.6	5.1	0.0	5.1	Mixed Am and Lr	13.6	63.1	9.5
35	-4.68183	55.4543	0.23	404.2	9.8	0.0	9.8	Mixed Sa and Rm	8.8	74.6	8.8

Site name	Latitude	Longitude	Elevation (m MTL)	Distance from shore (m)	TOC %	TIC %	TC %	Vegetation zone	Fine sand %	Coarse sand %	Silt and clay %
37	-4.68174	55.45422	0.29	393.3	19.9	0.9	20.8	Mixed Sa and Rm	4.4	85.7	3.6
42	-4.68155	55.45418	0.51	386.7	3.4	7.5	10.9	Terrestrial dominated	16.0	55.0	9.0
46	-4.68207	55.45386	0.61	354.9	3.7	9.7	13.4	Mixed Sa and Rm	27.6	39.5	6.5
47	-4.68217	55.45377	0.43	349.7	6.1	4.0	10.0	Mixed Sa and Rm	24.3	34.9	21.2
51	-4.68244	55.4536	0.34	336.8	5.4	8.2	13.6	Mixed Sa and Rm	51.1	15.3	14.1
55	-4.68246	55.45346	0.18	326.8	9.0	4.6	13.6	Mixed Sa and Rm	36.3	12.1	41.8
56	-4.68248	55.45357	0.21	323.3	2.3	7.3	9.6	Mixed Sa and Rm	60.2	7.7	16.8
57	-4.68239	55.45358	0.26	329.9	4.1	5.2	9.3	Mixed Sa and Rm	52.1	14.5	20.6
58	-4.68239	55.45348	0.23	317.2	5.8	5.9	11.7	Mixed Sa and Rm	28.9	49.1	6.5
59	-4.68237	55.45344	0.32	317.4	2.5	8.1	10.6	Mixed Sa and Rm	46.7	26.2	8.9
65	-4.68233	55.45364	0.36	342.9	6.3	3.2	9.5	Mixed Sa and Rm	17.6	59.5	12.2
67	-4.68217	55.45373	0.38	339.3	3.7	4.0	7.7	Mixed Sa and Rm	26.2	37.8	13.5
70	-4.68207	55.4535	0.7	321.7	1.8	9.9	11.6	Mixed Sa and Rm	24.6	42.5	4.8
71	-4.6821	55.45349	0.91	323.2	3.8	10.7	14.4	Terrestrial dominated	24.3	44.0	4.4
72	-4.68207	55.45351	1.19	322.8	2.0	10.4	12.4	Terrestrial dominated	26.4	34.6	8.9
73	-4.68214	55.45351	1.44	322.6	0.9	10.5	11.4	Terrestrial dominated	28.8	32.6	7.2
74	-4.68213	55.45351	1.65	322.3	1.0	10.9	11.9	Terrestrial dominated	26.6	29.6	15.9
79	-4.68226	55.45322	0.47	293.0	0.8	10.0	10.8	Mixed Sa and Rm	65.6	6.6	5.3
80	-4.68205	55.45318	0.82	286.7	0.0	10.1	10.1	Mixed Sa and Rm	29.5	37.1	3.7
81	-4.68269	55.45262	-0.43	231.5	4.6	8.5	13.1	Mixed Sa and Rm	76.0	7.4	2.6
82	-4.68277	55.4526	-0.38	230.5	3.8	9.8	13.6	Mixed Sa and Rm	68.2	11.5	4.0
83	-4.68271	55.45261	-0.34	231.4	1.2	9.8	11.0	Mixed Sa and Rm	67.8	10.0	3.6
84	-4.68272	55.4526	-0.32	236.8	1.1	9.5	10.6	Mixed Sa and Rm	69.8	6.0	6.1
85	-4.6827	55.4526	-0.23	238.5	0.6	9.9	10.4	Mixed Sa and Rm	65.5	10.5	6.8

Site name	Latitude	Longitude	Elevation (m MTL)	Distance from shore (m)	TOC %	TIC %	TC %	Vegetation zone	Fine sand %	Coarse sand %	Silt and clay %
86	-4.68272	55.45262	-0.18	241.4	1.7	9.0	10.7	Mixed Sa and Rm	73.7	5.2	7.1
87	-4.68274	55.45259	-0.11	243.1	3.6	8.2	11.9	Mixed Sa and Rm	62.2	12.6	10.4
88	-4.68267	55.45265	-0.06	243.9	0.0	9.7	9.7	Mixed Sa and Rm	65.9	15.9	4.1
89	-4.68276	55.45265	-0.09	245.3	1.9	8.1	10.0	Mixed Sa and Rm	59.7	12.5	8.5
90	-4.68278	55.45267	0.02	246.9	0.8	8.7	9.5	Mixed Sa and Rm	51.3	20.7	10.1
91	-4.68281	55.45274	0.08	249.3	0.3	8.1	8.4	Mixed Sa and Rm	47.7	26.7	5.6
92	-4.68279	55.45277	0.13	253.2	4.1	7.3	11.4	Mixed Bg and Rm	59.7	8.2	12.7
93	-4.68282	55.45274	0.19	257.1	5.2	7.8	13.0	Mixed Bg and Rm	50.6	22.0	8.3
94	-4.68283	55.45279	0.22	259.3	1.8	8.3	10.0	Mixed Bg and Rm	9.1	0.0	90.9
95	-4.68282	55.45286	0.27	262.1	2.2	8.6	10.8	Mixed Bg and Rm	57.5	13.1	11.2
122	-4.68252	55.45552	0.25	552.7	7.9	0.0	7.9	Mixed Am and Lr	12.9	49.8	31.3
126	-4.68263	55.45542	0.18	549.0	12.5	0.1	12.6	Mixed Sa and Rm	18.1	20.8	55.5
127	-4.68268	55.4555	0.11	551.2	21.9	0.2	22.0	Mixed Sa and Rm	20.4	5.9	70.2
128	-4.68272	55.45547	0.06	553.6	22.3	0.1	22.3	Mixed Sa and Rm	19.3	1.0	77.9
129	-4.6828	55.45559	0.23	561.7	6.6	0.0	6.6	Mixed Sa and Rm	7.4	77.9	5.9

Table A5: Surface sediment sample data for Anse Boileau (see Chapter five for method details and uncertainties). Latitude and longitude are in decimal degrees, see Appendix Figure A3 for distance from shore calculations. Fine sand (63-250 µm), coarse sand (>500 µm), silt and clay (<63 µm). Vegetation codes: Sa is Sonneratia alba, Rm is Rhizophora mucronata, Bg is Bruguiera gymnorrhiza, Am is Avicennia marina, Lr is Lumnitzera racemosa.

Site name	Latitude	Longitude	Elevation (m MTL)	Distance from shore (m)	TOC %	TIC %	TC %	Vegetation zone	Fine sand %	Coarse sand %	Silt and clay %
111	-4.70353	55.47561	0.2	57.5	0.0	10.5	10.5	Mixed Sa and Rm	51.2	16.2	5.3
114	-4.70343	55.47566	0.16	69.8	4.5	4.6	9.1	Mixed Sa and Rm	23.4	40.4	25.0
115	-4.70338	55.47573	0.12	79.2	4.2	5.1	9.3	Mixed Sa and Rm	24.6	37.6	25.5
116	-4.70339	55.47587	0.1	87.9	12.1	0.1	12.2	Mixed Sa and Rm	20.0	16.5	55.5
120	-4.70352	55.47582	0.42	73.8	2.2	7.3	9.5	Mixed Sa and Rm	25.8	44.1	11.7
150	-4.70345	55.47601	0.41	93.5	15.3	0.1	15.4	Mixed Sa and Rm	24.9	6.6	59.8
152	-4.70349	55.47612	0.43	98.1	18.6	0.1	18.7	Mixed Sa and Rm	20.1	3.6	72.4
155	-4.70357	55.47633	0.47	106.3	18.5	0.0	18.5	Mixed Sa and Rm	13.6	0.0	86.3
158	-4.70279	55.47617	-0.36	159.9	7.3	0.1	7.4	Mixed Sa and Rm	31.7	22.1	40.0
160	-4.70292	55.47618	-0.3	150.2	9.7	0.0	9.7	Mixed Bg and Rm	21.8	43.3	30.4
162	-4.70296	55.47624	-0.23	151.4	10.0	0.0	10.0	Mixed Bg and Rm	23.9	39.1	29.9
164	-4.7031	55.47636	-0.16	148.0	13.5	0.0	13.5	Mixed Bg and Rm	26.2	18.2	50.8
166	-4.70314	55.47647	-0.1	152.1	12.8	0.0	12.8	Mixed Bg and Rm	23.4	1.2	74.5
169	-4.70324	55.47663	-0.1	156.2	13.8	0.0	13.8	Mixed Bg and Rm	18.4	0.3	80.7
172	-4.70271	55.47622	-0.51	198.1	12.6	0.3	12.9	Mixed Sa and Rm	26.2	23.1	42.3
174	-4.70263	55.47664	0.08	207.7	6.0	0.0	6.0	Mixed Sa and Rm	14.8	59.6	13.3
176	-4.70278	55.47666	0.13	196.9	3.6	0.0	3.6	Am dominated	10.7	72.3	8.1
179	-4.70292	55.47678	0.18	190.2	3.5	0.0	3.5	Mixed Bg and Rm	21.2	51.8	12.6
185	-4.70323	55.47687	0.21	192.2	3.5	0.1	3.6	Mixed Bg and Rm	13.7	0.0	85.1
186	-4.70279	55.47701	0.22	220.8	3.0	0.0	3.0	Am dominated	7.2	71.4	14.3
187	-4.70282	55.47704	0.23	230.6	6.1	0.0	6.1	Am dominated	6.8	69.8	17.2

Site name	Latitude	Longitude	Elevation (m MTL)	Distance from shore (m)	TOC %	TIC %	TC %	Vegetation zone	Fine sand %	Coarse sand %	Silt and clay %
188	-4.70279	55.47713	0.27	236.1	4.9	0.0	4.9	Am dominated	5.7	72.6	16.3
190	-4.70285	55.47709	0.27	249.9	7.2	0.1	7.3	Am dominated	7.5	65.3	20.9
192	-4.70292	55.47717	0.32	260.3	6.9	0.0	6.9	Am dominated	6.3	65.8	23.5
197	-4.70259	55.47623	-0.3	183.5	7.0	0.1	7.1	Mixed Sa and Rm	16.0	28.8	51.1
198	-4.70261	55.47623	-0.28	183.5	6.1	0.1	6.1	Mixed Sa and Rm	24.9	30.4	38.0
199	-4.7026	55.47626	-0.23	183.4	8.2	0.1	8.3	Mixed Sa and Rm	10.9	64.1	19.0
200	-4.70255	55.47625	-0.07	183.6	2.7	0.0	2.7	Terrestrial dominated	10.2	62.5	20.9
201	-4.70254	55.47624	0.04	183.9	1.6	0.0	1.6	Terrestrial dominated	6.4	77.5	10.7
202	-4.70249	55.47627	0.26	184.2	1.3	0.0	1.3	Terrestrial dominated	11.4	56.1	24.4

Figure A1: Sample sites analysed for biomarkers highlighted. Dashed white line is approximate mangrove zone, light blue line is the River Dauban.

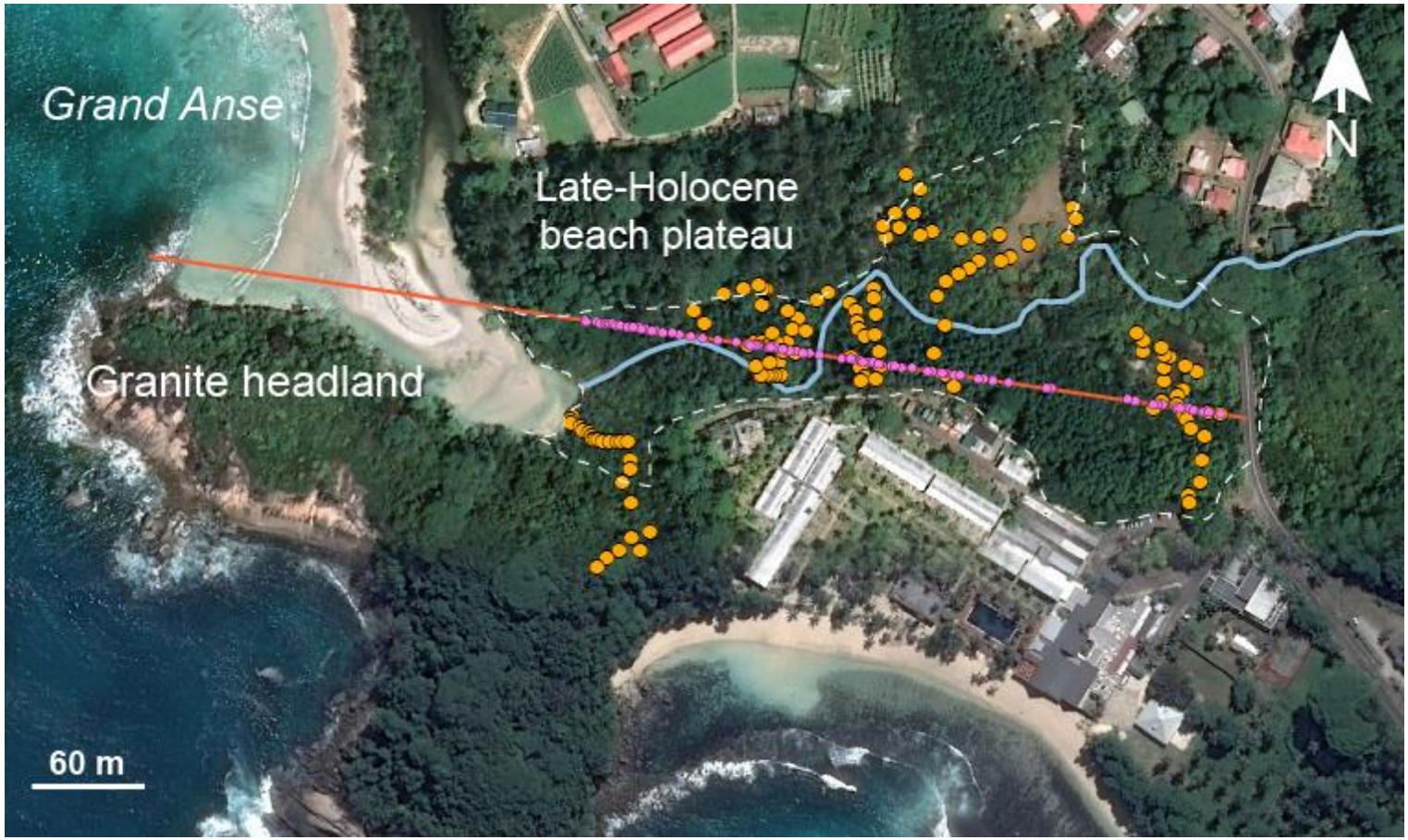

Figure A2: Total number of sample sites (vegetation, elevation, surface sediments) at the Grand Anse mangrove, with calculations for distance from shore visualised (sample sites data in Tables A2 and A4). The orange line is a 'cross-section', to which sample sites are linearly interpolated (the pink dots). Distance from shore is calculated with the 0 value marking the marine end of the cross-section line. The dashed white line is approximate mangrove zone, and the light blue line is the River Dauban.

Figure A3: Total number of sample sites (vegetation, elevation, surface sediments) at the Anse Boileau mangrove, with calculations for distance from shore visualised (sample site data in Tables A3 and A5). The green line is a 'cross-section', to which sample sites are linearly interpolated (the pink dots). Distance from shore is calculated with the 0 value marking the marine end of the cross-section line. The dashed white line is approximate mangrove zone, and the light blue line is the River Cayman.

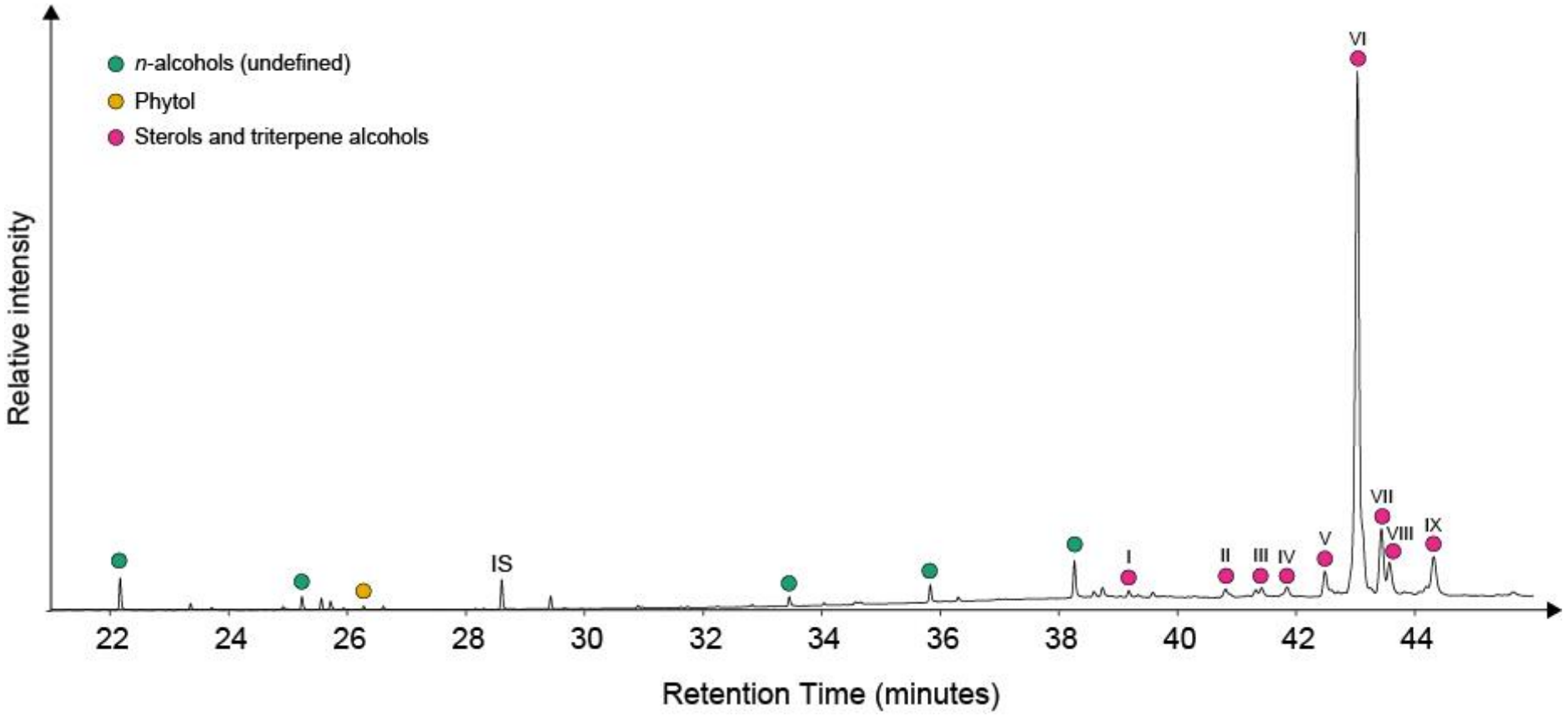

Figure A4: A typical GC-MS chromatogram of the polar fraction of a surface sediment sample from Grand Anse (sample 58). IS is the internal standard (5α-androstanol), and sterols and triterpene alcohols are as follows: I) cholesterol, II) campesterol, III) poriferasterol, IV) β-stigmasterol, V) sitosterol, VI) taraxerol, VII) β-amyrin, VIII) germanicol, IX) lupeol.

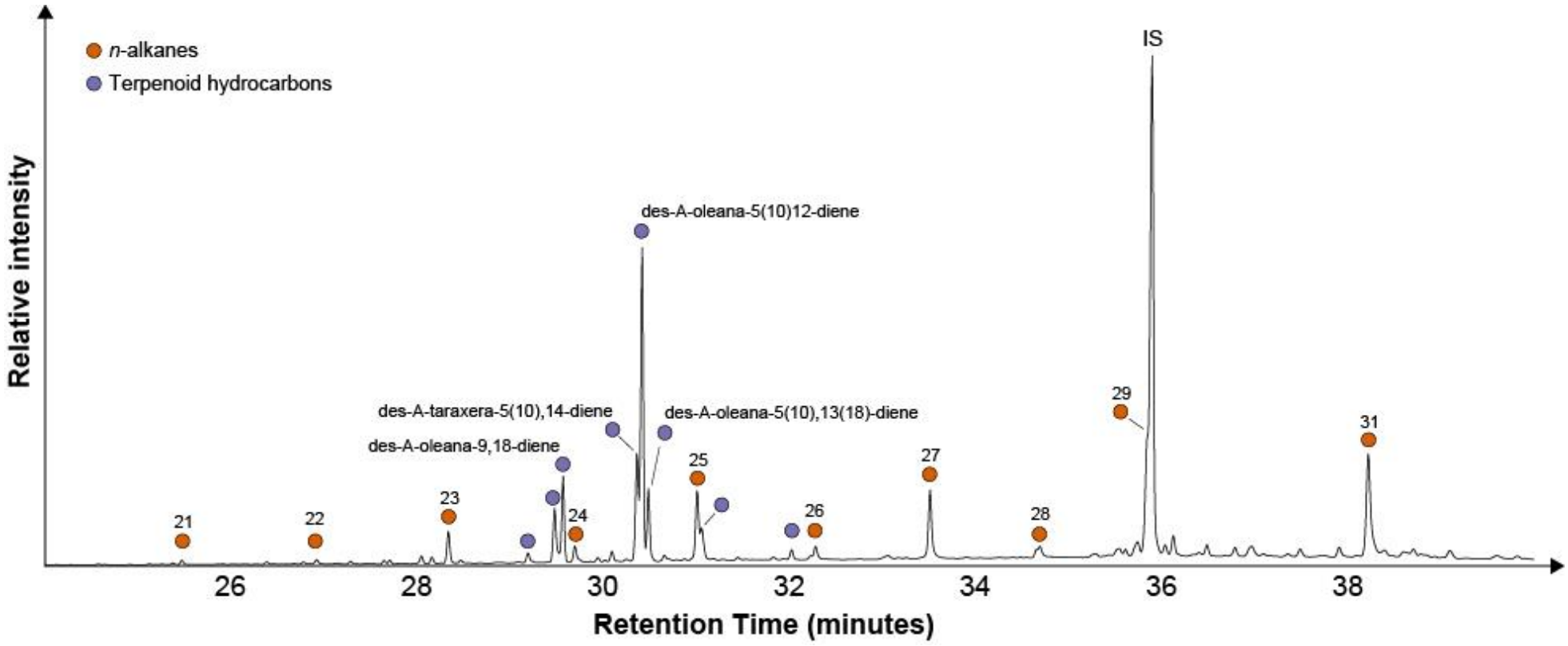

Figure A5: A typical GC-MS chromatogram for the apolar fraction a surface sediment sample from Grand Anse (sample 5). IS is the internal standard (5α-cholestane, which is co-eluting with the C29-alkane).

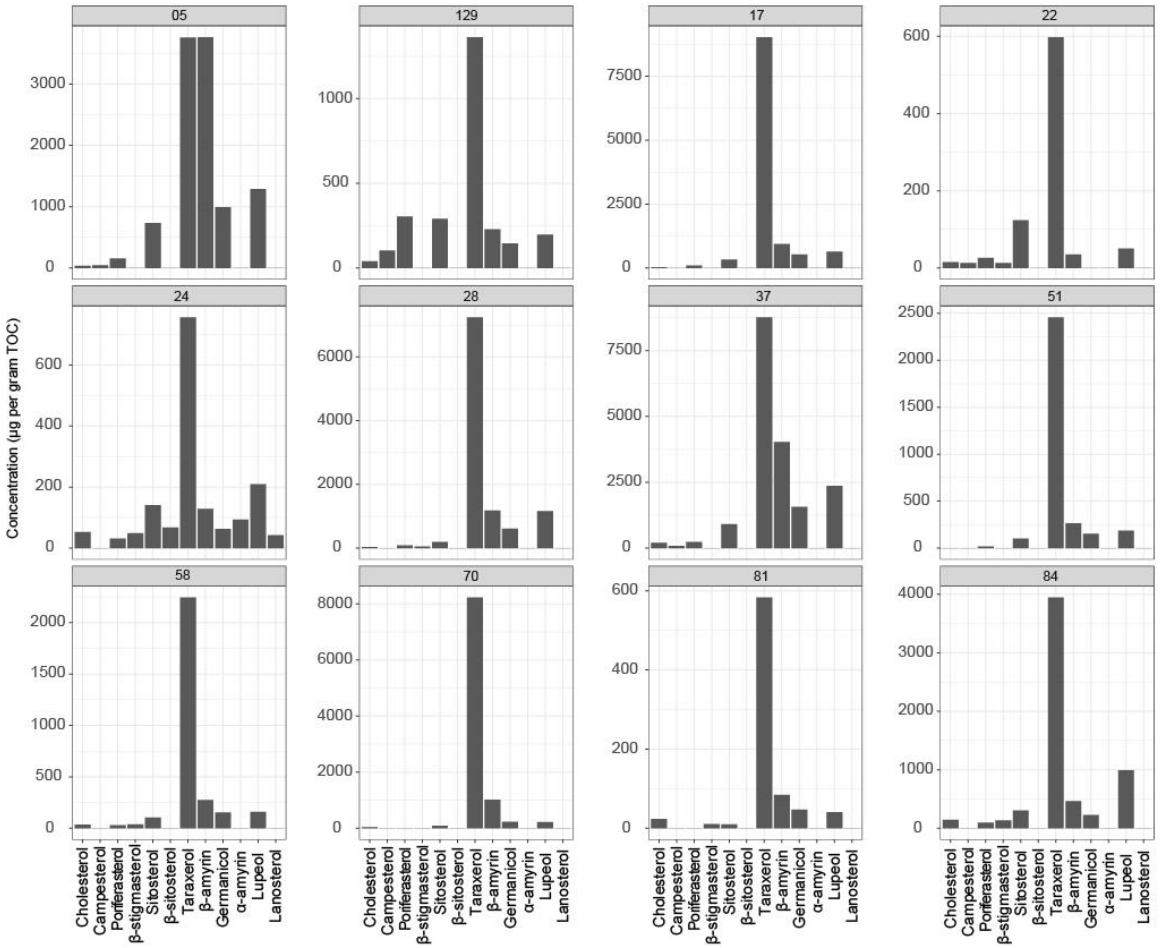

Figure A6: Concentrations (µg per gram of TOC) of identified sterols and triterpene alcohols in the Grand Anse surface sediment samples.

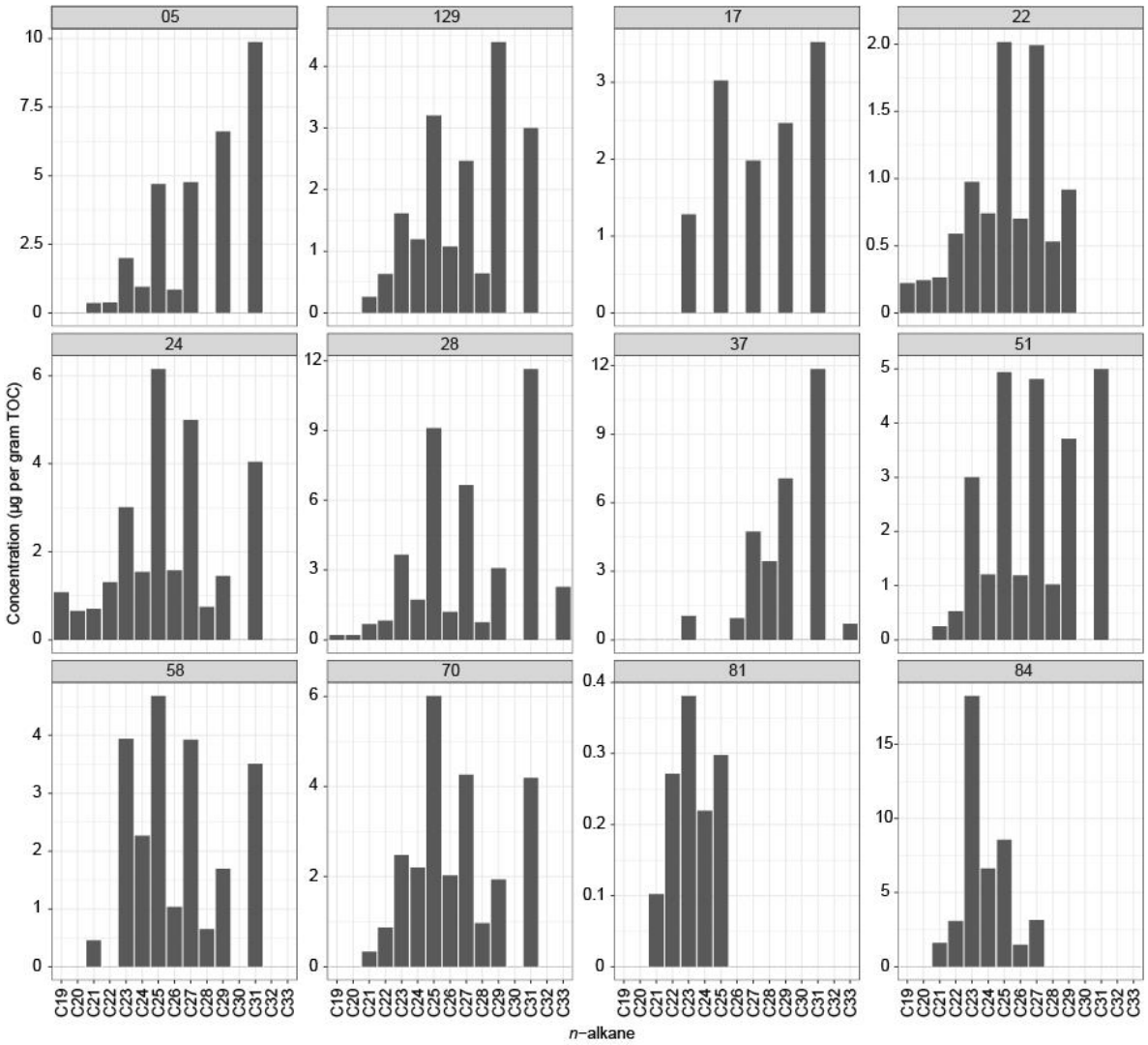

Figure A7: n-alkane distributions (concentration µg per gram TOC) for each surface sediment sample from Grand Anse.

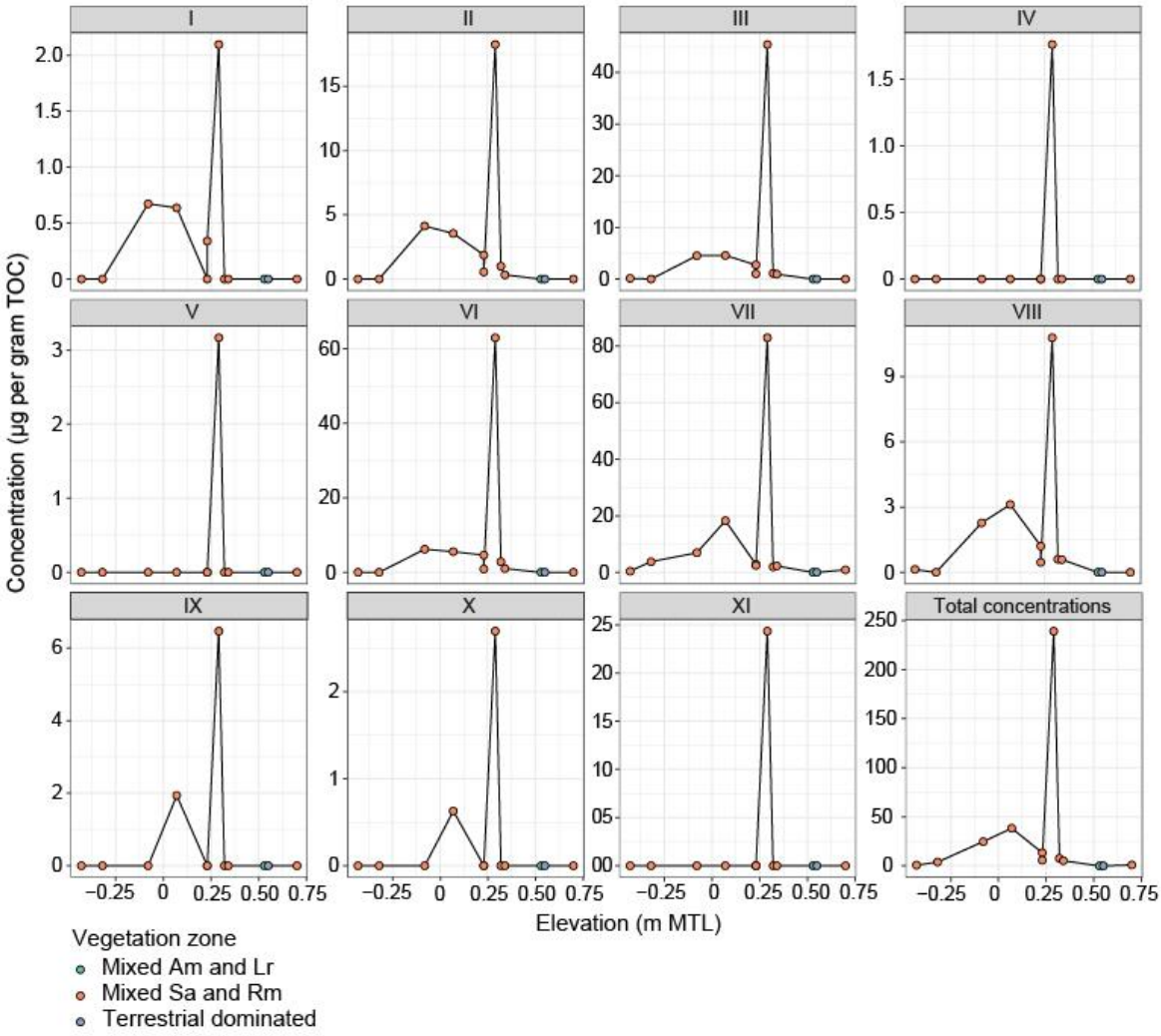

Figure A8: Terpenoid hydrocarbons tentatively identified in the Grand Anse surface sediment samples. Only six out of eleven have been identified to compound level: III) des-A-oleana-9,18-diene, IV) des-A-oleana-5(10),6,12-triene, VI) des-A-taraxera-5(10),14-diene, VII) des-A-oleana-5(10),12-diene, VIII) des-A-oleana-5(10),13(18)-diene, XI) 24-Norlup-22(29)-ene.

Table A6: n-alkane concentrations (µg per gram total organic carbon).

sample	C19	C20	C21	C22	C23	C24	C25	C26	C27	C28	C29	C30	C31	C32	C33	total
81	0.00	0.00	0.10	0.27	0.38	0.22	0.30	0.00	0.00	0.00	0.00	0.00	0.00	0.00	0.00	1.27
84	0.00	0.00	1.60	3.08	18.27	6.62	8.57	1.47	3.14	0.00	0.00	0.00	0.00	0.00	0.00	42.75
17	0.00	0.00	0.00	0.00	1.28	0.00	3.02	0.00	1.98	0.00	2.47	0.00	3.52	0.00	0.00	12.28
5	0.00	0.00	0.35	0.37	1.99	0.95	4.69	0.85	4.77	0.00	6.61	0.00	9.87	0.00	0.00	30.45
129	0.00	0.00	0.26	0.63	1.61	1.19	3.20	1.08	2.47	0.64	4.39	0.00	3.00	0.00	0.00	18.47
58	0.00	0.00	0.45	0.00	3.94	2.26	4.68	1.03	3.92	0.65	1.69	0.00	3.51	0.00	0.00	22.15
37	0.00	0.00	0.00	0.00	1.03	0.00	0.00	0.94	4.73	3.44	7.06	0.00	11.85	0.00	0.70	29.77
28	0.21	0.21	0.68	0.83	3.65	1.72	9.11	1.19	6.66	0.76	3.09	0.00	11.64	0.00	2.27	42.00
51	0.00	0.00	0.25	0.53	3.00	1.21	4.94	1.19	4.81	1.02	3.71	0.00	5.00	0.00	0.00	25.65
24	1.08	0.65	0.71	1.31	3.01	1.54	6.15	1.58	4.99	0.75	1.45	0.00	4.04	0.00	0.00	27.27
22	0.22	0.24	0.26	0.59	0.98	0.74	2.02	0.70	1.99	0.53	0.92	0.00	0.00	0.00	0.00	9.19
70	0.00	0.00	0.34	0.86	2.48	2.20	6.01	2.03	4.26	0.96	1.94	0.00	4.19	0.00	0.00	25.26

Table A7: Terpenoid hydrocarbon concentrations (µg per gram total organic carbon). Only six out of eleven have been identified to compound level: III) des-A-oleana-9,18-diene, IV) des-A-oleana-5(10),6,12-triene, VI) des-A-taraxera-5(10),14-diene, VII) des-A-oleana-5(10),12-diene, VIII) des-A-oleana-5(10),13(18)-diene, XI) 24-Norlup-22(29)-ene.

sample	I	II	III	IV	V	VI	VII	VIII	IX	X	XI	XII	XIII	totals
81	0.00	0.00	0.14	0.00	0.00	0.00	0.47	0.13	0.00	0.00	0.00	0.00	0.00	0.75
84	0.00	0.00	0.00	0.00	0.00	0.00	3.81	0.00	0.00	0.00	0.00	0.00	0.00	3.81
17	0.67	4.13	4.52	0.00	0.00	6.23	6.93	2.28	0.00	0.00	0.00	0.00	0.00	24.76
5	0.64	3.55	4.60	0.00	0.00	5.56	18.26	3.12	1.94	0.63	0.00	0.00	0.00	38.30
129	0.00	1.88	2.74	0.00	0.00	4.65	2.84	1.21	0.00	0.00	0.00	0.00	0.00	13.32
58	0.34	0.55	1.04	0.00	0.00	0.94	2.53	0.46	0.00	0.00	0.00	0.00	0.00	5.86
37	2.10	18.26	45.41	1.76	3.17	62.93	82.93	10.78	6.47	2.70	2.44	0.00	0.00	238.94
28	0.00	0.99	1.10	0.00	0.00	2.87	1.98	0.61	0.00	0.00	0.00	0.00	0.00	7.56
51	0.00	0.33	0.95	0.00	0.00	1.05	2.28	0.59	0.00	0.00	0.00	0.00	0.00	5.21
24	0.00	0.00	0.00	0.00	0.00	0.00	0.00	0.00	0.00	0.00	0.00	0.00	0.00	0.00
22	0.00	0.00	0.00	0.00	0.00	0.00	0.00	0.00	0.00	0.00	0.00	0.00	0.00	0.00
70	0.00	0.00	0.00	0.00	0.00	0.00	0.94	0.00	0.00	0.00	0.00	0.00	0.00	0.94

Table A8: n-alkane indices for Grand Anse surface samples. CPI (carbon preference index), ACL (average chain length), Paq (aquatic vs. terrestrial organic matter index).

sample	CPI	ACL	Paq
81	1.36	25.00	1.00
84	1.45	25.54	1.00
17	0.00	28.18	0.42
5	14.48	28.67	0.29
129	4.49	28.10	0.39
58	3.49	27.58	0.62
37	5.55	29.70	0.05
28	8.92	28.47	0.46
51	5.39	27.95	0.48
24	4.29	27.41	0.63
22	2.49	26.55	0.77
70	3.16	27.53	0.58

Table A9: n-alcohol totals and phytol concentrations (µg per gram total organic carbon) for Grand Anse surface sediments.

sample	phytol	*n*-alcohol totals
81	20.74	32.53
84	290.15	292.83
17	34.14	961.67
5	0.00	632.57
129	65.11	1501.87
58	26.41	264.34
37	103.11	681.35
28	148.30	485.54
51	13.34	217.59
24	158.09	195.00
22	116.06	89.77
70	0.00	229.57

Table A10: Sterol and triterpene alcohol distributions in µg per gram TOC. Compounds are A: Cholesterol, B: Campesterol, C: Poriferasterol, D: ß-stigmasterol, E: Sitosterol, F: ß-sitosterol, G: Taraxerol, H: ß-amyrin, I: Germanicol, J: α-amyrin, K: Lupeol, L: Lanosterol.

sample	A	B	C	D	E	F	G	H	I	J	K	L	totals
81	23.18	0.00	0.00	10.27	9.77	0.00	582.88	84.34	46.98	0.00	40.53	0.00	797.94
84	143.19	0.00	96.08	132.36	304.52	0.00	3944.97	461.83	226.56	0.00	992.11	0.00	6301.63
17	31.75	0.00	100.30	0.00	334.74	0.00	9021.48	939.53	528.63	0.00	642.60	0.00	11599.02
5	36.90	44.34	156.83	0.00	731.37	0.00	3760.32	3763.32	992.96	0.00	1286.71	0.00	10772.76
129	39.56	104.09	303.94	0.00	290.20	0.00	1361.74	228.21	145.00	0.00	196.15	0.00	2668.88
58	34.86	0.00	29.03	36.44	103.97	0.00	2243.54	274.99	153.41	0.00	158.51	0.00	3034.75
37	197.15	79.67	229.75	0.00	908.41	0.00	8759.60	4032.76	1567.81	0.00	2358.33	0.00	18133.48
28	29.17	0.00	87.88	47.16	197.12	0.00	7241.96	1176.35	612.74	0.00	1159.82	0.00	10552.20
51	0.00	0.00	17.83	0.00	102.16	0.00	2456.25	265.78	154.19	0.00	187.01	0.00	3183.22
24	52.17	0.00	31.73	48.48	140.75	67.53	755.69	128.67	62.45	93.61	209.51	41.99	1632.60
22	15.25	13.25	26.33	13.24	124.06	0.00	597.48	35.00	0.00	0.00	50.30	0.00	874.91
70	36.98	0.00	0.00	0.00	85.84	0.00	8227.11	1013.09	233.54	0.00	213.78	0.00	9810.34

Table A11: Detailed core descriptions as per described in Figure 3.3. Note core descriptions for Core A and Core B were completed as part of the Woodroffe et al. (2015a) study. Lithology is grouped as described in Figure 3.3, and the detailed description is recorded according to the Troels-Smith (1955) classification of unconsolidated sediments.

Core name	Depth (cm)	Lithology	Troels-Smith description
Core 1	0-34	Organic carbonate sand	Ga4, Gs+, Dl+, Th+
	34-45	Organic carbonate sand	Ga3, Gs1, Dl+, Th+, Sh+
	45-50	Organic carbonate sand	Ga4, Gs+, Dl+, Th+
Core 2	0-10	Organic coarse granitic sand	Ga3, Th1, Sh+
	10-50	Sandy peat	Ga1, Th1, Sh2, Ggmin+, Gs+, Dl+
Core A	0-15	Organic coarse granitic sand	Ga3, Sh1, Th+
	15-27	Sandy peat	Ga1, Gs1, Sh2, Th+
	27-85	Peat	Sh2, Th2, Dg+, Gs+
	85-91	Organic carbonate sand	Gs2, Dg1, Th1, Sh1
Core 3	0-50	Peat	Th3, Sh1, Ag+, Dl+, Ggmin+, Gs+
Core 4	0-37	Coarse granitic sand	Gs3, Th1, Dl+, Ggmin+
	37-100	Peat	Th3, Dl1, Gs+, Ag+
Core B	0-28	Coarse granitic sand	Gs2, Ga1, Ag1, Gg(min)+
	28-113	Peat	Dg2, Sh1, Th1, Gs+
	113-250	Organic coarse granitic sand	Gs2, Sh2, Dg+, Th+